DOCTOR OF SCIENCES

Copper resistance in Caulobacter crescentus
Characterization of the Pco operon and of an ABC transporter permease

Gillet, Sébastien

Award date:
2019

Awarding institution:
University of Namur

Microorganisms
Biology
Research
Unit

Copper resistance in *Caulobacter crescentus* - Characterization of the Pco operon and of an ABC transporter permease

Dissertation authored by **Sébastien Gillet**
in preparation of the degree of Ph.D. in Sciences

2019

Jury members:

Pr. Collet Jean-François (de Duve Institute, Belgium)
Pr. Devos Damien (Centro Andaluz de Biología del Desarrollo, Spain)
Dr. Van Houdt Rob (SCK-CEN, Belgium)
Pr. De Bolle Xavier (president, University of Namur, Belgium)
Pr. Jean-Yves Matroule (promoter, University of Namur, Belgium)

UNIVERSITÉ
DE NAMUR

Copper resistance in *Caulobacter crescentus* - Characterization of the Pco operon and of an ABC transporter permease

Gillet Sébastien

Summary

Selective pressure has driven evolution through the ages, forcing organisms to adapt time and again. Organisms developed strategies to face environmental stresses and maintain their fitness. In this context, *Caulobacter crescentus*, an oligotrophic alphaproteobacterium, has been studied to discover different systems it acquired during evolution to resist against metal stresses.

In the first part of this thesis, we characterize the Pco system of *C. crescentus*, providing answers about the functions and localizations of two proteins, PcoA and PcoB. We demonstrate that PcoA is a multicopper oxidase detoxifying the periplasm of *C. crescentus* by oxidizing copper cations. Additionally, we show that PcoB acts like an efflux pump, exporting copper ions outside the bacterium. We also investigate the role of another system, the Cus system, in the resistance against copper stresses. Finally, we conduct a large-scale *in silico* study, hoping to determine whether correlations exist between the conservation of genes and the behaviors, lifestyles, and environments of alphaproteobacteria.

In the second part of the thesis, we characterize an ABC transporter permease and provide data suggesting that this protein would act like a cysteine exporter. Transporting cysteine from the cytoplasm towards the periplasm could help *C. crescentus* resist to stresses caused by several transition metals, including copper, silver, and cadmium.

“I’ll be there where fire makes you dance”

- Ronnie James Dio

Table of Content

Results - Part I

Results - Part II

Discussion

Experimental procedures

Supplementary and annexes

Acknowledgement

Après plus de 4 ans (5, en comptant l'année du mémoire) passés en URBM, il est étrange de se retourner un moment et se remémorer ce qui a composé ce voyage. Le labo est un peu la proverbiale maison bleue de la chanson de Maxime Le Forestier (les hippies en moins) : Des gens y viennent, y restent un peu, puis repartent, avant de revenir éventuellement des années après pour boire un coup à la beer-hour ou pour y travailler à nouveau (pas vrai, Charles, pas vrai, Fanélie ?). Le turn-over fréquent des membres du labo permet beaucoup de rencontres, ce qui a d'ailleurs tendance à allonger drastiquement les listes de remerciements des mémoires et autres thèses.

Il m'est bien sûr impossible de ne pas commencer par remercier Jean-Yves, qui m'a permis de tenter ma chance au FRIA, et qui m'a encadré ces dernières années. Toujours disponible, il a cette faculté de trouver le bon côté dans chaque résultats, que l'expérience soit une réussite ou un échec. Ca permet de garder le moral plus facilement, même dans les passages les plus cahoteux de la thèse. Merci également aux autres P.I. de l'URBM pour leur conseils judicieux, surtout Xavier (qui, en plus des conseil et en plus d'être président de mon Jury, nous permet aussi de nous dérouiller au kicker).

Merci bien sûr à toute la BEAR team, passée et présente. Eme qui m'a formé (je reste son mémo n°1) et Lio bien entendu, mais aussi les plus récents membres de l'équipe, ainsi que les mémos et stagiaires que j'ai pu encadrer. Gwen, Pauline, merci pour vos coups de main ainsi que les fous rires, je vous souhaite de continuer à faire vivre la BEAR team comme il se doit. Un tout grand merci évidemment à Françoise pour son aide précieuse. En plus de nous réserver le meilleur matériel (privilège d'équipe), elle a aussi abattu un boulot colossal qui m'a permis de boucler certaines expériences dans les temps en fin de thèse. Merci également à Maffiou non seulement pour la collection apparemment sans fond de vannes vaseuses, mais aussi pour tout le reste : La musique, les discussions et le travail qu'il réalise au quotidien sans lequel plus rien ne tournerait au labo.

Un grand merci aux gens qui sont venus et repartis, et qui ont contribué à rendre ces années si agréables : Doudou, Simon, Mich-Mich, J-F, Mel ou encore Séverin, ainsi qu'à tous ceux qui sont encore là et qui maintiennent cette ambiance propre à l'URBM : Pierre C-137 qui sort des blagues d'une autre dimension, Kévin, Fanélie, Charles, Mathilde, Agnès, Aurore, Jérome, Caro et tous les autres. Une mention particulière pour mes 4 camarades de galère que sont Oli, Carlo, Vicky et Katy avec qui j'aurai partagé non seulement l'angoisse de la présentation FRIA mais aussi les quatre années qui ont suivi, jusqu'à la rédaction de la thèse. Vous êtes super et je vous souhaite à tous le meilleur pour la suite.

Je ne pourrais pas non plus passer à côté des remerciement pour mes amis et ma famille, qui m'ont soutenu ces dernières années, même si je suspecte qu'ils se demandent toujours à quoi ces recherches peuvent bien servir. Enfin, un merci tout particulier à Hadeline qui a du me supporter plus que les autres, y compris (et surtout !) en fin de cette 4^{ième} année, sans qui j'aurais sans doute eu nettement plus de mal à finir cette thèse.

Last but not least, I'd like to thank the members of my Jury: the Pr. Jean-François Collet, Pr. Damien Devos, Dr. Rob Van Houdt, and Pr. Xavier De Bolle, not only to have accepted this role, but also for the insightful discussions during the private defense.

List of abbreviations

ABC	ATP Binding Cassette
Ag	Silver
Ala	Alanine
CA	Correspondence Analysis
Cd	Cadmium
CDF	Cation Diffusion Facilitator
Cu	Copper
Cys	Cysteine
Fe	Iron
GSH	Glutathione
His	Histidine
IM	Inner Membrane
MCO	Multicopper Oxidases
Met	Methionine
MFP	Membrane Fusion Protein
Mn	Manganese
MT	Metallothionein
NBD	Nucleotide Binding Domain
Ni	Nickel
OM	Outer Membrane Protein
OMP	Outer Membrane Protein
Pb	Lead
PD	Predivisional cell
Pro	Proline
RND	Resistance-Nodulation-Division (protein family)
ROS	Reactive Oxygen Species
SOD	Superoxide Dismutase
ST	Stalked cell
SW	Swarmer cell
TM	Transition Metal
TMD	Transmembrane Domain
Zn	Zinc

Introduction

Environment

1. Variability of the ecological factors

Environmental studies often stress the importance of the ecological niche. This concept is not recent: the idea of a strong interdependency between an organism and its environment long predates modern ecology, going back to Ancient Greece (Pocheville 2015). While the concept did not bear the name of "ecological niche" yet, it was commonly accepted that a given environment is composed of a wide array of specific biotic and abiotic factors, and that these factors would suit some species better than others. Biotic factors have been described as the relationships developed between different organisms or species, such as predation, competition or symbiosis (Van Beneden 1878; Pocheville 2015). The abiotic factors, on the other hand, encompass the various inorganic parameters, such as temperature, light, pressure, or pH (Haferburg & Kothe 2007; Levin & Carpenter 2009).

Charles Darwin, in "On the Origin of Species", improved the notion of ecological niche. The idea that organisms "*adapts through the means of natural selection"* suggests they did not randomly settle in a perfect pre-existing niche. Rather, organisms would have co-evolved with the environment until their biological parameters for optimal fitness coincide with the ecological factors of the niche.

In the late fifties, George Evelyn Hutchinson further refined the concept. Hutchinson coined the "multidimensionality" of the niches, where the different dimensions (the biotic and abiotic factors) are considered according to their accessibility. For instance, if two species are competing for the same nutrient, its presence in the environment does not equal its accessibility. He also acknowledges the "ebb and flow" nature of a niche, meaning that environmental factors can fluctuate over time, either transiently or in a more permanent way (Levin & Carpenter 2009; Pocheville 2015). A competing species can disappear from the niche; the temperature can change, so does the pH, and so on. These natural or anthropogenic variations could drastically reshape the environment as a whole.

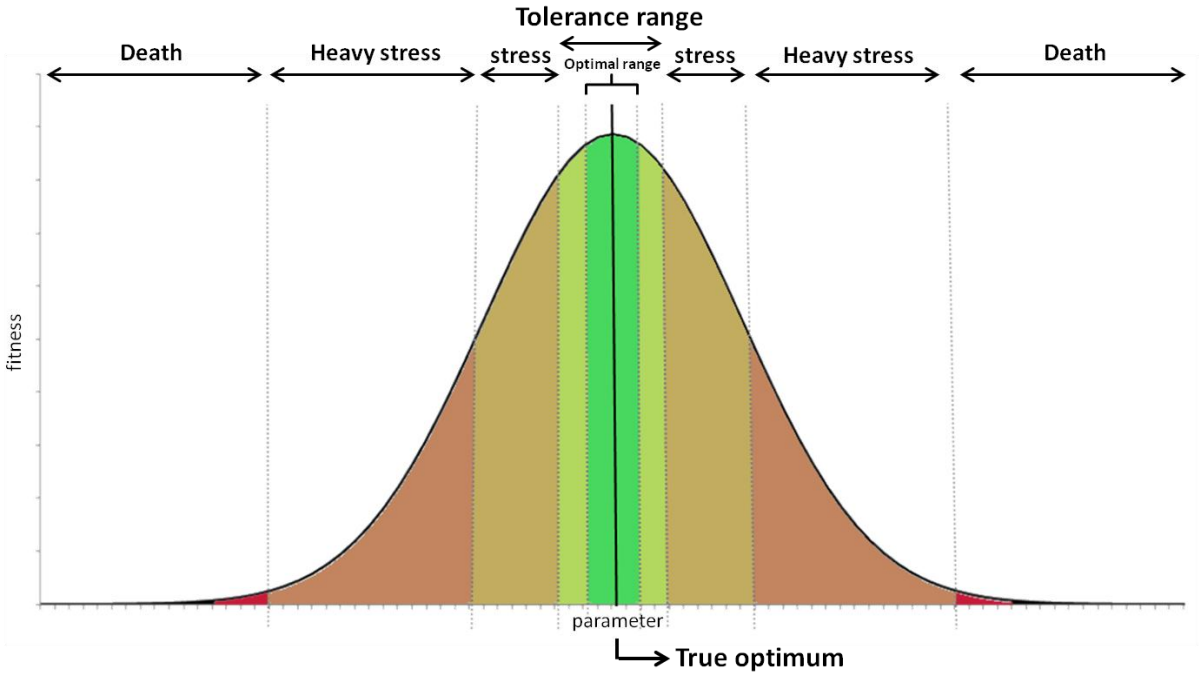

Fig. 1: Normal distribution illustrating the concept of ecological amplitude. For a defined parameter (temperature, pH, oxygen level…) a species will have an optimum point at which its fitness is maximum. Small variations around this theoretical "true optimum" that induce virtually no response from the organism define the "optimal range". The "tolerance range" is defined as the range in which variations may or may not induce a response from the organism, but without affecting its phenotype, growth rate and apparent fitness. Diverging from this range will increase the chance to trigger an important stress, ultimately setting the organism into a "death zone".

2. Limits of tolerance and stresses

In order to maintain their fitness, organisms have thus to cope with these variations. Species can often tolerate small variations of a parameter from an optimum. For instance, the commensal bacterium *Escherichia coli* has an optimal growth temperature of 37°C. Yet, it can still survive and thrive in environment at 33°C without apparent phenotype issues, with little to no change in the genome expression (Polissi et al. 2003). However, as the temperature progressively differs from this temperature range, the growth is increasingly hindered. Morphology defects arise, and important changes are observed at the transcriptomic level. Under these conditions, the expression level of several dozen proteins is modified significantly (Polissi et al. 2003; Gadgil et al. 2005; Noor et al. 2013). The bacteria are then undergoing a stress.

"Stress", in biology, is a poorly defined notion. As Hans Seyle stated it, not without irony: *"Everybody knows what stress is and nobody knows what it is"* (Seyle 1973). In the broad sense of the term, a stress is anything that "impairs Darwinian fitness" (Bijlsma 1997). However, a stress must be characterized at least through the level of the stress and its intensity. A change in the environment could impact an organism at the molecular level, without affecting its physiology or its phenotype. However, another stress could impact not only the physiology of the individual, but the species as a whole, making it a stress at the population level. Likewise, because any deviation from the optimal situation could arguably be regarded as a stress, it is necessary to assess the "intensity" of the stress, although the threshold may seem arbitrary (Bijlsma 1997).

These observations gave birth to the concept of "ecological amplitude" or "ecological valence": an organism can tolerate moderate variations from an optimum without being in a "stress state", until these variations exceed a threshold that will, in turn, trigger a response from the organism or results in its death (Fig. 1).

Among the various abiotic factors that can trigger a stress is the lack or the excess of metals.

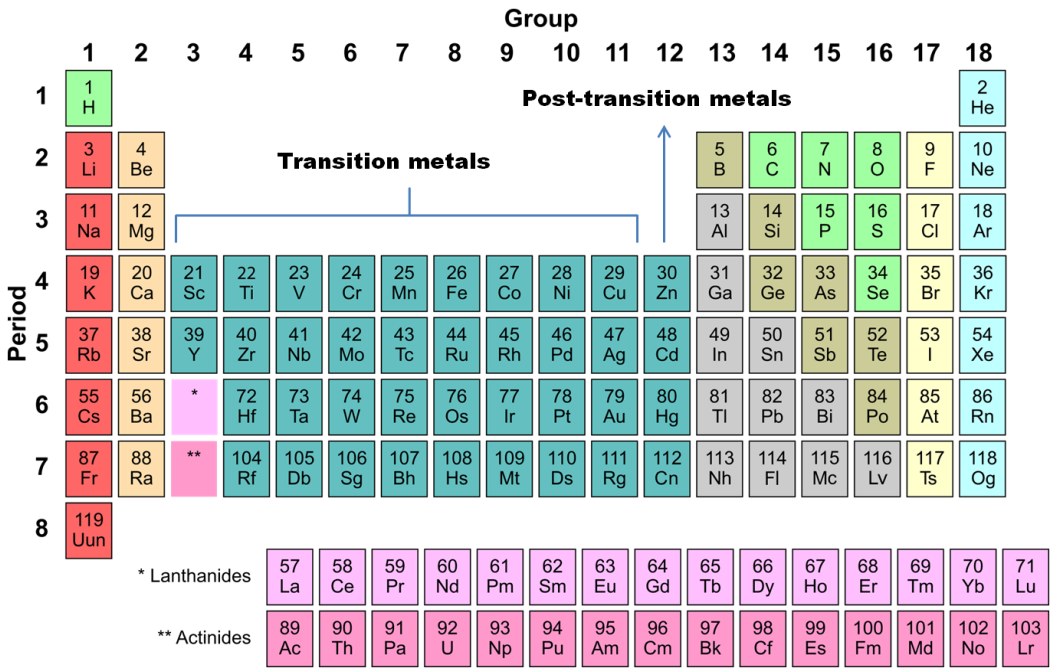

Fig. 2: Periodic table of elements. The transition and posttransition metals, located from period 4 to 7 and from group 3 to 12, are colored in turquoise. Modified from a public domain image created by Offnfopt, uploaded on Wikimedia Commons.

The Copper Case

From a chemical point of view, Cu is a natural element that exists in several ionic forms. The most common forms are Cu^{+} and Cu^{2+}. Both of these forms can potentially damage the cell, although the reduced Cu^{+} is regarded as slightly more toxic than the oxidized form Cu^{2+} (Osman & Cavet 2008). Interestingly, Earth (and Life) witnessed a major shift in Cu bioavailability. Until 2.5 billion years ago, the Earth had a reducing atmosphere, which maintained the majority of Cu in the insoluble cuprous form (Cu^{+}). At the time, most of the oxygen was chelated by dissolved Fe ions. During the Great Oxygenation Event (GOE), the Earth atmosphere underwent a rapid and massive increase of O_2, generating an oxidative environment (Margulis & Sagan 1987; Hao et al. 2016). As O_2 increased with the GOE, soluble Fe^{2+} was oxidized into the less soluble Fe^{3+}, and insoluble Cu^{+} was oxidized into soluble cupric form (Cu^{2+}). This event marked a shift in metalloproteins composition, as they began to favor Cu as a cofactor (Hao et al. 2016).

From a physicochemical point of view, Cu is a ductile and conductive metal, which is naturally present in the environment, such as in soils, sediments or water. Cu concentration displays important variations, either due to natural factors (e.g., the presence of Cu veins or deposits) or anthropogenic pollution. In non-polluted soils, the average Cu concentration is around 30 mg/kg (Adriano 2001; Komárek et al. 2010). In water, the reported average Cu concentration varies between 0.2 and 200 µg/L. However, in case of pollution, these numbers can increase thousandfold (reaching up to a few g/kg and mg/L, respectively) (Monteiro et al. 2010; Hu et al. 2005; Nirel & Pasquini 2010; Moran 2004). However, absolute concentrations are not always meaningful indicators. What often matters for most living organisms is the free or bioavailable Cu more than the biochemically inert or inaccessible Cu.

1. The two faces of a same (copper) coin

Cu shares a long history with humankind. The Chalcolithic period, covering roughly 9000 to 3500 B.C., is called the “Copper Age”, and marks the time in which humanity began to use Cu by inventing metallurgy. Cu is thus likely to be the oldest metal used by mankind. Nowadays, Cu is used for its physical properties in plumbing, in the automobile industry, in electronic components, wires… Moreover, importantly, Cu is also used for its toxic properties.

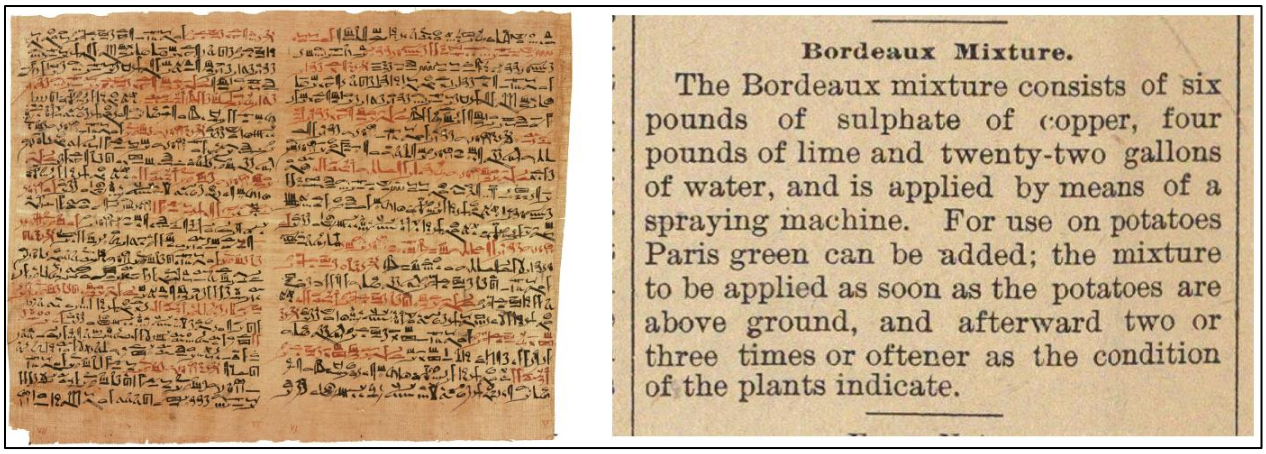

Bordeaux Mixture.

The Bordeaux mixture consists of six pounds of sulphate of copper, four pounds of lime and twenty-two gallons of water, and is applied by means of a spraying machine. For use on potatoes Paris green can be added; the mixture to be applied as soon as the potatoes are above ground, and afterward two or three times or oftener as the condition of the plants indicate.

Fig. 7: Examples of Cu usage for its antimicrobial properties. On the left is photography of section of the Edwin Smith Papyrus, in which Cu is presented as beneficial for wound treatments (Photography originally taken from the Rare Book Room, New York Academy of Medicine, Public domain, and recovered from http://nyam.org/news//2493.html). On the right is a digitized extract from Ann Arbor Argus (June 3, 1892, Public domain), depicting the recipe for the Bordeaux Mixture, used as an anti-fungal on potato cultures.

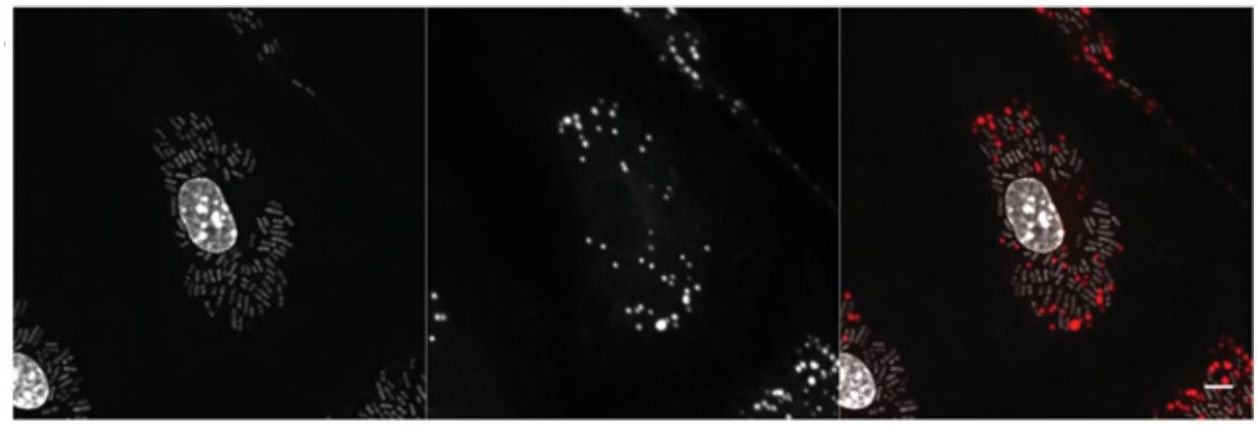

Fig. 8: Cu redistribution in Murine macrophages. Murine macrophage were fixed and stained with DAPI (left) and a Cu specific probe (middle). Right image is the overlay with probed Cu in red, and both Macrophages and Salmonella DNA stained by DAPI in grey Picture from (Achard et al. 2012)

Although the mechanisms of Cu toxicity were not always understood, Cu has empirically been used as an antimicrobial, antiviral or antifungal solution for a long time. We can trace its use back to Ancient Egypt, where Cu tools were employed in medicine and Cu concoction prepared to cure various ailments (Fig. 7) (Breasted 1930; Grass et al. 2011). The new world pioneers used to put copper coins in water barrels in order to increase the time of use (Borkow & Gabbay 2005). In agriculture, the Bordeaux Mixture (mostly composed of $CuSO_4$ and $Ca(OH)_2$) has been used since the 19th century on vines, to prevent mildew infections (Fig. 7) (Hobman & Crossman 2015; Komárek et al. 2010). Cu is also used in boat paint as an anti-fouling means to prevent algae and microorganisms from adhering to the hull, or as a treatment against various diseases (Borkow & Gabbay 2005). Recently, the medical field renewed with the idea of using dry Cu as a means to limit nosocomial infections and encouraged hospitals to plate surfaces such as door handles or bed railings with Cu or Cu alloys (Hodgkinson & Petris 2012).

Because Cu is essential at low dose and toxic as its concentration increases (Cfr. “Metal Stress”, point 2a. and 2b.), tuning the internal Cu concentration is similar to walking a thin line. Pathogens, for instance, often engage in a “tug-o-war” competition with the host, the latter trying to starve the former of this essential nutrient (Braymer & Giedroc 2014; Espart et al. 2015; Becker & Skaar 2014). Alternatively, the host can also try to kill the pathogen by accumulating Cu at the entry site of the infection, as it was observed in murine macrophages upon *Salmonella* (Fig. 8) or *Cryptococcus neoformans* infections (Achard et al. 2012; Espart et al. 2015).

2. Cu acquisition

Cu entry in bacteria has been studied for years, although it remains elusive in most bacterial models (Porcheron et al. 2013; Argüello et al. 2013). For instance, there is no real consensus on how Cu ions enter *E. coli* cells. Most hypotheses formulated for Cu entrance in this organism come from indirect evidence. In *E. coli*, Cu acquisition was suggested to rely at least partially on porins (Lutkenhaus 1977; Argüello et al. 2013). *E. coli* strains lacking the "protein B porin" (later renamed OmpB) were described to be more resistant to Cu stress (Lutkenhaus 1977). The porin had been shown *in-vitro* to be a non-specific importer (Nakae 1976), able to transport various compounds across reconstituted vesicles. This led to think Cu may simply enter the cells in a non-specific way through OmpB.

Recently, however, a new Cu acquisition pathway was discovered in a pathogenic strain of *E. coli*. In UPEC strain, Cu would be imported by the Yersiniabactin (Ybt) metallophore (Koh et al. 2017). The *ybt* gene is found in a pathogenicity island and was originally characterized in *Yersinia pestis.* The Ybt metallophore was first described to help the bacterium resist Cu stress. Ybt would bind free Cu ions to prevent toxicity (Chaturvedi et al. 2013; Koh & Henderson 2015). However, recent developments indicate that in case of Cu deficiency, Cu-Ybt complexes may also be uptaken by the FyuA OM protein. FuyA would then import them in the periplasm. The YbtP/Q protein tandem, anchored in the IM, may be involved in Cu-Ybt dissociation, or even in Cu transport toward the cytoplasm (Koh et al. 2017).

In other bacteria, some Cu importers have been identified. In *Enterococcus hirae,* the CopA protein, although usually regarded as an exporter (cfr. point 3.a.), was reported to be a Cu importer. However, the evidence sustaining the uptake function remain indirect (Odermatt et al. 1993; Solioz & Stoyanov 2003).

In the alphaproteobacterium *Rhodobacter capsulatus,* Cu is likely to be imported in the cytoplasm by CcoA, a transporter belonging to the major facilitator superfamily (Khalfaoui-Hassani et al. 2018). Interestingly, CcoA homologs, despite being absent in *C. crescentus*, are found in several other alphaproteobacteria, including *S. meliloti* or *Ochrobactrum anthropi*. In *E. coli,* this cytoplasmic import could be performed (in addition to the YbtPQ pathway described above) by the hypothetical importer PcoD, localized in the IM (Argüello et al. 2013). However, the fact most cuproenzymes are located in the periplasm led some authors to think the cytoplasmic Cu import would be so limited it may not require specific transporters (Argüello et al. 2013; Osman & Cavet 2008).

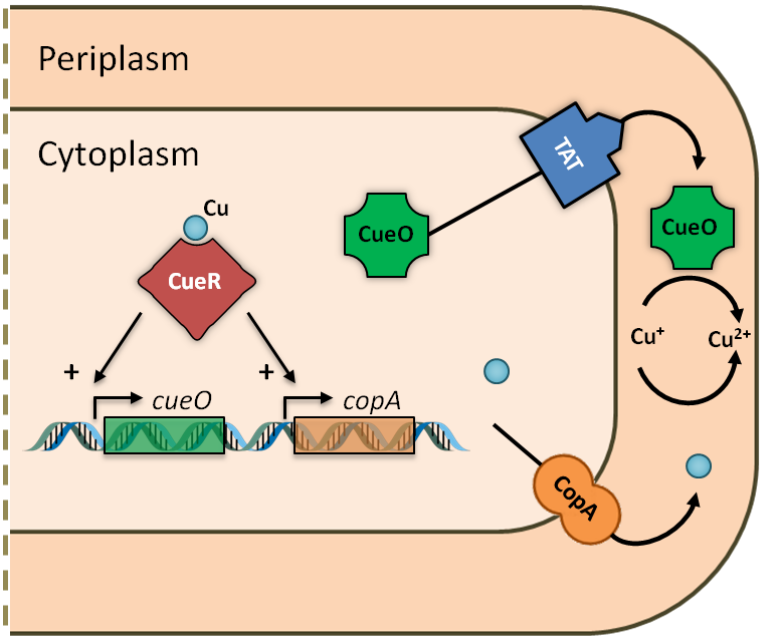

Fig. 9: Schematic overview of the Cue system in *E. coli*. Upon Cu sensing, the CueR protein will upregulate the transcription of the *cueO* and *copA* genes. The CopA ATPase will anchor in the inner membrane and channel Cu^{+} ions to the periplasm, where the CueO MCO will detoxify them by oxidizing them in Cu^{2+}

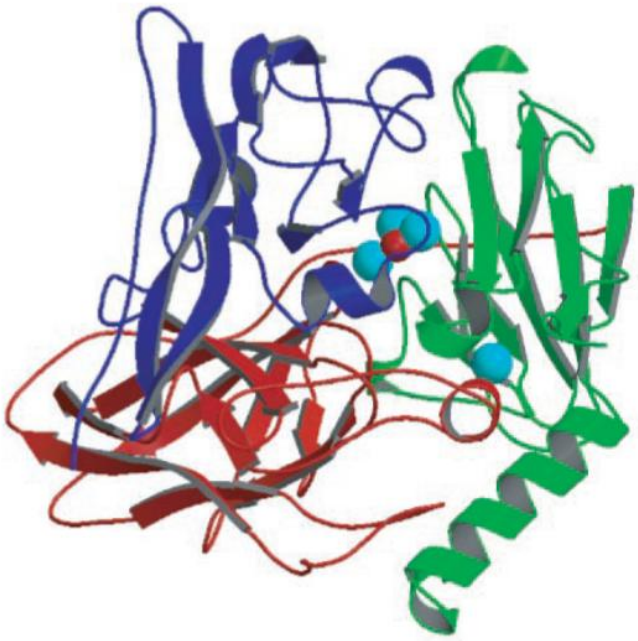

Fig. 10: Ribbon drawing of the crystal structure of *E. coli* CueO. The T1 Cu and Cu3O clusters are depicted as spheres. The 3 domains are colored separately. Image from (Roberts et al. 2002)

3. The major Cu resistance systems of the *E. coli* model

In the *E. coli* model for the transition metals homeostasis, the 3 main copper resistance systems are the Cue system, the Cus system, and the Pco system.

a. The Cue system

The first line of defense is thought to be the Cue system, composed of CueR, CueO, and CopA. A Cu cytoplasmic censor (the CueR protein, acting both as a sensor and a transcriptional regulator) detects free Cu ions in the cytoplasm. Upon detection, CueR activates the transcription of the *copA* gene, encoding the CopA P_{1b}-type ATPase (Fig. 9).

P_{1b}-type ATPases typically share a distinctive Cu-binding motif composed of 2 cysteines (CXXC) in the cytoplasmic N-terminus, before the transmembrane helices (Hodgkinson & Petris 2012). In *E. coli* CopA, CGHC and CASC can be found in the position 14-17 and 112-115, respectively, both before the first TMD in position 185. Additionally, P_{1b}-type ATPases usually feature a conserved HP or CP(C/H) motif in the sixth TMD (Argüello et al. 2011). This CPC pattern can be found in position 497-499 in CopA (Rensing & Franke 2013; Rensing et al. 2000).

CopA homologues have been found in many bacterial species, including *B. subtilis*, *Sinorhyzobium meliloti, Legionella pneumophila,* and *E. hirae* (Porcheron et al. 2013; Patel et al. 2014; Argüello et al. 2013; Multhaup et al. 2001). As mentioned in the previous point, in *E. hirae,* CopA was first characterized as an importer. The export function would then be carried out by the CopB ATPase (Odermatt et al. 1993). It is interesting to note that CopA does not bind free soluble Cu ions, which would be highly toxic in the cytoplasm, but receives the ions from a transporter (see chaperone section below).

Along with the *copA* transcription, CueR also upregulates the expression of *cueO*, coding for a periplasmic MCO involved in Cu detoxification (Fig. 9 and Fig. 10).

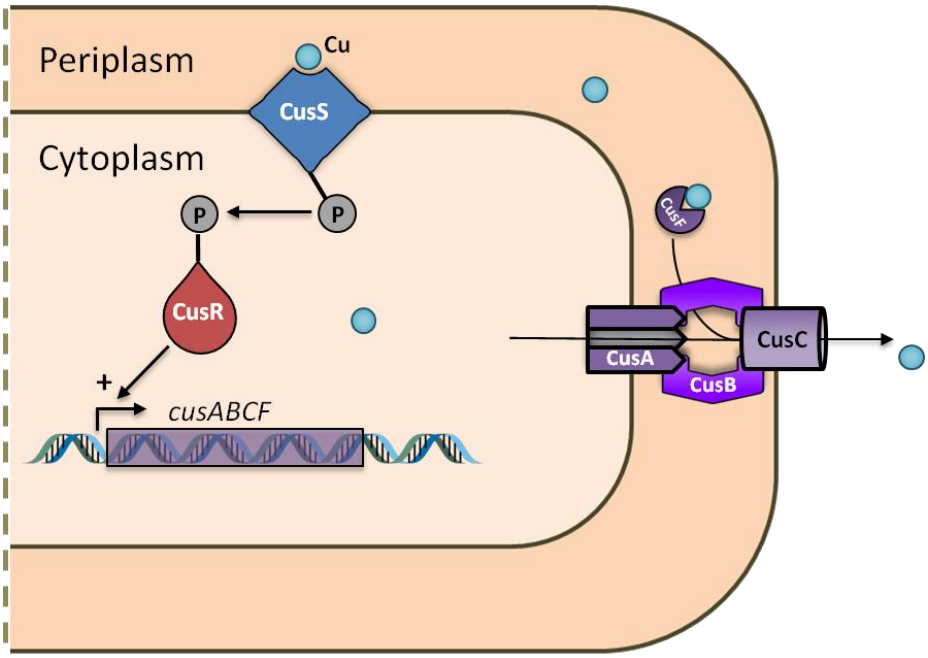

Fig. 11: Schematic overview of the CuS system in *E. coli*. The histidine kinase CusS, anchored in the IM, acts as a Cu sensor. Upon detection, the signal will be transmitted to the transcriptional activator CusR. CusR will upregulate the transcription of the *cusABCF* operon, encoding for a HME-RND type export system.

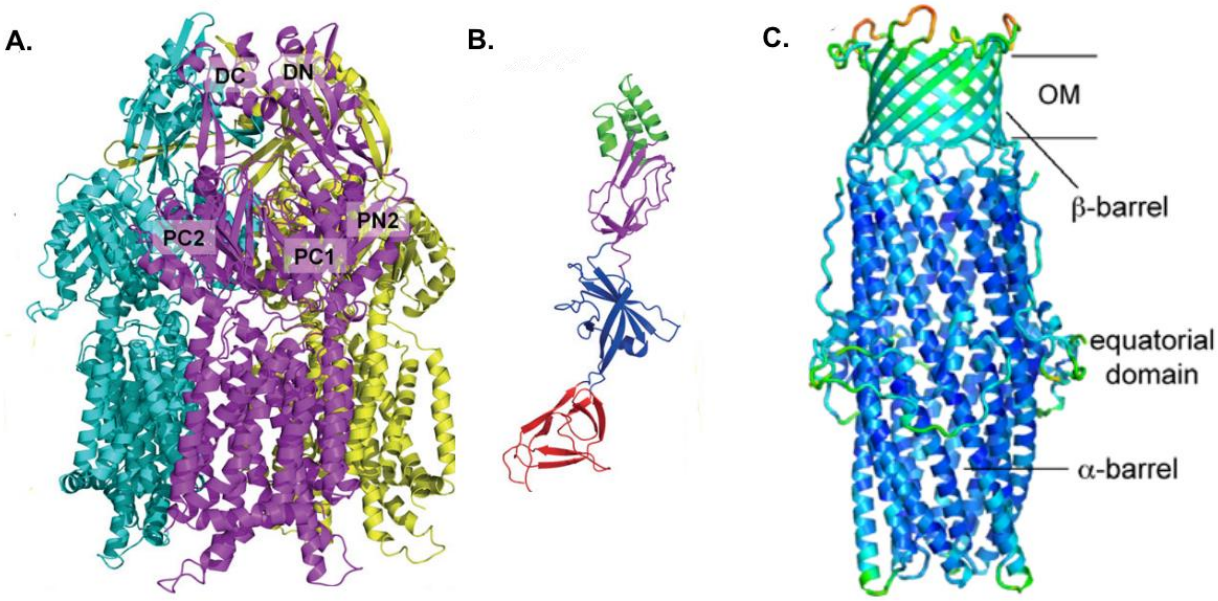

Fig. 12: Ribbon drawing of the crystal structure of *E. coli* CuSA, CusB and CusC. A) Ribbon drawing of the assembly of CusA homotrimer B) Ribbon diagram of the CusB protomer. C) Ribbon representation of the CusC trimer. Picture assembled with images taken from (Long et al. 2012; Kulathila et al. 2011)

MCOs use Cu ions as cofactors to oxidize a broad range of substrates (Solomon et al. 1996; Komori & Higuchi 2015). In *E. coli*, CueO oxidizes Cu^{+} into the less toxic Cu^{2+} by using O_2 as a final acceptor (Grass & Rensing 2001). Cu^{+} oxidation will therefore result in a 4 electrons reduction of O_2 into 2 H_2O molecules (Grass & Rensing 2001; Djoko et al. 2010). Classically, MCOs harbor three Cu binding sites. The mononuclear T1 Cu site accepts electrons and transfer them to a trinuclear cluster, which is composed of a mononuclear T2 Cu site and a binuclear T3 Cu center, binding and reducing O_2 (Solomon et al. 1996; Galli et al. 2004). Specific MCOs are involved in metal resistance by using the metal as a substrate (Solomon et al. 2008; Butterfield et al. 2013). Near the T1 Cu site, CueO also displays a methionine-rich region binding a labile Cu ion in the context of a phenol oxidase activity (Roberts et al. 2003; Cortes Castrillona et al. 2015; Djoko et al. 2010). CueO is translocated into the periplasm through the TAT pathway, where it detoxifies Cu^{+} into Cu^{2+}.

b. The Cus system

The Cus system acts as the second line of defense for *E. coli*. While the threshold for its activation seems to be twenty times higher than the Cue threshold (Outten et al. 2001), the Cus system is critical for the cell when the Cue system is saturated and overwhelmed by the Cu stress.

The inner membrane sensor CusS is a histidine kinase that autophosphorylates upon Cu detection. CusS~P then transfers its phosphate to the transcriptional activator CusR. CusR~P stimulates the transcription of the *cusABCF* operon encoding a HME-RND complex, which then pumps Cu ions from the cytoplasm or the periplasm to the extracellular space (Fig. 11) (Osman & Cavet 2008; Long et al. 2012). Interestingly, the CusABC complex may not be entirely specific to Cu and might also exports Ag^{+} (Franke et al. 2003).

The integral inner membrane CusA is the RND protein *per se*, and forms a homotrimer (Fig. 12 A) (Kim et al. 2011). A large periplasmic domain allows the interaction with CusB and CusC, while a smaller additional domain protrudes in the cytoplasm (Delmar et al. 2013). CusA binds cytoplasmic Cu^{+} or Ag^{+} ions through Met residues (M_{573}, M_{623} and M_{672}). Additional Met clusters in the periplasmic domains are thought to create a “methionine relay network”, transporting the cations to the CusC OMP via CusB, the MFP (Delmar et al. 2013).

CusB is spanning across the periplasm and bridges CusA to CusC. It can also bind Cu^{+} or Ag^{+} ions directly from the periplasmic chaperone CusF (Fig. 11). CusB comprises four domains (Fig. 12 B), 3 of which are mostly composed of β-strands.

The fourth domain is slightly different and consists in a three- α-helices bundle, whose function is poorly understood (Delmar et al. 2013; Kim et al. 2011). Indeed, this fourth domain is not found in any other described bacterial MFP, making homology comparison virtually impossible. It is thought to interact with CusC, facilitating the delivery of cations to the OMP (Delmar et al. 2013).

CusC is a 12-stranded β-barrels forming a channel in the outer membrane for membrane ions export (Fig. 12 C). It is a trimeric complex, each monomer comprising 4 β-strands each. As the structure of CusC does not point toward any metal-specific feature, the specificity of the CusABC complex is thought to rely on CusA and CusB (Delmar et al. 2013).

The fourth member of the cus operon encodes the small periplasmic CusF chaperone (Fig. 11). CusF binds Cu^{+} ions and delivers them for export to CusB within the CusABC RND efflux pump (Bagai et al. 2008). CusF is reported to bind Cu^{+} and Ag^{+} through an HMM motif (H_{36} M_{47} M_{49}), as well as a Trp residue (W_{44}) (Loftin et al. 2007; Loftin & Mcevoy 2009). The Trp generates a π-interaction, weaker than the bond with the metal cation that would result from a third Met residue. This reduced affinity is crucial to allow the transfer of the metal to CusB (Loftin & Mcevoy 2009)

c. The Pco system

The third major system for Cu resistance in *E. coli* presented here is the Pco system. The Pco system was identified in *E. coli* strains isolated from feces of pigs whose diet had been supplemented with Cu (Tetaz & Luke 1983). Cu has been known to improve growth and mass gain in livestock and poultry (Silveira et al. 2014; Shurson et al. 1990; Lewis 1995). While the mechanisms promoting this growth have yet to be completely elucidated, it is thought to be due to the bactericidal effect of Cu. Cu acts as a pseudo-antibiotic treatment, preventing common diarrheal diseases that slow down the growth of the animals (Yazdankhah et al. 2014). However, due to Cu toxicity, new regulations have been set. For instance, the European Union now limits Cu in diet to a maximum of 175 ppm (Silveira et al. 2014).

In response to the Cu-enriched diet, the flora of the animals was forced to adapt, and new resistance systems appeared. Among them was the plasmid-borne *pco* system, carried on the pRJ1004 conjugative vector, and found in some *E. coli* strains (Tetaz & Luke 1983; Brown et al. 1995). On the pRJ1004, the Pco system is encoded by seven genes (*pcoA; pcoB; pcoC; pcoD; pcoR; pcoS and pcoE*), distributed in three clusters. The first cluster is the *pcoABCD* operon, the second is the *pcoRS* operon and, finally, *pcoE*, located further down the genome.

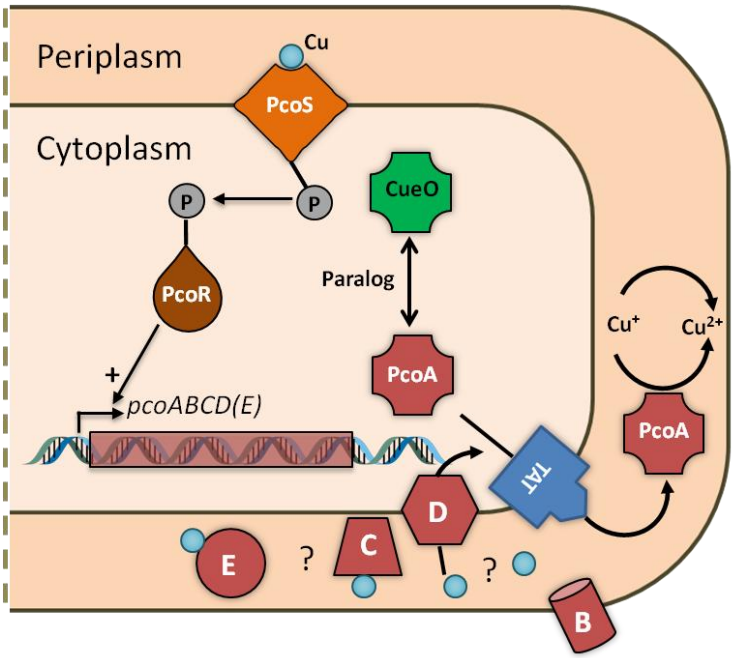

Fig. 13: Schematic overview of the Pco system in *E. coli*. The histidine kinase PcoS, anchored in the IM, acts as a Cu sensor. Upon detection, the signal will be transmitted to the transcriptional activator PcoR. PcoR upregulates the transcription of the *pcoABCD(E)* operon. PcoA is a periplasmic MCO that, akin to CueO, detoxifies the periplasm by oxidizing Cu^{+} into Cu^{2+}. PcoB is predicted to be an export system in the OM, driving Cu outside the cell. PcoC is thought to be a Cu-binding protein that delivers Cu cations to either PcoA or PcoD. PcoD is predicted to be a Cu importer in the IM, and PcoE a periplasmic Cu chaperone.

The PcoRS proteins are part of a two-component system strikingly similar to CusRS and function the same way. PcoS is the sensor and PcoR the transcriptional activator that upregulates the transcription of the *pcoABCDE* genes. Interestingly, CusRS can compensate for the absence of PcoRS and can ultimately activate the transcription of the *pco* operon (Franke et al. 2003).

The PcoABCDE proteins are involved in Cu detoxification and export, but not all of them are thoroughly characterized (Fig. 13). PcoA is a periplasmic MCO, paralog of CueO. Less is known about PcoB. *In-silico* analyses predicted a possible interaction with PcoA and is thought to export Cu (Hobman & Crossman 2014). PcoC is a methionine-rich Cu binding protein, whose function remains elusive despite a solved crystal structure (Wernimont et al. 2003). The current hypothesis is that PcoC feeds PcoA or PcoD with Cu^{+} for detoxification (Fig. 13). PcoD is predicted to be an inner membrane protein containing 8 transmembrane domains, which would import Cu from the periplasm to the cytoplasm (Rensing & Grass 2003). Finally, PcoE is a putative periplasmic chaperone of unknown function (Fig. 13) (Argüello et al. 2013).

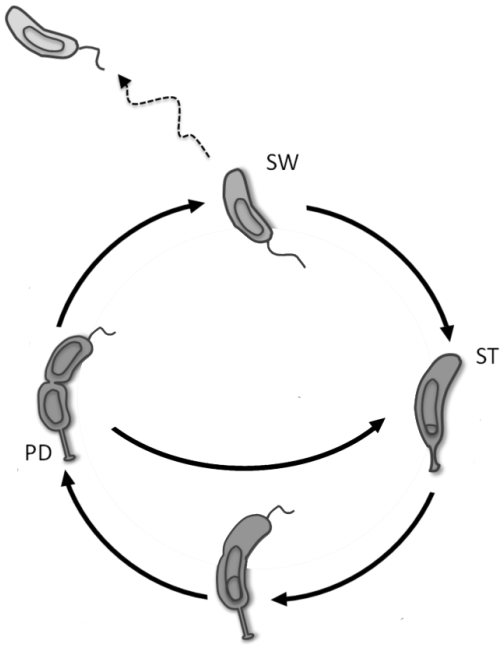

Fig. 14: ***C. crescentus*** **cell cycle**. The ST cell initiates DNA replication, leading to the formation of a PD cell. The PD cell will yield a new SW cell and a ST cell upon cell division. The motile SW can potentially explore new environments, but has to undergo a differentiation process and differentiate into a ST cell in order to replicate its chromosome and to divide.

Caulobacter crescentus

1. A free-living alphaproteobactrium

Isolated for the first time at the end of the 19th century by Loeffler, and observed more thoroughly in the dawn of the 20th century by Jones, *Caulobacter* was not properly characterized until a few decades later, when Henrici and Johnson established *Caulobacter vibrioides*, also called *Caulobacter crescentus*, as the representative species of the *Caulobacter* genus (Henrici & Johnson 1935; Abraham et al. 1999). The work of Poindexter will flesh out the genus further (Poindexter 1964), and many others afterwards will make of *C. crescentus* a model species for cell cycle progression and regulation (see below).

Albeit ubiquitous, *C. crescentus* was long regarded as a mostly aquatic alphaproteobacterium (Abraham et al. 1999). However, a recent development tends to indicate that *C. crescentus* would rather be mostly present in soils, in addition to other environments such as water bodies (Wilhelm 2018). Early on, *Caulobacter* ability to thrive in low-nutrient and toxic environments was reported (Poindexter 1981; Poindexter 1964). Therefore, *Caulobacter* is regarded as a pioneer genus, able to colonize oligotrophic and polluted environments.

2. Caulobacter crescentus cell cycle

C. crescentus became a model for its dimorphism. It is one of the most striking examples of asymmetric cell cycle, a hallmark in many alphaproteobacteria. *C. crescentus* cell cycle culminates with an asymmetrical cell division, yielding two morphologically and physiologically distinct progenies, one flagellated swarmer (SW) cell and one sessile stalked (ST) cell.

The SW cell is limited to the G1 phase and is therefore unable to replicate its DNA. In the context of a differentiation process, the SW cell will loosely attach to a surface, shed its flagellum, retract its pili and synthesize a stalk at the same pole. The resulting ST cell is now strongly bound to the surface via a polysaccharidic holdfast located at the tip of the stalk and immediately starts chromosome replication (S phase). After completion of DNA replication, the growing ST cell enters the G2 phase and turns into a predivisional (PD) cell that will grow a new flagellum at the pole opposite to the stalk (Fig. 14).

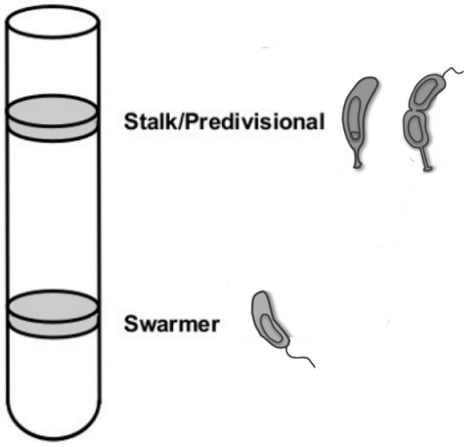

Fig. 15: Schematic representation of the result of a silicate gradient synchrony of *C. crescentus*. The surface capsule possessed by the ST and PD cells makes them less dense. They will therefore not migrate as far as the SW cell in the silicate gradient upon centrifugation. The upper band contains a mix of ST and PD cell, while the lower band contains the SW cells. The SW cell population can be recovered for further experiments. Cartoon modified from (Schrader & Shapiro 2015)

The PD cell will then undergo an asymmetrical cell division yielding a new SW cell and a ST cell, the later immediately starting a new round of DNA replication (Fig. 14) (Curtis & Brun 2010).

The presence of a capsule at the ST and PD cell surface lowers their density and therefore facilitates the isolation of SW cells by centrifugation in a silicate gradient, where the more dense SW cells will accumulate deeper in the gradient (Fig. 15). The SW cell population can be recovered, washed and placed in fresh medium. The bacteria will then progress throughout their cell cycle in a synchronized manner, allowing the monitoring of the different stages of the cycle (Kirkpatrick & Viollier 2012; Schrader & Shapiro 2015).

4. *C. crescentus* defense strategy against metals – A brief overview

C. crescentus is known to colonize polluted environments and to resist various metals, such as cadium, chromium or selenium (Braz & Marques 2005; Kavamura & Esposito 2010; Hu et al. 2005; Yung et al. 2014). High-throughput transcriptomic studies were conducted to establish the profile of gene expression underlying these resistance processes. Genes encoding efflux pumps, heat-shock proteins and resistance systems against oxidative stress were found to be overexpressed upon exposure to these metals.

Interestingly, *C. crescentus* was also shown to be highly resistant to Uranium (U) (Yung & Jiao 2014; North et al. 2004; Yung et al. 2015; Hu et al. 2005). In case of U stress, *C. crescentus* seems to operate in a two-steps strategy. Firstly, *C. crescentus* induces the biomineralization of U ions through the PhoY phosphatase, likely decreasing its toxicity. The biomineralization process precipitates the U in the form of U-phosphate, depleting the bioavailable phosphate from the cell. This phosphate starvation is compensated by the upregulation of the transcription of a phytase, which is likely to supply phosphate to the bacterium during the U stress condition (Yung & Jiao 2014; Yung et al. 2014). As some bacterial phytases can hydrolyse a broad range of substrates (Konietzny & Greiner 2004; Priyodip et al. 2017), they might use various phosphorylated compounds, such as ATP or Glucose 6-phosphate, to make up for the phosphate starvation induced by the U stress.

Despite the high-throughput analysis, not much is known about the biochemical functions of the various metal homeostasis or resistance systems. Many of them are probably still undiscovered or at least not annotated. The work presented in this thesis aim to contribute to the characterization of systems involved in the detoxification of the periplasmic space of *C. crescentus*.

Objectives

Objective

Owing to their ambivalent nature, transition metals represent a potential threat for living organisms and their concentration needs to be tightly regulated. Bacteria have developed a broad diversity of systems throughout evolution to regulate this concentration or to counteract the various adverse effects the metal stresses can generate.

This thesis aims to elucidate some of the strategies that *C. crescentus*, a model alphaproteobacterium known to colonize oligotrophic and polluted environments, has acquired and set up to face Cu and other metallic stresses. More specifically, this work will focus on the periplasm of *C. crescentus*, as the periplasm is known to harbor most of the cuproproteins (Argüello et al. 2013). It is likely to be one of the first lines of defense against extracellular metallic ions (or at least Cu ions) that could create cellular damage.

This thesis will be divided into 2 main part. The first section will be dedicated to the Pco and Cus systems, known in *E. coli* for their role against Cu stress. The objective is to see whether they are present or not in *C. crescentus,* and whether there are involved in Cu resistance and detoxification. The Pco system, poorly described in *E. coli*, will be characterized functionally. At the end of this first chapter, a large bioinformatic study will be described. The objective of this analysis is to elucidate whether or not a correlation exists between the conservation of the Pco and Cus system in alphaproteobacteria and their lifestyle.

The second part of the thesis will be centered on another metal resistance system of *C. crescentus*, and ABC transporter permease discovered during a genetic screen performed by the research group. The objective is to characterize its function, its intracellular localization, and eventually its expression throughout the cell cycle.

RESULTS – Part I

Table 1: Result of the ortholog search with *E. coli* proteins as query sequence against the *C. crescentus* proteome.

E. coli protein	Homolog in *C. crescentus*	E value	Score	Query cover	Identity
PcoA	CCNA_01015	0	546	99%	47%
PcoB	CCNA_01016	8E-36	125	85%	35%
PcoC	X	/	/	/	/
PcoD	X	/	/	/	/
PcoE	X	/	/	/	/
PcoR	CCNA_02845	6E-62	193	97%	44%
	CCNA_01351	2E-54	175	97%	46%
	CCNA_00296	3E-44	148	96%	38%
	CCNA_03130	2E-39	148	97%	38%
	...	...	...	...	...
PcoS	CCNA_03326	1E-20	91.7	45%	32%
	CCNA_01239	3E-20	89.7	56%	31%
	CCNA_00983	2E-19	87.8	43%	31%
	CCNA_02842	1E-18	85.1	65%	25%
	...	...	...	...	...

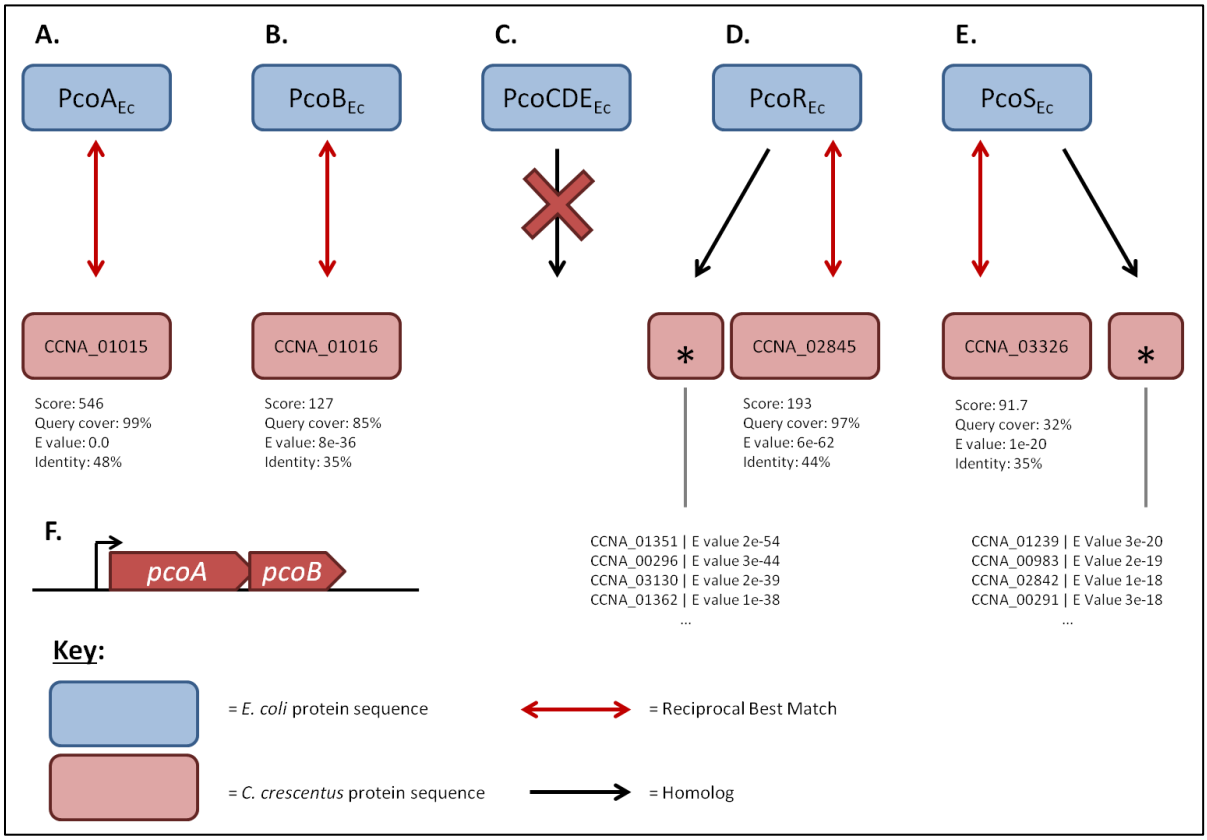

Fig. 16: Conservation of the *E. coli* Pco system in *C. crescentus*. Double-headed arrows indicate a reciprocal best match. One-way arrows indicate simple homology. A. Results with PcoA$_{Ec}$ as query sequence B. Results with PcoB$_{Ec}$ as query sequence C. No results could be found with PcoC$_{Ec}$, PcoD$_{Ec}$ or PcoE$_{Ec}$ as query sequences. D. Results with PcoR$_{Ec}$ as query sequence E. Results with PcoS$_{Ec}$ as query sequence F. Organisation of the PcoAB operon.

The Pco and Cus systems

1. The Pco System detoxifies the periplasm of *Caulobacter crescentus*

a. Bioinformatics – establishing the hypothetical model

i. Search for orthologs from *E. coli* sequences

E. coli is a model for TM resistance and homeostasis systems. Many of these systems are conserved in other species of the proteobacteria phylum. To obtain a general idea of which Cu resistance systems are conserved in *C. crescentus*, a search for orthologs was conducted. We assessed the presence of *E. coli* Pco protein orthologs in our strain of interest, the *C. crescentus* CB15N (synonymous of NA1000). The NCBI BLAST+ 2.4.0 package was employed, with an E value threshold of 9e-16. The amino acid (AA) sequences of the 7 Pco proteins of *E. coli* were taken as the query. These proteins will be referred from now on with the $_{Ec}$ suffix (e.g., $PcoA_{Ec}$, indicating the *E. coli* version of PcoA). The proteins listed without any suffix belong to *C. crescentus*. The resulting best matches are listed in Table 1. $PcoC_{Ec}$, $PcoD_{Ec}$ and $PcoE_{Ec}$ analysis did not provide any results matching the search criteria, likely indicating the absence of orthologs in *C. crescentus* (Table 1 & Fig. 16 C). However, several matches were found for $PcoA_{Ec}$, $PcoB_{Ec}$, $PcoR_{Ec}$ and $PcoS_{Ec}$.

The best match recovered from the $PcoA_{Ec}$ "blast" is CCNA_01015, a 571 AA protein encoded by the eponymous gene (Table 1). Running the reverse research with the CCNA_01015 AA sequence as the query against the *E. coli* proteome leads to $PcoA_{Ec}$ as the first result, indicating a reciprocal best match (Fig. 16 A). Both proteins match each other as the highest scoring candidate in the other proteome.

The blast search for $PcoB_{Ec}$ returned CCNA_01016 as the best hit. This 303 AA protein is encoded by a gene neighboring the $PcoA_{Ec}$ ortholog candidate, CCNA_01015 (Table 1). $PcoB_{Ec}$ and the *C. crescentus* homolog are listed as reciprocal best matches (Fig. 16 B). Interestingly, the CCNA_01015 and CCNA_01016 genes seem to work in operon. There is a 3 base pairs overlap between the two genes, and no distinct promoter for CCNA_01016 could be predicted (Fig. 16 F).

The $PcoR_{Ec}$ and $PcoS_{Ec}$ results are less straightforward to interpret. The blast search returned many matches as potential ortholog candidates (Fig. 16 D&E), which may not be so surprising. $PcoR_{Ec}$ and $PcoS_{Ec}$ are indeed a very classical two-component system, with a histidine kinase and a response regulator. Such systems are generally well conserved, and paralogs can be found scattered all over the genome.

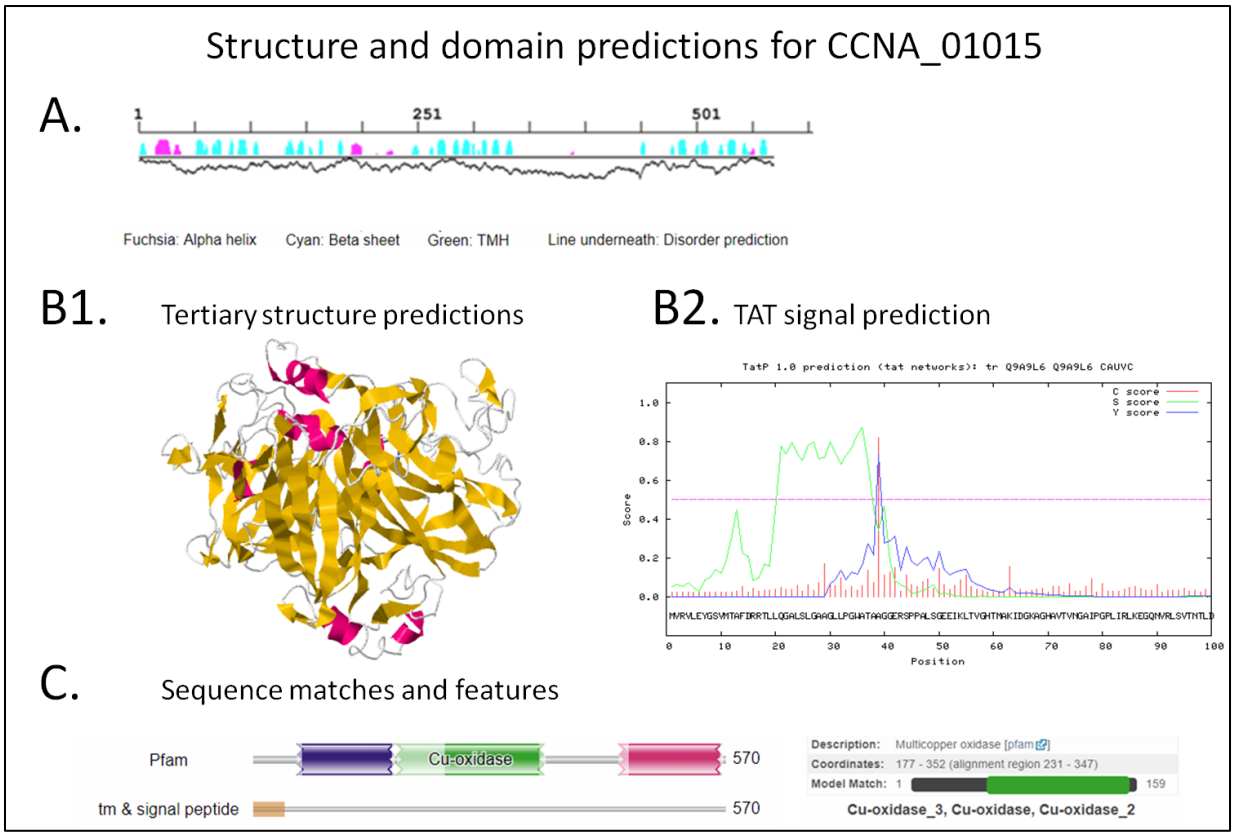

Fig. 17: Structure and domain prediction for CCNA_01015 (PcoA). A. Result of the Foundation analysis. Secondary structures are represented along with their sequence position on the X axis. α-helices are represented in fuchsia and β-strands in cyan. The wiggly line beneath the secondary structure represents disorder. The further away from the X axis, the more the disorder. **B1** Tertiary structure prediction through I-Tasser. The secondary structure composing the 3D model are color-coded. α-helices are represented in fushia, β-strands in yellow. **B2.** TAT signal prediction. **C.** Results of the HMMER domain prediction. The three domains (violet, green and pink) correspond to three Cu oxidase subdomains.

This may explain why CusRS could replace PcoRS in the absence of the latter in *E. coli* (Franke et al. 2003). Indeed, both systems are strikingly similar, which makes ortholog search complicated. Multiple good matches are to be expected. Despite the status of reciprocal best matches for both $PcoR_{Ec}$ and $PcoS_{Ec}$, it is unclear whether these candidates are involved in Cu sensing and in the regulation of the *pcoAB* operon. The *C. crescentus* predicted *pcoR* and *pcoS* are both isolated in the genome, and physically apart from *pcoA* and *pcoB*. It is therefore unlikely that CCNA_02845 and CCNA_03326 are the functional orthologs of $PcoR_{Ec}$ and $PcoS_{Ec}$.

PcoA

The protein sequence of PcoA was thoroughly analysed through a series of bioinformatic tools, allowing us to obtain predictions about its structure and domains.

ii. Structure

The PcoA protein sequence was first introduced in Foundation, a "protein sequence features visualizer" from the CADB (Centro Andaluz de Biología del Desarrollo, Sevilla) (Fig. 17 A). Foundation aggregates result from three different software: Psi-pred, predicting 2nd structures, IUPred, assessing disorder, and TMHMM, looking for transmembrane helices.

PcoA displays a majority of β-sheets, with a few α-helices scattered mostly in the first half of the protein (from position 16 to 37 and 191 to 251). A large disordered region is located from position 348 to 423. These predictions are in line with the solved structure of $PcoA_{Ec}$. For further comparison, two additional analyses were carried out.

The first one is another secondary structure prediction made by the Quick2D aggregative tool. Quick2D, akin to Foundation, requires several other tools to perform the prediction. However, Quick2D pings the same request to several different algorithms dedicated to the same function and crosschecks the results. It will therefore return, for instance, multiple calculation results for the disordered or for the α-helices/β-sheets structures. Albeit a bit more complete (Quick2D also report coiled-coil and π-helices if any), the results are slightly redundant with those obtained with Foundation (Fig. S1).

The second supplementary analysis was a tertiary structure prediction, performed by I-TASSER (Iterative Threading ASSEmbly Refinement). I-TASSER is an online web-service dedicated to protein structure and function prediction. I-TASSER uses a user input (i.e. the query AA sequence) and tries, by homology, to find similar folds or known templates from PDB ("The Protein Data Bank", one of the largest database of 3D structures, gathering published crystallography, Cryo-electron microscopy or NMR spectroscopy results).

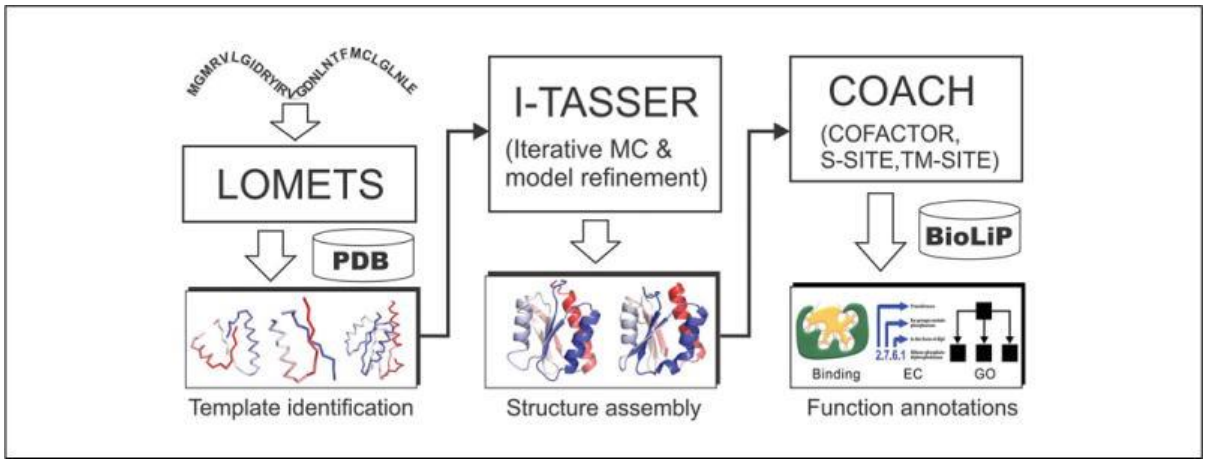

Fig. 18: I-Tasser pipeline. The input sequence is processed by several algorithms to create a 3D model and predict functions. (Yang & Zhang 2015)

I-TASSER then aligns the query and the model, and builds a 3D structure for the matching regions. For the non-matching regions (that do not align with known templates), I-TASSER will try to create a model *ab initio*, based on the sequence itself and the biochemical properties of the different amino acids. The different fragments will subsequently be assembled. Usually, there will be some uncertainties about the correct 3D conformation of the protein. I-TASSER will therefore run a large set of possible structures and use the SPICKER algorithm to cluster these hypothetical models. It will compare similarity and identify the lowest free-energy state that would be more favorable for the protein (and therefore more likely to be correct). Based on SPICKER results, I-TASSER will report the five most probable results with a score of confidence (Yang & Zhang 2015).

These models can be evaluated manually and refined with any supplementary information not computed by the service. Additionally, one can choose to input the resulting structure for a second prediction process with the COACH program that will attempt to predict and annotate the function of the query protein (Fig. 18).

The I-TASSER prediction for PcoA can be seen in Fig. 17 B1. The model seems consistent with the known structure of the *E. coli* ortholog (Fig. 10).

iii. Signals and domains prediction

Additional bioinformatic analyses were achieved to predict signal peptides and enzymatic domains. The TatP 1.0 server is an online service that looks for Twin-Arginine signal peptide in a given sequence, via the recognition of conserved cleavage sites and consensus patterns. PcoA is predicted to possess a TAT signal at the N-Terminus (Fig. 17 B2). The cleavage site would be around position 38 and a typical TAT recognition pattern (DRRTLL) can be found. This pattern is similar to the SRRXFLK consensus motif reported in the literature (Stanley 2000). This is consistent with what is known for $PcoA_{Ec}$, reported to have a similar TAT signal for periplasm export (Sun et al. 2002). PcoA would thus fold in the cytoplasm before being exported into the periplasm of *C. crescentus*.

Finally, the PcoA sequence was entered in the HMMER webserver. HMMER is an online platform building profile hidden Markov models for a query sequence, which uses this profile to screen similarities in large databases and libraries. This allows gathering of various information, including prediction about protein domains (Potter et al. 2018).

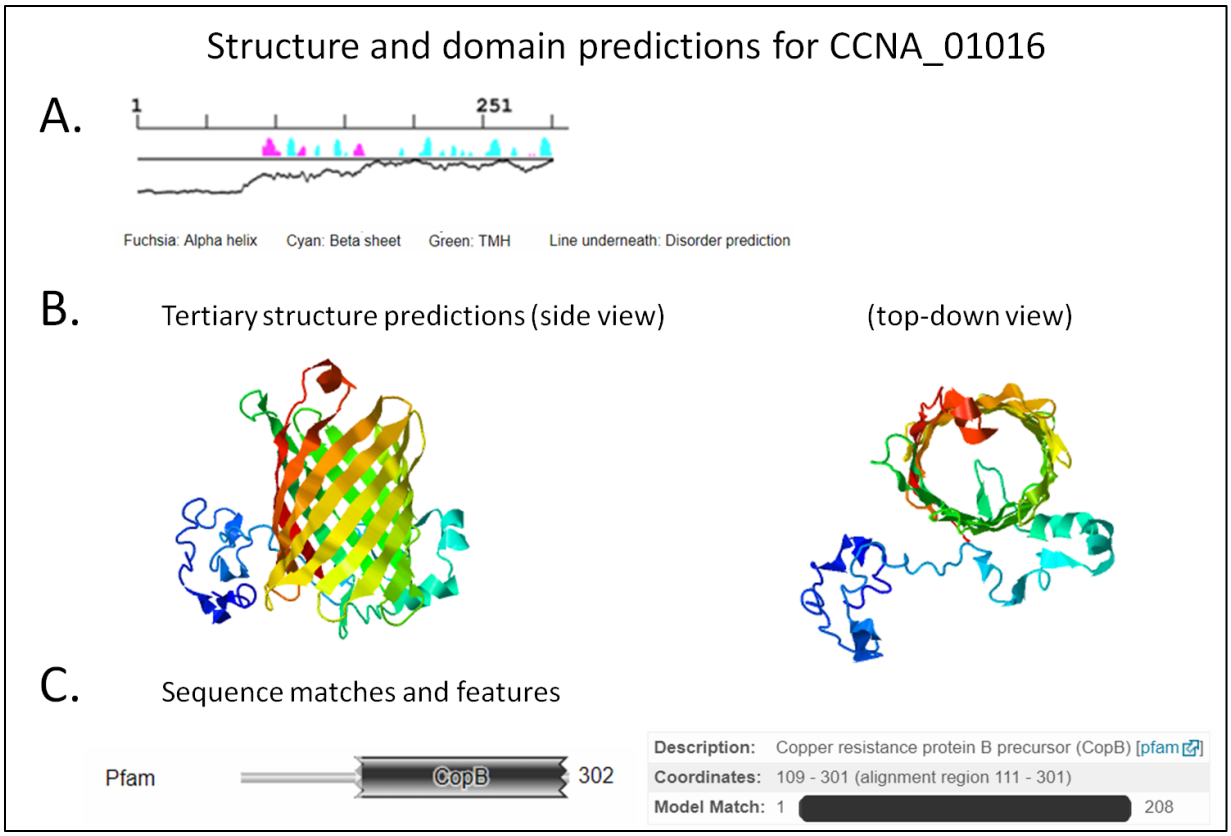

Fig. 19: Structure and domain prediction for CCNA_01016 (PcoB). **A.** Result of the Foundation analysis. Secondary structures are represented along with their sequence position on the horizontal axis. α-helices are represented in fushia and β-strands in cyan. The wiggly line in beneath the secondary structure represents disorder. The further away from the horizontal axis, the more the disorder. **B** Tertiary structure prediction through I-Tasser, both inside and top-down view. **C.** Results of the HMMER domain prediction. The only predicted domain corresponds of Cu resistance domain precursor.

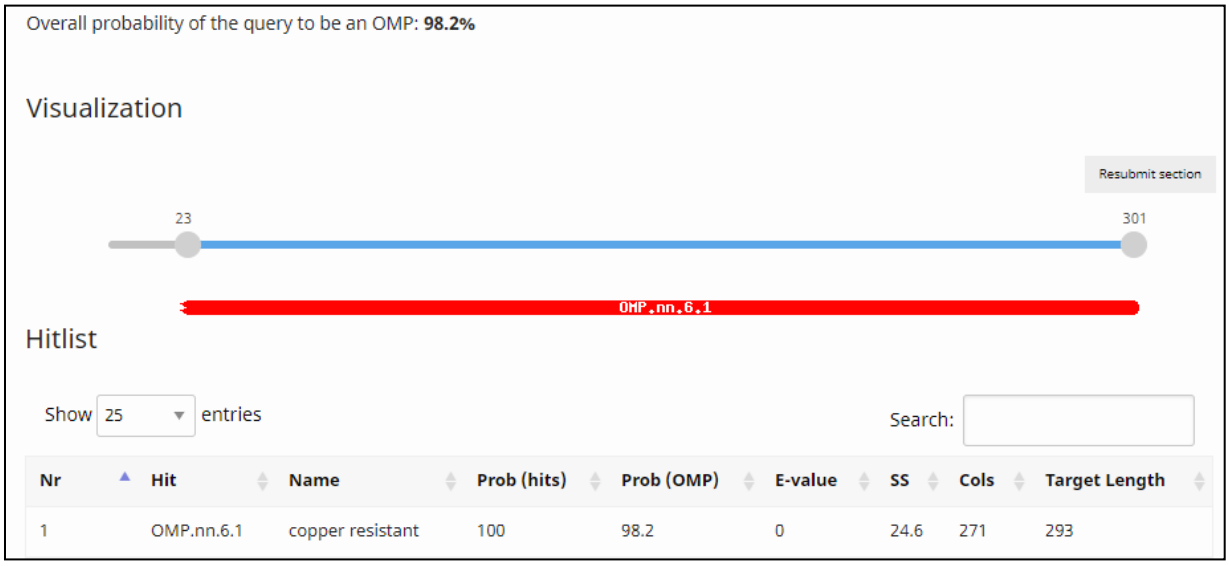

Fig. 20: HHomp prediction. HHomp screen for outer membrane features based on homologies found in various protein databases. The probability for the query sequence to be an OMP is summarized at the top of the image, with more details in the bottom line.

Three Cu oxidase domains are detected in PcoA, forming an expected multicopper oxidase complex (Fig. 17 C). Taken together, bioinformatics suggests that PcoA is very likely to be a functional MCO. Every domain and the signal peptide from the *E. coli* ortholog seem to be conserved, and the predicted secondary and tertiary structure are equally similar.

PcoB

ii'. Structure

Similar bioinformatic analyses were performed on PcoB, using the same parameters except for the query input corresponding to the CCNA_01016 AA sequence.

PcoB N-terminus seems to have no defined and only disordered secondary structure. From position 90 to 160, α-helices and β-strands interweave before a long sequence of low disorder displaying several β-sheets (Fig. 19 A). Although not completely clear (Fig. S2), there seems to be 12 β-strands. A succession of 12 β-strands can be indicative of a β-Barrel protein, like the NanC porin or TolC transporter in *E. coli* (Fairman et al. 2012). β-Barrels can be formed from 8 to 24 β strands (Fairman et al. 2012).

This β-barrel hypothesis is supported by the I-TASSER tertiary structure prediction, as the resulting PcoB 3D model seems to form a β-barrel-like channel (Fig. 19 B).

iii'. Domain prediction

No signal peptide could be detected via the TatP algorithm. Other signal prediction tools detected neither TAT nor SEC signal. If PcoB is indeed an OM protein as it was suggested for the *E. coli* ortholog, no obvious translocation motif can explain how PcoB is exported from the cytoplasm to the OM. However, a manual analysis reveals a potential poorly conserved SEC motif, characterized by AXA repeated patterns (positions 13-15, 20-22 and 34-36) and a high occurrence of hydrophobic AA in the PcoB N-terminus (Payne et al. 2012).

Alternatively, PcoB could be translocated through a "hitchhiking" system, as shown for several proteins, like the HybC / HybO tandem from *E. coli* (Rodrigue et al. 1999). In this context, the protein lacking the TAT signal is co-translocated with an interacting partner in a "piggyback-ride" fashion (Palmer & Berks 2012).

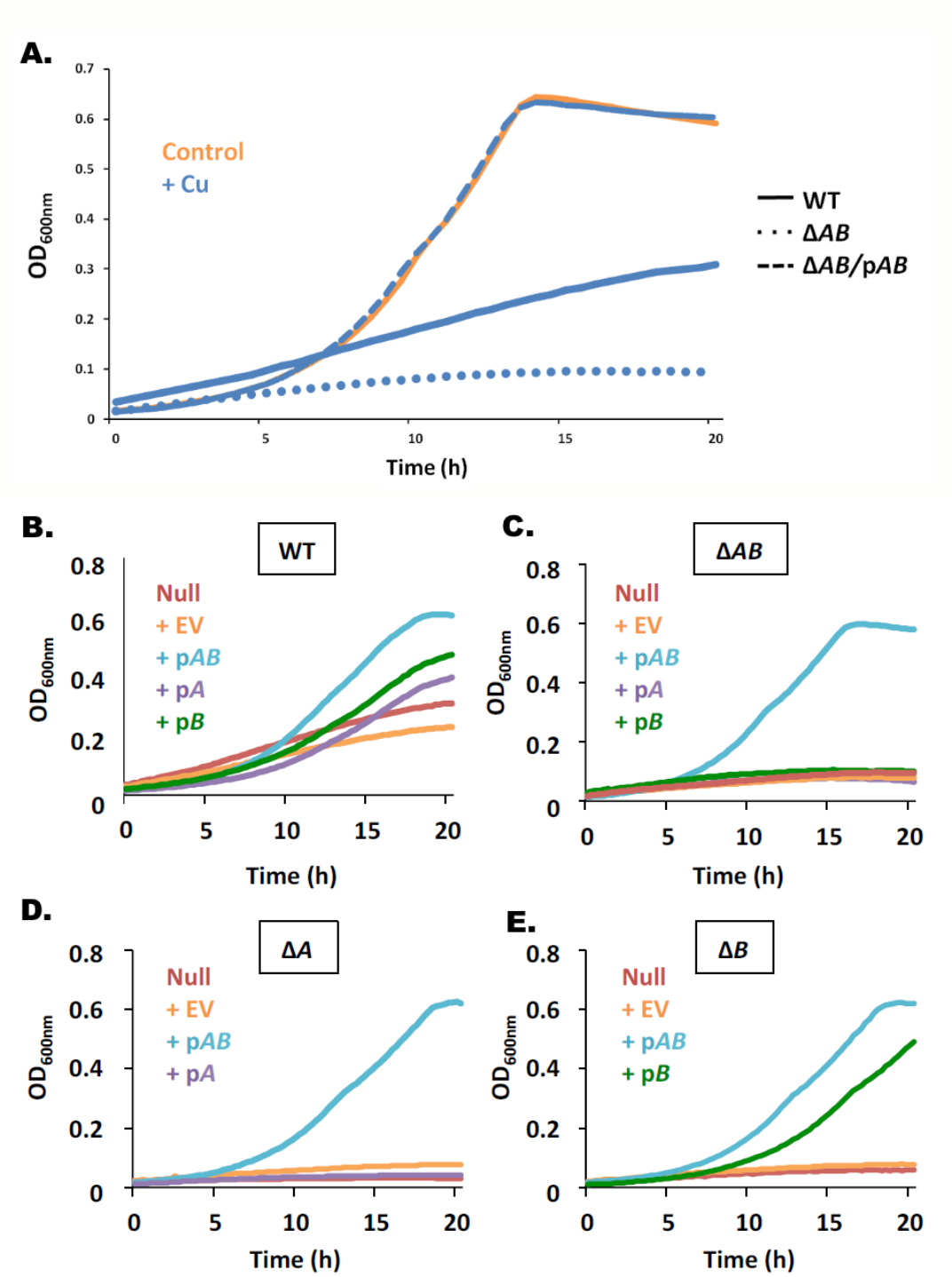

Fig. 21: Implication of PcoA and PcoB in Cu resistance. A. Phenotype of the WT, Δ*AB* and *ΔAB/pAB* strains in HIGG defined medium under control (orange) or 1,16 mM Cu stress (blue) conditions. **B, C, D and E.** Growth profiles of the *ΔAB*, Δ*A* and Δ*B* strains, respectively, transformed with the empty vector (EV), pAB, pA or pB, or not transformed (Null condition – no vector) under a 1.16 mM Cu stress in HIGG defined medium.

Using HMMER, a CopB domain was predicted in PcoB (Fig. 19 C). This Cu resistance system domain is also found in $PcoB_{Ec}$, comforting this idea of functional orthology between $PcoB_{Ec}$ and CCNA_01016.

Finally, HHomp, working on the same principle than HHMER, was used to assess the presence of any OM feature in PcoB. A hit was detected, and the probability the query sequence to be an OMP was evaluated at 98.2%, strongly supporting the putative OM localization of PcoB (Fig. 20).

b. Importance of the Pco system in Cu resistance

To assess the role of the Pco system in *C. crescentus* Cu resistance, several clean knock-out strains were engineered. A knock-out strain for the *pcoAB* operon was constructed (ΔAB strain), as well as single knock-out strains for *pcoA* (ΔA) and *pcoB* (ΔB). The genetic backgrounds were tested in presence of various Cu sources ($CuSO_4$, $CuCl_2$) and in different media (HIGG, PYE), allowing to determine for each medium a typical "stress condition" where the general fitness is negatively impacted. The ΔAB strain displays a higher sensitivity to Cu than the WT, suggesting that PcoA and PcoB are involved in Cu resistance as expected (Fig. 21 A). Interestingly, the single knock-out strains resulted in the same phenotype as the ΔAB background, strongly hinting that both PcoA and PcoB are working together, and both are required for the Pco system to be functional (figure Fig. 21 C, D, & E).

The complementation strain ΔAB/pAB restored the WT phenotype and even slightly potentiated Cu resistance (Fig. 21 A). This effect has been imputed to the overexpression of both PcoA and PcoB resulting from the choice of vector and the promoter. Indeed, the complementation strain carries the *pco* operon on a pMR10 replicative plasmid under the control of a strong pLac promoter. Because the pMR10 is likely to be present in more than one single copy and because the pLAC is probably stronger than the endogenous *pcoAB* promoter, the complementation strain likely contains more copies of the PcoAB proteins than the WT, resulting in a higher resistance to Cu.

The introduction of a valid functional copy of *pcoB* on a plasmid in the ΔB (ΔB/pB) strain also saved the phenotype (figure 18 E). However, a similar attempt for the pcoA knock-out (ΔA/pA) was infructuous in restoring the WT phenotype (Fig. 21 D), indicating that *pcoA* deletion has a polar effect on *pcoB*. This may not be surprising considering the operon organization and the overlap between the two genes.

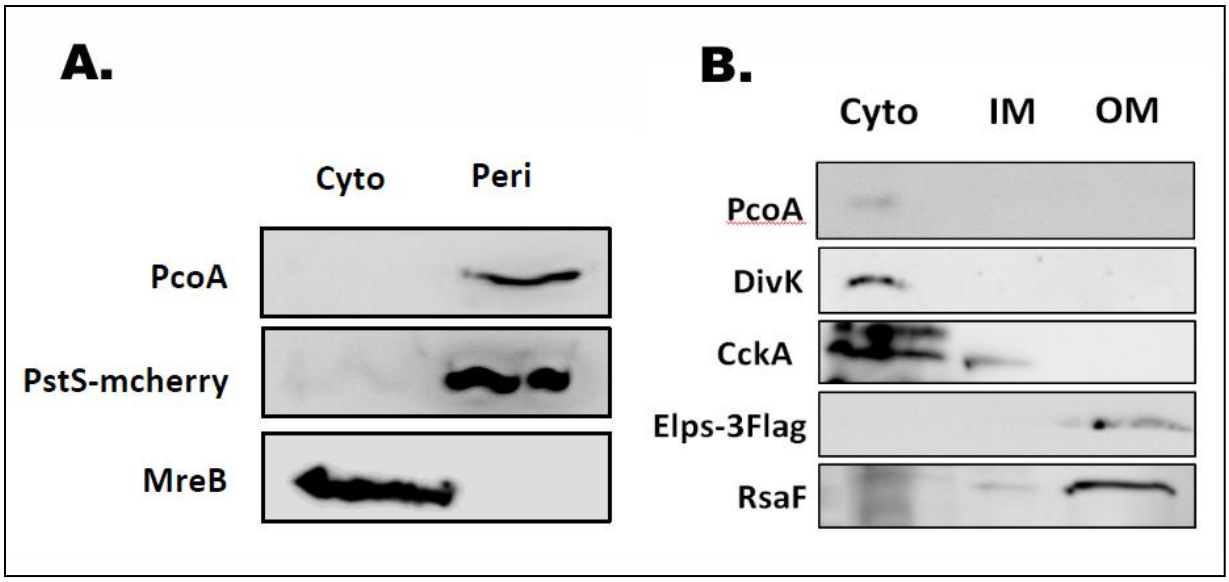

Fig. 22: **A.** Expression levels of PcoB in the cytoplasm (Cyto), and periplasm (Peri). MreB and PstS-mcherry were used as Cyto and Peri controls, respectively. **B.** Expression levels of PcoB in the cytoplasm inner membrane (IM) and outer membrane (OM). DivK, CckA and ElpS-3Flag and RsaF were the Cyto, IM and OM controls, respectively.

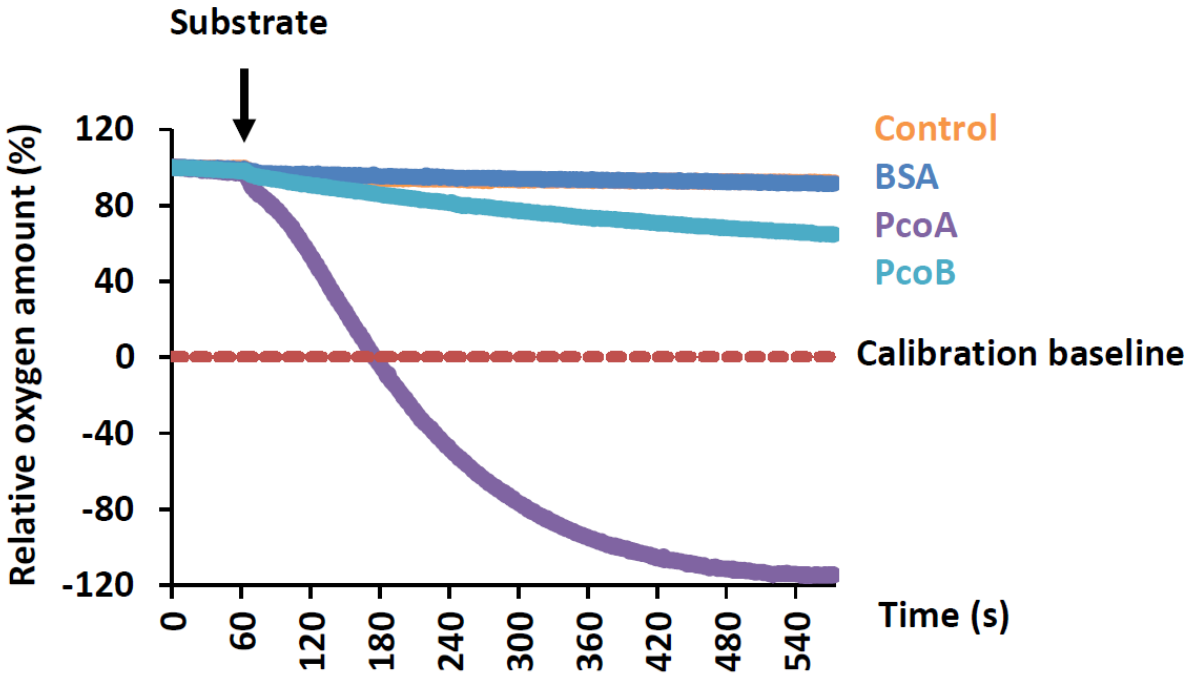

Fig. 23: Relative oxygen concentration (%) over time measured with a control buffer, purified BSA, purified PcoA and purified PcoB. The red dotted line represents the calibration baseline.

All together, these data tend to support the hypothetical model according to which PcoA is a periplasmic MCO oxidizing Cu^{+} into Cu^{2+}.

c. Biochemical characterization of PcoA: localization and function

While the previous experiments shed light on the importance of the Pco system under Cu stress, they did not address the biochemical mechanisms underlying Cu resistance provided by this system. Therefore, PcoA was characterized, based on the assumption that it works in a similar fashion as its *E. coli* ortholog.

i. PcoA is located in the periplasm

A fractionation assay, separating the periplasm from the cytoplasm, was performed. PcoA was immunodetected in the periplasmic fraction, consistent with its predicted role of periplasmic MCO. In this experiment, MreB was used as a cytoplasmic control, while the PstS-mCherry fusion serves as the periplasmic control (Fig. 22 A) (Schlimpert et al. 2013). However, in this assay, the periplamic fraction is not pure, and also contains the OM. To rule out the possibility of PcoA anchoring in the OM, an additional purification step isolating the OM and the IM was carried out. This experiment was negative for the immunodetection of PcoA, suggesting that PcoA is a soluble periplasmic protein. The Divk and CckA proteins were used as cytoplasmic and IM control, respectively, while both a ElpS-3flag fusion and RsaF were picked as OM controls (le Blastier et al. 2010; Lam et al. 2003; Yung et al. 2015).

ii. PcoA acts as a periplasmic MCO

Based on the similarities between $PcoA_{Ec}$ and its paralog $CueO_{Ec}$, we hypothesized that PcoA could be a MCO, and we decided to assess the capacity of the protein to oxidize Cu^{+} into Cu^{2+} . During Cu oxidation process, MCOs reduce O_2 in H_2O as a byproduct of the reaction. Recording the variation in O_2 concentration when purified PcoA is mixed with a Cu^{+} source would therefore provide a way to confirm or refute our hypothesis. This experiment was done via an oxygraph. The source used was Copper(I) tetrakis(acetonitrile) hexafluorophosphate ([Cu(CH3CN)4]PF6), a “caged” copper component that stabilizes the Cu core to prevent self-oxidation.

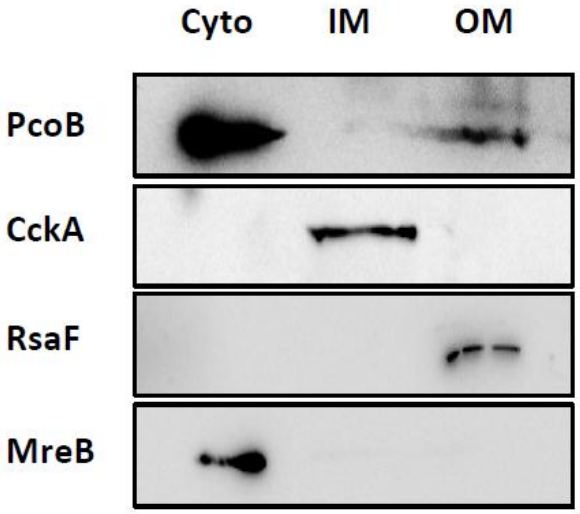

Fig. 24: Expression level of PcoB in the cytoplasm (Cyto), inner membrane (IM) and outer membrane (OM). MreB, CckA and RsaF were used as Cyto, inner membrane (IM) and outer membrane (OM) controls, respectively.

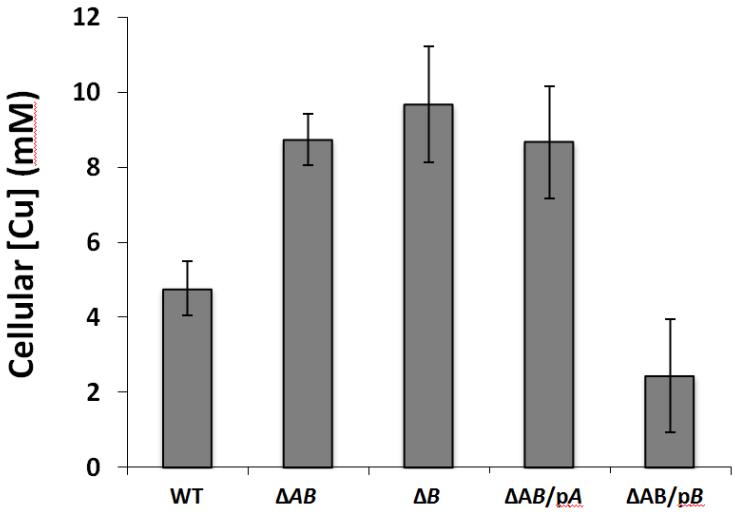

Fig. 25: Intracellular Cu concentrations in the WT, ΔAB, ΔB, ΔAB/pA and ΔAB/pB strains under a moderate Cu stress (5 minutes of 1.16 mM $CuSO_4$ in HIGG defined medium).

Purified PcoA-His is placed in an oxygraph chamber where an electrode monitors the O_2 content. At a defined time, the Cu-based substrate is injected in the chamber through a syringe. If PcoA is indeed a MCO, the O_2 concentration in the chamber will decrease. The condition with a control buffer and the condition with BSA did not react to the Cu substrate. However, the PcoA condition immediately showed a drastic decrease in O_2 concentration (Fig. 23). The PcoB condition displays a slow, albeit noticeable, O_2 decrease, possibly because the protein is interacting with Cu, destabilizing the substrate and favoring auto-oxidation.

d. Biochemical characterization of PcoB: localization and function

i. PcoB localizes in the OM of *C. crescentus*

Similarly to PcoA, a membrane fraction assay was performed. PcoB displays an OM localization, consistent with its putative role as an efflux pump (Fig. 24). CckA serves as IM control, while RsaF is used as an OM fraction control. MreB has been included as the cytoplasmic fraction control.

ii. PcoB acts as a Cu efflux pump

We sought to assess the ability of PcoB to export Cu outside the cell. By combining flow cytometry, which allows for cell counting, and Atomic Absorption Spectrometry (AAS), which can be used to measure the absolute Cu concentration in a sample, we were able to average the Cu concentration per cell (Lawarée et al. 2016). This experiment was performed in several genetic backgrounds by Emeline Lawarée in the context of her own PhD thesis. The ΔAB mutant seems to accumulate twice as much intracellular Cu as the WT strain (Fig. 25), potentially explaining the growth defect observed with that strain when placed in contact with a moderate amount Cu (Fig. 21 A). Interestingly, the internal Cu concentration for both the ΔB and the ΔAB/pA strains are on the same range than the double knock-out (Fig. 25). This would indicate that in absence of PcoB, the cell either accumulates Cu at a faster rate, or is unable to export it out of the cell. This is further supported by the result of the ΔAB/pB background, mimicking a ΔA mutant, where the expression of PcoB on a plasmid is restoring the WT phenotype. The slight overexpression of PcoB actually makes the intracellular Cu concentration drop even lower than the wild type strain, strongly suggesting an efflux pump role for PcoB.

Table 2: Result of the Cus homolog research with *E. coli* proteins as query sequence against *C. crescentus* proteome

E. coli protein	Homolog in *C. crescentus*	E value	Score	Query cover	Identity
CusA	CCNA_02473	0	601	99%	35%
	CCNA_02809	1E-174	541	99%	33%
	CCNA_03301	7E-69	246	99%	20%
	CCNA_03219	4E-51	192	46%	25%
	CCNA_00850	1E-50	191	98%	23%
	...	...	...	...	...
CusB	CCNA_01261	2.00E-08	52.4	83%	26%
	CCNA_02472	2.00E-05	43.1	94%	26%
	CCNA_03218	6.00E-05	41.6	82%	24%
CusC	CCNA_00849	1E-96	300	98%	37%
	CCNA_01863	4E-31	121	99%	27%
	CCNA_03299	6E-18	83.2	99%	25%
	CCNA_02471	1.7	27.7	23%	37%

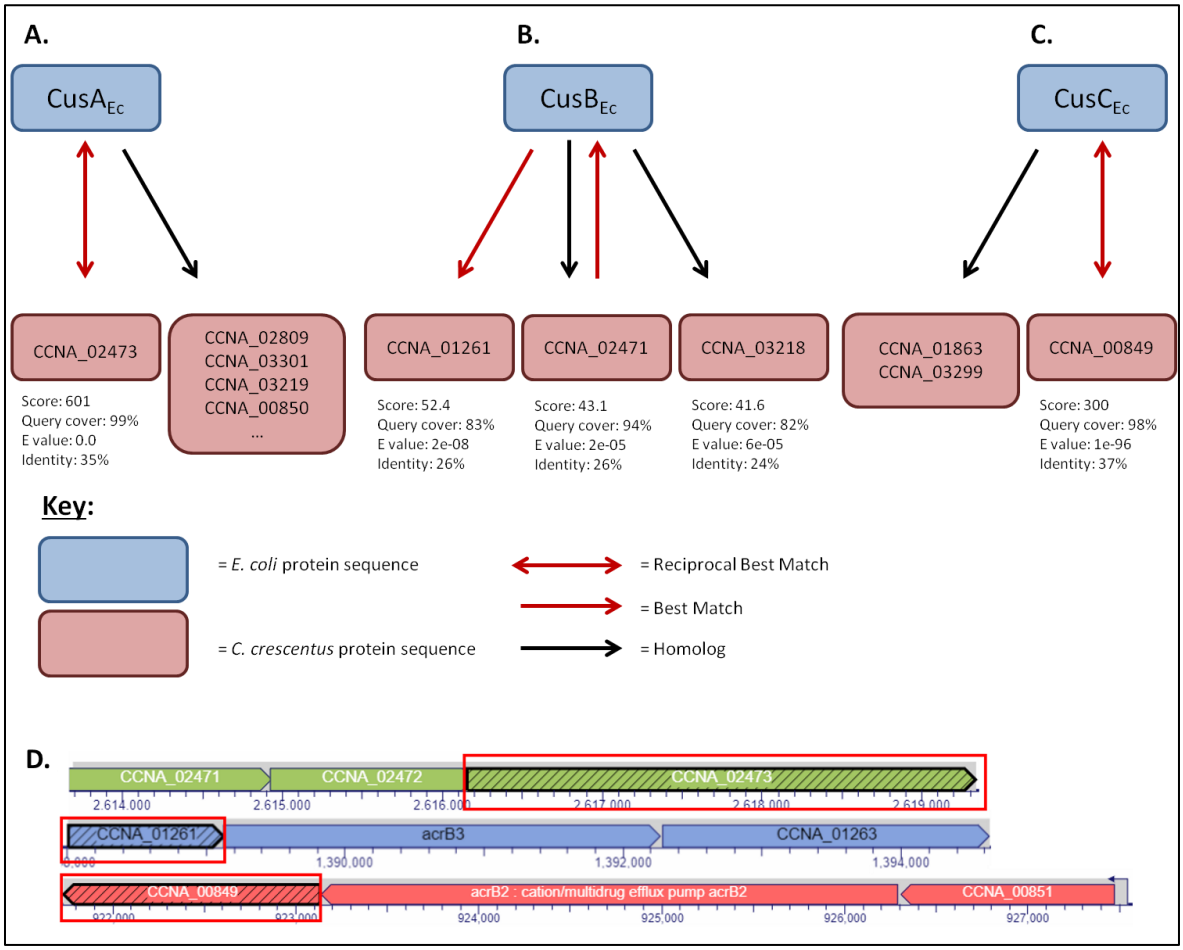

Fig. 26: Conservation of the *E. coli* CusABC system in *C. crescentus*. Red double-headed arrows indicate a reciprocal best match. Red one-way arrow indicate the best ortholog candidate. One-way black arrows indicate simple orthology. A. Results with CusA$_{Ec}$ as query sequence B. Results with CusB$_{Ec}$ as query sequence C. Results with CusC$_{Ec}$ as query sequence. D. Operon and gene neighborhoods of the best matches. Red frames indicate the genes selected for the knockouts.

However, one should remember that this strain does not grow well in presence of Cu stress (Fig. 26 C). This likely indicate that both PcoA and PcoB are equally important. PcoA thus seems crucial to detoxify the Cu present in the periplasm, even though PcoB would be actively exporting Cu in the extracellular environment.

2. The involvement of *C. crescentus* Cus System in Cu resistance is unclear

a. Bioinformatics – establishing a hypothetical model

i. Homologs research from *E. coli* sequences

The search for orthologs of the *E. coli* Cus system has been more complicated than expected. The *E. coli* Cus system is a complex belonging to the HME-RND family, which is widespread in bacterial species. There is often multiple (HME-)RND operons scattered over the genome, each one coding for an export complex with its cognate substrate (antibiotics, metals, …). Because of their similarities, any homology search is likely to give several matches, regardless the actual substrate specificity.

$CusA_{Ec}$, $CusB_{Ec}$ and $CusC_{Ec}$ AA sequences were used as query, and "blasted" against the *C. crescentus* proteome. $CusA_{Ec}$ blast search resulted in several good matches (Table 2), although the first homolog listed (CCNA_02473) is undeniably the best candidate with a 0.00 E value and a Reciprocal Best Match (Fig. 26 A). The gene coding for CCNA_02473 works in operon with the *CCNA_02471* & *CCNA_02472* genes predicted to encode a Co-Zn-Cd resistance system.

The orthologs search for $CusB_{Ec}$ returned three potential candidates. CCNA_01261 is the best result, but not a reciprocal best match (Fig. 26 B). However, the second best match is CCNA_02472, encoded by a gene neighboring the *CCNA_02473* gene, which is the best candidate for *cusA*. In addition, blasting CCNA_02472 against the *E. coli* proteome returns $CusB_{Ec}$ as the best match. It is worth noting that E values for these candidates are close to the threshold, and the bit scores are around 10 times lower than for the $CusA_{Ec}$ orthologs search.

The $CusC_{Ec}$ orthologs search returned three hits. The best candidate is CCNA_00849. It stands above the other two in terms of score and E value and is a reciprocal best match (Fig. 26 C). Surprisingly, the best match is thus not CCNA_02471 as we could have expected (considering CCNA_02472 and CCNA_02473 were good matches for $CusB_{Ec}$ and $CusA_{Ec}$, respectively).

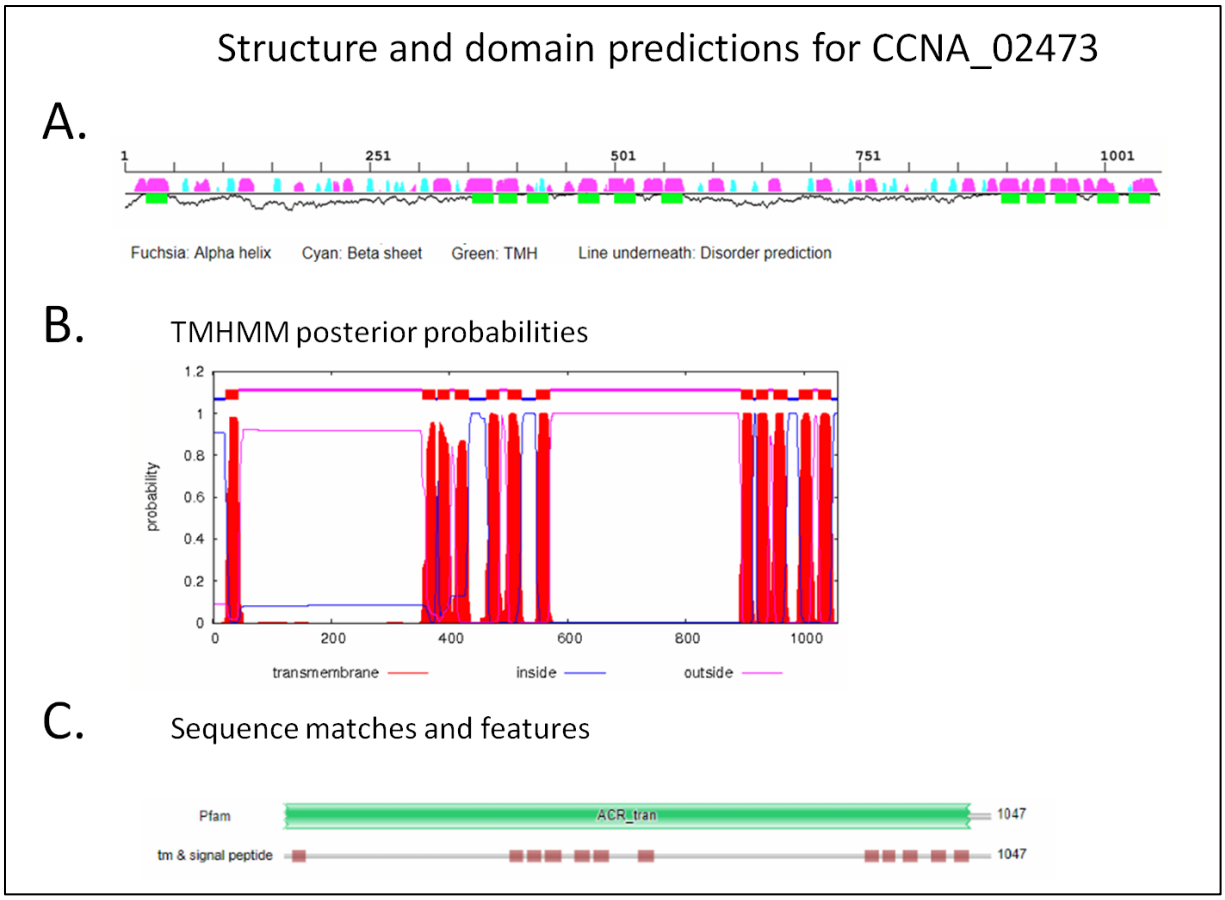

Fig. 27: Structure and domain prediction for CCNA_02473 (CusA). **A.** Result of the Foundation analysis. Secondary structure are represented along with their sequence position on the horizontal axis. α-helices are represented in fushia and B-strands in cyan. The wiggly line in beneath the secondary structure represents disorder. The further away from the horizontal axis, the more the disorder. **B** TMHMM results, prediction transmembrane domain and helices. **C.** Results of the HMMER domain prediction.

In fact, CCNA_02471 is even filtered out by the selected E value threshold and is only found after removing the threshold constraint (Table 2).

These data suggest that several similar protein complexes co-exist in *C. crescentus*, each encoded by a different operon. However, no operon clearly stands out as the best homolog of the *cusABC*$_{Ec}$ one. The best match for each of the proteins were further examined through bioinformatics predictions.

ii. Structures & Domains

CusA

CCNA_02473 was chosen as the CusA ortholog in *C. crescentus*. The CCNA_02473 protein sequence possesses numerous α-helices and β-strands (Fig. 27 A) as well as twelve transmembrane helices (TMH), as predicted by TMHMM 2.0 (Fig. 27 B). An ACR-like domain was also predicted (Fig. 27 C). ARC domains are derived from the AcrB/ArcD/ArcF protein family, whose members are known to be membrane proteins, involved in the export of a broad range of substrates. These predictions are perfectly in line with what is known for CusA$_{Ec}$, which is also predicted to have 12 TMH and an ACR domain.

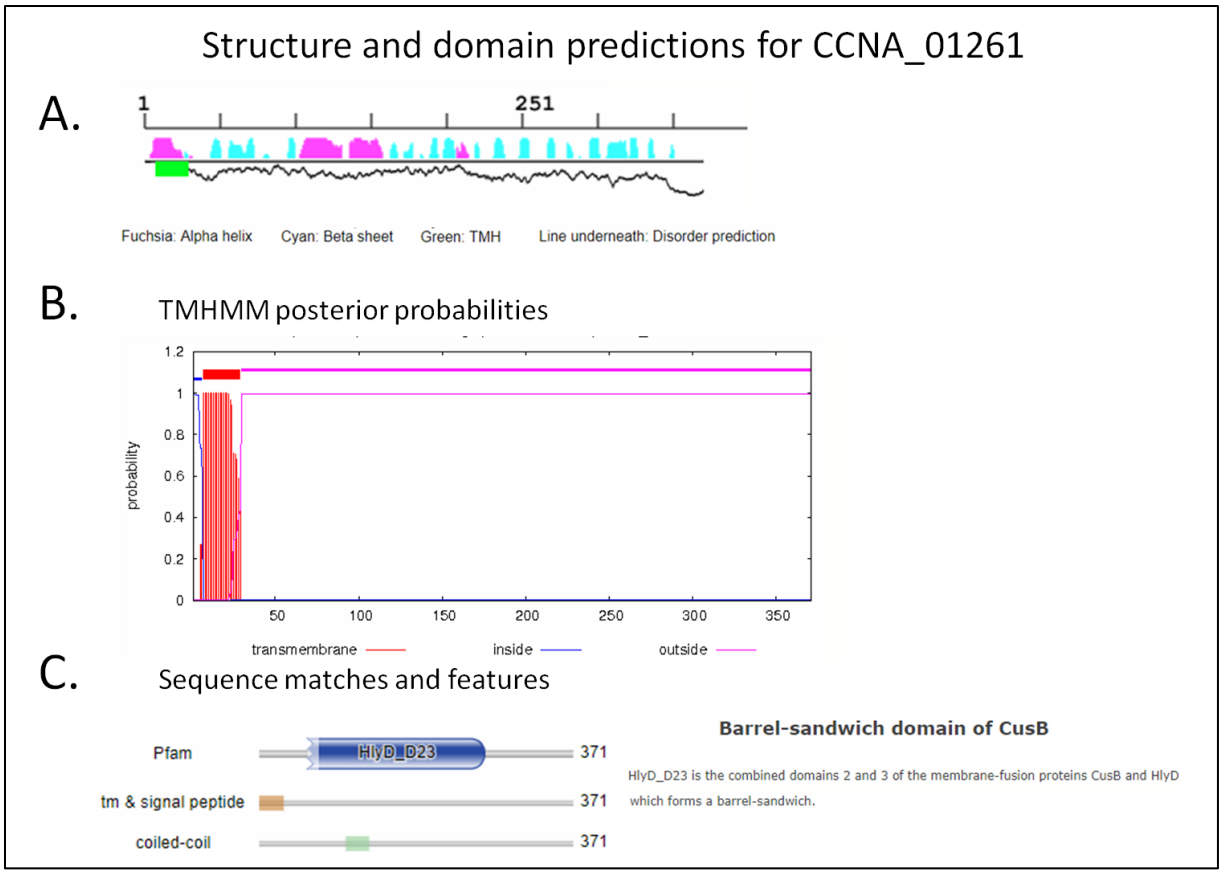

Fig. 28: Structure and domain prediction for CCNA_01261 (CusB). **A.** Result of the Foundation analysis. Secondary structure are represented along with their sequence position on the horizontal axis. A-helices are represented in fushia and β-strands in cyan. The wiggly line in beneath the secondary structure represents disorder. The further away from the horizontal axis, the more the disorder. **B** TMHMM results, prediction transmembrane domain and helices. **C.** Results of the HMMER domain prediction.

CusB

CCNA_01261 was chosen as the CusB candidate. The protein seems to be mostly composed of β-strands, with a few clusters of α-helices in the first half of the sequence (Fig. 28 A). A TMH domain is predicted in the N-terminus region (Fig. 28 B). A HlyD domain is predicted, which corresponds to the barrel-sandwich domain of CusB (Fig. 28 C). These predictions support the hypothesis that CCNA_01261 could indeed be a functional homolog of $CusB_{Ec}$.

CusC

CCNA_00849 is predicted as a $CusC_{Ec}$ homolog. The secondary structure of the protein seems mostly composed of α-helices but very few β-strands (Fig. 29 A) No transmembrane region was predicted (Fig. 29 B), which is similar to the $CusC_{Ec}$ predictions. Two outer membrane efflux protein domains are predicted (Fig. 29 C). These data suggest a role of CCNA_00849 as an outer membrane protein, and reinforces the hypothesis of a functional homology between CCNA_00849 and $CusC_{Ec}$.

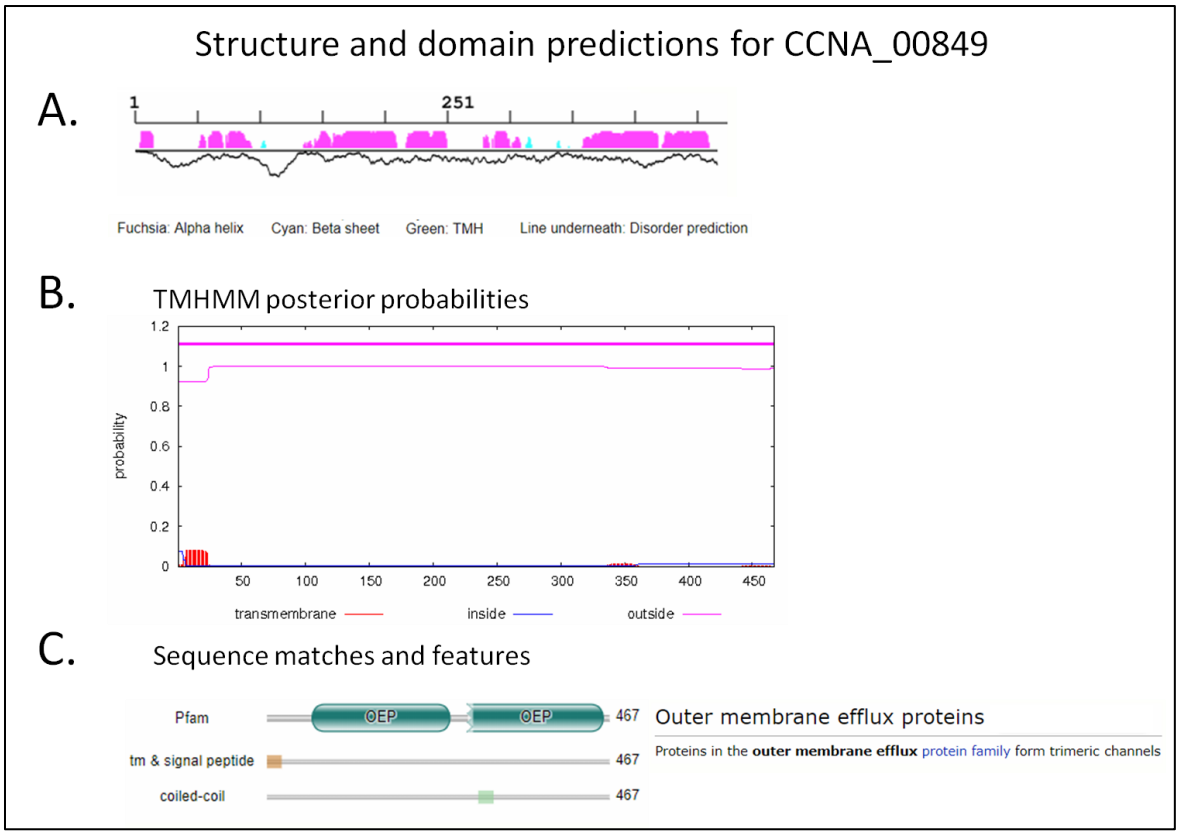

Fig. 29: Structure and domain prediction for CCNA_00849 (CusC). A. Result of the Foundation analysis. Secondary structure are represented along with their sequence position on the horizontal axis. A-helices are represented in fushia and β-strands in cyan. The wiggly line in beneath the secondary structure represents disorder. The further away from the horizontal axis, the more the disorder. **B** TMHMM results, prediction transmembrane domain and helices. **C.** Results of the HMMER domain prediction.

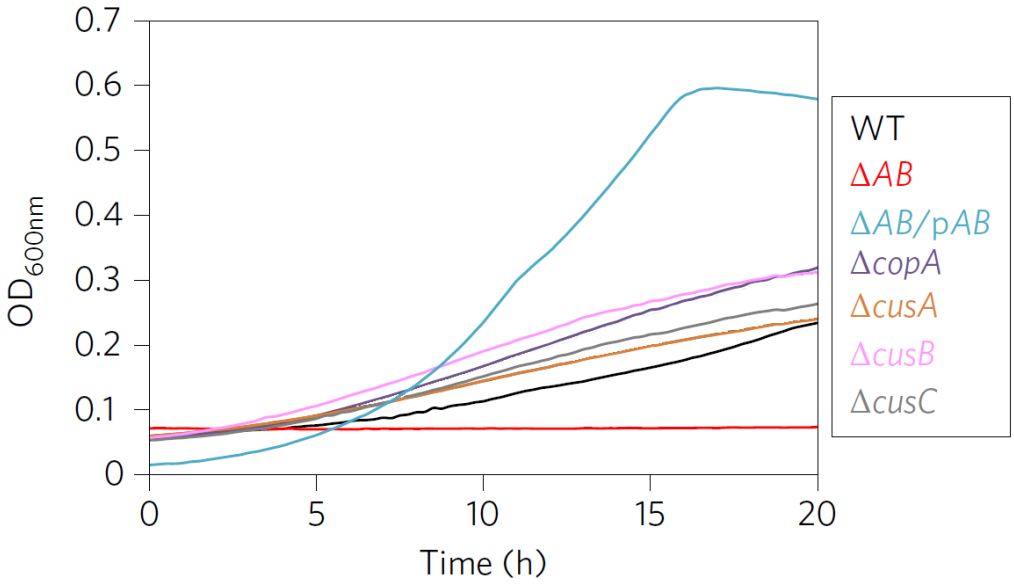

Fig. 30: Growth profiles of WT, *ΔAB*, *ΔcopA*, *ΔcusA*, *ΔcusB*, *ΔcusC* and *ΔAB/pAB* strains subjected to a moderate Cu stress (1.16 mM $CuSO_4$ in HIGG medium) (mean, relative standard deviation between 0.0087 and 0.1413, biological replicates = 3, technical replicates = 2) (Lawarée et al. 2016)

b. Impact of the Cus System on Cu resistance of *C. crescentus*

To evaluate the importance of the Cus system in *C. crescentus* resistance to Cu, *cusA*, *cusB* and *cusC* disruption mutants were obtained in the context of Emeline Lawaree's thesis by inserting a mini-transposon in the middle of each respective gene sequence (Fig. 26 D). Growth curves measurements under a moderate Cu stress condition were performed (Lawarée et al. 2016). Surprisingly, none of the three single mutants were more sensitive to the Cu stress than the WT strain (Fig. 30).

These results suggest that the CusABC system is not crucial for *C. crescentus* to handle Cu stress under these conditions, and that it is less preeminent than the Pco system. This observation contrasts with what is known in *E. coli*, where Cue and Cus are considered as the first lines of defense and the Pco system acts when the formers are overwhelmed (Outten et al. 2001; Rensing & Grass 2003).

A genetic screen performed in the lab support these results. A mini-Tn5 transposon has been employed to generate, by conjugation, a library of mutants. The mutants are plated both on a Cu-containing medium and a control medium and screened for Cu sensitivity. Sensitive mutants are then sequenced from the transposon to identify the transposon insertion site and therefore a candidate gene potentially involved in Cu resistance or homeostasis. Despite over 45,000 clones screened (theoretically close to the statistical saturation), none of the Cus orthologs candidate genes were recovered in the screen. This suggests that, if the mini-Tn5 was inserted in their sequence, it did not generate a mutant more sensitive to a moderate Cu stress. However, the genetic screen highlighted the implication of the *CCNA_00851* gene located in the same operon as our *cusC* candidate (*CCNA_00849*, part of a three genes operon) (Fig. S3). It may indicate that, while the operon could be involved in Cu resistance, CusC function could be redundant. In this case, a single knockout would fail to highlight this effect, as no Cu sensitive phenotype would emerge.

In the context of protein characterization, qPCR experiments have been conducted and the transcription of several genes in the presence and absence of a moderate Cu stress has been monitored. Inducibility upon Cu sensing could argue in favor of a role in Cu resistance. The transcription of *cusA*, *cusB*, *cusC*, *cusR* and *cusS* has been monitored, as well as the 16S control. A first sample of a WT culture of *C. crescentus* was collected before Cu stress (T0). Then, the culture was mixed with 1.16 mM of $CuSO_4$ (HIGG medium, equivalent to a 175 µM condition in PYE) and samples were collected after 15 minutes (T15), 30 minutes (T30) and 60 minutes (T60). Samples were treated according to the established protocol.

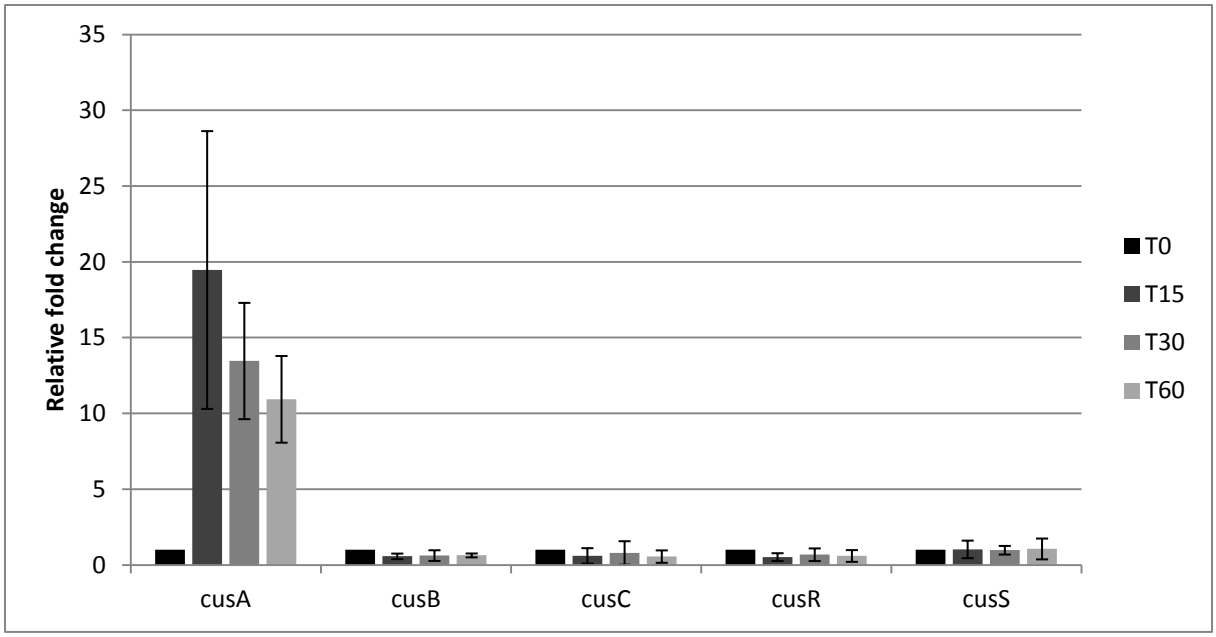

Fig. 31: qPCR performed on *cusA*, *cusB*, *cusC*, *cusR* and *cusS*. Results expressed in relative fold changes compared to the T0 control condition and calculated as $2^{-\Delta\Delta Ct}$. (biological replicates = 3, technical replicates ≥ 6). P value for CusA T15, T30 T60 = 0.0731; 0.0302; and 0.0265, respectively. The 16sRNA was used as control.

The cells were lysed, the RNA was extracted and treated with DNAse. The purified RNA was subsequently reverse-transcribed and the resulting cDNA was subjected to qPCR. Target mRNA levels were compared to the T0 control condition without $CuSO_4$. mRNA fold changes between conditions were calculated following the ΔΔCt method.

Surprisingly, *cusA* seems to be strongly induced by the $CuSO_4$, while the expression of the other *cus* genes does not show any significant difference compared to the T0 control (no matter the time condition) (Fig. 31).While the T15 19-fold increase is not statistically significant ($p = 0.0731$; likely due to the high standard deviations measured), the 13-fold T30 increase and 11-fold T60 increase are ($p = 0.0302$ and 0.0265, respectively). This suggests a rapid induction of the *cusA* gene. This induction might result in a massive increase of the CusA protein level in the cell, possibly helping the bacterium to fight a Cu stress.

3. Evolution and Phylogeny of Cu Resistance system

The results described above highlight the role of the Pco and Cus system in Cu resistance. It points out that Cu resistance systems that have been demonstrated as crucial in one species may not be as important in another species (e.g., the Cus system in *E. coli* and *C. crescentus*). Therefore, the conservation of such systems may be driven by natural selection and environemental pressure. In this context, we chose to investigate the evolution and phylogeny of the Pco and Cus system in the alphaproteobacteria class.

a. Alphaproteobacteria are formidable in their diversity.

The Alphaproteobacteria bacterial class belongs to the proteobacteria phylum. Alphaproteobacteria harbor an astonishing diversity of lifestyles, comprising pathogenic bacteria, symbionts, commensal bacteria, or free-living organisms (Pini et al. 2011; Curtis & Brun 2014). They live in a broad range of environments, from soil to fresh and sea water, and from plant roots to mammals (Pini et al. 2011).

Several studies drew attention to a possible link between the conservation of specific subsets of genes by a bacterium and its lifestyle, or the environment in which it lives. In the alphaproteobacteria, it was found that plant-associated bacteria (would it be by symbiosis or free-living association) tend to

have larger genomes, and are likely to share a particular common set of genes, despite sometimes a rather large phylogenic distance (Pini et al. 2011). In Enterobacteria, belonging to the Gammaproteobacteria class, the “Copper Homeostasis And Silver Resistance Island” (CHASRI) is suggested to have spread across species in response to increased metal stress in the environment (Staehlin et al. 2016). The actinobacterium *Frankia* has been reported to accumulate more metal resistance systems to increase its chances to enter the roots of plants growing on contaminated soils (Furnholm & Tisa 2014). In addition, murine macrophages have been demonstrated to accumulate Cu when infected with *Salmonella enterica.* Conversely, *S. enterica* fights this stress by expressing the MCO CueO (Achard et al. 2012). This reinforces the natural idea that the constraint introduced by the environment or lifestyle could drive the conservation and spread of specific sets of genes.

For this reason, we analyzed the conservation of the Pco and Cus system in the alphaproteobacteria and tried to determine whether there was a correlation between the conservation of Cu resistance systems and bacterial lifestyle or environments, as well as the mobility of bacteria. These criteria were chosen as they fit with several examples of ecological pressure described in the literature. Both the lifestyle and environment will modulate the frequency at which you may face a metal stress. Motility was taken into account owing to the fact it may influence the conservation of metal resistance systems, too. It was demonstrated in *C. crescentus* that the SW cells, motile, were not expressing the PcoAB system, while the ST and PD cells, sessile (and therefore unable to flee a Cu stress), were expressing it (Lawarée et al. 2016).

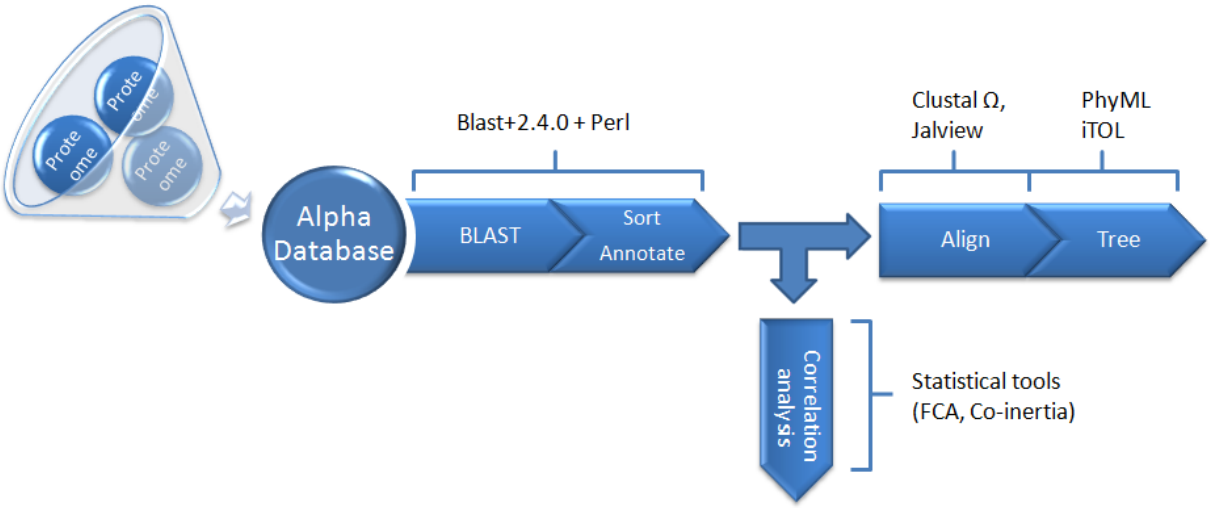

Fig. 32: Schematic representation of the workflow. The small circle indicates the proteomes of the different species, assemble into a single big database. The arrow represent the different step of the workflow, with the different tools or plateforms used.

b. Conservation of Pco and Cus system in the Alphaproteobacteria

i. General conservation across the alphaproteobacteria - The Pco system does not seem as well conserved as the Cus system

To achieve this *in silico* analysis, a semi-automated pipeline was established. The general idea of the workflow was to (i) search orthologs of the proteins of interest in the proteomes of the alphaproteobacteria, (ii) extract the name of the species that conserved at least one homologous protein, determine whether the homologs are carried on a plasmid or on the chromosome, and annotate its lifestyle, environment and motility, (iii) analyse the correlation between the conservation and the different annotations (iii') perform an alignment of the AA sequence of the proteins, and build a phylogenetic tree (Fig. 32). This workflow would therefore try to trace the evolution of the Pco/Cus system and correlate the presence or absence of homologs with bacterial lifestyle, environment or motility.

The NCBI Entrez E-Utilities suite was used to assemble and download the database needed for the initial blast search. NCBI provides freely accessible data that can be retrieved from their servers. The proteome of all referenced alphaproteobacteria was fetched. Proteomes belonging to undefined species or strains were filtered out.

The resulting database contained more than 5 million protein sequences, belonging to 1274 species or strains. However, as one of the goals was to assess the conservation rate of the various proteins of interest, it was necessary to curate this database to remove as much artificial bias as possible. The most characterized genus naturally tend to have a higher number of sequenced strains, and many different well studies species. This overrepresentation could tip the balance and artificially inflate the conservation rate of the proteins for which these genus have homolog for. Therefore, synonymous entries were first removed (e.g., *C. crescentus* and *C. vibrioides*), and we limited the number of species to one per genus. This restricted database comprises 206 genus/species entries.

It served as the basis for ortholog search through the BLAST+2.4.0 package. The $PcoA_{Ec}$, $PcoB_{Ec}$, $PcoC_{Ec}$, $PcoD_{Ec}$, $PcoE_{Ec}$, $CusA_{Ec}$, $CusB_{Ec}$ and $CusC_{Ec}$ AA sequences were used as a query. PcoR and PcoS were excluded from the search, as they were likely to have many homologs unrelated to Cu resistance owing to their widespread structure. Each search generated a file containing the AA sequences of all the potential orthologs in FASTA format. The accession numbers of the proteins were extracted by a custom PERL script, and were automatically compared with a database containing all the proteins annotated as having a plasmidic origin.

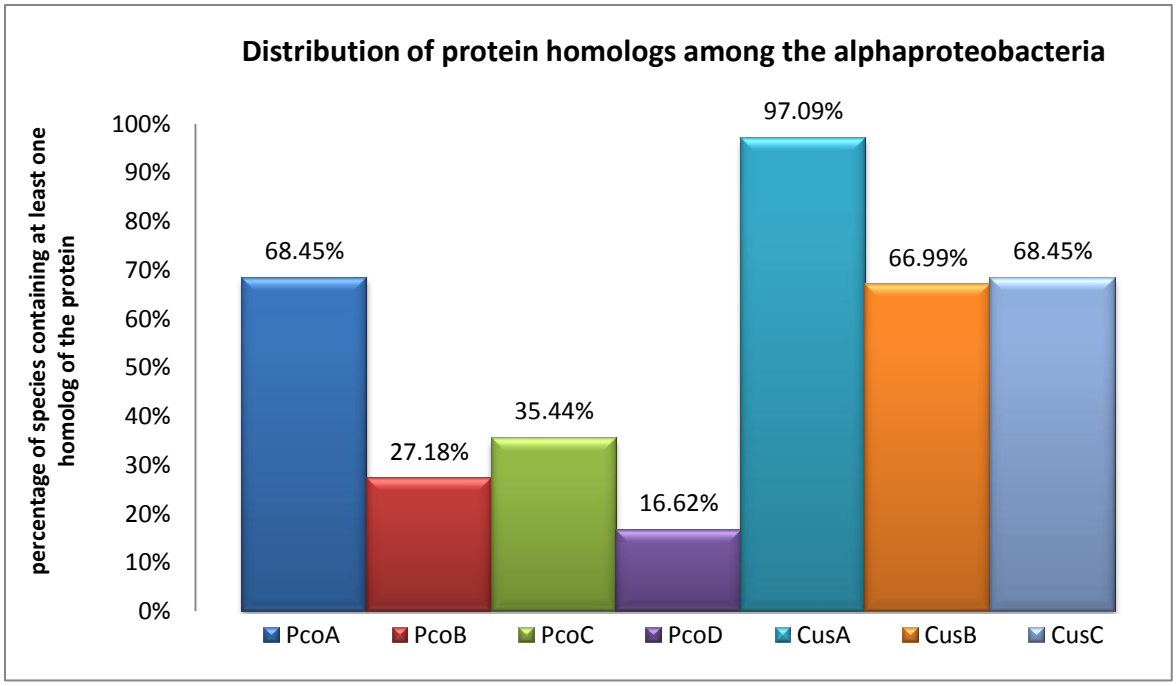

Fig. 33: Conservation of the Pco and Cus proteins in the alphaproteobacteria. The Pco_{Ec} and Cus_{EC} AA sequence were used as a query for the BLAST ortholog search. Percentages indicate what proportion of the 206 species presents in the curated database possess at least one homolog for the protein of interest.

This permitted the classification of the homologs according to their origin, chromosomal or plasmidic. Additionally, the blast results were sorted to exclude candidates that did not meet certain criteria (e.g., e value threshold or AA length threshold). The names of the different species were extracted. For comparison purpose, the same search was conducted on the non-curated database of 1274 species.

A second database was then established manually. For each of the 206 species comprised in the curated database, information about its lifestyle, the environment from which it has been isolated, and its motility were annotated.

Among these 206 species, it appears that the conservation of the different proteins presents important variations. The Cus system seems overall relatively well conserved. 97% of the species contained in the database possess at least one homolog to CusA (Fig. 33). CusB and CusC seem slightly less conserved, with respectively 67% and 68% of conservation (Fig. 33). The close conservation rates between CusB and CusC may suggest that both work together as it is the case in *E. coli*, while the higher conservation level of CusA might indicate that CusA alone could be of use for some species.

The conservation of the Pco system is less homogenous. PcoA is the most conserved, with around 68% of the 206 selected species possessing at least one PcoA homolog (Fig. 33). It is worth noting that, because CueO is a paralog of PcoA, we had to rule out false positives. Species that did possess a PcoA homolog that was also found as a CueO homolog were investigated more thoroughly and counted as negative if the homology score for CueO was higher than for PcoA. PcoB is apparently less conserved, with only 27% of conservation across the 206 alphaproteobacterial species (Fig. 33). This is somewhat surprising considering its crucial role in *C. crescentus*, where a Δ*pcoB* mutant is as sensitive to Cu stress as the Δ*pcoAB* mutant, hinting toward an important role for both the PcoA and PcoB proteins. PcoC displays a 35% conservation rate, while PcoD seems to be present in only 16% of the selected strains.

$PcoE_{Ec}$ is the only one for which no homolog was not found at all in the alphaproteobacteria class, at least with our parameters. PcoE is found neither in the 206 selected species nor in the 1274 complete database. Outside of the additional PcoRS tandem, this would make the Pco system a 4-protein system in the alphaproteobacteria.

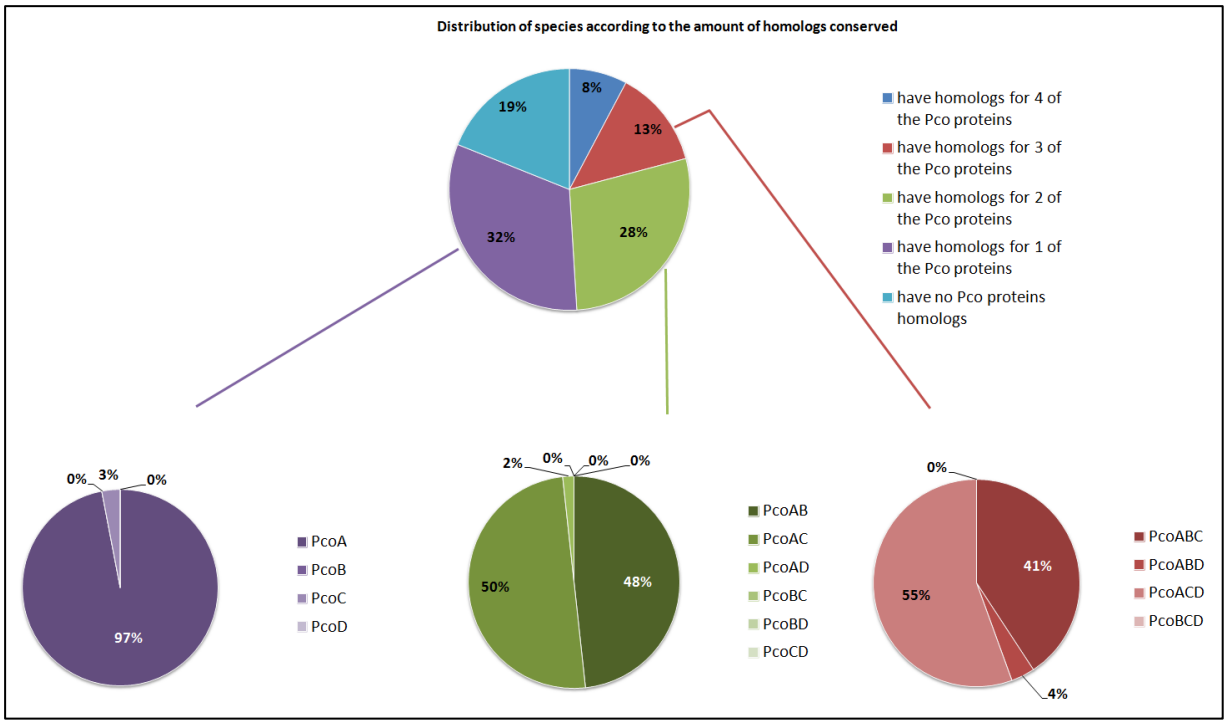

Fig. 34: Distribution of species according to the amount of Pco homologs conserved. The 206 species are categorized according to their conservation of the Pco proteins and the different possible conservation combinations.

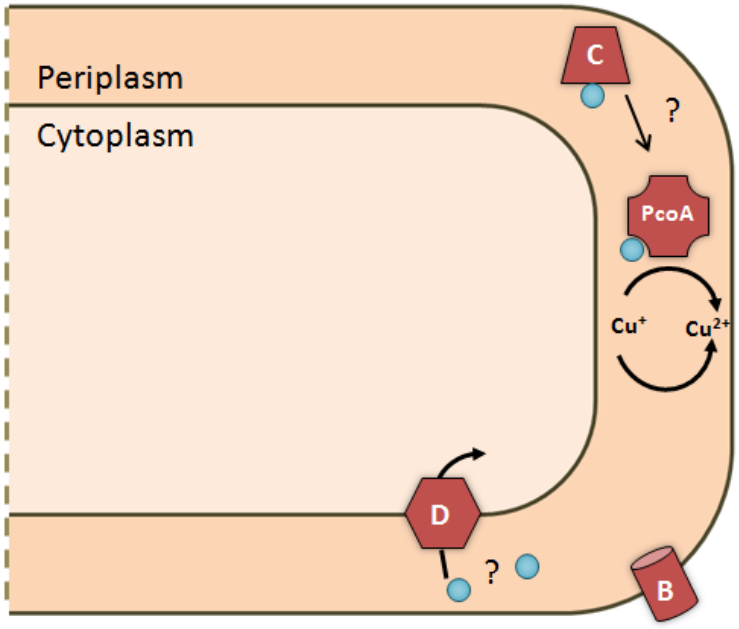

Fig. 35: Reminder of the predicted function for PcoA, PcoB, PcoC and PcoD. PcoA is a periplasmic MCO that detoxifies the periplasm by oxidizing Cu^{+} into Cu^{2+}. PcoB is predicted to be an export system in the OM, driving Cu outside the cell. PcoC is thought to be a Cu-binding protein that delivers Cu cations to either PcoA or PcoD. PcoD is predicted to be a Cu importer in the IM.

It is worth mentioning that, aside for PcoC, these results do not differ much from the conservation rate obtained when the search is performed on the total database containing the 1274 species/strains (65%; 23%; 21% and 13% for PcoA, PcoB, PcoC, and PcoD, respectively).

ii. Interdependency – PcoA and CusA may be able to work without their comrades-in-arm.

Following these observations, we sought to assess the interdependency of the proteins. If PcoA orthologs can be found alone in some species, without orthologs for the other Pco proteins, is the reverse also true? Can PcoB, PcoC or PcoD be found without PcoA?

The conservation data were therefore further analyzed. Among the alphaproteobacteria, we quantified the segregation of the genes to determine whether some particular subsets were more conserved than others. Only 8% of the 206 species possess homologs for the 4 proteins of the Pco system (PcoABCD, as PcoE is notably absent of all the alphaprotebacteria tested) (Fig. 34). 13% percent conserved 3 of the 4 proteins. Among these 13%, 41% of them possess the PcoABC combination, 55% the PcoACB combination, and only 4% the PcoABD arrangement. The PcoBCD subset was not found (Fig. 34). This seems to underline the importance of PcoA for the system. While several combinations were possible, all of the ones that were found contained PcoA. Subsets without PcoA do not seem advantageous for the cells, as it does not appear to exist or at least was not conserved enough to be detected by the ortholog search.

28% of the 206 selected species have been found to hold homologs for 2 of the 4 Pco proteins. Among them, 48% contain PcoAB, akin to *C. crescentus*. 50% conserved PcoAC, and only 2% were found to possess PcoAD. The remaining three combinations (PcoBC, PcoBD, and PcoCD) were not present in the results (Fig. 34). This once again seems to stress the importance of PcoA.

In 32% percent of the 206 species, only one of the four proteins could be detected. In those cases, PcoA is without surprise overwhelmingly present, with a 97% conservation rate among this category. 3% seems to have conserved PcoC only, without the three other actors (Fig. 34).

The very variable level of conservation may make sense, as the prediction function for these Pco proteins could suggest relative independence between PcoA, PcoB, and PcoD (Fig. 35). The PcoC protein, however, is thought to either interact with PcoA or PcoD. Based on our result, the PcoA interaction seems more likely, as there are very few cases where a PcoC homolog is found without PcoA, while plenty of species seems to possess a PcoC homolog without PcoD.

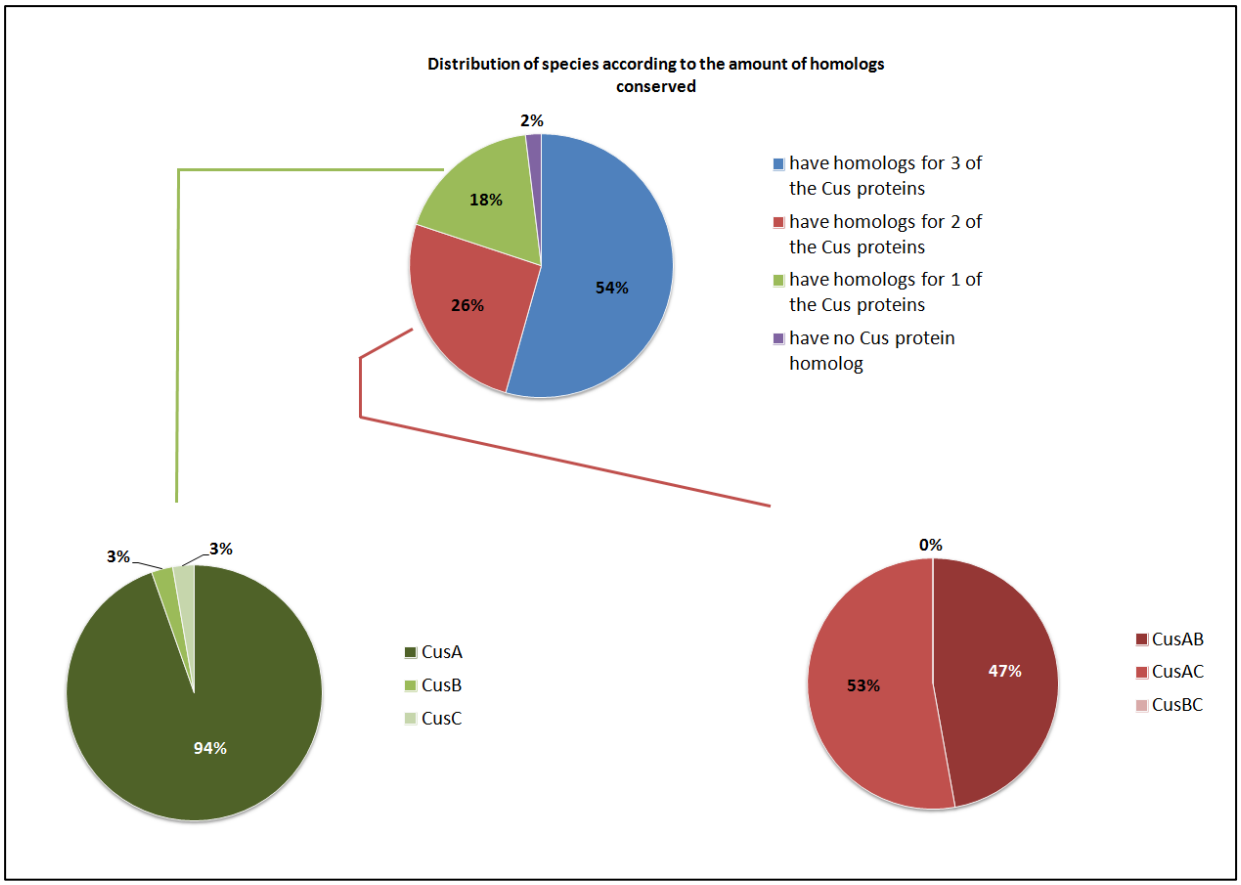

Fig. 36: Distribution of species according the amount of Cus homologs conserved. The 206 species are categorized according to their conservation of the Cus proteins and the different possible conservation combinations.

A majority (54%) of the 206 species retained the three Cus proteins (Fig. 36). 26% conserved 2 of the 3 proteins. In these species, among the three possible associations (CusAB, CusAC and CusBC), only CusBC is not represented. The CusAB and CusAC associations display a conservation rate of 47% and 53%, respectively. Finally, among the 18% of the 206 species that conserved only one Cus protein, the overwhelming majority (94%) kept CusA. CusB and CusC alone represents only 3% each (Fig. 36). This could indicate that CusA is able to have a function on its own, maybe as an IM transporter exporting substrate to the periplasm, or maybe an unrelated function, while CusB and CusC are unlikely to be functional if not paired with CusA.

These conservation results were superimposed with the database containing information about motility, lifestyle, and environment (Fig. S4). Several fuzzy correspondence analyses (FCA), followed by co-inertia analyses, were conducted. The FCA were performed via the Ade4 R package, with the Duality Diagram functions (dudi functions).

These analyses are descriptive tools. A Correspondence Analysis (CA) serves to find, in a table, association patterns between the row labels (e.g., the organisms) and the columns labels (e.g., the traits).

The CA will compute Expected Values (EV = row average * column average / total average) and Residuals Values (RV = actual value of the table cell – expected value). Positive residual values tend to indicate a correlation, while a negative value indicates an anti-correlation (Bock 2015). However, it is important to keep in mind that, because the population average is used to calculate the residual value, the result will always be relative to the population. For instance, if all the organisms share a trait in the table, the residual value is likely to be close to 0, despite being indeed a characteristic associated with the organism.

	Trait 1 (e.g., longevity)	Trait 2 (e.g., agressivity)	Trait 3	Average
Organism 1	89	63	100	84
Organism 2	45	0	91	45
Organism 3	95	12	89	65
Organism 4	17	99	90	69
Organism 5	72	24	85	60
Average	64	40	91	65

Fig. 37: Mock-up table of a dataset for CA. The data presented here are made up and represent a fictive example of a dataset that can be computed by CA. The rows are the values for the different organisms (called the row labels), while the columns are the different traits (column labels).

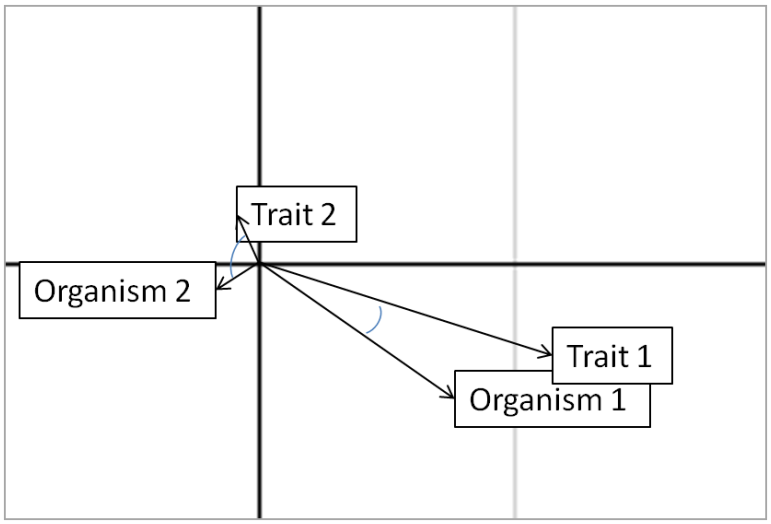

Fig. 38: Mock-up of the kind of scatterplot resulting from the CA. This example suggests that the organism 1 and the trait 1 present a strong correlation, at least stronger than the relation between the organism 2 and the trait 2. They are further away from the barycenter, indicating they a stronger distinction from the background noise. The proximity and smaller angle between the two elements reinforce this suggestion of correlation.

In the example presented in Fig. 37, the RV for the Trait 2 of the organism n°4 equals 57, which indicate a relatively strong correlation between this organism and this trait. As the actual value was high (99) and above the values of the other organisms, this was expected. More surprisingly, the residual value for the Trait 3 of the same organism is -7, which would mean an anti-correlation. Yet, the actual value is still high (90), but due to the population average, this trait does not stand out for this organism.

Once computed, these residual values will be presented on a scatterplot. This scatterplot is a planar representation of the multidimensional analysis. Three elements are important to interpret the plot.

The barycenter of the graph indicates a relative neutrality. The further away an element is from this center, the more this element will stand out from the rest of the dataset (Fig. 38). Traits shared by an overwhelming majority of the population, or traits shared uniformly in various groups without a strong correlation, tend to remain close to the origin, akin to background noises.

The proximity of two different elements (one row label and one column label) suggests a correlation. The closer they are, the more associated they are likely to be (Fig. 38). If a row label (e.g., the organism name) and a trait are on the opposite part of the plot, they may be anticorrelated.

The angle between two elements, i.e. formed if two lines were traced from these elements to the barycenter, is also indicative of an association (Fig. 38). The smaller the angle, the stronger the association. On the contrary, a 90° angle means there is no correlation, while a 180° would mean a perfect anticorrelation.

Despite all the information given by the (F)CA, it remains a descriptive tool. It is simply used to have a better view on relationships that could exist within a table. In any case, any correlation should be verified with the raw data, as RV can sometimes be counterintuitive. Besides, in the case of where a trait is only shared by a small percentage of the population, it may under- or overestimate the strength of a correlation, due the the small size of the sample (Husson & Josse 2014).

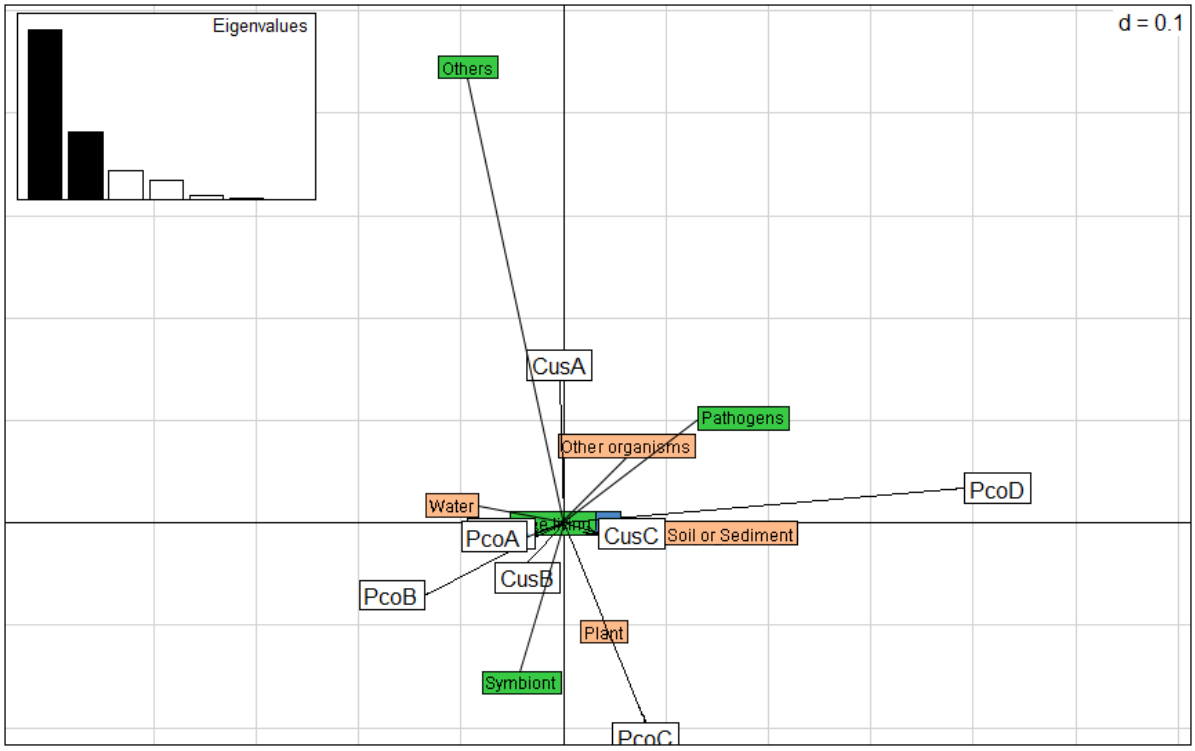

Fig. 39: Correlation of the conservation of the Pco and Cus proteins with the motility, the environment, and lifestyle as per the CA. The distance from the origin indicates a specificity, a small distance between elements from the different categories suggests an association and the angle between two elements formed by abstract line to the center indicate the strength of the correlation. Total inertia of the analysis = 57%.

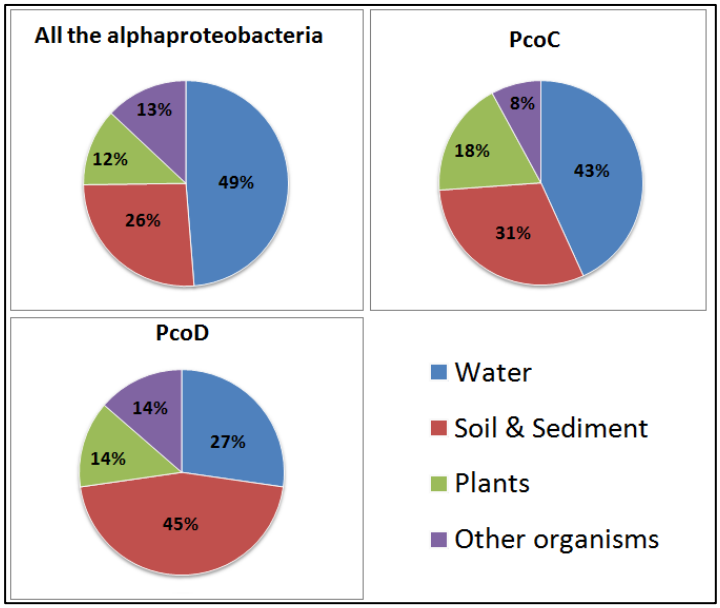

Fig. 40: Repartition of the environment for several categories of alphaproteobacteria. The top left quadrant indicates the reparation of the environmental niches for the 206 alphaproteobacteria of the database. The top right quadrant is the same repartition for all the alphaproteobacteria possessing at least one PcoC homolog, and the bottom left quadrant is for the ones possessing at least one PcoD homolog. The aquatic environment is color-coded in blue, the soil and sediment category in red, the plant environment in green, and the fraction of bacteria isolated on or in other organisms is depicted in violet.

Several FCA were conducted, correlating both the species and their environment (water, soil and sediment, plants or in other living organisms), lifestyle (pathogen, symbiont, free-living, or other) and motility (motile or non-motile), but also the conservation of the Pco and Cus system (Fig. 39, 42 and 44). In addition, a co-inertia analysis was performed. The co-inertia analysis was originally developed to study species-environment relationships, and aims to detect correlations between two tables of values (Dolédec & Chessel 2006). This allowed us to get an additional qualitative assessment of the correlations found, in this case between the different proteins of the Pco and Cus system, and the table containing information about the environment and the lifestyle.

The first analysis was done with the different Pco and Cus proteins independently from each other (Fig. 39). The correlation between these proteins, the species, and their motility (in blue), their environment (in orange) and lifestyle (in green) was assessed. The total inertia of the analysis was 57%, which was deemed acceptable. PcoC seems to stand out and appear to be slightly correlated with plants environment, and possibly the symbiotic lifestyle. The CA also suggest an association between the PcoD and the "Soil or sediment" environment. No effect of the motility was apparent. The co-inertia analysis reinforced these results, indicating a relatively high correlation value (0.8061) for PcoD and the Soil/Sediment environment, and a moderate positive value for PcoC and the plants (0.3056). We therefore went back to the raw data and plotted a comparison between the repartition of the environments for the general alphaproteobacteria population (n = 206 species) and the environment occupied by species that had at least one protein homologous for PcoC or PcoD (Fig. 40).

The PcoC correlation is not striking (18% isolated from a plant, instead of 12% in the general population). Nonetheless, if we run the reverse search, looking at all the species annotated as symbionts in the database, it appears that 69% of them possess at least PcoC (Fig. 41), while the conservation rate for PcoC is otherwise only half as high (35%) (Fig. 33). For PcoD, the correlation with soils or sediment seems more prominent. 45% of the alphaproteobacteria possessing at least one homolog of PcoD were isolated in the ground, compared to only 26% in the general population (Fig. 40).

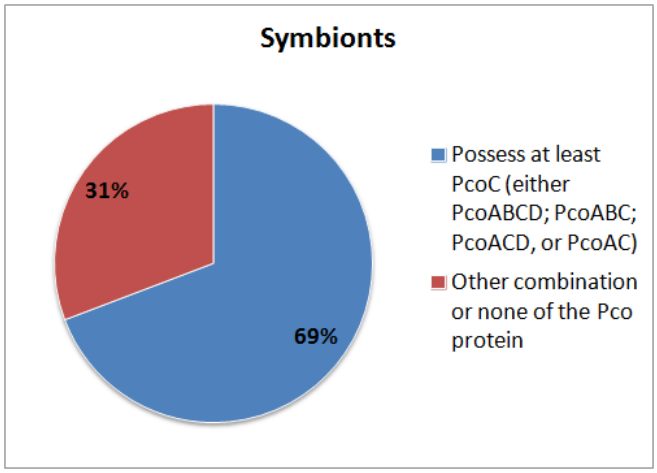

Fig. 41: Repartition of symbionts according to their conservation of PcoC. Symbiotic alphaproteobacteria that possess at least one homolog for the PcoC protein or a combination containing PcoC are color-coded in blue, those who do not are in red.

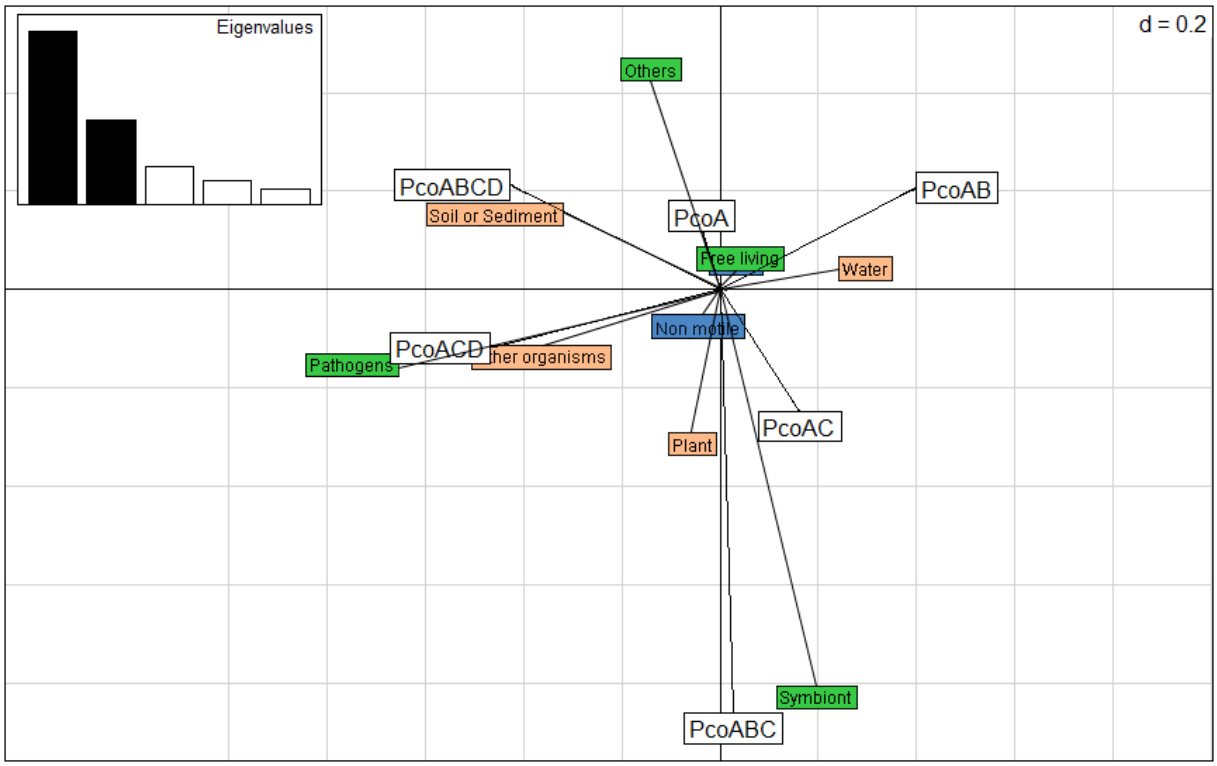

Fig. 42: Correlation of the conservation of the different Pco proteins subsets with the motility, the environment, and lifestyle as per the CA The distance from the origin indicate a specificity, a small distance between elements from the different categories suggests an association and the angle between two elements formed by abstract line to the center indicate the strength of the correlation. Total inertia of the analysis = 50.5%.

However, analyzing all the proteins independently may introduce background noise that would drag everything closer to the barycenter. As most of the alphaproteobacteria conserved a homolog of CusA (Fig. 33) and a majority of them also possess homologs for PcoA, CusB, and CusC (Fig. 33), these proteins are likely to stay relatively close to the origin of the plot. This may be the case here for PcoA, CusB, and CusC. CusA seems dragged toward the top of the plot, possibly attracted by the "others" lifestyle category, which contains very few species, and which correlation strength may therefore be overestimated by the CA.

Another CA was thus performed, this time with a clusterization of the conservation categories. We grouped the different combinations of the Pco system (PcoABCD, PcoABC, PcoACD, PcoAB, PcoAC, PcoAD, and PcoA) and tried to evaluate their respective associations with the lifestyle and environment as previously (Fig. 42).

This time, stronger associations appear to arise. While the motility still does not seem to be associated with a particular trait, the protein groups may be more specific to some environments or lifestyles. Bacteria that have conserved the four proteins (PcoABCD) seem to express a strong correlation with the soil/sediment environment (Fig. 42). PcoABC appears to be strongly associated with the symbiotic lifestyle, and possibly with the "plants" environmental category. PcoACD is suggested to be paired with the pathogenic lifestyle and, logically, would be found on or in other organisms (Fig. 42). The co-inertia analysis supported these observations, with a positive correlation value of 1.1542; 2.8129; 0.6219; 2.2600 and 0.2074, respectively.

The raw data, however, only partially supported these correlation results. The PcoABCD correlation seems to hold true, as a vast majority (67%) of the species which conserved PcoABCD indeed have been isolated from soils or sediment, compared to only 26% of the general population of the alphaproteobacteria (Fig. 43 A).

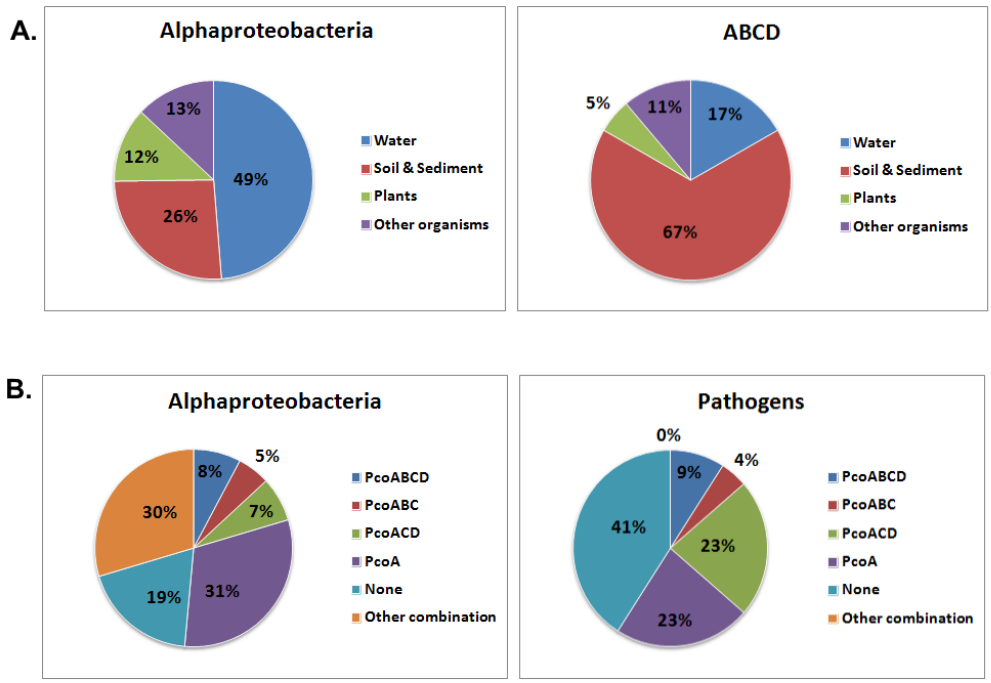

Fig. 43 Repartition of alphaproteobacteria according to their environment or lifestyle. A) The top row displays the repartition of the alphaproteobacteria according to their environmental niche. Left quadrant indicates the reparation of the 206 alphaproteobacteria of the database. The right quadrant is the same repartition for all the alphaproteobacteria the PcoABCD protein combination. B) The bottom row displays the segregation of homologs according to the lifestyle of the bacteria — left quadrant the proteins group for the 206 alphaproteobacteria of the database. Right quadrant is the same analysis for the pathogens only.

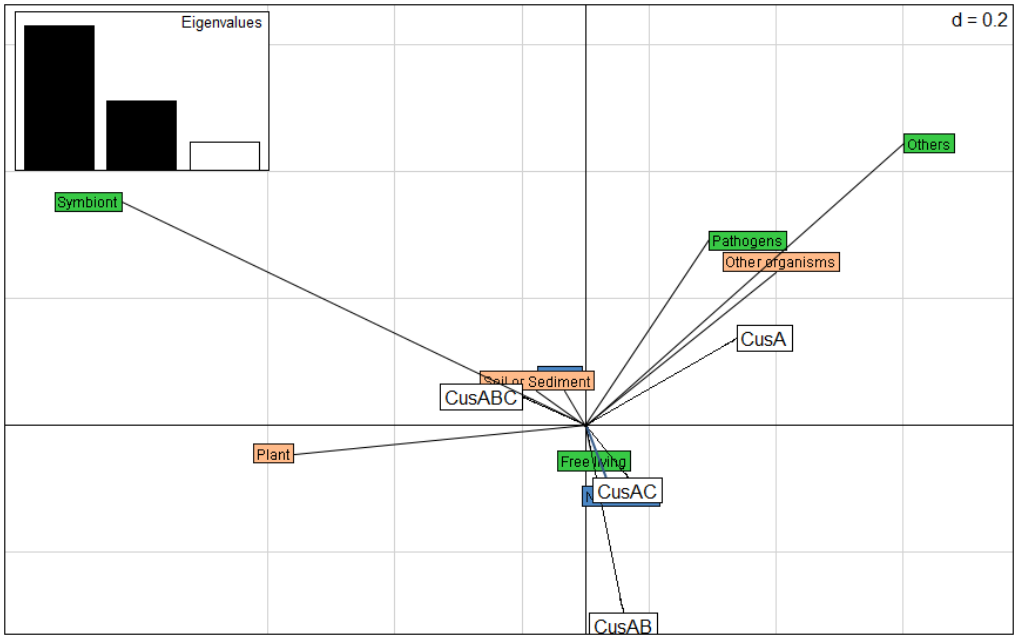

Fig. 44: Correlation of the conservation of the different Cus proteins subsets with the motility, the environment, and lifestyle as per the CA. The distance from the origin indicates a specificity, a small distance between elements from the different categories suggests an association and the angle between two elements formed by abstract line to the center indicate the strength of the correlation. Total inertia of the analysis = 88.37%.

The PcoACD association with pathogens is also partially found in the raw data. While the PcoACD combination represents only 7% of the alphaproteobacteria, it is found in nearly ¼ of the pathogens of this class (Fig. 43 B). However, nearly half of the pathogen do not possess any Pco homolog. This may indicate a fracture in the pathogen group, where two different clusters would not have the same need regarding Cu resistance.

A third CA was performed, similarly to the one done with the Pco proteins group, although this time with the different grouping for the Cus system (Fig. 44).

Although two correlations seem to stands out (CusA with the pathogens category and CusAC with free-living one), the co-inertia value are slightly more moderate than for the Pco analysis (0.6091 and 0.1257143). Besides, going back to the raw data does not provide much more hindsight on this correlation, possibly due to the ubiquist properties of CusA. 97% of the alphaproteobacteria appears to have at least one CusA homolog (Fig. 33), which makes difficult for a category to stand out based on its conservation.

While some of these correlations seem interesting, it is still unknown if they are based on simple phylogeny or if they are due to an evolutive pressure that would have driven the bacteria to acquire and keep these resistance mechanisms due to their lifestyle. For instance, a strong correlation between the PcoABCD system and bacteria living in soil or sediment have been suggested. It would be interesting to know whether these bacteria are phylogenetically close to each other (in which case the conservation of PcoABCD may be irrelevant to their environment), or whether the evolutive distance between them is important. The latter may suggest that the four PcoABCD proteins are important to optimize the evolutive fitness when living in the soil or sediments.

To answer this question, we aimed to superimpose the CA data to a phylogenetic tree of the 206 alphaproteobacteria. To build this tree, the 30S ribosomal protein S1 was selected as its basis. The 30sS1 sequences of the 206 species were aligned with Clustal Omega. Clustal Omega is a command-line based software able to align multiple protein sequences. The resulting file needed to be curated, in order to remove the mostly non-conserved region that would bring on the table more noise than actual information. This reduction of the signal-to-noise ratio is important to build a phylogenetic tree as accurate as possible. Curating the alignment can be done manually via a software like Jalview, or via automated tools. If done manually, this critical step requires at the very least a rough knowledge of the protein of interest. It is valuable to know where the important regions of the sequence are located. This will reduce the risk of removing a poorly conserved region that is essential for a certain number of organisms present in the alignment (Castresana 2000).

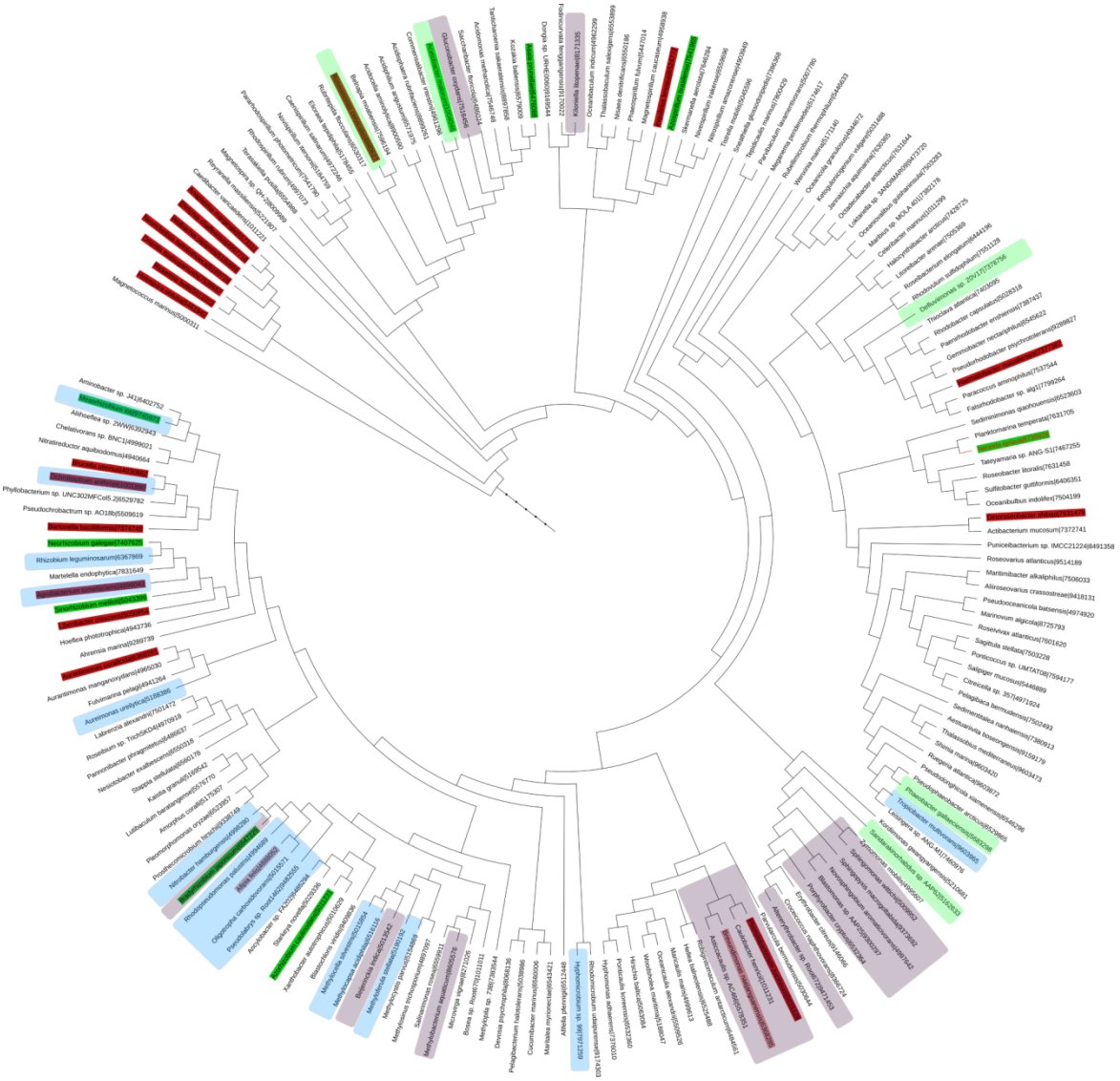

Fig. 45: Phylogenetic tree of the 206 species of alphaproteobacteria contained in the database. The tree was constructed with PhyML, using BIONJ starting tree with NNI improvement, and an aLRT SH-like statistical test for branch support. Pathogens are highlighted in dark red, symbionts in dark green. The light, semi-transparent boxes highlight various Pco proteins grouping. Bacteria having conserved PcoABCD are highlighted in light purple, the PcoACD subset is shown in light blue, and the PcoABC combination is in light green.

This kind of information, useful for the editing process, can be acquired experimentally or predicted by various bioinformatics tools. Here, we used several of them, including Foundation, Biocyc, HHPred, SignalP, or HMMER. The curated alignment was sent to PhyML, which is described as a "fast but accurate algorithm" to build a phylogenetic tree (Guindon & Gascuel 2003). The parameters utilized were an AIC selection with a BIONJ starting tree with NNI improvement and an aLRT SH-like statistical test for branch support. The resulting tree can be seen in Fig. 45. The tree appears conform to trees already published in the literature (Williams et al. 2007), although a small group of Rhodobacteraceae seems misplaced. The tree has been annotated, with the pathogens highlighted in dark red, and the symbionts in dark green (Fig. 45). Pathogens look mostly spread in two clusters, one in the Rhizobiales order, and the other in the rickettsiales. Symbionts are more evenly spread. We superimposed on the tree the 3 Pco conservation subsets that gave a strong correlation in the previous analysis. The PcoABCD (in light purple) seems mostly clustered in one part of the tree (Fig. 45). This support the hypothesis that the tree is phylogenetically correct. However, that also suggests this PcoABCD conservation may not be related to the lifestyle, but would rather be a product of an unrelated evolutive process. Indeed, soils and sediment bacteria are spread rather homogeneously in the tree. The important cluster of soil bacteria possessing PcoABCD may over-represent the correlation between the environment and the Pco system.

Similarly, the PcoACD subset (light blue), correlated with the pathogen in the FCA, is mostly present in the Rhizobiales order (Fig. 45). While it is indeed present in a number of Rhizobiales pathogens, this particular grouping is not present in pathogens of other orders, such as the Rickettsiales pathogens. This may indicate that the pathogenic lifestyle does not especially require PcoACD as the CA could have suggested. However, it might also simply indicate the two orders face slightly different selective pressure, and that the Rhizobiales may encounter Cu or Ag stresses more frequently than the Rickettsiales during their infectious cycle.

The PcoABC subset (in light green), correlated with the symbiotics bacteria and bacteria isolated from plants, is more homogenously distributed (Fig. 45), which may means the PcoABC combinations is relatively important for such lifestyle and environment.

RESULTS – Part II

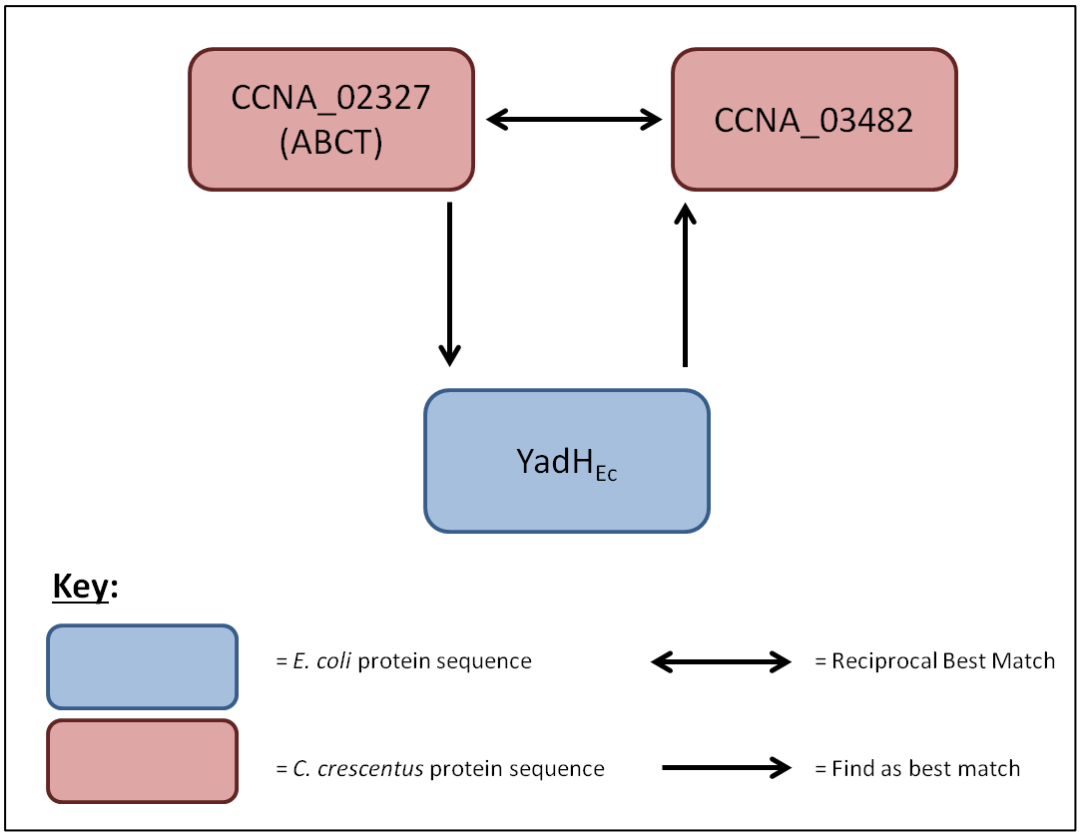

Fig. 46: Conservation of the TmrP protein of *C. crescentus* in *E. coli*. Double-headed arrows indicate a reciprocal best match. One-way arrows indicate that the first protein find the second as best match in blast..

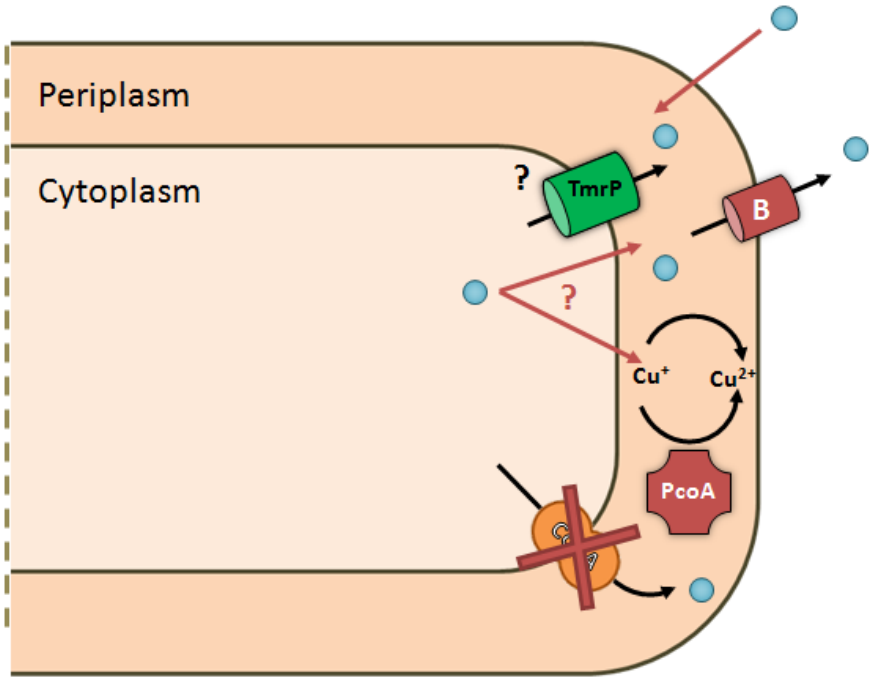

Fig. 47: First hypothetical work model for TrmP. The PcoAB system is likely to manage Cu cations (depicted here blue spheres) entering the cell from the extracellular environment. However, Cytoplasmic Cu may need to be exported to the periplasm for detoxification and export. However, experimental data suggest that CopA might not fill this role in *C. crescentus*. Therefore, our first hypothesis was for another protein, here the TmrP permease, to perform this Cu transport.

TmrP – An uncharacterized protein involved in metal resistance

After the characterization of the Pco system in *C. crescentus*, several questions were still pending. One of them concerned the way Cu is transported from the cytoplasm to the periplasm. What is feeding the Pco system with Cu? PcoA and PcoB are likely to regulate the excess Cu that enters the cell from the extracellular space. The cytoplasmic Cu level needs to be regulated as well. Ions may be driven to the periplasm by a specific protein to alleviate the risk of DNA damage. In *E. coli*, the P1B- ATPase CopA is reported to fulfill this role. This IM protein works in tandem with CueO (and therefore, possibly with the CueO paralog $PcoA_{Ec}$), driving excess Cu from the cytoplasm to the periplasm for detoxification.

However, in *C. crescentus*, the reported CopA homolog does not seem to be crucial for Cu resistance. The disruption of the gene does not seem to increase the Cu sensitivity of the resulting mutant cells (Fig. 30). Functional homologues were then sought.

The previously described genetic screen (Fig. S3) revealed several genes likely involved in *C. crescentus* Cu resistance, such as *CCNA_02327* annotated as a gene coding for an ABC Transporter permease protein, hereafter referred to as "TmrP" (For Transition metals resistance Permease). TmrP candidate was identified nine times in the screen. Interestingly, the *tmrP* gene only encodes the permease part of the transporter, and the gene encoding the ATPase domain is not neighboring it. As ABC Transporters are generally localized in the IM, we first hypothesized it could play the role of CopA in *C. crescentus* and characterized this candidate further (Fig. 47).

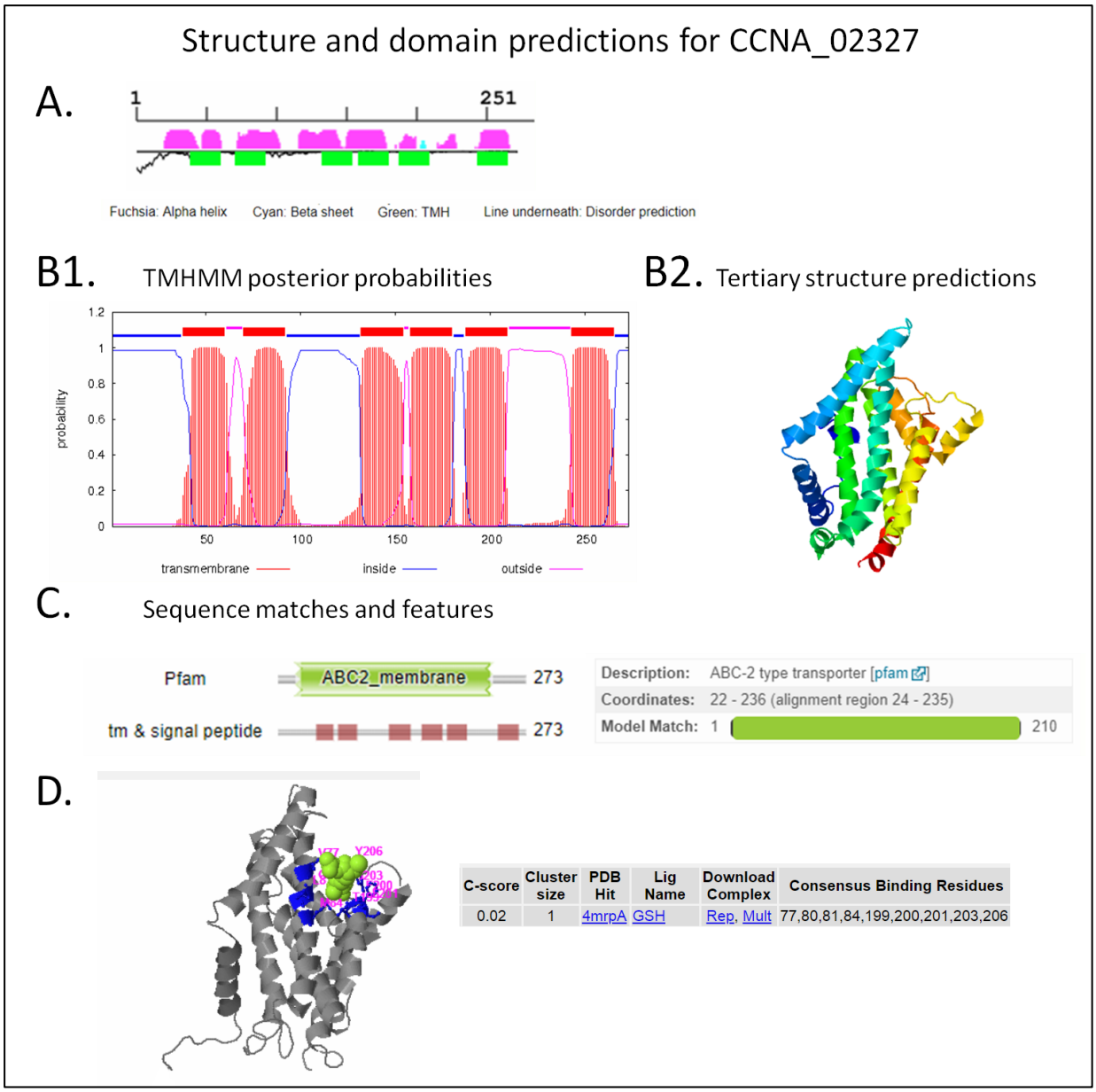

Fig. 48: Structure and domain prediction for CCNA_02327 (TmrP). **A.** Result of the Foundation analysis. Secondary structure are represented along with their sequence position on the horizontal axis. α-helices are represented in fushia and β-strands in cyan. The wiggly line in beneath the secondary structure represents disorder. The further away from the horizontal axis, the more the disorder. **B1** TMHMM results, prediction transmembrane domain and helices. **B2** I-Tasser tertiary structure prediction results. **C.** Results of the HMMER domain prediction. **D.** Results of the COACH prediction, predicting eventual binding sites and ligands.

a. Bioinformatics – establishing an hypothetical model

i. Homologs research from *E. coli* sequences

When blasting the TmrP protein sequence of *C. crescentus* as a query against the *E. coli* proteome, the best resulting match is the poorly characterized YadH ABC transporter protein. Interestingly, the reverse search, using the YadH protein sequence as the query against the *C. crescentus* proteome, does not return TmrP as the best match, but rather the uncharacterized CCNA_03482 ABC transporter permease, which has not been found in the genetic screen. However, CCNA_03482 still bears striking similarities with TmrP. Both proteins are reciprocal best matches within the *C. crescentus* proteome (Fig. 46).

ii. Structure and domains

TmrP displays classic ABC Transporter features in the structure prediction. It seems mostly composed of α-helices and is predicted to possess 6 transmembrane helices (Fig. 48 A and 48 B1), which is quite standard for an ABC transporter permease (ter Beek et al. 2014).

Domain predictions suggest the presence of a large ABC-2 type transporter domain (Fig. 48 C). Although Type 2 ABC transporters are most often described as importers (ter Beek et al. 2014), several well characterized exporters possess type-2 like sequences such as NodJ, which is part of the NodIJ complex exporting the nodulation inducers in some plant symbionts, like *Rhizobium leguminosarum* or *Bradyrhizobium japonicum* (Fath & Kolter 1993) (Fig. S5). *In silico* protein-ligand binding site prediction performed by both COACH and TM-SITE indicates several potential ligand, although with poor confidence score. Both plateform predict GSH as a potential ligand (Fig. 48 D)

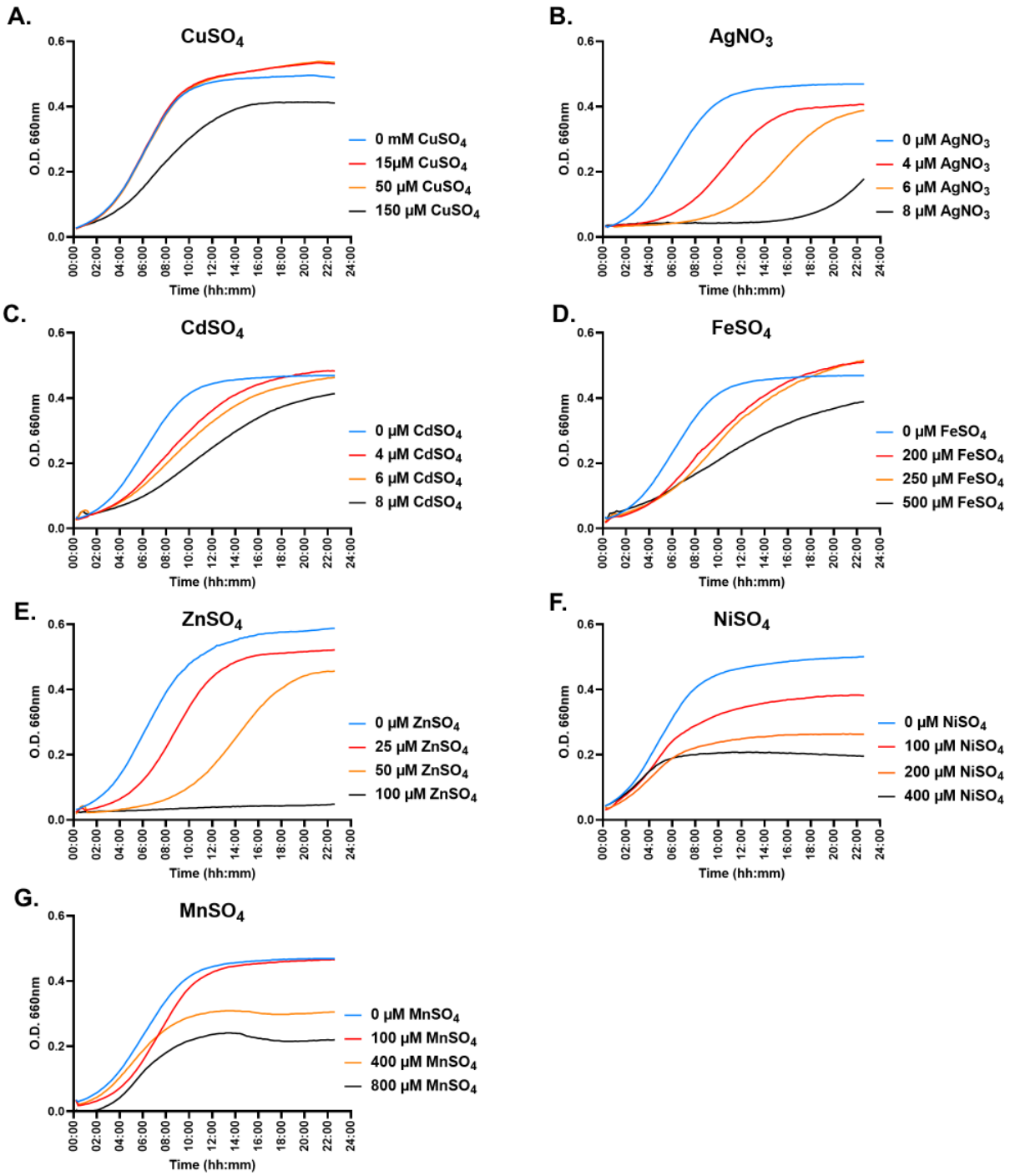

Fig. 49: Growth profiles of the WT strains under various metal stresses in PYE medium. From A to G are the growth curves for $CuSO_4$, $AgNO_3$, $CdSO_4$, $FeSO_4$, $ZnSO_4$, $NiSO_4$, $MnSO_4$, respectively. (Biological replicate = 3 for each metal; technical replicates for each biological replicate = 3 for $CuSO_4$, $CdSO_4$, $AgNO_3$, $FeSO_4$ and 2 for $ZnSO_4$, $NiSO_4$, $MnSO_4$). Relative standard deviation between 6e-03 and 0.172.

b. TmrP is a system involved in metal resistance

The implication of TmrP in metal resistance has first been tested through growth curves experiments. A clean Δ*tmrP* knockout strain has been obtained by allelic replacement. In parallel, a second strain, harboring a replicative pMR10 plasmid carrying a copy of the *tmrP* gene under the control of the Lac promoter (Δ*tmrP* pMR10 *tmrP*), was engineered.

Moderate stress levels were determined for each of the metal salts (Fig. 49). The stresses increased in a dose-dependent manner, hindering the growth of *C. crescentus* either by reducing the growth rate or by elongating the lag phase before the growth start (Fig. 49). "Moderate stresses" were defined as concentrations to which the growth of the strain of interest is negatively impacted but still ongoing. The selected metal concentrations for $CuSO_4$, $AgNO_3$, $CdSO_4$, $FeSO_4$, $ZnSO_4$, $NiSO_4$, and $MnSO_4$ were 150µM, 6µM, 6µM, 500µM, 50µM, 200µM, and 400µM, respectively.

The different genetic backgrounds were tested in the presence of 150 µM of $CuSO_4$. The *ΔtmrP* strain exhibits an increased sensitivity to Cu compared to the WT strain (Fig. 50A). We sought to assess the specificity of this system. The Pco system was shown to be specific to Cu (Lawarée et al. 2016). If TmrP is indeed working alongside the Pco system as hypothesized, then perhaps it might have the same Cu specificity. We therefore tested the sensitivity of the strains to several TM in the form of $ZnSO_4$, $NiSO_4$, $FeSO_4$, $MnSO_4$, $CdSO_4$ and $AgNO_3$.

The Δ*tmrP* mutant does not display any increased growth delay or defect compared to the WT cells upon $ZnSO_4$, $NiSO_4$, $FeSO_4$ or $MnSO_4$ exposure (Fig. 50 D to 50 G). Interestingly, the *ΔtmrP* mutant seems more sensitive to $CdSO_4$ and $AgNO_3$ than the WT cells (Fig. 50 B and 50 C). In each of these case, the *ΔtmrP* pMR10 *tmrP* restored the WT phenotype. In addition, the complemented strain may slightly increase the resistance to $NiSO_4$ (Fig. 50 E). While the growth rate seems similar, the plateau phase reaches a slightly higher O.D.

These data suggest that TmrP is not entirely specific to Cu, and is involved in the resistance against at least three different TM stresses, suggesting that TmrP does not mirror the function of the Cu-specific CopA transporter in *E. coli* (Futai et al. 2004). However, TmrP could be a non specific IM metal transporter feeding the periplasmic Pco system with Cu ions. In order to test this hypothesis, TmrP was further characterized for its function and localization.

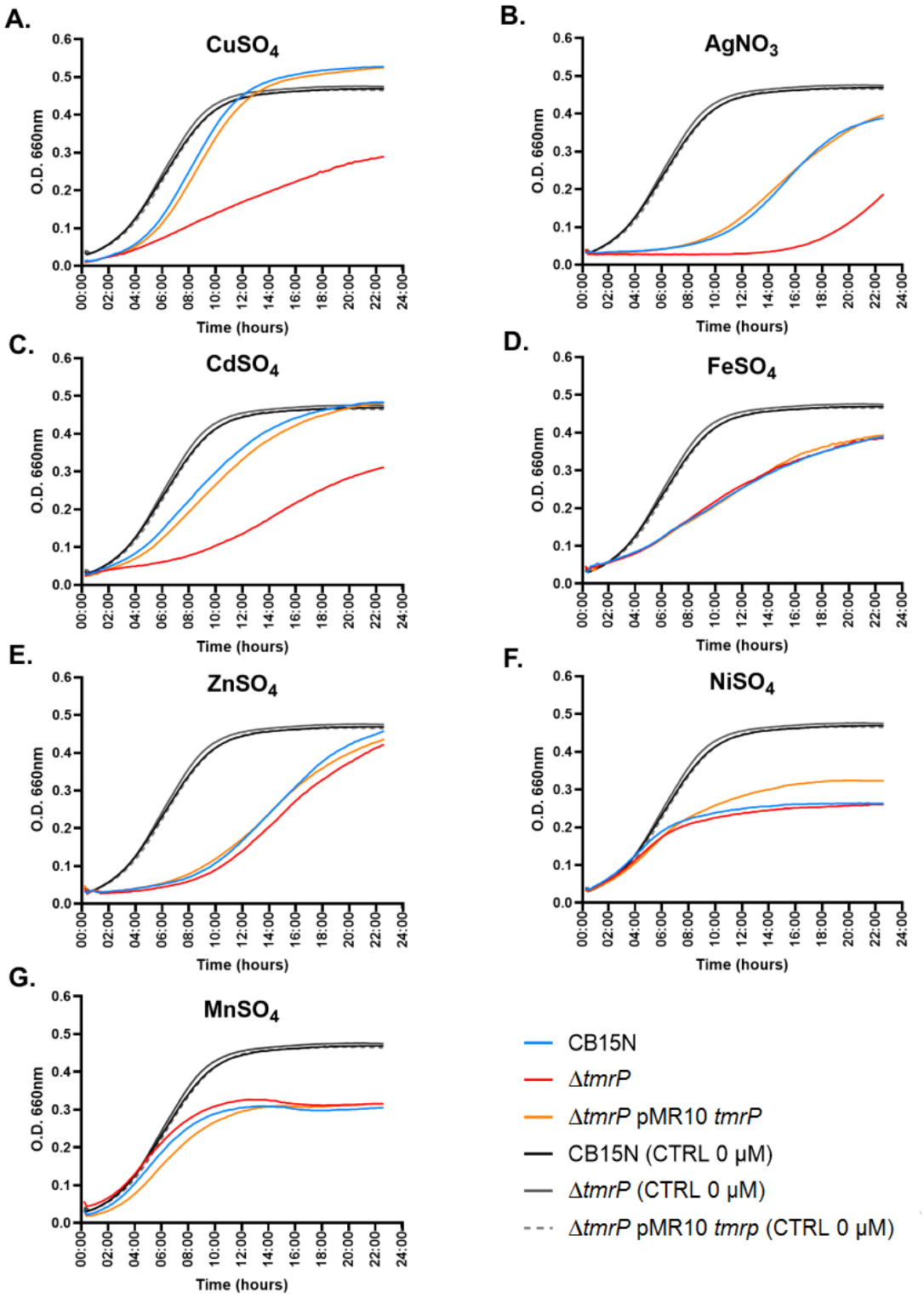

Fig. 50: Growth profiles of the WT, *ΔtmrP* and *ΔtmrP* pMR10 TmrP strains under various metal stresses in PYE medium. From A to G are the growth curves for $CuSO_4$, $AgNO_3$, $CdSO_4$, $FeSO_4$, $ZnSO_4$, $NiSO_4$, $MnSO_4$ in 150µM, 6µM, 6µM, 500µM, 50µM, 200µM, 400µM, respectively. (Biological replicate = 3 for each metal; technical replicates for each biological replicate = 3 for $CuSO_4$, $CdSO_4$, $AgNO_3$, $FeSO_4$ and 2 for $ZnSO_4$, $NiSO_4$, $MnSO_4$). Relative standard deviation between 4e-04 and 0.154.

c. Biochemical characterization of TmrP: localization and function

i. TmrP localizes in the IM

In order to establish whether TmrP is indeed an IM protein, a membrane fractionation assay has been performed, similarly to the experiment realized with PcoB. This experiment aims to isolate the IM from the OM. An immunodetection is carried out as a follow-through, to detect in which cellular fraction the protein is located.

However, as no antibodies for TmrP were available, a tagged strain was designed. The mCherry fluorescent tag was amplified by PCR from a reference strain and fused to the N-terminus of the *tmrP* gene sequence. This fusion was integrated in a pMR10 replicative plasmid and placed under the control of the strong Lac promoter. The vector was sent by electroporation in a *ΔtmrP* background, creating a mCherry-TmrP fusion that was used to perform the fractionation assay and the immunodetection.

The Cytoplasm, IM and OM fractions of the WT and the mCherry-TmrP strains have been isolated, and the immunodetection has been carried out. The mCherry-TmrP was localized in the IM (Fig. 51A), strengthening the hypothesis of a IM permease.

Fluorescence microscopy has also been performed with the mCherry-TmrP strain. The fluorescence reveals a faint peripheral halo, as well as bright fluorescent spots (Fig. 51 B). The halo likely marks the position of one of the two membranes, possibly the IM where mCherry-TmrP is supposed to localize. We currently have no conclusive explanation for the cytoplasmic spots. While they may be part of the natural expression of the protein, they could also indicate protein clustering. This could be due to the potential overexpression of the mCherry-TmrP fusion protein, which could trigger the formation of inclusion bodies. The cytoplasmic spots do not systematically localize at the same intracellular location. Preliminary 1 hour timelapse experiments failed to highlight any movement of these spots. Further experiments and longer observations may gather additional data about the nature of these fluorescents spots.

Taken together, these findings support the model of TmrP acting as an IM permease, part of an ABC transporter complex. However, these data do not provide any information about the permease substrate.

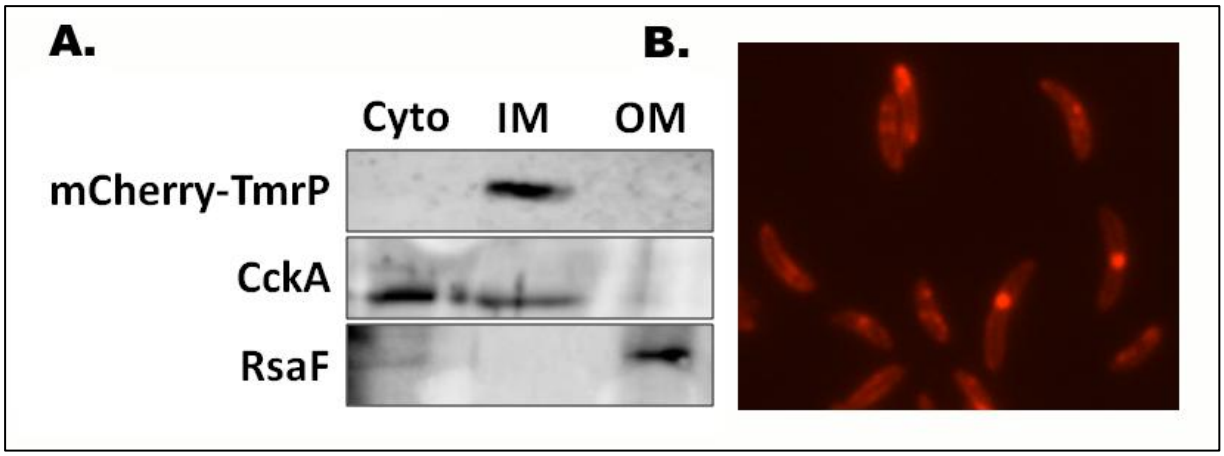

Fig. 51: **A.** Expression level of PcoB in the cytoplasm (Cyto), inner membrane (IM) and outer membrane (OM). CckA and RsaF were used as inner membrane (IM) and outer membrane (OM) controls, respectively. **B.** Picture of the mCherry-TmrP strain under fluorescence microscopy.

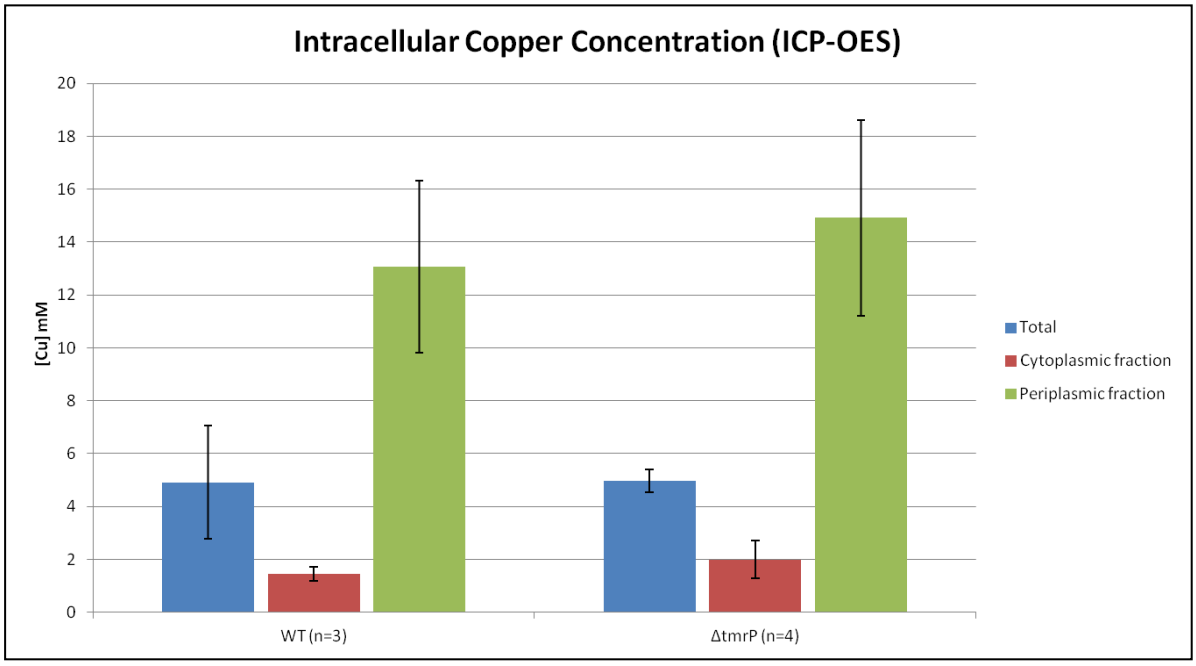

Fig. 52: **ICP-OES Cu concentration measurement.** Cu concentration in the different cellular fractions of WT and *ΔtmrP* strain. Total Cu measure on cell lysate is in blue, Cu mesure from cytoplasmic fraction is colored in red and Cu measured in the periplasmic fraction is colored in green. (Biological replicates = 3; technical replicates = 3). Differences between WT and *ΔtmrP* for their respective fraction at the 0.05 α level are not significant. (Respectively p = 0.9571; p = 0.2710 and p = 0.5211 for the Total comparison, cytoplasmic comparison and periplasmic comparison)

ii. TmrP may export cysteine toward the periplasm

Despite the bioinformatic analysis and the preliminary characterization, little is known about the cognate substrate of the TmrP. Our working model is that TmrP transports Cu, Ag and Cd from the cytoplasm to the periplasm where they could be detoxified and/or expelled out of the cell. By combining the previously described fractionation assay and Inductively Coupled Plasma - Optical Emission Spectrometry (ICP-OES), we were able to quantify the Cu concentration in periplasmic and cytoplasmic fractions of different genetic backgrounds. A "total fraction" condition, consisting of whole cell lysate, was also sampled.

Surprisingly, no statistically significant differences in the Cu concentrations could be highlighted between the periplasms of WT and the *ΔtmrP* strains (p value = 0.5211) (Fig. 52). Similarly, no statistical differences could be measured between their respective cytoplasm (p value = 0.2710) or total fractions (p = 0.9571). Two other preliminary experiments have been performed, trying to measure Ag and Cd in a similar fashion. Akin to the results obtain with Cu, neither the Ag nor the Cd concentration seemed to vary in the different cellular fractions between the WT and the *ΔtmrP* strains. However, the Ag and Cd results should be treated with caution, as they are preliminary (biological replicate = 2). Taken together, these data therefore do not support the proposed model according to which TmrP would export Cu cations from the cytoplasm to the periplasm.

TmrP thus seemingly does not transport metals, but could perhaps provides protection against Cu, Cd and Ag stress via another fashion.

The genetic screen performed in the laboratory suggests the involvement of a cysteine synthase gene (*CCNA_01493*) in the Cu resistance (Fig. S3), since transposon insertion in the *CCNA_01493* gene increases Cu sensitivity relative to the WT strain. This sensitivity has been confirmed by growth curves experiments (Fig. 53).

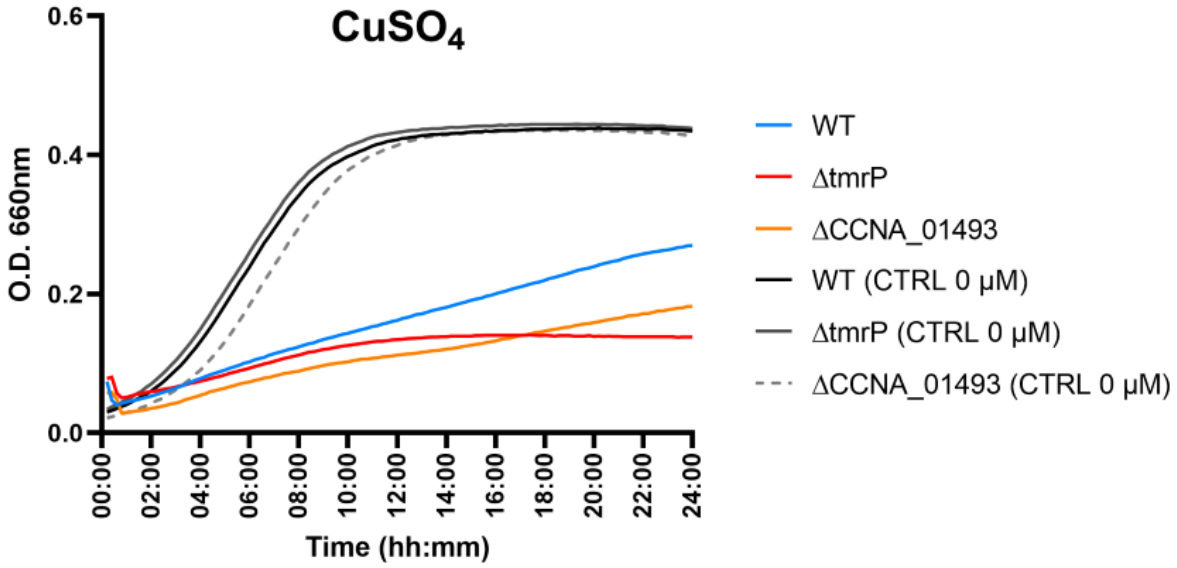

Fig. 53: Growth profiles of the WT, *ΔtmrP* and *ΔCCNA_01493* strains under a 200 µM $CuSO_4$ stress in PYE medium. The control conditions without Cu are depicted in black, dark grey or dashed dark grey. (Biological replicate = 2 for each metal; technical replicates for each biological replicate = 2). Relative standard deviation between 0.0015 and 0.087.

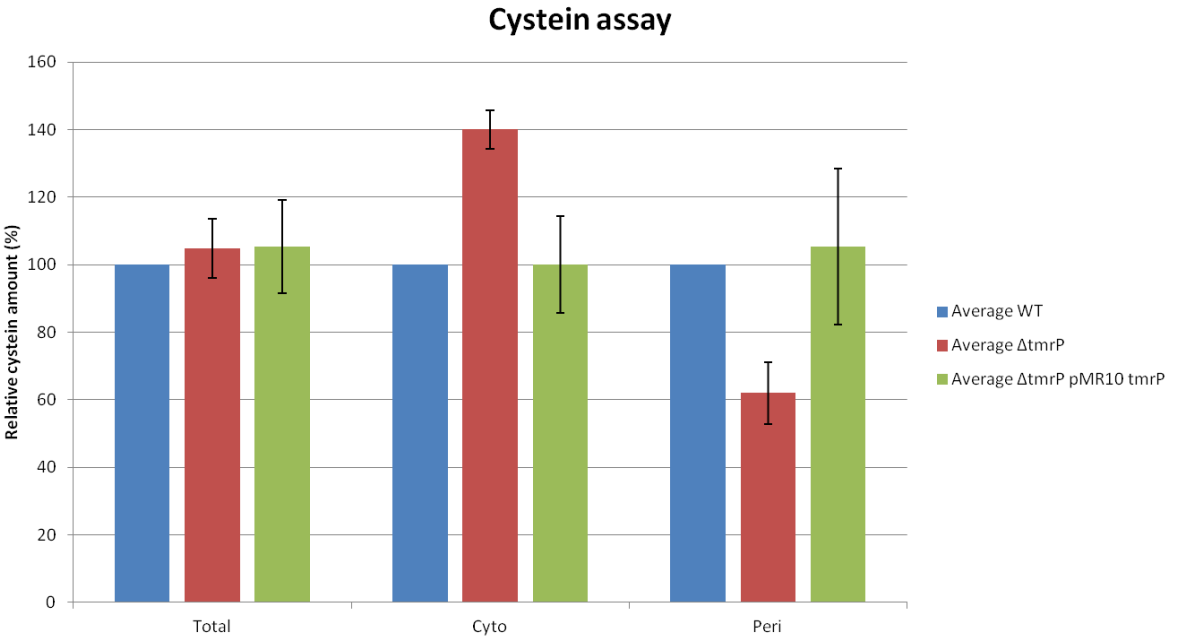

Fig. 54: Quantification of cysteine in different cellular fractions by a colorimetric technique in three different strains (WT, *ΔtmrP* and *ΔtmrP* pMR10 *tmrP*). The Cys content of the total, cytoplasmic (Cyto) and periplasmic (Peri) are estimated, and normalized by the WT values for comparison purpose (Biological replicates = 6 for WT and *ΔtmrP* and n = 3 for *ΔtmrP* pMR10 *tmrP*. Technical replicates = 3). One-sample t-tests were conducted, comparing the *ΔtmrP* and *ΔtmrP* pMR10 tmrP strains to a known mean of 100 (the normalized WT background value). P values for *ΔtmrP* total, cyto and peri fractions = 0.2389; 0.000012 and 0.0002, respectively. P value for *ΔtmrP* pMR10 tmrP total, cyto and peri fractions = 0.3867; 1 and 0.5928.

Cysteine (Cys) is a soluble amino acid, characterized by a thiol side chain. Highly reactive Cys serves both structural and functional purposes in many proteins (Ohtsu et al. 2010). Cys is also the key to the “oxidative folding” of a protein. The thiol of two Cys residues of a polypeptide can indeed form a disulfide bond, stabilizing the protein in a certain conformation (Holyoake et al. 2015).

Cys is also the precursor of various molecules, such as glutathione or cystine (product of Cys disulfide bond-mediated dimerization) and a component of metallothioneins (Masip et al. 2006; Hamer 1986). These molecules play a role in dampening the metal toxicity (Cfr. introduction – Metal dedicated resistance system). Morover, the sulfhydryl (-SH) group of the Cys can react with H_2O_2, a potential byproduct of some metal stress, in a redox reaction, as it was observed in yeasts (Hohmann & Mager 2003). This reaction catalyzes the formation of cystine and H_2O, thus reducing the ROS concentration in the cell (Ohtsu et al. 2010):

H_2O_2 + 2 L-cysteine --> $2H_2O$ + L-cystine

In *E. coli*, the YdeD transporter has been shown to be involved in the defense against H_2O_2 stress by translocating Cys from the cytoplasm to the periplasm (Ohtsu et al. 2010). The YecS importer, in turn, imports the resulting cystine back to the cytoplasm to regenerate the Cys pool (Ohtsu et al. 2015). In *E. coli* the CydDC ABC Transporter complex was demonstrated to export Cys and glutathione and seems to be required for Cytochrome assembly (Pittman et al. 2005; Pittman et al. 2002; Shepherd 2015; Holyoake et al. 2015; Cruz-ramos et al. 2004).

Considering Cys could thus counters the toxic byproducts of metal stresses or metals themselves, we hypothesized that TmrP could be involved in Cys transport from the cytoplasm to the periplasm in order to detoxify periplasmic Cu. Experiments were then performed to assess the ability of TmrP to transport Cys. While Cys-containing molecules are therefore known to help resist against a metal stress and Cys known to bind Cu, the eventuality Cys alone could provide resistance against metal in bacteria is less studied.

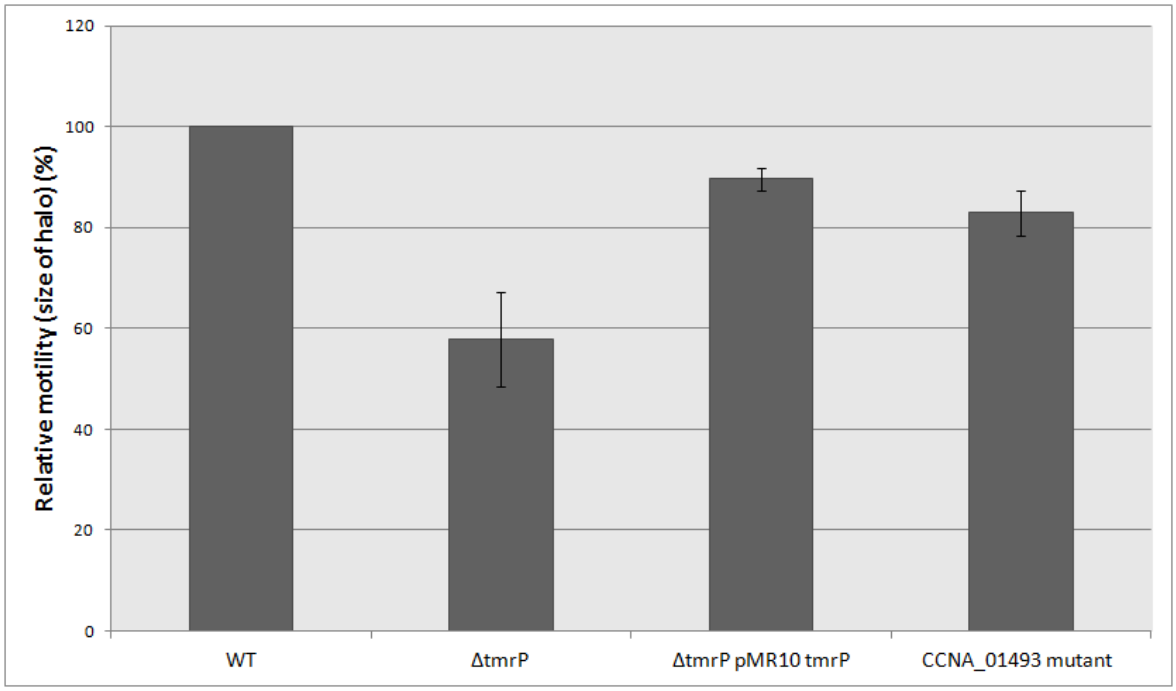

Fig. 55: Quantification of motility by a swarming motility assay. The motility of each genetic background has been estimated by measuring the size of the dispersion halo (M2G 0.25% agar). Measurements have been normalized by the WT value for comparison purpose. Biological replicates = 3. P values for *ΔtmrP*, *ΔtmrP* pMR10 *tmrP* and CCNA_01493 mutant backgrounds = 0.0160; 0.0155 and 0.0218, respectively.

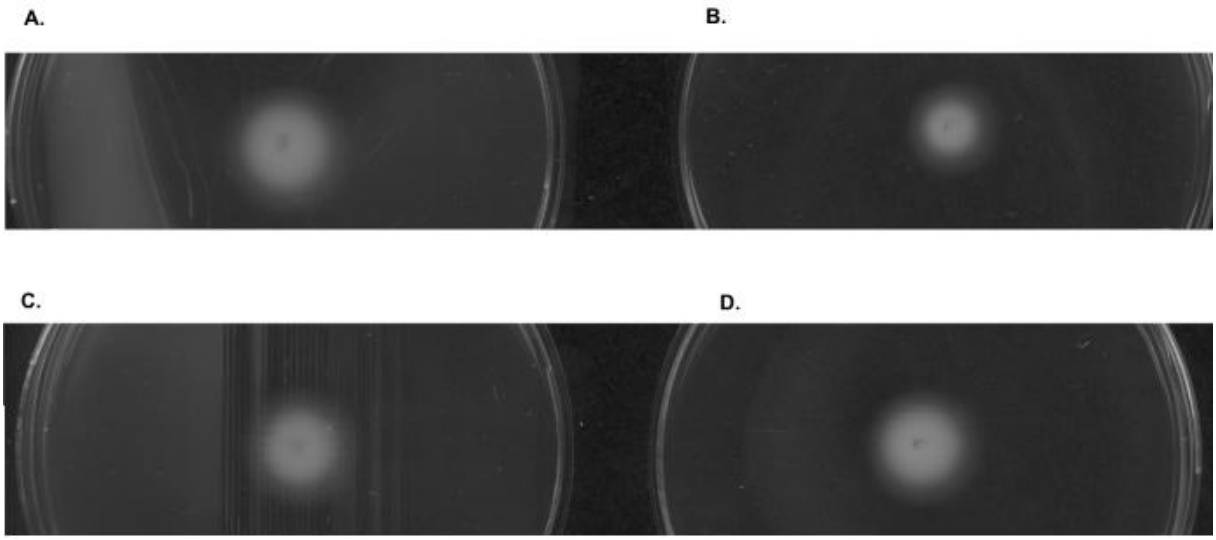

Fig. 56: Scan of the motility halo for one of the replicate of the motility assay. From A to D, halo for the WT, *ΔtmrP*, *ΔtmrP* pMR10 *tmrP* and CCNA_01493mutant background respectively.

Cys concentration can be determined via a colorimetric method involving ninhydrin (Gaitonde 1967). Under acidic condition, Ninhydrin reacts with L-Cys and turns the sample pink that can be quantified by measuring the O.D. $_{560\,nm}$ with a spectrophotometer (Gaitonde 1967; Ohtsu et al. 2010). This reaction has been reported to be quite specific to L-Cys. Ninhydrin will not react, under these conditions, with Cys-bearing complexes such as Cystine or Gluthathione, nor with other AA such as Proline or Citrulline (Gaitonde 1967). This protocol was used in combination with the fractionation assay to assess the presence of Cys in the periplasmic and cytoplasmic fractions of different genetic backgrounds. The WT, *ΔtmrP* and *ΔtmrP* pMR10 *tmrP* strains were tested. The *ΔtmrP* strain seems to accumulate 40% more Cys in the cytoplasm than the WT (Fig. 54). Conversely, it has roughly 40% less Cys in the periplasm. These differences are statistically significant (One-sample t-test; p = 0.000012 and 0.0002, respectively). The *ΔtmrP* pMR10 *tmrP* complement the phenotype, restoring WT level of Cys in both fractions. This result argues in favor of the cystein exporter model. TmrP would be anchored in the IM and transport Cys from the cytoplasm towards the periplasm.

Periplasmic Cys has been reported as crucial for proper motility in *E. coli* (Pittman et al. 2002). Mutation in the CydDC ABC Cys exporter would reduce Cys amount in the periplasm and trigger motility defects. As it may trigger similar effects in *C. crescentus*, we performed a motility assay. The *ΔtmrP* strains exhibited a 32% decrease in swarming motility (calculated from the size of the swarming halo, cfr. Fig. 56 for an example of halo pictures) compared to WT (Fig. 55). This difference is stastically significant (One-sample t-test, p value = 0.0160) The *ΔtmrP* pMR10 *tmrP* strain exhibits a near-complete restoration of the WT phenotype (92% of the WT motility). An additional genetic background was tested. Alternatively, the *CCNA_01493* knockout strain (knockout by disruption of a Cys synthase gene) displayed an intermediate phenotype with a 24% decrease compared to WT. However, it should be noted that *CCNA_01493* possess a paralog. The *CCNA_03740* gene encodes for a second Cys synthase, which may explain why the *CCNA_01493* knockout strain only results in an intermediate phenotype in the motility assay.

These results tend to corroborate those from the Cys assay, and support the hypothesis that TmrP exports Cys to the periplasm of *C. crescentus*.

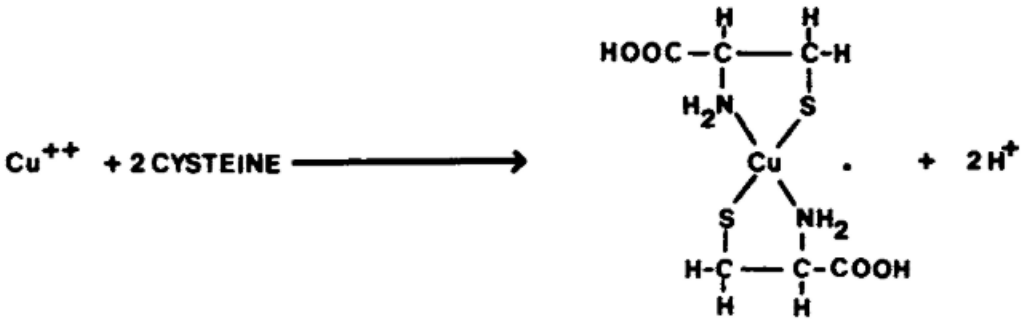

Fig. 57: Proposed model for the chelation of Cu^{2+} by Cys (Baker & Czarnecki-maulden 1987).

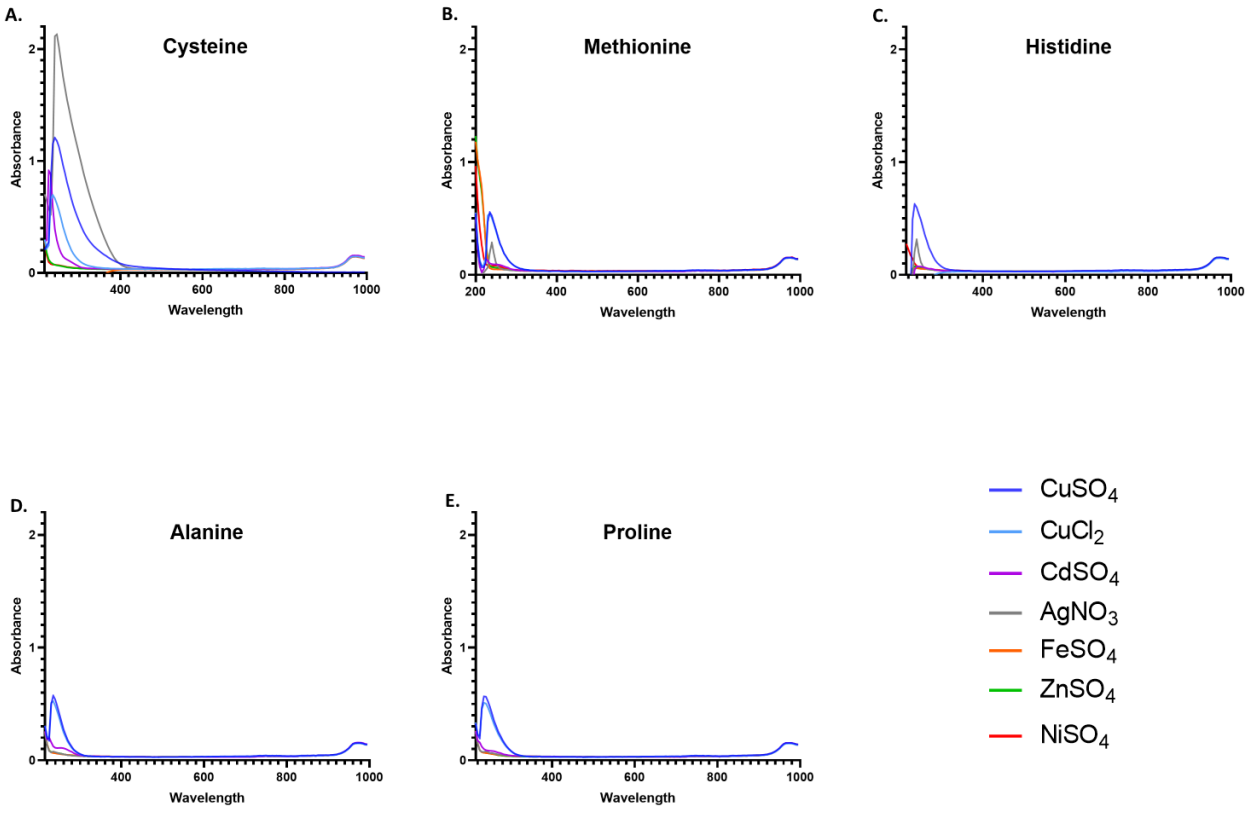

Fig. 58: Impact of metals on the absorbance of AA. Difference between the absorbance of AA alone and AA with metals, with the controls subtracted. Range of read from 201nm to 998nm. From A. to E.: 500 µM of L-Cys, L-Met, L-His, L-Ala or L-Pro, respectively, each one in when placed in contact with 50 µM of either $CuSO_4$, $CdSO_4$, $AgNO_3$, $FeSO_4$, $ZnSO_4$ or $NiSO_4$

iii. Cysteine is involved in metal resistance

In eukaryotes, Cys was proposed to chelate heavy metals and trace elements, limiting the amount of free ions able to damage the cell (Baker & Czarnecki-maulden 1987). In the case of Cu, this would be done by 2 Cys binding to Cu^{2+} through their sulfhydryl group (Fig. 57) Cys was shown to bind Cu *in vitro.* The affinity of Cu for Cys thiol group was investigated by Mass Spectrometry (Wu et al. 2010). Cu^{+} cations were shown to react with the –SH or $–SO_3H$ group. Additionally, the formation of Cys-Cu complexes was evidenced by Spectrometry, Electro Spin Resonance (ESR) and Nuclear Magnetic Resonance (NMR) (Rigo et al. 2004).

In order to assess the involvement of Cys in metal resistance, we first tried to assess the ability of Cys and several other AA (Met, His, Ala and Pro) to bind TM directly. Using a spectrometry-based protocol, we measured the absorbance of 50 µM of $CuSO_4$, $CdSO_4$, $AgNO_3$, $FeSO_4$, $ZnSO_4$ and $NiSO_4$ before ("T0" condition) and 5 minutes after they were mixed with 500 µM of L-Cys, L-Met, L-His, L-Ala or L-Pro ("T5" condition). A plate reader scanned and recorded the absorbance from 201 nm to 998 nM in the different conditions. All 6 tested metallic salts had a maximum absorption peak in the UV range (225 nm, 220 nm, 230 nm, 200 nm, 200 nm and 200 nm, respectively). The raw absorbance reads can be plotted, showing the differences between the T0 and T5 conditions (e.g., Fig. S6). However, to highlight the changes, the controls (the blank, AA and metal absorbance values) were subtracted from the T5 condition, so that the plotted curve only represent the effect the AAs had on the metals (Fig. 58 and Fig. S6).

When mixed with 0.5 mM L-Cysteine, the absorbances for $CuSO_4$, $AgNO_3$ and $CdSO_4$ increased drastically, while the absorbances for $FeSO_4$, $ZnSO_4$ and $NiSO_4$ seemed less impacted (Fig. 58 A). The $CuSO_4$ absorbance peak was slightly displaced to the right, now reaching its maximum at 245 nm (instead of 225 nm), and creating a right-sided shoulder on the curves (Fig. 58 A and Fig S5). The 245nm absorbance increased two-fold. A similar, albeit slightly weaker effect was observed for $CuCl_2$ and $CdSO_4$ (Fig. 58 A). The $AgNO_3$ condition also followed a similar trend (Fig. 58 A). Although the absorbance peak stayed at 230 nm like the T0 condition, the absorbance was increased and a shoulder can be observed on the right side of the slope (Fig. 48 A and Fig. S6). The $FeSO_4$, $ZnSO_4$, and $NiSO_4$ did not seem to react as strongly with Cys, although we cannot rule out the possibility that an effect would exist outside the recorded range, e.g., below 201 nm.

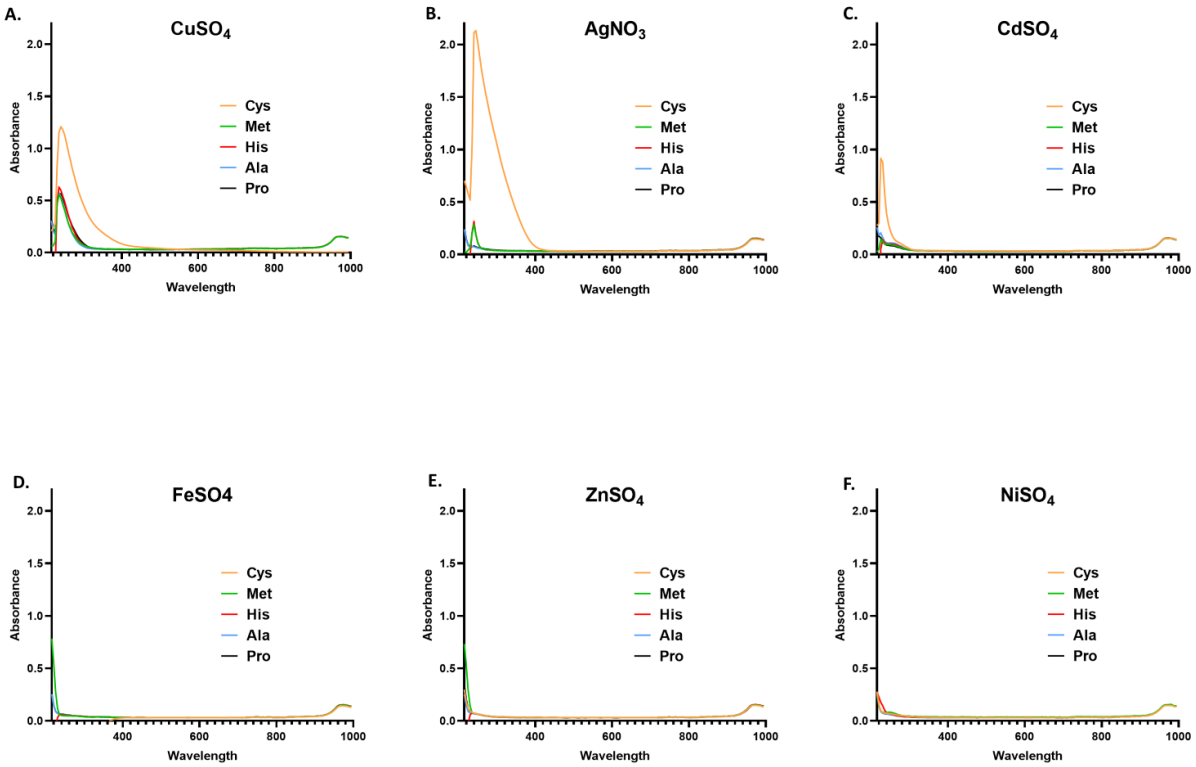

Fig. 59: Impact of AA on the absorbance of AA. Difference between the absorbance of metal alone and metals with AA, with the controls subtracted. Range of read from 201nm to 998nm. From A. to F.: 50 µM of $CuSO_4$, $CdSO_4$, $AgNO_3$, $FeSO_4$, $ZnSO_4$ and $NiSO_4$, respectively, each one in when placed in contact with 500 µM of either of L-Cys, L-Met, L-His, L-Ala or L-Pro

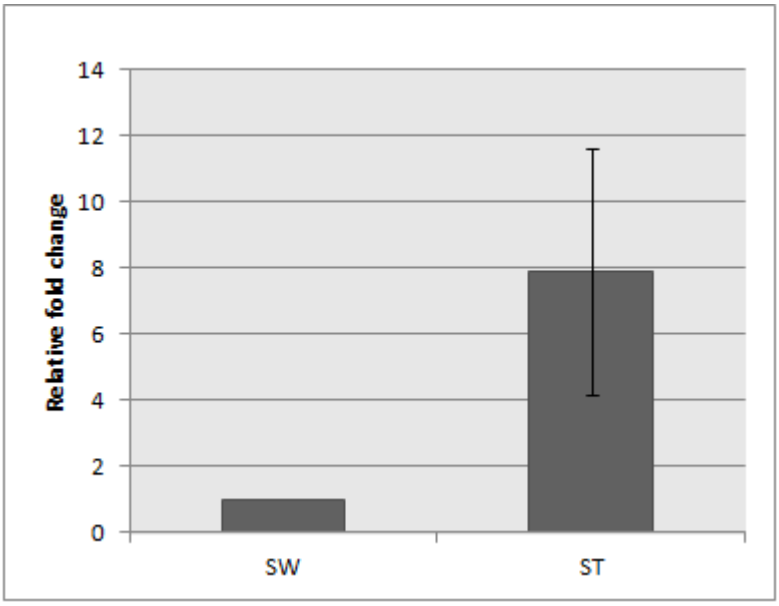

Fig. 60: qPCR performed on TmrP. The results is expressed in relative fold changes compared to the SW condition and calculated as $2^{-\Delta\Delta Ct}$. (biological replicates = 3, technical replicates 3). P value for the ST condition = 0.0851. The 16sRNA was used as control.

The experiment was also done with other AAs. $CuSO_4$ seems to react with every one of them, although in a lesser way than with L-Cys (Fig 58 A to E and Fig. 59 A). L-Met also seems prone to chelate metals. Outside of $CuSO_4$, L-Met also appears to bind $AgNO_3$, $FeSO_4$, and $ZnSO_4$ (Fig. 58 B). This is in line with the literature, as Met has been shown to bind a broad range of TM (Osman & Cavet 2008; Hilal et al. 2016; Bampidis et al. 2018; Deepak et al. 2017). The other tested AA do not highlight a strong interaction with the tested metals other than Cu, although a slight effect can be seen for some, for instance L-His with $AgNO_3$. In any case, the differences are milder than with Cys (Fig. 58 C to E). The changes in the peak of absorbance of $AgNO_3$ with L-Cys, for instance, is 5 times stronger than the changes with L-Met or L-His (Fig 59 B).

These data support the idea that Cys could chelate Cu^{2+}, Cd^{2+} and Ag^{+} but not Fe^{2+}, Ni^{2+} or Zn^{2+}. This is consistent with the role of TmrP in resistance against Cu, Cd and Ag. However, Cys may also have a more indirect effect through redox reaction, handling ROS and toxic by-products of metal excess.

iv. TmrP might more expressed in the ST cells than in the SW cells.

As the SW cells of *C. crescentus* can flee a stress (Lawarée et al. 2016), it may be less essential for them to possess numerous resistance and detoxification mechanisms, as it could be more costly energetically speaking. It has been demonstrated that there is very little PcoA and PcoB proteins present in the SW, while the number of transcript and protein increase drastically in the ST and PD cells, sessile (Lawarée et al. 2016). To investigate if a similar distribution applies to TmrP, we conducted qPCR experiment during the cell cycle.

A WT culture was synchronized. It was sampled a first time during the G1 SW phase, and a second time right before the G2 phase, when cells are in ST phase. Cells were lysed and RNA extracted, treated with DNAse and reverse-transcribed for qPCR. The *tmrP* mRNA level in the ST was compared to SW mRNA level. mRNA fold changes between conditions were calculated following the ΔΔCt method (Fig. 60). Despite a 8 fold change mean, the results is not quite statistically significant ($p = 0.0851$), possibly due the relatively low number of technical replicates (n=3) and/or biological replicates (n = 3).

More experiment would be needed to confirm or disprove this trend. Immunodetection could also be used to assess the protein level rather than the mRNA level.

Discussion

Impact of the Pco and Cus system on *C. crescentus* resistance to Cu

The periplasm of Gram-negative bacteria is likely to represent an important line of defense against exogenous metal stress. Therefore, identifying periplasmic resistance systems is of utmost interest to acquire a better understanding of the molecular mechanisms at play in these bacteria. In *C. crescentus*, we showed that a functional Pco system detoxifies and exports Cu outside the cell. However, the Cus system could not be confirmed as having the same Cu export function than it has in *E. coli*.

1. The role of PcoA and PcoB

Unsurprisingly, experimental data confirmed that PcoA is a periplasmic MCO. However, we also managed to shed some light on the function of PcoB, still poorly characterized even in the *E. coli* model. The experiments conducted on a *ΔpcoB* background hinted toward a role of efflux pump in *C. crescentus*. A fractionation assay successfully localized PcoB in the OM. However, albeit these data are consistent with the *in silico* predictions, several questions remain. Importantly, the way PcoB would be energized remains elusive. No ATPase domains are predicted in PcoB. As the periplasmic Cu concentration is often higher than the extracellular Cu concentration (Lawarée et al. 2016), a gradient-based may be possible. However, it could be argued that the Cu measured in this experiment is the total amount of Cu and not the free Cu that would contribute to the gradient. Hence, the presence and direction of an eventual gradient is unknown. It is not impossible however that the intrinsic physiochemical properties of PcoB would allow the export of Cu cations through PcoB without a third-party source of energy (Argüello, personal communication). Besides, the crystallization of PcoB may provide some additional clues about the energization question, although crystal structures of membrane proteins are usually difficult to obtain. The first crystallization attempts of PcoB, performed in collaboration with the chemistry department, proved unsuccessful. The ability for PcoB to bind Cu could, however, be tested in vitro, for instance via Microscale Thermophoresis (MST). MST is a fluorescence-based technique that can be used to measure the interaction between a known biomolecule and a ligand (Jerabek-willemsen et al. 2014). This technique could reinforce the hypothesis that PcoB is indeed a Cu efflux pump.

Another question that remains unanswered so far is the interaction between PcoA and PcoB. We tried to assess this interaction with a co-immunoprecipitation experiment but were unable to highlight any interaction in our test conditions. However, it may not be that surprising. As PcoB seems to be able to function alone (Fig. 25), one could argue it does not interact with PcoA. However, crystallization could once again bring further information on the issue.

2. The dynamic between the Pco and Cus system of C. crescentus seem peculiar

The Pco system appears crucial for *C. crescentus* resistance to Cu, while the Cus system does not seems to have much impact on it. Disruption mutants for the different Cus actors indeed did not increase Cu sensitivity in the tested condition (Fig. 30). This is a bit surprising considering it goes against what was known so far in the *E. coli* model. In *E. coli*, it had been reported that the Cue and Cus systems were acting as the first and second line of defense (Osman & Cavet 2008). The Pco system would be an auxiliary system, stepping in if the other 2 were overwhelmed by the Cu stress (Osman & Cavet 2008). The *Caulobacte*r case would therefore be rather peculiar, although some counterarguments have to be taken in account.

The proteins we labeled as the different Cus orthologs were selected via an *in silico* analysis, picking the best match from each Blast search. However, this led to the selection of proteins that are encoded by genes in three different operons, which is rather odd. In *E. coli*, the Cus complex is encoded by a single group of three genes, controlled by the same promoter. This may hint toward one or multiple duplications in *C. crescentus*, where the three operons would be paralogs. The duplications would create redundancy and would explain why no Cu sensitive phenotype was detected in the single-mutant growth curves experiments. This hypothesis also fits the results of the genetic screen performed by the group, where none of the genes encoding for the chosen proteins were found. Interestingly, the protein chosen as the CusA ortholog was still induced by a moderate Cu stress, and a gene (CCNA_0851) in operon with our *cusC* candidate was highlighted by the genetic screen (Fig. S3). This suggests that their two respective operons may still be involved in Cu resistance.

It would be interesting to engineer multi-knockout strains where all the 3 operons are impaired, for instance by excising all the orthologous genes for *cusB* or *cusC*. This could bring new information about the function of the Cus system in *C. crescentus*, and its importance for metal resistance. In addition, we could try growth curves experiments with other metals, like $AgNO_3$, as the Cus system in *E. coli* was shown to be not completely specific to Cu.

3. Evolution and Conservation of the Pco and Cus systems

a. Variation of conservation

The conservation of the Pco and Cus proteins varies. Both PcoA and CusA are the most conserved protein of their respective system. While *C. crescentus* needs both PcoA and PcoB to resist Cu in the conditions we tested, it is not farfetched to imagine that PcoA alone could be sufficient in some other species, or at least to imagine a system where the Cu ions detoxified by PcoA would be exported by another efflux system than PcoB. This would be similar to the Cue system, where no protein dedicated to the export of the Cu cations detoxified by CueO has been described.

Interestingly, our analyses might provide hindsight about a long-lasting question, which is the role of PcoC. PcoC is poorly characterized in *E. coli.* It is predicted as a Cu-binding protein that would interact with either PcoD or PcoA. Conservation data indicated that when a PcoC homolog is conserved, PcoA is nearly always present. However, the presence of PcoD does not seem mandatory. This suggest an interaction with PcoA rather than with PcoD. Co-immunoprecipitation or two-hybrids experiments may bring a more definitive closure to the subject.

CusA is more conserved than CusB or CusC. Akin to the hypothesis formulated for PcoA, maybe CusA could act independently of CusB and CusC in some bacteria. CusA might then function as a Cu-binding protein, or as a IM transporter, binding Cu cations in the cytoplasm and exporting them to the periplasm. This hypothesis is partially supported by the fact CusA has been shown to remain functional in absence of CusC in *E. coli* (Franke et al. 2003). While CusF and CusC were needed to provide complete and optimal resistance to Cu, CusA and CusB alone were sufficient to provide protection against a lesser Cu stress (Franke et al. 2003). This is a bit puzzling considering CusB had initially been described only as a relay bridging CusA to CusC, and helping to channel the ions through the periplasm. However, it also has been later described as accepting ions from the CusF chaperone. Recent developments put emphasis on the latter function, suggesting it may be CusB primary role, and stating that the metal relay hypothesis may be wrong (Chacón et al. 2014). Beside, CusB also has been reported as acting as a "switch" for CusA, allowing it to accept ions from CusF (Chacón et al. 2014; Delmar et al. 2015). This function may not be needed in the eventuality of CusA acting solely as an IM transporter.

However, there is another important point to consider. The blast search does not discriminate between orthologs and paralogs, and does not give any solid information about the function. Although we often tend to assume that two homologous proteins share the same role, the function of a protein may very well have slowly drifted over time. This can explain why some homologs of proteins usually belonging to a multipartite complex are found isolated in the genome.

For instance, it has been reported that, in *S. meliloti*, a "CusA-like" protein is present. This CusA-like protein is necessary not only to increase metal resistance in both *S. meliloti* and its host after symbiosis, but also to help symbiosis in the first place (Lu et al. 2017). A plant infected by a *ΔcusA*-like strain exhibits a lower number of nodules, and difficulties to grow even on uncontaminated soils (Lu et al. 2017). This CusA-like protein was described to have a 97% identity with the regular Cu/Ag exporting CusA of *S. meliloti*, and is thought to have emerged from a duplication event. It was found to be slightly truncated (Lu et al. 2017; Fagorzi et al. 2018). The gene encoding for this CusA-like protein is part of a four genes operon, comprising *copG*, the *cusA-like* gene, a *fixH*-like gene, and gene coding for a protein of unknown function (Fagorzi et al. 2018).

While this particular finding may not have influenced our results here (as all the symbionts but one possess the whole CusABC complex), it highlights the importance of discriminating between the protein of interest and eventual paralogs that would have drifted away from the original function. Besides, as the CusA-like protein is still reported to be important for Cu resistance, it could suggest it can work outside the CusABC complex and again explain why some species only possess CusA and not CusB and CusC.

It would therefore be necessary to run additional *in silico* analysis to ensure that the homologs found in the 206 species of alphaproteobacteria are indeed orthologs of the genes of interest and not homologs with a different function. We may also need to revise the thresholds selected, and set up stricter e value or AA length similarity filters.

b. Pathogenesis correlation

The correlation with pathogenesis also raises questions. The nutritional immunity strategy described in the literature would lead to think that pathogens do not need Cu resistance systems as much as other bacteria, as the host cell would try to deprive them of Cu (Braymer & Giedroc 2014; Espart et al. 2015). However, the strategy described in murine macrophages in case of salmonella infection is to increase the Cu concentration at infection site (Achard et al. 2012), which would argue in favor of a strong need for Cu resistance system for pathogens.

The pathogens in the alphaproteobacteria seem to be generally split into two clusters, one in the rhizobiales, and one in the rickettsiales (Fig. 45). As the rickettsiales seem largely deficient in Pco homologs, it would be interesting to analyze what are the differences with the rhizobiales pathogens. Both seem to share some similarities in term of hosts (several rhizobiales and rickettsiales both infect mammalians cells, for instance) but maybe the mean of infection, the subcellular replication niche, or mechanisms to avoid immune system detection are different. This could leads to different reaction of the immune system, maybe avoiding the Cu stress strategy of defense. If Rhizobiales are more likely to face toxic Cu concentration from the host, then it would make sense for this group to keep Pco proteins homologs. Rickettsiales are however known for their surprisingly small genome, and for their ability to escape the immune system (Merhej et al. 2011). This may be part of the explanation to why they seemingly do not require Pco homologs.

c. More information could be extracted from the *in silico* data

More information could be annotated on the phylogenetic tree. The origin of the homologs (whether they are encoded by a gene carried on a plasmid or a chromosome) could be mapped, as well as the environment. Additionally, it would be interesting to find a way to discriminate between a vertical transmission, inherited from a common ancestor, and homologs acquired by horizontal gene transfer (HGT). Detecting HGT events is known to be challenging (Adato et al. 2015; Trappe et al. 2016). Several detection methods exist. The phylogeny-based approach constructs the phylogeny lineage of the gene of interest, and compares it to a phylogenetic tree built with a reference gene (Adato et al. 2015). The comparison between the 2 may highlight HGT events. However, this approach is highly dependent on the target itself, as some genes may be not suited to infer a reliable tree, making the comparison difficult. The composition-based approach relies on detecting anomalies at the sequence level (changes in codon bias, GC content, etc.) to infer HGT events. This is not always perfect, as it would fail to detect HGT between species sharing roughly the same composition characteristics (Adato et al. 2015) . HGT events also can, in some cases, be detected by the traces they left, as some specific sequences or patterns can sometime be found flanking the inserted element (Cuecas et al. 2017).

Synteny-based search could also be performed. By looking at the positions of genes and their genomic environment, species-to-species divergences may be highlighted. Synteny-based comparison tools have been shown to work reliably and are freely available (Adato et al. 2015). In our analysis, however, these techniques would be difficult to set up. Most of them require to work on the nucleotides sequences, while our database is composed of AA sequences. The phylogeny-based approach could be attempted, as it can be performed with proteins instead of genes.

Characterization of the TmrP protein

We suggested a function for a uncharacterized ABC Transporter permease of *C. crescentus.* TmrP has been shown to be an IM protein involved in Cu, Cd and Ag resistance. Experiments imply that it exports Cys to the periplasm, which could provide resistance to these metals. Spectrometry also indicates that Cys could bind Cu, Cd, and Ag directly, but not the others tested metals.

This suggests that the observed effect on metal resistance may be due, at least partially, to direct chelation.

Direct binding of metal by Cys was demonstrated already (Wu et al. 2010; Rigo et al. 2004). While this chelation was proposed to play a role against metal toxicity in general (Rigo et al. 2004), it was not linked to an *in vivo* case in a particular bacteria. However, MT are shown to chelate similar metals (Cd, Ag, Cu, but also Zn, Hg or As) *in vivo* and are composed of up to 30% of Cys. MT and the Cys transported by TmrP are therefore likely to play a similar role. Indirect roles of Cys in metal resistance are also known, for instance via the formation of GSH. GSH has been shown to chelate metals, but is also likely, due to its antioxidant effect, to neutralize the ROS created by metal stress. The Cys exported by TmrP might be used for other processes in the periplasm, too.

However, as with Cu, Cys can rapidly become toxic as its concentration increases. The toxicity likely comes from the –SH group, highly reactive (Guédon & Martin-Verstraete 2006). Cys production and export therefore need to be tightly regulated. In *E. coli*, the CysB transcriptional regulator controls Cys synthesis. CysB is a multi-target activator, regulating positively many Cys-related genes. The *cysB gene* possesses two homologs in *C. crescentus*. Interestingly, both of them (CCNA_03625 and CCNA_01174) are found in the genetic screen done by the team, suggesting a relation to Cu resistance.

In addition, transcriptomic data provided by Laurens Maertens indicated that the expression of both *tmrP* and CCNA_01493, the Cys synthase identified in the genetic screen, may be induced by Cu. However, CCNA_03187, a homolog of *ydeD*, is not. In *E. coli*, *ydeD* encodes for a L-Cys transporter required for H_2O_2 tolerance (Ohtsu et al. 2010). However, these high-throughput transcriptomic data could be confirmed and expanded. For instance, in addition to the response to Cu, the induction by Cd and Ag stresses could be tested. Besides, we could test the inducibility at the protein level through the immunodetection of a tagged strain.

1. TmrP might react with other metals

These results shape a hypothesis where Cu (and potentially other metals) stresses may induce the expression of Cys synthases and Cys exporters. The efflux of Cys toward the periplasm would temporarily increase, allowing for periplasm detoxification by metal chelation. However, a question remains: Why does this putative chelation effect was only observed with 3 metals so far? Why would TmrP (or rather, the Cys it exports) confer resistance against Cu, Ag, Cd, but not the other metal we tested?

Although Cu, Ag and Cd are often cited together when it comes to resistance systems (Culotta & Scott 2013), Zn is generally considered in the same category. Yet, Zn resistance was not shown to be potentiated by Tmrp. Why?It might be related to atomic orbitals and the size of these atom nucleus.

The electronic configuration of Cu is [Ar]4s1 3d10. Thefore, the configuration of Cu^{2+} is [Ar]4s0 3d9, as the 4s subshell electron is removed first (flowing the “highest n” rule), then the one on 3d subshell. The configuration for Ag is [Ar]5s1 4d10. Ag^{+} is therefore [Ar]5s0 4d10. The configuration for Cd is [Kr]5s2 4d10, resulting thus for Cd^{2+} in [Kr] 5s0 4d10.

Cd and Ag have a similar electronic configuration. They are both in the 5th period of the periodic table, and both their respective ionic forms end up in a 4d10 configuration. Cu, however, is in 3d9. Both 4d10 and 3d9 configurations tend to react with sulfhydryl groups, as the reaction would be energetically favorable.

Curiously, Zn^{2+} ions also are in a 4d9 configuration, like Cu, and yet, do not appear to react with Cys in our condition. This might be explained by the nucleus size. Zn nucleus is smaller, and therefore the electrons spread around it are closer together than they would be if they were around a bigger nucleus, like the Cu nucleus. This proximity makes the disruption of the electron interactions harder. It may therefore take more energy to do so, or require an dedicated enzymatic process.

This hypothesis could be partially verified by testing other metals. According to this model, TmrP should confer resistance to Hg and Au as well. This could be tested by growth curves experiments.

2. The TmrP ATPase has yet to be identified, and the complex could interact with other proteins

As mentioned, the *tmrP* gene only encodes for the permease domain of the ABC transporter complex, and the gene encoding for the ATPase domains remains elusive so far. However, two potential candidates were identified, *CCNA_00188* and *CCNA_03681*. Both are annotated as genes encoding for ABC transporter ATP-binding proteins. Besides, both are not predicted to be in operon with a neighboring permease. *CCNA_00188* have been found several time among the hits of the genetic screen done by the group, and is *in silico* analysis predict its protein could be interacting with TmrP. *CCNA_03681* has not been found in the genetic screen yet, but preliminary mass spectrometry data (data not shown) suggested it could be in interaction with TmrP as well.

We engineered disruption strains for the genes encoding these two proteins. If one of these two proteins interacts with TmrP, then the mutant strain may present the same phenotype to Cu, Cd and Ag stress than the Δ*tmrP*. We are currently performing the growth curves measurements for these mutants in presence of the metals already tested with the Δ*tmrP*.

As a prospect, we also plan to check their interaction by an immunoprecipitation assay. In addition, we also would like to test the interaction of the TmrP with CCNA_01493, the Cys synthase found in the results of the genetic screen. However, it should be noted that the precise site of interaction is not known, and we ignore if CCNA_01493 would be interact with the ATPase domain or with the cytoplasmic part of the permase domain.

3. Is TmrP unique?

One of the questions that remains to be answered is how common this system would be. Is Cys export a widespread strategy to face transition metal stress? Is this another particularity of *C. crescentus*? We intend to answer this question by conduction bioinformatics analyses and estimate if we can extrapolate this system to other alphaproteobacteria.

Experimental procedures

Bioinformatics

1. Ortholog search

Ortholog searches were performed with the NCBI BLAST+ 2.4.0 command-line package, with an E value threshold of 9e-16. The "blastp" command was used on a database composed of proteomes of alphaproteobacteria recovered on NCBI via the Entrez utility. The "–num_descriptions 9999" and "-num_alignments 9999" were added as additional parameters.

2. Predictive tools

Various platforms and service were employed to make *in silico* predictions about the different Pco and Cus proteins, as well as the ABCT protein. The tools or website used were Foundation (http://www.pvcbacteria.org/foundation/prg/foundation_01.cgi), Biocyc (http://biocyc.org), HHPred, PatternSearch, HHOMP, Quick2D which all can be found in the MPI bioinformatic toolkit (https://toolkit.tuebingen.mpg.de). SignalP (http://www.cbs.dtu.dk/services/SignalP/), HMMER (https://www.ebi.ac.uk/Tools/hmmer/) and I-Tasser (https://zhanglab.ccmb.med.umich.edu/I-TASSER/). These services were used according to their respective guidelines.

3. Phylogenetic Tree

Alignments of the sequence were made via the command-line based version of Clustal Omega and the curation the resulting alignment was performed with Jalview (http://www.jalview.org). The phylogenetic tree was assembled via PhyML. The parameters used were an AIC selection, a BIONJ starting tree with NNI improvement and an aLRT SH-like statistical test for branch support. The visualization and annotation of the tree were done via the iTOL (interactive tree of life - http://itol.embl.de) online tool.

Strains, plasmids and growth conditions

The *C. crescentus* NA1000 WT strain was grown at 30°C, under moderate shaking, in Peptone Yeast Extract (PYE) medium (Poindexter 1981) with 5 µg/ml kanamycin, 5 µg/ml Nalidixic acid, and/or CuSO4.5H2O when required. Cultures in exponential phases were used for all experiments. Plasmids were mobilized from a DH10B *E. coli* strain into *C. crescentus* by triparental mating conjugation (Glazebrook & Walker 1991). The strains and plasmids are listed in Tables 3 and 4. The growth curves experiments on the Cus mutants were conducted by E. Lawarée and performed in Hutner base-Imidazole-buffered-Glucose-Glutamate (HIGG) minimal medium. Cysteine assays were performed in M2G (M2 minimal salts with a glucose carbon source, as detailed in (Hottes et al. 2004)). Synchronization experiments were performed according to (Evinger & Agabian 1977).

Table 3: **Table of the strains used for the experiments presented in this work**

Strains	Relevant genotype or description
CB15	Wild-type strain of C. crescentus
WT	CB15N (NA1000) synchronizable variant strain of CB15
ΔAB	Knockout strain for pcoAB genes
ΔAB EV	Knockout strain for pcoAB genes carrying an empty pMR10 KanR
ΔAB/pAB	Knockout strain for pcoAB genes carrying a copy of pcoAB of the pMR10 under control of the lac promoter; KanR
ΔABpA	Knockout strain for pcoAB gene carrying a copy of pcoA on the pMR10 under control of the lac promoter; KanR
ΔABpB	Knockout strain for pcoAB genes carrying a copy of pcoB on the pMR10 under control of the lac promoter; KanR
ΔA	Knockout strain for pcoA gene
ΔA EV	Knockout strain for pcoA genes carrying an empty pMR10 ;KanR
ΔApAB	Knockout strain for pcoA gene carrying a copy of pcoAB on the pMR10 under control of the lac promoter; KanR
ΔApA	Knockout strain for pcoA gene carrying a copy of pcoA on the pMR10 under control of the lac promoter; KanR
ΔB	Knockout strain for pcoB gene
ΔB EV	Knockout strain for pcoB genes carrying an empty pMR10; KanR
Δtmrp	Knockout strain for tmrp gene
Δtmrp/ptmrp	Knockout strain for tmrp gene carrying a copy tmrp on the pMR10 under control of the lac promoter
mCherry-tmrP	Knockout strain for *tmrp* gene carrying a copy of mCherry-tagged tmrp on the pMR10 under control of the lac promoter
dCCNA_001493	Mini-TN5 disruption knockout for the CCNA_001493 gene encoding for a cysteine synthase
dCCNA_02473	Mini-TN5 disruption knockout for the CCNA_02473 gene encoding for a CusA homolog
dCCNA_01261	Mini-TN5 disruption knockout for the CCNA_001261 gene encoding for a CusB homolog
dCCNA_00849	Mini-TN5 disruption knockout for the CCNA_00849 gene encoding for a CusC homolog
dCusR	Mini-TN5 disruption knockout for a gene encoding for a CusR homolog
dCusS	Mini-TN5 disruption knockout for a gene encoding for a CusS homolog
DH10B	DH10B *E. coli* strain used for transformation and conjugation
S17-1	*E. coli* strain RP4-2, Tc::Mu, KM-Tn7, for plasmid mobilization

1. Construction of clean knockout mutants

The respective upstream and downstream regions (500 bp each) of the target genes were amplified by PCR from the NA1000 genomic DNA (The respective primer sequences are listed in Table 4). The up- and downstream PCR products were cloned separately into a pSK-oriT plasmid linearized by the EcoRV from Roche with the SuRE/Cut Buffer System. Each insert was then excised from the plasmid by using restriction enzymes and cloned together into a pNPTS138 plasmid restricted with the 5' restriction enzyme from the upstream insert and 3' enzyme from the downstream one. The ligation product was transformed in DH10B E. coli strain. A triparental mating was performed between the DH10B *E. coli* strain (now carrying the pNPTS138 with the flanking region of the target gene), an *E. coli* Helper strain and the NA1000 strain. The pNPTS138 integrative vector carries genes coding for kanamycin resistance and sucrose sensitivity. The plasmid is unable to replicate in *C. crescentus*. A first selection for kanamycin-resistant clones was conducted to select for bacteria that have integrated the plasmid in their genome by homologous recombination. The second recombination event was selected by growing kanamycin-resistant clones overnight in PYE medium and then plating bacteria on PYE plates containing 3% sucrose. The loss of the plasmid therefore resulted in either a clean knockout for the target gene or a wild-type strain. A last PCR was performed to determine the genotype of each clone and the strain was sequenced to ensure the lack of mutation.

2. Construction of complementation strain

The genomic sequence of the target gene was amplified from the NA1000 by PCR. The was inserted into an EcoRV-linearized pSK-oriT vector. The insert was then excised using restriction enzyme and ligated into a replicative pMR10 plasmid, previously restricted with the same enzymes. Via triparental mating, the resulting plasmid was then introduced into a *C. crescentus*, mutated for the target gene (clean knockout or disruption knockout). The clones containing the pMR10-carrying gene were checked by a diagnostic and sequenced

Table 4: **Table of the primers used for the various genetic constructions presented in this work**

Primer name	5' to 3' primer sequence
Am_02327_ER1_F	GAATTCGAGGGAGCCGCGCGGCCCGACAGG
Am_02327_Xba1_R	TCTAGACGGCGGATCTCACGCTGGTAGAGC
Av_02327_XbaA_F	GCTCTAGACTCGATCGCGATCGGCGTCG
Av_02327_BamH1_R	CGGGATCCATCCGGTAGATATTGGAGACG
AmontpcoAFEcorI	CGGAATTCCGCAGCGCTACTCCGCCACGAT
AmontpcoARXbaI	GCTCTAGAGCCTTGGGTATCACGCGAGCCA
AvalpcoAFXbaI	GCTCTAGAGCAGCCCGGCGACTGGGCCTTC
AvalpcoARHindIII	CCCAAGCTTGGGGGCCTTCAGGCCCTCCAGCT
AmontpcoBFEcoRI	CGGAATTCGCCTCTATCCGCCCAAGGAC
AmontpcoBRXbaI	GCTCTAGAGCCCTGTGATGGGCGTGCGG
AvalpcoBFXbaI	GCTCTAGAATGTCGGCGTGGTGCGCGAG
AvalpcoBRHindIII	CCCAAGCTTAGCTGCGCGAAGGTCGTCTC
pPcoAFEcoRI	CGGAATTCCAGGCGGGCTTGCCGTCCAG
PcoARSacI	CGAGCTCTCACGCGGCGGCTCCATCGA
pPcoARNcoI	CATGCCATGGTTGGGTATCACGCGAGCCAT
pcoBFNcoI	CATGCCATGGACGAGCCCGGCGACTGGGCC
mCherry_F_Nt_H3	CCCAAGCTTATGGTGAGCAAGGGC
mChe_R_Nt_EcoRI	GAGAATTCTCTTGTACAGCTCGTCC
ABCT_F_MchNT_EcI	AGAATTCTCATGAGAGACACGGCCGAGAGC
ABCT_R_MchNT_SPI	CACTAGTTCAGCTCTTGAGACGGTAACCG
ABCT_F_MchCt_H3	CCCAAGCTTATGAGAGACACGGCCGAGAGC
ABCT_R_MchCt_EcI	GAGAATTCTGCTCTTGAGACGGTAACCG
mCherry_F_Ct_EcI	AGAATTCTCATGGTGAGCAAGGGCGAGG
mChe_R_Ct_SPEI	GACTAGTTTACTTGTACAGCTCGTCCATGC

Protocols

1. Growth curve measurements

C. crescentus cultures were collected in exponential growth phase (O.D. $_{660\ nm}$ of 0) and diluted in PYE medium to a final O.D. $_{660\ nm}$ of 0.05. Bacteria were inoculated in 96-well plates with appropriate $CuSO_4$, $ZnSO_4$, $CdSO_4$, $AgNO_3$, $FeSO_4$, $NiSO_4$ or $MnSO_4$ concentrations if needed. Bacteria were then grown for 24 h at 30°C under continuous shaking in an Epoch 2 Microplate Spectrophotometer from BioTek. The absorbance at O.D. $_{600\ nm}$ was measured every 10 min.

2. Membrane fractionation assays

The inner and outer membrane fractions of *C. crescentus* were harvested by ultracentrifugation after Sodium Lauryl Sarconisate (SLS) and Sodium Carbonate treatment as described in (Cao et al. 2012). 400 ml of cell culture were grown in PYE at 30°C to an O.D.660 of 0.4. Bacteria were centrifuged for 10 min at 4000 x g at 4°C, and washed 3 times in 50 ml of 50 mM (pH 8) Ammonium bicarbonate (AmBic). Cells were finally resuspended in 5 ml AmBic and sonicated on ice (20 rounds of 5 seconds sonication at maximum intensity). The lysate was centrifuged for 20 min at 12,000 x g at 4°C and the pellet containing the unbroken cells and debris was discarded. The supernatant was then ultracentrifuged for 40 min at 100,000 x g in order to dissociate the cytoplasmic fraction (supernatant) from the total membrane fraction (pellet). The pellet was then resuspended in 1 ml of 1% Sodium Lauryl Sarconisate and centrifuged for another 40 min at 100,000 x g and 4°C. The subsequent supernatant contains the solubilized inner membrane (SIM). The pellet containing the outer membrane (OM) fraction was washed in 1 ml of 2.5 M NaBr and incubated for 30 min on ice. It was then ultracentrifuged for 40 min at 100,000 x g at 4°C. The supernatant was discarded and the pellet was incubated for 1 h in 1 ml of 100 mM Na2CO3 for further enrichment of the outer membrane fraction, before being spun again for 40 min at 100,000 x g at 4°C. The various fractions collected were as samples for immunodetection experiments.

3. Immunodetection (Western blotting)

Exponentially growing cells were pelleted and resuspended in SDS-PAGE loading buffer. Boiled protein samples were then resolved on 12% sodium dodecyl sulfate-polyacrylamide gels and electrotransferred to Nitrocellulose membranes. Nitrocellulose membranes were probed with polyclonal rabbit anti-PcoA (1:5000), anti-PcoB (1:1000), anti-dsRed (1:5000), anti-CtrA (1:5000), anti-CckA (1:5000), anti-RsaF (1:5000) or anti-DivK (1:1000) antibodies. Polyclonal goat antirabbit immunoglobulins/HRP secondary antibody is used at 1:5000 (DAKO).

4. Fluorescence microscopy

Cells in exponential growth phase were immobilized on 1.5% agarose M2G pads. Fluorescence microscopy was performed using a Zeiss Axio Imager.Z1 microscope equipped with a Zeiss 100X/1.3 Oil Ph3 objective and appropriate filter sets. Images were collected with a Hamamatsu C11440 digital camera. All image capture and processing were performed with the Zen Pro 2012 software (blue version).

5. Oxidase assay

The oxidase activity of PcoA and PcoB was assessed in vitro by measuring their oxygen consumption rate with an oxygraph (Hansatech Instruments Ltd) when mixed with a Cu^{+} substrate as described for CueO in (Achard et al., 2010). Briefly, 50 µg of recombinant PcoAHis or PcoB-His are resuspended in 700 µL of 0.1 M sodium acetate buffer (pH 5.5), loaded in the Oxygraph sensor cell and supplemented with 1 mM CuSO4 in order to fill the labile copper ligation site. Three min later, 500 µM solubilized Tetrakis(acetonitrile)copper(I) hexafluorophosphate ([Cu(CH3CN)4]PF6, Sigma Aldrich) substrate are added as a caged source of Cu+. The oxygen consumption is recorded with the Oxygraph for 30 min, and the data are then plotted. Bovine Serine Albumin (50 µg) was used as a negative control.

6. Cellular fractionation for Cysteine assays and ICP-OES

C. crescentus cultures (30 ml) are grown up to exponential phase ($O.D._{660\ nm}$ = 0.4). A 5 minute Cu treatement is done if necessary. The cultures are split in two sample of 15ml each and centrifuged for 5 min at 8000 x g at 4°C. The resulting pellet is resuspended in 15 ml of PFA 2% and incubated on ice for 20 min for fixation. The cells are then centrifuged and washed 3 times (5 min at 8000 x g at 4°C and washed in 5 ml of Cold Wash Buffer (10 mM Tris-HCl, pH 6.8 + 100 µM EDTA). After the third wash, the supernatant is discarded. One of the 2 pellet is resuspended in 2 ml of HNO3 1M – this will be the total fraction. The other pellet is mixed with 3 ml of Zwittergent 0.25%. The resulting mix was incubated for 10 minutes at room temperature and centrifuged for 15 min at 19,000 x g. The supernatant, containing the periplasmic components, was separated from the cytoplasmic pellet.

For Cysteine assays: The periplasmic fraction is kept as is. The cytoplasmic fraction is resuspended in 2 ml of ZW buffer. The sample are kept overnight at 4°C. The total and cytoplasmic fractions are then lysed via French Press, and all fractions are centrifuged a last time (5 min at 6000 x g). The supernatant is then processed as described in pt. 7.

For ICP-OES analyses: The periplasmic fraction is mixed with HNO3 10M for a final concentration of HNO3 1M. The cytoplasmic fraction is resuspended in 2 ml HNO3 1M. The sample are kept overnight at 4°C. The total fraction is then lysed via French Press, and all fractions are centrifuged a last time (5 min at 6000 x g). Inductively coupled plasma - optical emission spectrometry measurement were conducted on Total, periplasmic and cytoplasmic fractions.

7. Cysteine Assay

Quantification of Cys in different samples was assessed through a colorimetric method. *C. crescentus* cultures were grown in M2G to exponential phase (60 ml; $O.D._{660\ nm}$ = 0.4). A fractionation assay was conducted as described above (cfr. Cellular fractionation for ICP-OES) to recover the total, periplasmic and cytoplasmic fraction of the different strains. The nihydrin colorimetric assay was then performed according to the protocol described in (Gaitonde 1967).

8. Motility Assay

C. crescentus cultures were grown in M2G to exponential phase (5 ml; $O.D._{660\ nm}$ = 0.4). The cultures were then diluted to 0.5 and inoculated with sterile toothpicks on a M2G swarming plates (M2G + 0.25% agar). The plates were incubated at 30°C for 3 days, then scanned. The area of the motility halos were then measured via the analyze/measure function of ImageJ.

9. Absorbance peak

The Epoch 2 Microplate Spectrophotometer from BioTek was used to measure the absorbance of 50 µM of $CuSO_4$, $CdSO_4$, $AgNO_3$, $FeSO_4$, $ZnSO_4$ and $NiSO_4$ in water, and in solutions containing 500 µM of L-Cys, L-Met, L-His, L-Ala, or L-Pro. The mix was prepared and injected into the wells of a 96-wells plate and placed in the microplate reader after 5 minutes. The wavescan function was employed. The absorbance of each well from 201 nm to 998 nm was recorded.

10. qPCR

Bacteria (50 ml) cultivated in HIGG at 30 °C (OD660 = 0.4) were collected by centrifugation. The recovered pellet was washed twice in sterile PBS and finally resuspended in 100 µl of 10% SDS and 20 µl proteinase K (proteinase K, recombinant, PCR Grade, Roche). The resuspended pellet was incubated for 1 h at 37 °C under mild shaking. A guanidinium thiocyanate-phenol-chloroform extraction was then conducted with TriPure Isolation Reagent (Roche), as described in the protocol available on the manufacturer's website. RNA (2 µg) was treated for 30 min with DNAse I (Thermo Scientific) at 37 °C followed by DNAse I inactivation with 50 mM EDTA for 10 min at 65 °C. The RNA was then reverse transcribed with Superscript II reverse transcriptase (Invitrogen) with hexamer random primers as described by the manufacturer. A condition without reverse transcriptase was also conducted in parallel as a negative control. cDNA (0.3 µg) was then mixed with SybrGreen mix (FastStart Universal SYBR Green Master (Rox); Roche) and the appropriate primers sets and subjected to qPCR in a LightCycler96 (Roche). A total of 45 three-step cycles were performed as follows: 95 °C for 10 s, 60 °C for 10 s and 72 °C for 10 s. Melting curves were then performed to assess primer specificity. Target mRNAfold change was calculated as $2^{-\Delta\Delta Ct}$, where 16S RNA was used as the reference gene.

Bibliography

Abraham, W. et al., 1999. Phylogeny and polyphasic taxonomy of Caulobacter species. Proposal of Maricaulis gen. nov. with Maricaulis maris (Poindexter) comb. nov. as the type species, and emended description of the genera Brevundirnonas and Caulobacter. *International Journal of Systematic Biology*, 49, pp.1053–1073.

Achard, M.E.S. et al., 2012. Copper redistribution in murine macrophages in response to Salmonella infection. *Biochemical Journal*, 444, pp.51–57.

Adato, O. et al., 2015. Detecting Horizontal Gene Transfer between Closely Related Taxa. *PLoS Computational Biology*, 11(10), pp.1–23.

Adriano, D., 2001. *Trace Elements in Terrestrial Environments: Biogeochemistry, Bioavailability, and Risks of Metals*, Springer Science+Business Media LLC.

Almiron, M. et al., 1992. A novel DNA-binding protein with regulatory and protective roles in starved Escherichia coli. *Genes and Development*, 6(12 B), pp.2646–2654.

Andrews, S.C., Robinson, A.K. & Rodríguez-Quiñones, F., 2003. Bacterial iron homeostasis. *FEMS Microbiology Reviews*, 27(2–3), pp.215–237.

Argüello, J.M., Gonzalez-Guerrero, M. & Raimunda, D., 2011. Bacterial Transition Metal P1B - ATPases, Transport Mechanism and Roles in Virulence. *Biochemistry*, 50(46), pp.9940–9949.

Argüello, J.M., Raimunda, D. & Padilla-Benavides, T., 2013. Mechanisms of copper homeostasis in bacteria. *Frontiers in Cellular and Infection Microbiology*, 3(November), pp.1–14. Available at: http://journal.frontiersin.org/article/10.3389/fcimb.2013.00073/abstract.

Bagai, I. et al., 2008. Direct Metal Transfer between Periplasmic Proteins Identifies a Bacterial Copper Chaperone. *Biochemistry*, 47(44), pp.11408–11414.

Baker, D. & Czarnecki-maulden, G., 1987. Pharmacologie Role of Cysteine in Ameliorating or Exacerbating Mineral Toxicities1. *The Journal of Nutrition*, 117(6), pp.1003–1010.

Ballatori, N., 1994. Glutathione Mercaptides as Transport Forms of Metals. *Advances in Pharmacology*, 27(C), pp.271–298.

Bampidis, V. et al., 2018. Safety of zinc chelate of methionine sulfate for the target species. *EFSA Journal*, 16(10).

Barkay, T., Miller, S.M. & Summers, A.O., 2003. Bacterial mercury resistance from atoms to ecosystems. *FEMS Microbiology Reviews*, 27(2–3), pp.355–384.

Becker, K.W. & Skaar, E.P., 2014. Metal limitation and toxicity at the interface between host and pathogen. *FEMS Microbiology Reviews*.

ter Beek, J., Guskov, A. & Slotboom, D.J., 2014. Structural diversity of ABC transporters. *The Journal of General Physiology*, 143(4), pp.419–435.

Beinert, H., 2000. Iron-sulfur proteins: ancient structures, still full of surprises. *Journal of Biological Inorganic Chemistry*, 5(1), pp.2–15. Available at: http://link.springer.com/10.1007/s007750050002.

Van Beneden, P.J., 1878. *Les commensaux et les parasites dans le règne animal* Nabu Press., Germer Baillère.

Benson, D.R. & Rivera, M., 2013. *Metallomics and the Cell*, Available at: http://link.springer.com/10.1007/978-94-007-5561-1.

Bijlsma, R., 1997. *Environmental Stress , Adaptation and Evolution* Springer. R. Bijlsma & V. Loeschchke, eds., Springer Basel AG.

Blanco, P. et al., 2016. Bacterial Multidrug Efflux Pumps: Much More Than Antibiotic Resistance Determinants. *Microorganisms*, 4(1), p.14. Available at: http://www.mdpi.com/2076-2607/4/1/14.

le Blastier, S. et al., 2010. Phosphate starvation triggers production and secretion of an extracellular lipoprotein in Caulobacter crescentus. *PLoS ONE*, 5(12).

Bleriot, C. et al., 2011. RcnB is a periplasmic protein essential for maintaining intracellular Ni and Co concentrations in Escherichia coli. *Journal of Bacteriology*, 193(15), pp.3785–3793.

Bock, T., 2015. Using Correspondence Analysis to Find Patterns in Tables. *Displayr*. Available at: https://www.displayr.com/correspondence-analysis-to-find-patterns-in-tables/ [Accessed January 5, 2019].

Borkow, G. & Gabbay, J., 2005. Copper as a biocidal tool. *Current medicinal chemistry*, 12(18), pp.2163–2175.

Braymer, J.J. & Giedroc, D.P., 2014. Recent developments in copper and zinc homeostasis in bacterial pathogens. *Current Opinion in Chemical Biology*, 19, pp.59–66. Available at: http://dx.doi.org/10.1016/j.cbpa.2013.12.021.

Braz, S. & Marques, M. V, 2005. Genes involved in cadmium resistance in Caulobacter crescentus. *FEMS Microbiology Letters*, 251, pp.289–295.

Breasted, J.H., 1930. *The Edwin Smith Surgical Papyrus - Published in facsimile and hieroglyphic transliteration with translation and commentary* The Univer. J. H. Breasted, ed., Chicago.

Brown, N.L. et al., 1995. Molecular genetics and transport analysis of the copper-resistance determinant (pco) from Escherichia coil plasmid pRJ1004. *Molecular Microbiology*, 17(6), pp.1153–1166.

Bruins, M.R., Kapil, S. & Oehme, F.W., 2000. Microbial Resistance to Metals in the Environment. *Ecotoxicology and Environmental Safety*, 45(3), pp.198–207. Available at: http://linkinghub.elsevier.com/retrieve/pii/S0147651399918602.

Butterfield, C.N. et al., 2013. Mn(II,III) oxidation and MnO2 mineralization by an expressed bacterial multicopper oxidase. *Proceedings of the National Academy of Sciences*, 110(29), pp.11731–11735. Available at: http://www.pnas.org/cgi/doi/10.1073/pnas.1303677110.

Cao, Y., Johnson, H.M. & Bazemore-Walker, C.R., 2012. Improved enrichment and proteomic identification of outer membrane proteins from a Gram-negative bacterium: Focus on Caulobacter crescentus. *Proteomics*, 12(2), pp.251–262.

Carrondo, M.A., 2003. Ferritins, iron uptake and storage from the bacterioferritin viewpoint. *EMBO Journal*, 22(9), pp.1959–1968.

Castresana, J., 2000. Selection of Conserved Blocks from Multiple Alignments for Their Use in Phylogenetic Analysis. *Molecular Biology and Evolution*, 17(4), pp.540–552.

Chacón, K.N. et al., 2014. Tracking metal ions through a Cu/Ag efflux pump assigns the functional roles of the periplasmic proteins. *Proceedings of the National Academy of Sciences*, 11(43), pp.15373–15378.

Chandrangsu, P., Rensing, C. & Helmann, J.D., 2017. Metal homeostasis and resistance in bacteria. *Nature Reviews Microbiology*, 15(6), pp.338–350.

Changela, A. et al., 2003. Molecular basis of metal-ion selectivity and zeptomolar sensitivity by CueR. *Science (New York, N.Y.)*, 301(5638), pp.1383–1387.

Chao, Y. & Fu, D., 2004. Kinetic Study of the Antiport Mechanism of an Escherichia coli Zinc Transporter, ZitB. *Journal of Biological Chemistry*, 279(13), pp.12043–12050.

Chaturvedi, K.S. et al., 2013. The siderophore yersiniabactin binds copper to protect pathogens during infection. *Nature chemical biology*, 8(8), pp.731–736.

Chloupková, M., LeBard, L.S. & Koeller, D.M., 2003. MDL1 is a high copy suppressor of ATM1: Evidence for a role in resistance to oxidative stress. *Journal of Molecular Biology*, 331(1), pp.155–165.

Cobine, P. et al., 1999. The Enterococcus hirae copper chaperone CopZ delivers copper(I) to the CopY repressor. *FEBS Letters*, 445(1), pp.27–30.

Cobine, P.A. et al., 2002. Copper transfer from the Cu(I) chaperone, CopZ, to the repressor, Zn(II)CopY: Metal coordination environments and protein interactions. *Biochemistry*, 41(18), pp.5822–5829.

Colaço, H.G. et al., 2016. Roles of Escherichia coli ZinT in cobalt, mercury and cadmium resistance and structural insights into the metal binding mechanism. *Metallomics*, 8(3), pp.327–336. Available at: http://xlink.rsc.org/?DOI=C5MT00291E.

Cortes Castrillona, L., Wedd, A.G. & Xiao, Z., 2015. The functional roles of the three copper sites associated with the methionine-rich insert in the multicopper oxidase CueO from E. coli. *Metallomics*. Available at: http://xlink.rsc.org/?DOI=C5MT00001G.

Cotton, G. et al., 1999. *Advanced Inorganic Chemistry, 6th edition* Wiley-In. W.- Interscience, ed., Wiley - Interscience.

Cruz-ramos, H. et al., 2004. Membrane topology and mutational analysis of Escherichia coli CydDC , an ABC-type cysteine exporter required for cytochrome assembly Printed in Great Britain. *Microbiology*, 150, pp.3415–3427.

Cuecas, A., Kanoksilapatham, W. & Gonzalez, J.M., 2017. Evidence of horizontal gene transfer by transposase gene analyses in Fervidobacterium species. *PLoS ONE*, 12(4), pp.1–21.

Culotta, V. & Scott, R.A., 2013. *Metals in Cells* V. Culotta & R. A. Scott, eds., Wiley.

Curtis, P.D. & Brun, Y. V., 2014. Identification of essential alphaproteobacterial genes reveals operational variability in conserved developmental and cell cycle systems. *Molecular Microbiology*, 93(July), pp.713–735. Available at: http://onlinelibrary.wiley.com/store/10.1111/mmi.12686/asset/mmi12686.pdf?v=1&t=hypmjt7y&s=77dffe4d27bea041ec0507bd14edb6704804d477.

Curtis, P.D. & Brun, Y. V, 2010. Getting in the loop: regulation of development in Caulobacter crescentus. *Microbiology and molecular biology reviews : MMBR*, 74(1), pp.13–41.

Dann, C.E. et al., 2007. Structure and Mechanism of a Metal-Sensing Regulatory RNA. *Cell*, 130(5), pp.878–892.

Das, S. & Dash, H.R., 2017. *Handbook of Metal-Microbe Interactions and Bioremediation* S. Das & H. R. Dash, eds., CRC Press.

Das, S. & Dash, H.R., 2018. *Microbial Diversity in the Genomic Era* S. Das & H. R. Dash, eds., Elsevier Academic Press.

Deepak, R.N.V.K., Chandrakar, B. & Sankararamakrishnan, R., 2017. Biophysical Chemistry Comparison of metal-binding strength between methionine and cysteine residues : Implications for the design of metal-binding motifs in proteins. *Biophysical Chemistry*, 224, pp.32–39. Available at: http://dx.doi.org/10.1016/j.bpc.2017.02.007.

Delmar, J., Su, C.-C. & Yu, E., 2013. Structural Mechanisms of heavy-metal extrusion by the Cus efflux system. *Biometals*, 26(4), pp.593–607.

Delmar, J.A., Su, C. & Yu, E.W., 2015. Heavy metal transport by the CusCFBA efflux system. *Protein Science*, 24, pp.1720–1736.

Djoko, K.Y. et al., 2010. Reaction mechanisms of the multicopper oxidase CueO from Escherichia coli support its functional role as a cuprous oxidase. *Journal of the American Chemical Society*, 132(6), pp.2005–2015.

Dolédec, S. & Chessel, D., 2006. Co-inertia analysis : an alternative method for studying species-environment relationships. *Freshwater Biology*, 3, pp.277–294.

Dupont, C.L., Grass, G.B. & Rensing, C., 2011. Copper toxicity and the origin of bacterial resistance - new insights and applications. *Metallomics*.

Espart, A. et al., 2015. Understanding the 7-Cys module amplification of *C . neoformans* metallothioneins: how high capacity Cu-binding polypeptides are built to neutralize host nutritional immunity. *Molecular Microbiology*, 98(5), pp.977–992. Available at: http://doi.wiley.com/10.1111/mmi.13171.

Evinger, M. & Agabian, N., 1977. Envelope-Associated Nucleoid from Caulobacter crescentus Stalked and Swarmer Cells. *Journal of Bacteriology*, 132(1), pp.294–301.

Fagorzi, C. et al., 2018. Harnessing Rhizobia to Improve Heavy-Metal Phytoremediation by Legumes. *Genes*, 9(542).

Failla, M.L., 2003. Trace Elements and Host Defense : Recent Advances and and Continuing Challenges. *Immunity*, pp.1443–1447.

Fairman, J.W., Noinaj, N. & Buchanan, S.K., 2012. The structural biology of β-barrel membrane proteins: a summary of recent reports. *Current Opinion in Structural Biology*, 21(4), pp.523–531.

Fath, M.J. & Kolter, R., 1993. ABC transporters: bacterial exporters. *Microbiol Rev*, 57(4), pp.995–1017. Available at: http://www.ncbi.nlm.nih.gov/pubmed/8302219.

Festa, R. a. & Thiele, D.J., 2011. Copper: An essential metal in biology. *Current Biology*, 21(21), pp.R877–R883. Available at: http://dx.doi.org/10.1016/j.cub.2011.09.040.

Fontecave, M. & Ollagnier-de-Choudens, S., 2008. Iron-sulfur cluster biosynthesis in bacteria: Mechanisms of cluster assembly and transfer. *Archives of Biochemistry and Biophysics*, 474(2), pp.226–237.

Franke, S. et al., 2003. Molecular Analysis of the Copper-Transporting Efflux System CusCFBA of Escherichia coli. *Journal of Bacteriology*, 185(13), pp.3804–3812.

Fullmer, C.S., Edelstein, S. & Wasserman, R.H., 1985. Lead-binding properties of intestinal calcium-binding proteins. *Journal of Biological Chemistry*, 260(11), pp.6816–6819.

Furnholm, T.R. & Tisa, L.S., 2014. The ins and outs of metal homeostasis by the root nodule actinobacterium Frankia. *BMC genomics*.

Futai, M., Wada, Y. & Kaplan, J.H., 2004. *Handbook of ATPases - Biochemistry, Cell Biology, Pathophysiology* Wiley-VCH. M. Futai, Y. Wada, & J. H. Kaplan, eds., Weinheim: Wiley.

Gadgil, M., Kapur, V. & Hu, W., 2005. Transcriptional Response of Escherichia coli to Temperature Shift. *Biotechnology progress*, 21, pp.689–699.

Gaitonde, M.K., 1967. A Spectrophotometric Method for the Direct Determination of Cysteine in the Presence of Other Naturally Occurring Amino Acids. *Biochemical Journal*, 104(2), pp.627–633.

Galli, I., Musci, G. & Bonaccorsi Di Patti, M.C., 2004. Sequential reconstitution of copper sites in the multicopper oxidase CueO. *Journal of Biological Inorganic Chemistry*, 9(1), pp.90–95.

Glazebrook, B.J. & Walker, G.C., 1991. Genetic Techniques in Rhizobium meliloti. , 204(1989), pp.398–418.

Gordge, M.P. et al., 1995. Copper chelation-induced reduction of the biological activity of S-nitrosothiols. *British journal of pharmacology*, 114(5), pp.1083–1089.

Graham, S.C. et al., 2006. Kinetic and crystallographic analysis of mutant Escherichia coli aminopeptidase P: Insights into substrate recognition and the mechanism of catalysis. *Biochemistry*, 45(3), pp.964–975.

Graham, S.C. & Guss, J.M., 2008. Complexes of mutants of Escherichia coli aminopeptidase P and the tripeptide substrate ValProLeu. *Archives of Biochemistry and Biophysics*, 469(2), pp.200–208.

Grass, G. & Rensing, C., 2001. CueO is a multi-copper oxidase that confers copper tolerance in Escherichia coli. *Biochemical and biophysical research communications*, 286, pp.902–908.

Grass, G., Rensing, C. & Solioz, M., 2011. Metallic copper as an antimicrobial surface. *Applied and Environmental Microbiology*, 77(5), pp.1541–1547.

Guan, G. et al., 2015. PfeT, a P1B4 -type ATPase, effluxes ferrous iron and protects Bacillus subtilis against iron intoxication. *Molecular Cell*, 98(4), pp.787–803.

Guédon, E. & Martin-Verstraete, I., 2006. Cysteine Metabolism and Its Regulation in Bacteria. In *Microbiology Monographs*.

Guindon, S. & Gascuel, O., 2003. A Simple, Fast, and Accurate Algorithm to Estimate Large Phylogenies. *Systematic Biology*, 52(5), pp.696–704.

Haferburg, G. & Kothe, E., 2007. Microbes and metals: Interactions in the environment. *Journal of Basic Microbiology*, 47(6), pp.453–467.

Hamer, D.H., 1986. Metallothionein. *Annual Review of Biochemistry*, 55, p.913.

Hao, X. et al., 2016. A role for copper in protozoan grazing - two billion years selecting for bacterial copper resistance. *Molecular microbiology*, pp.2–35. Available at: http://www.ncbi.nlm.nih.gov/pubmed/27528008.

Harrison, J.J., Turner, R.J. & Ceri, H., 2005. Persister cells, the biofilm matrix and tolerance to metal cations in biofilm and planktonic Pseudomonas aeruginosa. *Environmental Microbiology*, 7(7), pp.981–994.

Harrison, M.D., Jones, C.E. & Dameron, C.T., 1999. Copper chaperones: Function, structure and copper-binding properties. *Journal of Biological Inorganic Chemistry*, 4, pp.145–153.

Hawkes, S.J., 1997. What Is a "Heavy Metal"? *Journal of Chemical Education*, 74(11), p.1374. Available at: http://pubs.acs.org/doi/abs/10.1021/ed074p1374.

He, D. et al., 2016. Structural characterization of encapsulated ferritin provides insight into iron storage in bacterial nanocompartments. *eLife*, 5(AUGUST), pp.1–31.

Helbig, K. et al., 2008. Glutathione and transition-metal homeostasis in Escherichia coli. *Journal of Bacteriology*, 190(15), pp.5431–5438.

Henrici, A.T. & Johnson, D.E., 1935. Studies of freshwater bacteria. *Journal of Bacteriology*, 30(1), pp.61–93.

Higgins, C.F., 2001. ABC transporters: physiology, structure and mechanism--an overview. *Research in microbiology*, 152(3–4), pp.205–210.

Higuchi, T. et al., 2009. Crystal structure of the cytosolic domain of the cation diffusion facilitator family protein. *Proteins: Structure, Function and Bioinformatics*, 76(3), pp.768–771.

Hilal, E.Y., Elkhairey, M.A.E. & Osman, A.O.A., 2016. The Role of Zinc, Manganse and Copper in Rumen Metabolism and Immune Function: A Review Article. *Open Journal of Animal Sciences*, 6, pp.304–324. Available at: http://www.scirp.org/journal/ojas.

Hiniker, A., Collet, J.F. & Bardwell, J.C. a, 2005. Copper stress causes an in vivo requirement for the Escherichia coli disulfide isomerase DsbC. *Journal of Biological Chemistry*, 280, pp.33785–33791.

Hobman, J.L. & Crossman, L.C., 2014. Bacterial antimicrobial metal ion resistance. *Journal of Medical Microbiology*.

Hobman, J.L. & Crossman, L.C., 2015. Bacterial antimicrobial metal ion resistance. *Journal of Medical Microbiology*, 64(2014), pp.471–497.

Hodgkinson, V. & Petris, M.J., 2012. Copper Homeostasis at the Host-Pathogen Interface. *The Journal of antibiotics*, 287(17), pp.13549–13555.

Hohmann, S. & Mager, W.H., 2003. *Yeast Stress Response* Springer. S. Hohmann & W. H. Mager, eds., Springer-Verlag.

Holyoake, L. V, Poole, R.K. & Shepherd, M., 2015. *The CydDC Family of Transporters and Their Roles in Oxidase Assembly and Homeostasis* 1st ed., Elsevier Ltd. Available at: http://dx.doi.org/10.1016/bs.ampbs.2015.04.002.

Horsburgh, M.J. et al., 2002. Manganese: Elemental defence for a life with oxygen? *Trends in Microbiology*, 10(11), pp.496–501.

Hossain, M.A. et al., 2012. Molecular Mechanism of Heavy Metal Toxicity and Tolerance in Plants: Central Role of Glutathione in Detoxification of Reactive Oxygen Species and Methylglyoxal and in Heavy Metal Chelation. *Journal of Botany*, 2012(Cd), pp.1–37. Available at: http://www.hindawi.com/journals/jb/2012/872875/.

Hottes, A.K. et al., 2004. Transcriptional Profiling of Caulobacter crescentus during Growth on Complex and Minimal Media. *Journal of Bacteriology*, 186(5), pp.1448–1461.

Hu, P., Brodie, E. & Suzuki, Y., 2005. Whole-genome transcriptional analysis of heavy metal stresses in Caulobacter crescentus. *Journal of …*, 187(24), pp.8437–8449. Available at: http://jb.asm.org/content/187/24/8437.short.

Huang, X. et al., 2017. Bacillus subtilis MntR coordinates the transcriptional regulation of manganese uptake and efflux systems. *Molecular Microbiology*, (103), pp.253–268.

Husson, F. & Josse, J., 2014. Multiple Correspondence Analysis. In M. Greenacre & J. Blasius, eds. *The Visualization and Verbalization of Data*. New Tork Academic Press.

Imlay, J.A., 2014. The mismetallation of enzymes during oxidative stress. *Journal of Biological Chemistry*, 289(41), pp.28121–28128.

Inesi, G., Pilankatta, R. & Tadini-Buoninsegni, F., 2014. Biochemical characterization of P-type copper ATPases. *Biochem J*, 463(2), pp.167–176. Available at: http://www.ncbi.nlm.nih.gov/pubmed/25242165.

Jerabek-willemsen, M. et al., 2014. MicroScale Thermophoresis: Interaction analysis and beyond. *Journal of Molecular Structure*, 1077, pp.101–113. Available at: http://dx.doi.org/10.1016/j.molstruc.2014.03.009.

Johnson, J.M. & Church, G.M., 1999. Alignment and structure prediction of divergent protein families: Periplasmic and outer membrane proteins of bacterial efflux pumps. *Journal of Molecular Biology*, 287(3), pp.695–715.

Jones, P.M. & George, A.M., 2004. The ABC transporter structure and mechanism: Perspectives on recent research. *Cellular and Molecular Life Sciences*, 61(6), pp.682–699.

Kaur, S., Kamli, M.R. & Ali, A., 2009. Diversity of arsenate reductase genes (arsc genes) from arsenic-resistant environmental isolates of E. coli. *Current Microbiology*, 59(3), pp.288–294.

Kaur, T., Singh, A. & Goel, R., 2011. Mechanisms pertaining to arsenic toxicity. *Toxicology International*, 18(2), p.87. Available at: http://www.toxicologyinternational.com/text.asp?2011/18/2/87/84258.

Kavamura, V.N. & Esposito, E., 2010. Biotechnological strategies applied to the decontamination of soils polluted with heavy metals. *Biotechnology Advances*, 28(1), pp.61–69. Available at: http://dx.doi.org/10.1016/j.biotechadv.2009.09.002.

Kershaw, C.J., Brown, N.L. & Hobman, J.L., 2007. Zinc dependence of zinT (yodA) mutants and binding of zinc, cadmium and mercury by ZinT. *Biochemical and Biophysical Research Communications*, 364(1), pp.66–71.

Khalfaoui-Hassani, B. et al., 2018. Widespread Distribution and Functional Specificity of the Copper Importer CcoA : Distinct Cu Uptake Routes for Bacterial cytochrome c oxidases. *mBi*, 9(1), pp.1–15.

Kim, D.Y. et al., 2007. The ABC transporter AtPDR8 is a cadmium extrusion pump conferring heavy metal resistance. *Plant Journal*, 50(2), pp.207–218.

Kim, E.-H. et al., 2011. Switch or Funnel: How RND-Type Transport Systems Control Periplasmic Metal Homeostasis. *Journal of Bacteriology*, 193(10), pp.2381–2387.

Kirkpatrick, C.L. & Viollier, P.H., 2012. Decoding Caulobacter development. *FEMS Microbiology Reviews*, 36(1), pp.193–205.

Koh, E. et al., 2017. Copper import in Escherichia coli by the yersiniabactin metallophore system. *Nature chemical biology*, (July), pp.1–8. Available at: http://dx.doi.org/10.1038/nchembio.2441.

Koh, E. & Henderson, J.P., 2015. Copper-binding siderophores at the host-pathogen interface. *Journal of Biological Chemistry*, (June), pp.1–16.

Kolaj-Robin, O. et al., 2015. Cation diffusion facilitator family: Structure and function. *FEBS Letters*, 589(12), pp.1283–1295. Available at: http://dx.doi.org/10.1016/j.febslet.2015.04.007.

Komárek, M. et al., 2010. Contamination of vineyard soils with fungicides : A review of environmental and toxicological aspects. *Environment International*, 36, pp.138–151.

Komori, H. & Higuchi, Y., 2015. Structural insights into the O2 reduction mechanism of multicopper oxidase. *Journal of Biochemistry*, 158(4), pp.293–298.

Konietzny, U. & Greiner, R., 2004. Bacterial phytase: Potential application, in vivo function and regulation of its synthesis. *Brazilian Jounral of Microbiology*, 35, pp.11–18.

Kulathila, R. et al., 2011. Crystal Structure of Escherichia coli CusC , the Outer Membrane Component of a Heavy Metal Efflux Pump. *PLoS ONE*, 6(1), pp.1–7.

Laity, J.H., Lee, B.M. & Wright, P.E., 2001. Zinc finger proteins: New insights into structural and functional diversity. *Current Opinion in Structural Biology*, 11(1), pp.39–46.

Lam, H., Matroule, J.Y. & Jacobs-Wagner, C., 2003. The asymmetric spatial distribution of bacterial signal transduction proteins coordinates cell cycle events. *Developmental Cell*, 5, pp.149–159.

Lawarée, E. et al., 2016. Caulobacter crescentus intrinsic dimorphism provides a prompt bimodal response to copper stress. *Nature Microbiology*, 1(9), p.16098. Available at: http://www.nature.com/articles/nmicrobiol201698.

Leedjärv, A., Ivask, A. & Virta, M., 2008. Interplay of different transporters in the mediation of divalent heavy metal resistance in Pseudomonas putida KT2440. *Journal of Bacteriology*, 190(8), pp.2680–2689.

Letelier, M.E. et al., 2005. Possible mechanisms underlying copper-induced damage in biological membranes leading to cellular toxicity. *Chemico-Biological Interactions*, 151, pp.71–82.

Levin, S.A. & Carpenter, S.R., 2009. *The Princeton Guide to Ecology* Princeton. S. Levin, ed., Princeton University Press.

Lewis, A., 1995. The biological importance of copper, *Final report of International Copper Associatiation (ICA) - ICA Project n°223*

Loftin, I.R. et al., 2007. Unusual Cu (I)/ Ag (I) coordination of Escherichia coli CusF as revealed by atomic resolution crystallography and X-ray absorption spectroscopy. *Protein Science*, (I), pp.2287–2293.

Loftin, I.R. & Mcevoy, M.M., 2009. Tryptophan Cu(I)–π interaction fine-tunes the metal binding properties of the bacterial metallochaperone CusF. *Journal of Biological Inorganic Chemistry*, 14(6), pp.905–912.

Long, F. et al., 2012. Structure and mechanism of the tripartite CusCBA heavy-metal efflux complex. *Philosophical Transaction of the Royal Society B*, 367, pp.1047–1058.

Lu, M. et al., 2017. Transcriptome Response to Heavy Metals in Sinorhizobium meliloti CCNWSX0020 Reveals New Metal Resistance Determinants That Also Promote Bioremediation by Medicago lupulina in Metal-Contaminated Soil. *Applied and Environmental Microbiology*, 83(20), pp.1–18.

Lutkenhaus, J.F., 1977. Role of a Major Outer Membrane Protein in Escherichia coli. *Journal of Bacteriology*, 131(2), pp.631–637.

Macomber, L. & Imlay, J. a, 2009. The iron-sulfur clusters of dehydratases are primary intracellular targets of copper toxicity. *Proceedings of the National Academy of Sciences of the United States of America*, 106(20), pp.8344–8349.

Macomber, L., Rensing, C. & Imlay, J. a., 2007. Intracellular copper does not catalyze the formation of oxidative DNA damage in Escherichia coli. *Journal of Bacteriology*, 189(5), pp.1616–1626.

Maret, W., 2015. Analyzing free zinc(II) ion concentrations in cell biology with fluorescent chelating molecules. *Metallomics*, 7(2), pp.202–211. Available at: http://xlink.rsc.org/?DOI=C4MT00230J.

Margulis, L. & Sagan, D., 1987. *Microcosmos: Four billion years of evolution from our microbial ancestor* Allen & Un., University of California Press.

Masip, L., Veeravalli, K. & Georgiou, G., 2006. The Many Faces of Glutathione in Bacteria. *Antioxidant & Redow signaling*, 8(5), pp.152–162.

McDevitt, C.A. et al., 2011. A molecular mechanism for bacterial susceptibility to Zinc. *PLoS Pathogens*, 7(11).

Merhej, V., Georgiades, K. & Raoult, D., 2011. Intracellular Rickettsiales : Insights into manipulators of eukaryotic cells. *Trends in Molecular Medicine*, 17(10).

Meydan, S. et al., 2017. Programmed Ribosomal Frameshifting Generates a Copper Transporter and a Copper Chaperone from the Same Gene. *Molecular Cell*, 65(2), pp.207–219.

Molteni, C., Abicht, H.K. & Solioz, M., 2010. Killing of bacteria by copper surfaces involves dissolved copper. *Applied and Environmental Microbiology*, 76(12), pp.4099–4101.

Monteiro, S., Lofts, S. & Boxall, A., 2010. *Pre-Assessment of Environmental Impact of Zinc and Copper Used Animal Nutrition*,

Montoya, M., 2013. Bacterial glutathione import. *Nature Structural and Molecular Biology*, 20(7), p.775. Available at: http://dx.doi.org/10.1038/nsmb.2632.

Moore, M.J. et al., 1990. Organomercurial Lyase and Mercuric Ion Reductase: Nature's Mercury Detoxification Catalysts. *Accounts of Chemical Research*, 23(9), pp.301–308.

Moran, K., 2004. *Copper Sources in Urban Runoff and Shoreline Activities*,

Moussatova, A. et al., 2008. ATP-binding cassette transporters in Escherichia coli. *Biochimica et Biophysica Acta - Biomembranes*, 1778(9), pp.1757–1771.

Multhaup, G. et al., 2001. Interaction of the CopZ copper chaperone with the CopA copper ATPase of Enterococcus hirae assessed by surface plasmon resonance. *Biochemical and Biophysical Research Communications*, 288(1), pp.172–177.

Nakae, T., 1976. Identification of the outer membrane protein of that produces transmembrane channels in reconstituted vesicle membranes. *Biochemical and Biophysical Research Communications*, 71(3), pp.877–884.

Nies, D.H., 2003. Efflux-mediated heavy metal resistance in prokaryotes. *FEMS Microbiology Reviews*, 27(2–3), pp.313–339.

Nirel, P.M. & Pasquini, F., 2010. Differentiation of copper pollution origin : agricultural and urban sources Différentiation de l ' origine des pollutions en cuivre : caractérisation des sources agricoles et urbaines. , pp.1–7.

Noor, R. et al., 2013. Influence of Temperature on Escherichia coli Growth in Different Culture Media. *Journal of Pure and Applied Microbiology*, 7(2), pp.899–904.

North, N.N. et al., 2004. Change in Bacterial Community Structure during In Situ Biostimulation of Subsurface Sediment Cocontaminated with Uranium and Nitrate. *Applied and Environmental Microbiology*, 70(8), pp.4911–4920.

Odermatt, A. et al., 1993. Primary structure of two P-type ATPases involved in copper homeostasis in Enterococcus hirae. *Journal of Biological Chemistry*, 268(17), pp.12775–12779.

Ohtsu, I. et al., 2010. The L-Cysteine / L-Cystine Shuttle System Provides Reducing Equivalents to the Periplasm in Escherichia coli. *The Journal of Biological Chemistry*, 285(23), pp.17479–17487.

Ohtsu, I. et al., 2015. Uptake of L -cystine via an ABC transporter contributes defense of oxidative stress in the L -cystine export-dependent manner in Escherichia coli. *PLoS ONE*, 10(4), pp.1–14.

Ortiz, D.F. et al., 1992. Heavy metal tolerance in the fission yeast requires an ATP-binding cassette-type vacuolar membrane transporter. *The EMBO journal*, 11(10), pp.3491–3499.

Ortiz, D.F. et al., 1995. Transport of metal-binding peptides by HMT1, a fission yeast ABC-type vacuolar membrane protein. *Journal of Biological Chemistry*, 270(9), pp.4721–4728.

Osborne, F.H. & Ehrlich, H.L., 1976. Oxidation of Arsenite by a Soil Isolate of Alcaligenes. *Journal of Applied Bacteriology*, 41(2), pp.295–305.

Osman, D. & Cavet, J.S., 2008. Copper Homeostasis in Bacteria. *Advances in Applied Microbiology*, 65(08), pp.217–247.

Outten, F.W. et al., 2001. The Independent cue and cus Systems Confer Copper Tolerance during Aerobic and Anaerobic Growth in Escherichia coli. *Journal of Biological Chemistry*, 276(33), pp.30670–30677.

Palmer, T. & Berks, B.C., 2012. The twin-arginine translocation (Tat) protein export pathway. *Nature Reviews Microbiology*, 10(7), pp.483–496. Available at: http://dx.doi.org/10.1038/nrmicro2814.

Patel, S.J. et al., 2014. Functional diversity of five homologous Cu+-ATPases present in Sinorhizobium meliloti. *Microbiology (United Kingdom)*, 160, pp.1237–1251.

Payne, S.H. et al., 2012. Unexpected Diversity of Signal Peptides in Prokaryotes. *mBio*, 3(6), pp.1–6.

Peer, W.A. et al., 2006. *Molecular Biology of Metal Homeostasis and Detoxification* M. Tamas & E. Martinoia, eds., Available at: http://www.scopus.com/inward/record.url?eid=2-s2.0-33748917519&partnerID=tZOtx3y1.

Peng, C.T. et al., 2017. Structure-function relationship of aminopeptidase P from Pseudomonas aeruginosa. *Frontiers in Microbiology*, 8(DEC), pp.1–12.

Pini, F. et al., 2011. Plant-bacteria association and symbiosis: Are there common genomic traits in alphaproteobacteria? *Genes*, 2(4), pp.1017–1032.

Pittman, M.S. et al., 2002. Cysteine Is Exported from the Escherichia coli Cytoplasm by CydDC , an ATP-binding Cassette-type Transporter Required for Cytochrome Assembly. *The Journal of Biological Chemistry*, 277(51), pp.49841–49849.

Pittman, M.S., Robinson, H.C. & Poole, R.K., 2005. A Bacterial Glutathione Transporter (Escherichia coli CydDC) Exports Reductant to the Periplasm. *The Journal of Biological Chemistry*, 280(37), pp.32254–32261.

Pocheville, A., 2015. The Ecological Niche : History and Recent Controversies. In T. Heams et al., eds. *Handbook of Evolutionary Thinking in the Sciences*. Springer, pp. 547–568.

Poindexter, J.S., 1964. Biological Properties and Classification of the Caulobacter Group1. *Bacteriological reviews*, 28(3), pp.231–295.

Poindexter, J.S., 1981. The caulobacters: ubiquitous unusual bacteria. *Microbiological reviews*, 45(1), pp.123–179.

Polissi, A. et al., 2003. Changes in Escherichia coli transcriptome during acclimatization at low temperature. *Research in microbiology*, 154, pp.573–580.

Pontel, L., Checa, S. & Soncini, F., 2015. *Bacteria-Metal Interactions* Springer. D. Saffarini, ed., Springer.

Porcheron, G. et al., 2013. Iron, copper, zinc, and manganese transport and regulation in pathogenic Enterobacteria: correlations between strains, site of infection and the relative importance of the different metal transport systems for virulence. *Frontiers in Cellular and Infection Microbiology*, 3(December), pp.1–24. Available at: http://journal.frontiersin.org/article/10.3389/fcimb.2013.00090/abstract.

Potter, A.J., Trappetti, C. & Paton, J.C., 2012. Streptococcus pneumoniae uses glutathione to defend against oxidative stress and metal ion toxicity. *Journal of Bacteriology*, 194(22), pp.6248–6254.

Potter, S.C. et al., 2018. HMMER web server : 2018 update. *Nucleic acids research*, 46, pp.200–204.

Priyodip, P., Prakash, P.Y. & Balaji, S., 2017. Phytases of Probiotic Bacteria : Characteristics and Beneficial Aspects. *Indian Journal of Microbiology*, 57(2), pp.148–154.

Pulliainen, A.T. et al., 2005. Dps/Dpr ferritin-like protein: Insights into the mechanism of iron incorporation and evidence for a central role in cellular iron homeostasis in Streptococcus suis. *Molecular Microbiology*, 57(4), pp.1086–1100.

Radford, D.S. et al., 2003. CopZ from Bacillus subtilis interacts in vivo with a copper exporting CPx-type ATPase CopA. *FEMS Microbiology Letters*, 220(1), pp.105–112.

Radisky, D.C., Babcock, M.C. & Kaplan, J., 1999. The Yeast Frataxin Homologue Mediates Mitochondrial Iron Efflux. *Journal of Biological Chemistry*, 274(8), pp.4497–4499.

Rani, A. et al., 2014. Cellular mechanisms of cadmium-induced toxicity: A review. *International Journal of Environmental Health Research*, 24(4), pp.378–399.

Rensing, C. et al., 2000. CopA : An Escherichia coli Cu (I) -translocating P-type ATPase. *Proceedings of the National Academy of Sciences*, 97(2), pp.652–656.

Rensing, C. & Franke, S., 2013. Copper Homeostasis in Escherichia coli and Other Enterobacteriaceae. *EcoSal Plus*, (December 2013).

Rensing, C. & Grass, G., 2003. Escherichia coli mechanisms of copper homeostasis in a changing environment. *FEMS Microbiology Reviews*, 27(2–3), pp.197–213.

Rensing, C., Mitra, B. & Rosen, B.P., 1997. The zntA gene of Escherichia coli encodes a Zn(II)-translocating P-type ATPase. *Proceedings of the National Academy of Sciences of the United States of America*, 94(26), pp.14326–14331.

Rigo, A. et al., 2004. Interaction of copper with cysteine: stability of cuprous complexes and catalytic role of cupric ions in anaerobic thiol oxidation. *Journal of Inorganic Biochemistry*, 98, pp.1495–1501.

Roberts, S.A. et al., 2003. A Labile Regulatory Copper Ion Lies Near the T1 Copper Site in the Multicopper Oxidase CueO. *Journal of Biological Chemistry*, 278(34), pp.31958–31963. Available at: http://www.jbc.org/cgi/doi/10.1074/jbc.M302963200.

Roberts, S.A. et al., 2002. Crystal structure and electron transfer kinetics of CueO, a multicopper oxidase required for copper homeostasis in Escherichia coli. *Proceedings of the National Academy of Sciences*, 99(5), pp.2766–2771.

Rodrigue, A. et al., 1999. Co-translocation of a periplasmic enzyme complex by a hitchhiker mechanism through the bacterial tat pathway. *Journal of Biological Chemistry*, 274, pp.13223–13228.

Rodrigue, A. & Effantin, G., 2005. Identification of rcnA (yohM), a Nickel and Cobalt Resistance Gene in Escherichia coli Identification of rcnA (yohM), a Nickel and Cobalt Resistance Gene in Escherichia coli. *J. Bacteriol.*, 187(8), pp.2912–2916.

Sankari, S. & O'Brian, M.R., 2014. A bacterial iron exporter for maintenance of iron homeostasis. *Journal of Biological Chemistry*, 289(23), pp.16498–16507.

Santo, C.E. et al., 2008. Contribution of copper ion resistance to survival of Escherichia coli on metallic copper surfaces. *Applied and Environmental Microbiology*, 74(4), pp.977–986.

Santo, C.E., Morais, P.V. & Grass, G., 2010. Isolation and characterization of bacteria resistant to metallic copper surfaces. *Applied and Environmental Microbiology*, 76(5), pp.1341–1348.

Schiering, N. et al., 1991. Structure of the Detoxification Catalyst Mercuric Ion Reductase from Bacillus Sp Strain-Rc607. *Nature*, 352(6331), pp.168–172.

Schlimpert, S. et al., 2013. General Protein Diffusion Barriers create Compartments within Bacterial Cells. , 151(6), pp.1270–1282.

Schrader, J.M. & Shapiro, L., 2015. Synchronization of Caulobacter Crescentus for Investigation of the Bacterial Cell Cycle. *Journal of Visualized Experiments*, 2(98), pp.1–6. Available at: http://www.jove.com/video/52633/synchronization-caulobacter-crescentus-for-investigation-bacterial.

Schueck, N.D., Woontner, M. & Koeller, D.M., 2001. The role of the mitochondrion in cellular iron homeostasis. *Mitochondrion*, 1(1), pp.51–60.

Seyle, H., 1973. The Evolution of the Stress Concept: The originator of the concept traces its development from the discovery in 1936 of the alarm reaction to modern therapeutic applications of syntoxic and catatoxic hormones. *American Scientist*, 61(6), pp.692–699.

Sharma, J. et al., 2017. Metallothionein assisted periplasmic lead sequestration as lead sulfite by Providencia vermicola strain SJ2A. *Science of the Total Environment*, 579, pp.359–365. Available at: http://dx.doi.org/10.1016/j.scitotenv.2016.11.089.

Shepherd, M., 2015. The CydDC ABC transporter of Escherichia coli: new roles for a reductant efflux pump. *BIochemical Society Transaction*, 43(5), pp.908–912.

Sherrill, C. & Fahey, R.C., 1998. Import and metabolism of glutathione by Streptococcus mutans. *Journal of Bacteriology*, 180(6), pp.1454–1459.

Shurson, G.C. et al., 1990. Physiological relationships between microbiological status and dietary copper levels in the pig. *Journal of Animal Science*, 68, pp.1061–1071.

Silveira, E. et al., 2014. Co-transfer of resistance to high concentrations of copper and first-line antibiotics among Enterococcus from different origins (humans, animals, the environment and foods) and clonal lineages. *Journal of Antimicrobial Chemotherapy*, 69(4), pp.899–906.

Silver, S. & Misra, T.K., 1984. Bacterial transformations of and resistances to heavy metals. *Basic life sciences*, 28(67), pp.23–46. Available at: http://www.ncbi.nlm.nih.gov/pubmed/6367730.

Smirnova, G. V & Oktyabrsky, O.N., 2005. Glutathione in Bacteria. *Biochemistry*, 70(11).

Solioz, M. & Stoyanov, J. V., 2003. Copper homeostasis in Enterococcus hirae. *FEMS Microbiology Reviews*, 27(2–3), pp.183–195.

Solomon, E.I., Augustine, A.J. & Yoon, J., 2008. O2 Reduction to H2 O by the Multicopper Oxidases. *Dalton Transaction*, (30), pp.3921–3932.

Solomon, E.I., Sundaram, U.M. & Machonkin, T.E., 1996. Multicopper Oxidases and Oxygenases. *Chemical Reviews*, 96(7), pp.2563–2606. Available at: http://pubs.acs.org/doi/abs/10.1021/cr950046o.

Staehlin, B.M. et al., 2016. Evolution of a Heavy Metal Homeostasis/Resistance Island Reflects Increasing Copper Stress in Enterobacteria. *Genome biology and evolution*, 8(3), pp.811–826.

Stähler, F.N. et al., 2006. The novel Helicobacter pylori CznABC metal efflux pump is required for cadmium, zinc, and nickel resistance, urease modulation, and gastric colonization. *Infection and Immunity*, 74(7), pp.3845–3852.

Stanley, N.R., 2000. The Twin Arginine Consensus Motif of Tat Signal Peptides Is Involved in Sec-independent Protein Targeting in Escherichia coli. *Journal of Biological Chemistry*, 275(16), pp.11591–11596. Available at: http://www.jbc.org/cgi/doi/10.1074/jbc.275.16.11591.

Sun, M.L. et al., 2002. The Pco proteins are involved in periplasmic copper handling in Escherichia coli. *Biochemical and Biophysical Research Communications*, 295, pp.616–620.

Tamaki, S. & Frankenberger Jr, W., 1992. Environmental biochemistry of arsenic. *Reviews of Environmental Contamination and Toxicology;(United States)*, 124(March), p.71 pages. Available at: http://www.osti.gov/energycitations/product.biblio.jsp?osti_id=5752110.

Tetaz, T.J. & Luke, R.K.J., 1983. Plasmid-controlled resistance to copper in Escherichia coli. *Journal of Bacteriology*, 154(3), pp.1263–1268.

Tian, H., Boyd, D. & Beckwith, J., 2000. A mutant hunt for defects in membrane protein assembly yields mutations affecting the bacterial signal recognition particle and Sec machinery. *Proceedings of the National Academy of Sciences of the United States of America*, 97(9), pp.4730–4735.

Trappe, K., Marschall, T. & Renard, B.Y., 2016. Detecting horizontal gene transfer by mapping sequencing reads across species boundaries. *Bioinformatics*, 32, pp.595–604.

Turner, A.W., 1949. Bacterial Oxidation By Arsenite. *Nature*, 164, pp.915–916.

Valencia, E.Y. et al., 2013. Two RND proteins involved in heavy metal efflux in Caulobacter crescentus belong to separate clusters within proteobacteria. *BMC Microbiology*, 13, p.79. Available at: http://www.pubmedcentral.nih.gov/articlerender.fcgi?artid=3637150&tool=pmcentrez&rendertype=abstract.

Vergauwen, B. et al., 2013. Molecular and structural basis of glutathione import in Gram-positive bacteria via GshT and the cystine ABC importer TcyBC of Streptococcus mutans. *Molecular Microbiology*, 89(2), pp.288–303.

Wakeman, C.A. et al., 2014. Assessment of the requirements for magnesium transporters in bacillus subtilis. *Journal of Bacteriology*, 196(6), pp.1206–1214.

Waldron, K.J. & Robinson, N.J., 2009. How do bacterial cells ensure that metalloproteins get the correct metal? *Nature reviews. Microbiology*, 7, pp.25–35.

Wang, W. & Ballatori, N., 1998. Endogenous glutathione conjugates: occurrence and biological functions. *Pharmacological reviews*, 50(3), pp.335–356.

Wedepohl, K.H., 1995. The composition of the continental crust. *Geochimica et Cosmochimica Acta*, 59(7), pp.1217–1232.

Wei, Y. & Fu, D., 2005. Selective metal binding to a membrane-embedded aspartate in the Escherichia coli metal transporter YiiP (FieF). *Journal of Biological Chemistry*, 280(40), pp.33716–33724.

Wernimont, A.K. et al., 2003. Crystal structure and dimerization equilibria of PcoC, a methionine-rich copper resistance protein from Escherichia coli. *Journal of Biological Inorganic Chemistry*, 8, pp.185–194.

Wiethaus, J., Wildner, G.F. & Masepohl, B., 2006. The multicopper oxidase CutO confers copper tolerance to Rhodobacter capsulatus. *FEMS Microbiology Letters*, 256, pp.67–74.

Wilhelm, R.C., 2018. Following the terrestrial tracks of Caulobacter - redefining the ecology of a reputed aquatic oligotroph. *The ISME Journal*. Available at: http://dx.doi.org/10.1038/s41396-018-0257-z.

Williams, K.P., Sobral, B.W. & Dickerman, A.W., 2007. A Robust Species Tree for the Alphaproteobacteria. *Journal of Bacteriology*, 189(13), pp.4578–4586.

Winterbourn, C.C., 1995. Toxicity of iron and hydrogen peroxide: the Fenton reaction. *Toxicology Letters*, 82–83(C), pp.969–974.

Wu, Z., Fernandez-Lima, F. a. & Russell, D.H., 2010. Amino acid influence on copper binding to peptides: Cysteine versus arginine. *Journal of the American Society for Mass Spectrometry*, 21, pp.522–533.

Yang, J. & Zhang, Y., 2015. Protein Structure and Function Prediction Using I-TASSER. *Current protocols Bioinformatics*, 52, pp.1–24.

Yazdankhah, S., Rudi, K. & Bernhoft, A., 2014. Zinc and copper in animal feed–development of resistance and co-resistance to antimicrobial agents in bacteria of animal origin. *Microbial Ecology in Health and diseases*, 1, pp.1–7. Available at: http://www.ncbi.nlm.nih.gov/pmc/articles/PMC4179321/.

Yocum, C.F. & Pecoraro, V.L., 1999. Recent advances in the understanding of the biological chemistry of manganese. *Current Opinion in Chemical Biology*, 3(2), pp.182–187.

Yu, W. et al., 1996. Identification of SLF1 as a new copper homeostasis gene involved in copper sulfide mineralization in Saccharomyces cerevisiae. *Molecular and cellular biology*, 16(5), pp.2464–72. Available at: http://www.pubmedcentral.nih.gov/articlerender.fcgi?artid=231235&tool=pmcentrez&rendertype=abstract.

Yung, M., Ma, J. & Salemi, M., 2014. Shotgun Proteomic Analysis Unveils Survival and Detoxification Strategies by Caulobacter crescentus during Exposure to Uranium, Chromium, and Cadmium. *Journal of proteome …*. Available at: http://pubs.acs.org/doi/abs/10.1021/pr400880s.

Yung, M.C. et al., 2015. Transposon Mutagenesis Paired with Deep Sequencing of Caulobacter crescentus under Uranium Stress Reveals Genes Essential for Detoxification and Stress Tolerance. *Journal of Bacteriology*, 197(19), pp.3160–3172. Available at: http://jb.asm.org/lookup/doi/10.1128/JB.00382-15.

Yung, M.C. & Jiao, Y., 2014. Biomineralization of Uranium by PhoY Phosphatase Activity Aids Cell Survival in Caulobacter crescentus. *Applied and Environmental Microbiology*, 80(16), pp.4795–4804.

Zhao, G. et al., 2002. Iron and hydrogen peroxide detoxification properties of DNA-binding protein from starved cells. A ferritin-like DNA-binding protein of Escherichia coli. *Journal of Biological Chemistry*, 277(31), pp.27689–27696.

Supplementary and annexes

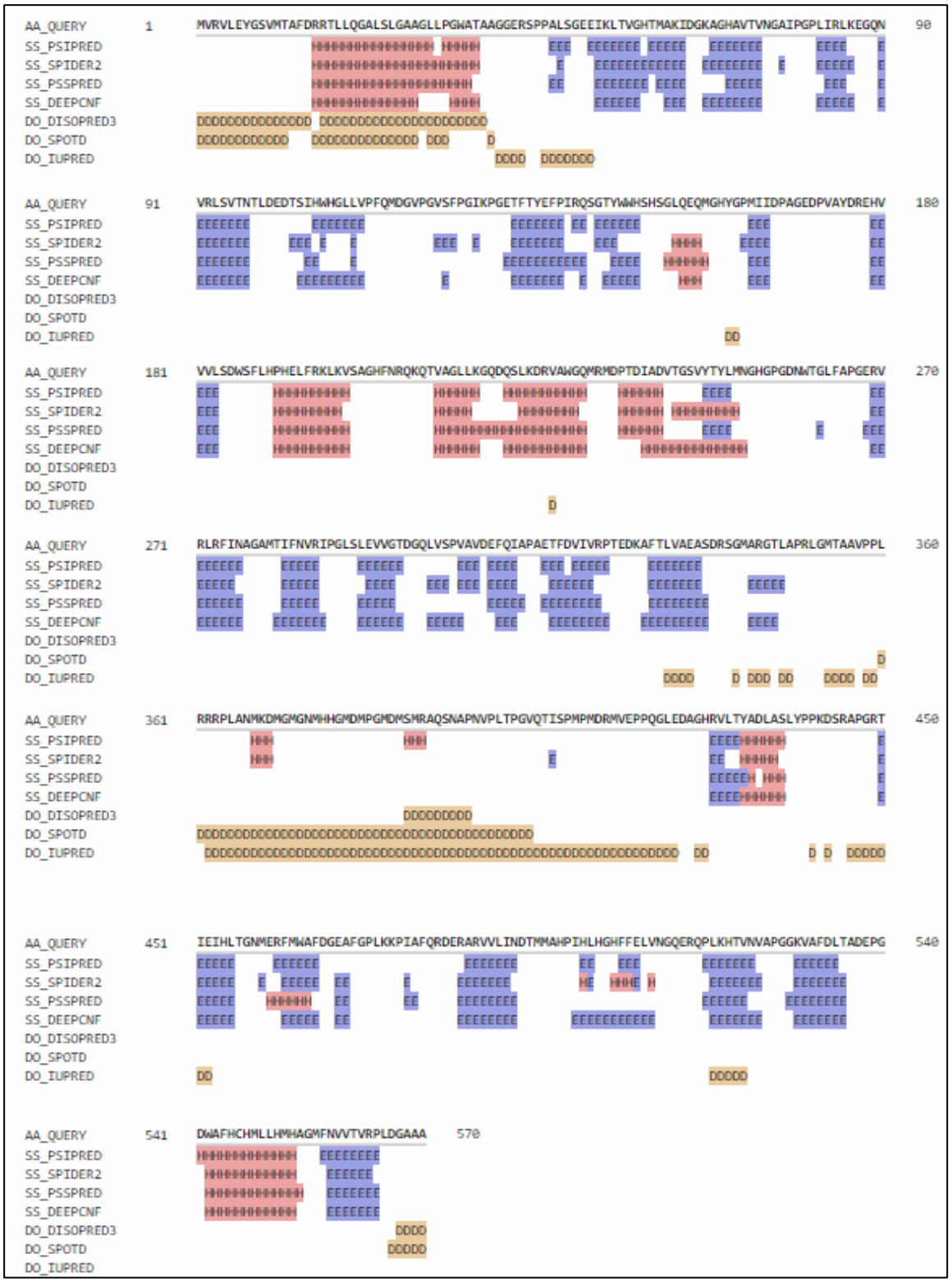

Fig. S1: Quick2D prediction for PcoA: The query sequence is run through several tools at once. Under the AA_Query line (the input AA sequence) are listed, line by line, the results for the different algorithms. The first four line indicate the secondary structures (β-strands in Blue E; α-helices in pink H). The last three tools are disorder prediction, and marks a yellow D at the position of predicted disorders.

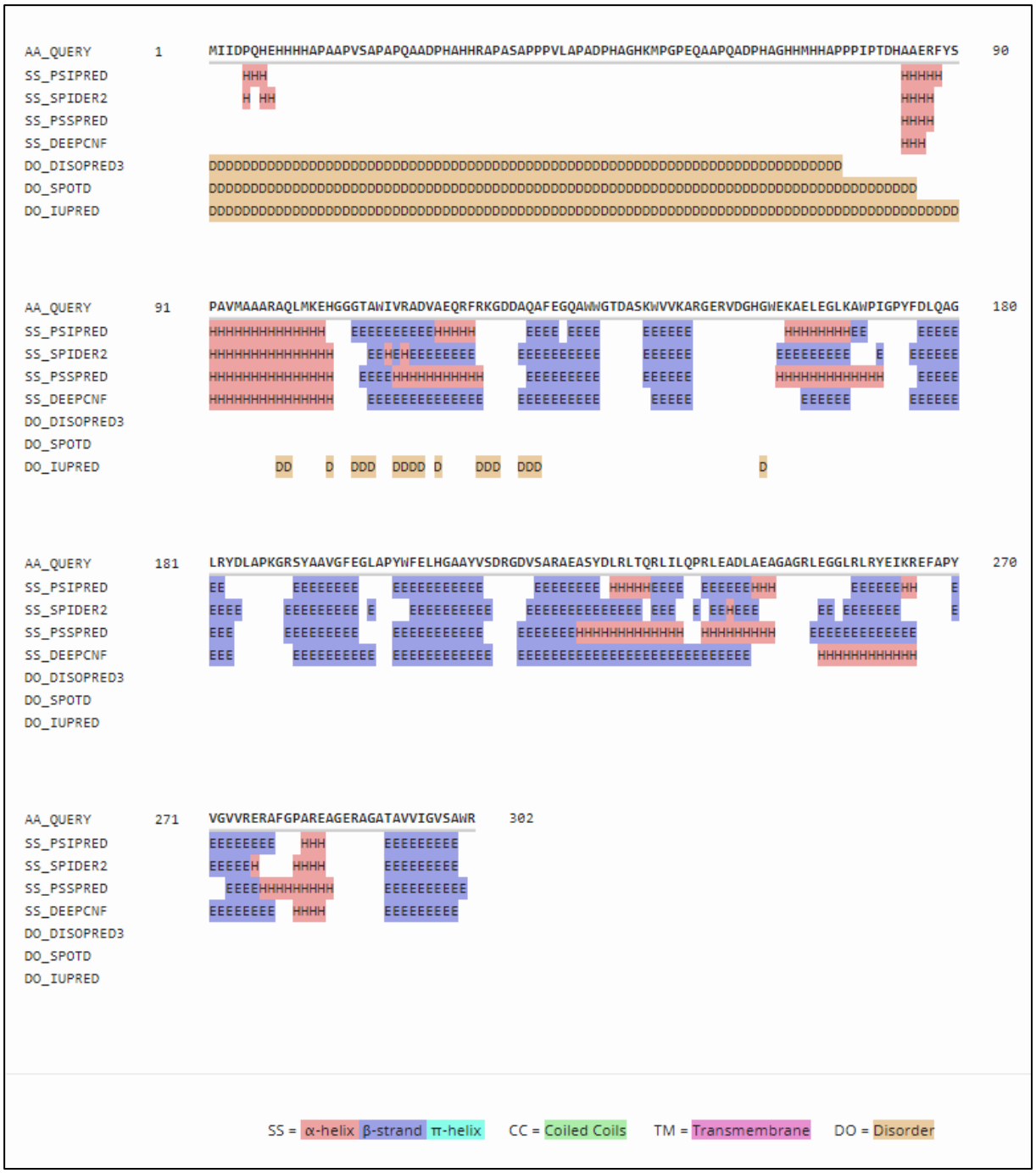

Fig. S2: Quick2D prediction for PcoB: The query sequence is run through several tools at once. Under the AA_Query line (the input AA sequence) are listed, line by line, the results for the different algorithms. The first four line indicate the secondary structures (β-strands in Blue E; α-helices with pink H). The last three tools are disorder prediction, and marks a yellow D at the position of predicted disorders.

CCNA	Number of time it was isolated	Predicted function
CCNA_00027	2	2OG-Fe(II) oxygenase
CCNA_00028	9	TonB-dependent receptor
CCNA_00033	1	polyribonucleotide nucleotidyltransferase/adenylyltransferase
CCNA_00043	1	NusA
CCNA_00112	1	glyoxalase family protein
CCNA_00188	4	ABC transporter ATP-binding protein
CCNA_00189	1	hypothetical cytosolic protein (ABC transporter ATP-binding protein)
CCNA_00236	2	conserved hypothetical protein ou prom de chvI
CCNA_00237	5	two-component response regulator chvI
CCNA_00302	1	parathion hydrolase
CCNA_00423	1	Phosphohdrolase MutT-nudix familly
CCNA_00454	1	transcriptional regulator, GntR family
CCNA_00459	2	NhaA Na+/H+ antiporter
NC region between CCNA_00460 and CCNA_00463	1	N/A
CCNA_00851	1	periplasmic multidrug efflux lipoprotein precursor
CCNA_00852	1	Transcriptional regulator
CCNA_01008	1	Urocanate hydratase
CCNA_01015 (*pcoA*)	6	PcoA
CCNA_01016 (*pcoB*)	5	copper resistance protein B (PcoB)
CCNA_01036	1	hyp, maybe peptidase
CCNA_01061	1	RsaE type I secretion adaptor protein
CCNA_01123	1	bacterial peptide chain Release factor 3 (RF-3)
CCNA_01174	1	transcriptional regulator, LysR family
CCNA_01175	1	uroporphyrin-III C-methyltransferase
CCNA_01198	1	dTDP-4-dehydrorhamnose reductase
CCNA_01246	1	methyltransferase
CCNA_01478	2	transcriptional regulator
CCNA_01493 (Cysteine synthase)	1	Cysteine synthase
CCNA_01542	1	ice nucleation protein
CCNA_01610	1	2-isopropylmalate synthase
CCNA_01622	1	ppGpp hydrolase-synthetase relA/spoT
CCNA_01736	1	Transcriptional regulator, TetR family
CCNA_01934	1	HesB protein family
CCNA_01938	1	ATP-dependent transporter sufC
CCNA_01940	1	ABC transporter-associated protein sufB
CCNA_02028	1	NTF2 enzyme family protein
CCNA_02066	1	Phytoene synthase family protein
CCNA_02081	1	Sec-independent protein translocase protein tatB
CCNA_02082	1	Sec-independent protein translocase protein tatA
CCNA_02083	1	segregation and condensation protein B scpB
CCNA_02085	1	anhydromuramoyl-peptide exo-beta-N-acetylglucosaminidase
CCNA_02327 (*tmrp*)	9	ABC transporter permease protein
CCNA_02431	2	histidinol dehydrogenase
CCNA_02466	1	UDP-glucose 4-epimerase
CCNA_02537	3	ribonuclease R
CCNA_03159	1	sulfite reductase (NADPH) flavoprotein alpha-component
CCNA_03164	1	protein translocase subunit secA
CCNA_03211	1	L-Ala-D/L-Glu racemase
CCNA_03271	1	methionine gamma-lyase
CCNA_03272	1	2 component sensor histidine kinase
CCNA_03362	1	ECF-family RNA polymerase sigma factor
CCNA_03527	1	glutamate-cysteine ligase (transposon in promoter region)
CCNA_03625	1	Régulateur transcriptionnel CztR
CCNA_03627	1	probable ATP phosphoribosyltransferase regulatory subunit
CCNA_03672	1	superoxyde dismutase
CCNA_03850	2	imidazoleglycerol-phosphate dehydratase
CCNA_03852	1	1-(5-phosphoribosyl)-5-((5-phosphoribosylamino)methylideneamino) imidazole-4-carboxamide
CCNA_03857	1	transporter
CCNA_03858	8	protein translocase subunit secB
CCNA_03872	1	tRNA synthase
CCNA_R0057	1	tRNAHis

Fig. S3: Results of the transposon-based genetic screen performed by the group. The mutants displaying higher Cu sensitivity were sequenced. The genes identified as mutated are listed in the first column. The second column list how many time this gene was found during the screening process, and the third column list the predicted function.

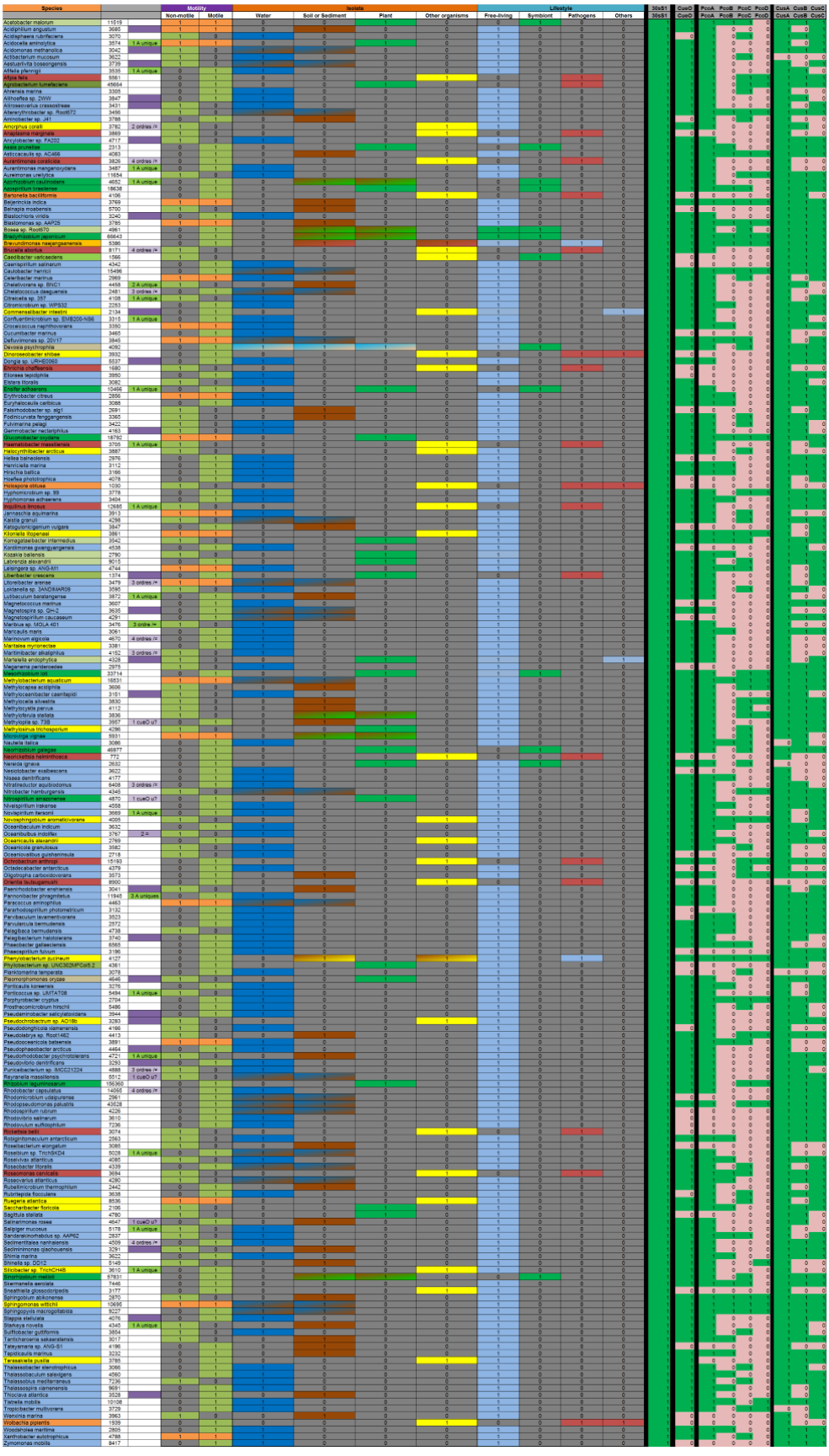

Fig. S4: Database containing the annotation of motility, environement and lifestyle of the 206 alphaproteobacteria species along with their conservation data A high-resolution picture of the database will be provided in a separate file.

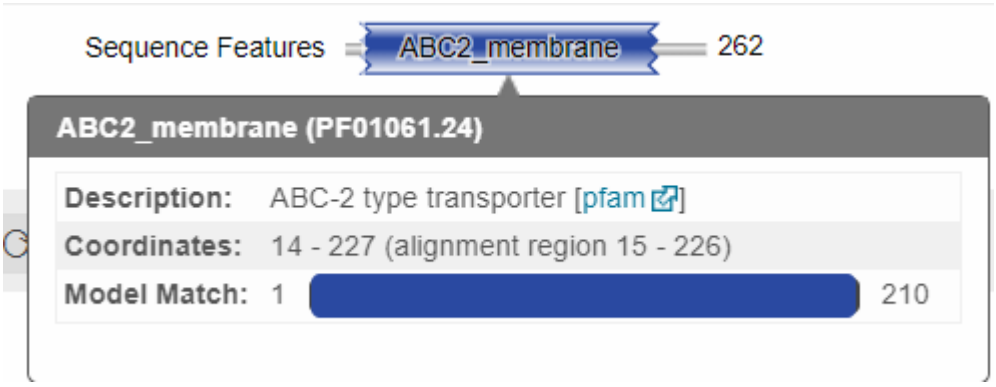

Fig. S4: Domain prediction for NodJ An ABC-2 type domain is predicted, similarly to the domain predicted for TmrP

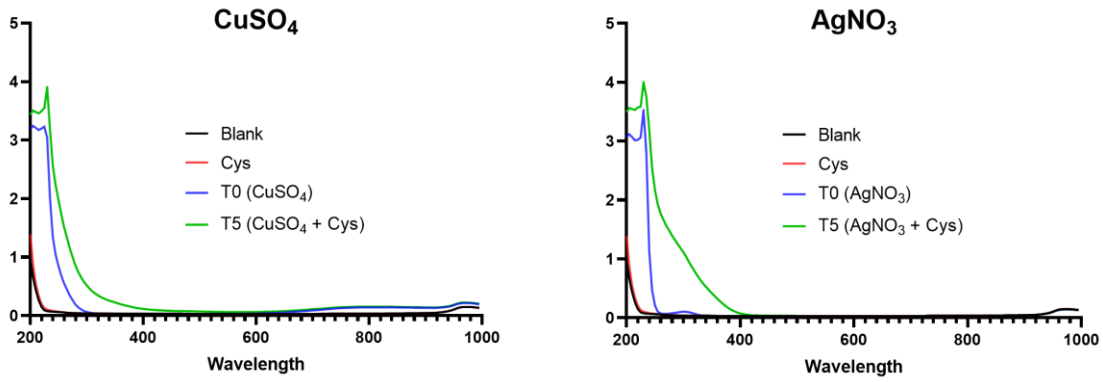

Fig. S5: Example of superposition of the absorbance curves – The blue ligne is the metal absorbance

During the course of this thesis, a few work in which I took part have been published:

- Gillet, S., Lawarée, E. & Matroule, J.-Y., 2018. Functional Diversity of Bacterial Strategies to Cope With Metal Toxicity. In S. Das & H. R. Dash, eds. Microbial Diversity in the Genomic Era. Elsevier Academic Press, pp. 409–426.

- Lawarée E., Gillet S., Louis G., Tilquin F., Le Blastier S, Cambier P and Matroule J-Y ; "Caulobacter crescentus intrinsic dimorphism provides a prompt bimodal response to copper stress"; Nature Microbiology ; 2016 ; 1 ; 16098

- Dufour YS, Gillet S, Frankel NW, Weibel DB, Emonet T; "Direct Correlation between Motile Behavior and Protein Abundance in Single Cells" ; 2016 ; PLoS Computational Biology; 12(9); e1005041

- Poncin K, Gillet S, De Bolle X ; "Learning from the master: Targets and functions of the CtrA response regulator in Brucella abortus and other alpha-proteobacteria" FEMS Microbiology Reviews, Volume 42, Issue 4, 1 July 2018, Pages 500–513, https://doi.org/10.1093/femsre/fuy019

The first two works will be added as annexes in the following pages

Chapter 23

Functional Diversity of Bacterial Strategies to Cope With Metal Toxicity

Sébastien Gillet, Emeline Lawarée and Jean-Yves Matroule

Molecular Biology Research Unit, NAmur Research Institute for LIfe Sciences (NARILIS)—Institute of Life, Earth, Environment (ILEE), University of Namur, Namur, Belgium

23.1 THE METALS

In the bacterial world, the great diversity of morphologies and physiological processes allowed bacteria to relentlessly adapt to a large number of environmental changes during the course of evolution. For instance, bacteria are often able to cope with an increase of concentration of specific metals in their environment, irrespective of their lifestyle, resulting in the onset of different survival strategies.

23.1.1 Metals Classification

Metals are ubiquitous in the environment, where their abundance may undergo important variations. Aluminum (Al), iron (Fe), or sodium (Na) are widely distributed, constituting 7.96%, 4.32%, and 2.36% of the earth continental crust, respectively (Wedepohl, 1995). Other metals such as silver (Ag) and cadmium (Cd) are considered as trace elements and accounts for only a fraction of 1% of the crust (Wedepohl, 1995). The classification of various metal elements has been the subject of a large debate, resulting in many blurred notions, such as "heavy metals," "trace metals," or "transition metals" (Hawkes, 1997). TMs, like Fe, copper (Cu), and nickel (Ni), encompass metal elements found in the d-block of the periodic table, ranging from group 3 to 11 and from period 4 to 7 (Fig. 23.1). They are mostly characterized by their electron shell and their redox properties. Group 12 elements, such as zinc (Zn), Cd, or mercury (Hg), are defined as "posttransitional metals" (Cotton et al., 1999). While technically not included in the transition metals group, they display similar biochemical properties as transition metals, which has led some authors to consider them as such. transition metals will be the focal point of this chapter and will be referred to as metals here below.

23.1.2 Metals and Bacteria—Coexisting for Better or Worse

23.1.2.1 There Would Be No Life Without Metal

Metals are essential to life. They are involved in many cellular processes, ranging from respiration to muscle contraction and nucleic acid stabilization. It is estimated that metalloproteins represent approximately 30% of the bacterial proteome (Waldron and Robinson, 2009). One of the major functions of metals is their role as essential cofactors. For instance, manganese (Mn) protects the cell against reactive oxygen species (ROS), as an obligate cofactor for certain types of catalase, peroxidase, and superoxide dismutase (SOD) (Horsburgh et al., 2002). SOD catalyzes the dismutation of two superoxide anions ($O_2^{\cdot -}$) into O_2 and the less reactive H_2O_2, which will be subsequently converted into H_20 by the peroxidase and the catalase (Becker and Skaar, 2014). Mn is essential in photosynthetic bacteria as well, where H_2O oxidation relies on a Mn metalloenzyme (Horsburgh et al., 2002). In *Escherichia coli*, Mn is also the catalytic factor of several exopeptidases, such as the aminopeptidase P (APPro), which possesses a binuclear Mn core. APPro proteins are conserved in the three domains of life (Graham and Guss, 2008) and are thought to have various biological functions, such as peptide degradation and proline recycling. APPro were also shown to be involved in the degradation

Microbial Diversity in the Genomic Era. DOI: https://doi.org/10.1016/B978-0-12-814849-5.00023-X

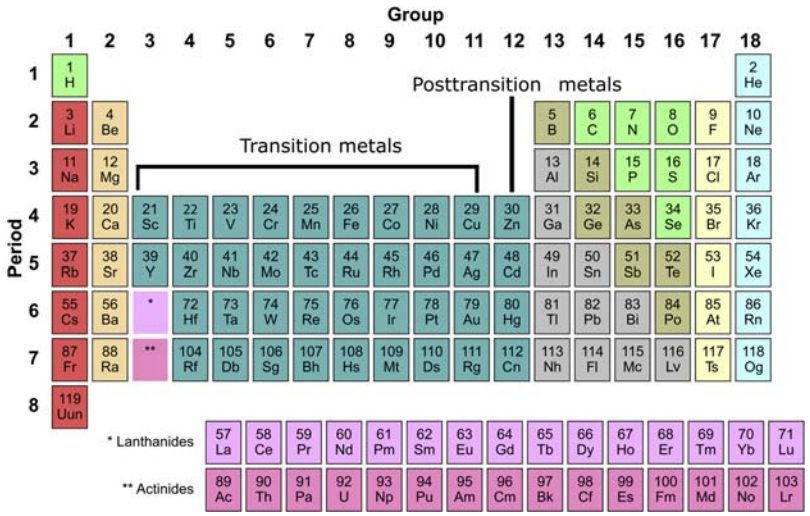

FIGURE 23.1 Periodic table of elements. The transition and posttransition metals, located from period 4 to 7 and from group 3 to 12, are colored in turquoise. *Modified from a public domain image created by Offnfopt, uploaded on Wikemedia Commons.*

of organophosphate compounds (Graham and Guss, 2008). In eukaryotes, they play a role in hormones maturation and activity regulation (Graham et al., 2006; Graham and Guss, 2008; Peng et al., 2017; Yocum and Pecoraro, 1999).

Similarly to Mn, Cu and Zn play a role in ROS detoxification through a structural and catalytic function in SOD, respectively. Cu/Zn SOD are very common in eukaryotes but are also conserved in bacteria, such as SodC in *E. coli* (Osman and Cavet, 2008).

Cu also serves as a catalytic cofactor for other enzymes, such as amino oxidases, NADH dehydrogenase-2, and cytochrome *C* oxidase, the latter being critical in cellular respiration (Festa and Thiele, 2011).

The interaction of metal ions with specific amino acids often ensures the proper conformation of metalloproteins (Festa and Thiele, 2011). Zn fingers are a prime example of metal-mediated structural motifs, where Zn stabilizes the protein in a certain fold. Zn fingers-containing proteins are often involved in transcription, DNA recognition, and apoptosis regulation (Laity et al., 2001).

In a similar way, Fe takes part in the electron transfer chain and in some cytochrome complexes, such as the succinate dehydrogenase (Failla, 2003). In addition, Fe displays a strong affinity for sulfides, enabling the formation of iron−sulfur (Fe−S) clusters. Fe−S clusters are so ubiquitous and abundant that they are sometimes regarded as one of the most prevalent prosthetic group and one of the very first catalyst in life (Beinert, 2000; Fontecave and Ollagnier-de-Choudens, 2008). Owing Fe crucial role in many cellular functions, Fe deprivation is often triggered by the host as a first-line of defense upon pathogen infection (Becker and Skaar, 2014). In order to adapt to this defense strategy, the causative agent of the Lyme disease *Borrelia burgdorferi* evolved by replacing Fe by Mn in its metalloproteins (Horsburgh et al., 2002). To overcome potential Fe limitation, bacteria also developed complex strategies. For instance, the small Fe-scavenging siderophores display a high affinity for Fe^{2+} or Fe^{3+} and are secreted in the extracellular space upon Fe starvation by several bacterial species. In Gram-negative bacteria, Fe-bound siderophores then bind TonB-dependent receptors at the bacterial surface allowing Fe to enter the cell. In Gram-positive bacteria, siderophores can bind directly to specific ATP-binding cassette (ABC) transporters anchored in the cytoplasmic membrane (Andrews et al., 2003; Benson and Rivera, 2013; Chandrangsu et al., 2017).

23.1.2.2 "The Dose Makes the Poison"—When Metals Turn Toxic

Despite their essential role in cellular processes, metals often turn toxic when their cellular concentration exceeds a specific threshold.

23.1.2.2.1 Mismetallation

Metals cytotoxicity mainly relies on their ability to compete with other metals and to cause mismetallation. In this context, the Irving−William series ranks transition metals according to the relative stability of the complexes they can form (Festa and Thiele, 2011; Waldron and Robinson, 2009), such that metals at the top of the series (like Cu) exhibit a higher affinity for a specific ligand, even at low concentration.

$$Mn^{2+} < Fe^{2+} < Co^{2+} < Ni^{2+} < Cu^{2+} < Zn^{2+}$$

Mismetallation may alter the conformation and therefore the function of a metalloprotein (Chandrangsu et al., 2017). In *E. coli*, Zn^{2+} was shown to decrease the activity of ribulose-3-phosphate 5-epimerase (RPE) by replacing the cognate Fe^{2+} cofactor in the enzyme (Imlay, 2014). Whether this effect is due to the high affinity of Zn for the ligand (preventing it from being released fast enough) or due to a structural alteration is not clear yet. This mismetallation is cytotoxic considering the role of RPE in sugar conversion (Imlay, 2014). When *Streptococcus pneumoniae* is subjected to a Zn stress, Zn^{2+} competes with Mn^{2+} within the Mn^{2+} PsaA importer. Although PsaA still retains a higher affinity for Mn^{2+}, Zn^{2+} binding seems significantly more stable, which may clog the importer and prevent further Mn import (McDevitt et al., 2011).

Mismetallation seems to be a widespread mechanism of toxicity. It has been observed in all three domains of life and has been reported with ions not listed in the Irving–William series, such as Cu^{+} (Chandrangsu et al., 2017), Ag^{+} (Das, 2017), Pb^{2+} (Fullmer et al., 1985), and Cd^{2+} (Hossain et al., 2012). Pb^{2+} displaces Ca^{2+} in calmodulin, disrupting cellular signaling in animal cells (Fullmer et al., 1985). A similar effect is observed in plants, where Ca^{2+} ions bound to calmodulin are displaced by Cd^{2+} (Hossain et al., 2012). Cd was also reported to bind sulfhydryl groups and to displace cognate metal cofactors from various metalloproteins including transcription factors (Kim et al., 2007).

Because of its high affinity for thiolate, Cu^{+} is proposed to disrupt Fe–S clusters (Dupont et al., 2011). In *E. coli*, it has been suggested that Cu^{+} damages Fe–S cluster dehydratases by displacing Fe atoms from the cluster, leading to the inactivation of the enzyme (Macomber and Imlay, 2009).

23.1.2.2.2 Oxidation of Cellular Substrates

Metals can also promote the generation of ROS leading to an oxidative stress. Fe^{2+} is a well-known catalyst of the Fenton reaction converting H_2O_2 into the highly toxic hydroxyl radical ($OH\bullet$) that potentially oxidizes DNA, lipids, and proteins (Winterbourn, 1995). Cd^{2+} is thought to induce lipid peroxidation when it interacts with cell membranes (Rani et al., 2014). Cu^{+} is also able to catalyze a Fenton-like reaction in vitro (Rensing and Grass, 2003; Santo et al., 2008), although the in vivo relevance of this process is still under debate due to the lack of evidence of Cu-induced ROS DNA damage (Macomber et al., 2007). Cu is also able to generate other kinds of ROS, at least in vitro, such as nitric oxides through the oxidation of S-nitrosothiol compounds (Achard et al., 2012; Gordge et al., 1995). Cd mismetallation can also indirectly promote oxidative stress by triggering the release of free Fe from various proteins, such as ferritins, which may in turn be involved in a Fenton reaction (Rani et al., 2014)

$$Fe^{2+} + H_2O_2 \rightarrow Fe^{3+} + HO\bullet + OH^{-}$$

In addition to ROS generation, Cu can potentially induce the formation of undesired disulfide bonds between two thiol groups (Hiniker et al., 2005). These disulfide bonds may impair protein conformation and lead to its inactivation, as it was shown with β-galactosidase (Hiniker et al., 2005; Tian et al., 2000).

Recent studies revealed that dry Cu surfaces have a strong bactericide or bacteriostatic potential, although the mechanisms underlying this toxicity have not been completely elucidated yet. It is proposed that dissolved Cu ions may enter the cells and induce the toxic mechanisms described above (Molteni et al., 2010). In addition, dry Cu has been reported to promote a rapid loss of the membrane integrity referred to as contact killing (Grass et al., 2011; Santo et al., 2010; Santo et al., 2008).

23.2 METAL-DEDICATED RESISTANCE SYSTEMS

Even though many metals share the same mechanisms of toxicity, bacteria evolved metal-and cellular compartment-specific defense strategies, indicating that a fine tuning of metal homeostasis is required for each metal in each cellular compartment to maintain bacterial fitness.

23.2.1 Extracellular Space—Dealing With an Invasive Friend

When the extracellular concentration of a given metal increases, the first "checkpoint" consists in limiting the entry of the metal in order to maintain a proper cellular metal homeostasis and to avoid cellular damage. A straightforward mean to handle this stress is to downregulate the expression of metal importers.

In *Bacillus subtilis*, Zn is sensed by the zinc uptake regulator (Zur) protein. When intracellular Zn concentration increases, the dimeric protein Zur binds DNA and represses the Zur regulon involved in Zn uptake

(Chandrangsu et al., 2017). A paralogous system exists for the Fe uptake regulation, where the ferric uptake regulator (Fur) protein represses Fe acquisition genes in a similar way. These regulators are conserved in many bacterial classes. For instance, the actinobacterium *Frankia* genome encodes the Fur, Zur, nickel uptake regulator (Nur), manganese uptake regulator (Mur), and Co-Fur proteins that regulate Fe, Zn, Ni, Mn, and Co import, respectively (Furnholm and Tisa, 2014).

In *B. subtilis*, the primary MgtE-dependent Mg import relies on a magnesium-sensitive riboswitch (Dann et al., 2007; Wakeman et al., 2014). Indeed, Mg^{2+} induces a conformational change of the mgtE mRNA, which promotes its compaction and the inactivation of an antiterminator structure, causing mgtE transcription arrest.

Chelation or precipitation of the soluble metal ions in the extracellular medium is another means to limit metal entry. In *Saccharomyces cerevisiae*, the SLF1 protein biomineralizes Cu at the surface of the yeast cells by converting $CuSO_4$ (soluble Cu^{2+}) into CuS (insoluble Cu^{+}), increasing the yeast Cu tolerance (Yu et al., 1996). A similar strategy is observed in Cu-exposed *Pseudomonas aeruginosa* biofilms, where brown Cu-containing precipitates can be found in the extracellular space, indicating a role of the biofilm in Cu chelation and cell protection (Harrison et al., 2005).

23.2.2 Intracellular Space—Keeping the Place Safe

Unlike Gram-positive bacteria which display one single lipid membrane, the cytoplasm of Gram-negative bacteria is isolated from the extracellular medium by the periplasm, which is delimited by the inner membrane (cytoplasmic side) and the outer membrane (extracellular side). The periplasm and the cytoplasm harbor distinct physiological activities under oxidative and reducing conditions, respectively, implying that metal toxicity will vary relative to the cellular compartment. Therefore, several strategies have been developed through evolution to cope with cellular metal stress, ranging from metal export to detoxification of metal ions or toxic by-products.

23.2.2.1 Efflux

The most common strategy to regulate metal homeostasis consists in decreasing cellular metal concentration with the use of efflux pumps. Several types of efflux pumps have been characterized in bacteria.

23.2.2.1.1 ATPases

P_{1b}-type ATPases (also known as E_1-E_2 ATPases) pumps are typical metal exporters and are conserved in many organisms, from bacteria to eukaryotes. These transporters use ATP hydrolysis as a source of energy to translocate a substrate across the cytoplasmic membrane. They typically contain six to eight transmembrane (TM) domains constituting the translocation channel. Three additional domains facing the cytoplasm are involved in ATP binding and hydrolysis, energy transduction, and regulation of the system (Fig. 23.2) (Argüello et al., 2011; Inesi et al., 2014). Cognate P_{1B}-type ATPase have been identified for the specific transport of Cu^{+}, Fe^{2+}, Zn^{2+}, and Co^{2+} (Culotta and Scott, 2013;

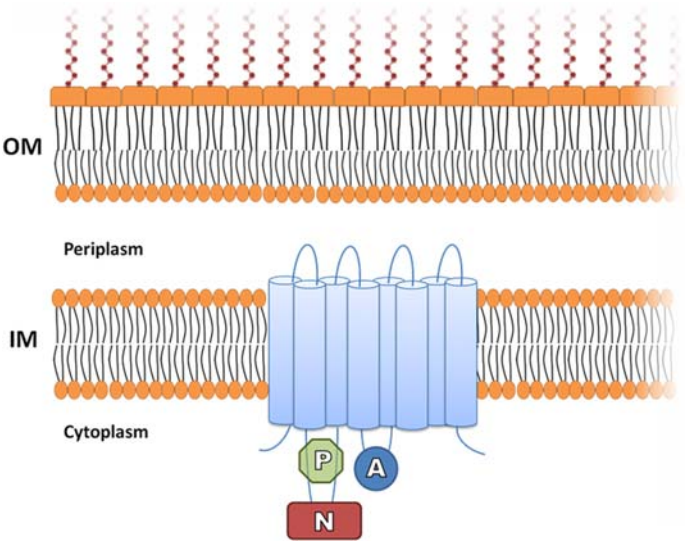

FIGURE 23.2 P1B-type ATPase contain six to eight transmembrane domains (TMD). These TMD forms the main translocation channel. Three additional domains are facing the cytoplasm: the phosphoryl domain (P, in green), the catalytic activation domain (A, in blue), and the ATP-binding domain (N, in red). *OM*, outer membrane; *IM*, inner membrane.

Guan et al., 2015). In *B. subtilis*, Fe^{2+} export is mediated by the PfeT ATPase (Guan et al., 2015). In *E. coli*, Zn^{2+} and Cu^{+} are transported from the cytoplasm to the periplasm by the ZntA and CopA P_{1b}-type ATPases, respectively (Rensing et al., 1997). CopA homologs have been found in many bacterial species, including *B. subtilis*, *Sinorhizobium meliloti, Legionella pneumophila*, and *Enterococcus hirae* (Argüello et al., 2013; Multhaup et al., 2001; Patel et al., 2014; Porcheron et al., 2013). Interestingly, *E. hirae* CopA was first reported to be a Cu importer, although the evidence sustaining the uptake function remain indirect (Odermatt et al. 1993; Solioz and Stoyanov 2003). The export function would then be carried out by another ATPase, CopB (Odermatt et al., 1993). It is interesting to note that CopA does not bind free soluble Cu ions directly, which would be highly toxic in the cytoplasm, but is rather relying on a dedicated transporter (see Section 23.2.3.1). Owing to their physicochemical properties, Cd^{2+}, Pb^{2+}, and Ag^{+} likely use noncognate ATPase (Argüello et al., 2011).

23.2.2.1.2 HME-RND

The resistance-nodulation-division (RND) transporters superfamily includes the heavy metal efflux (HME)-RND family, which is involved in metal homeostasis in several Gram-negative bacteria. An HME-RND transporter is typically a tripartite complex where the RND protein, generally anchored in the inner membrane, is linked to an outer membrane channel protein (OMP) via a periplasmic membrane fusion protein (MFP) (Fig. 23.3) (Nies, 2003; Valencia et al., 2013).

In *E. coli*, the CusABC pump mediates Cu efflux from the cytoplasm or the periplasm to the extracellular space (Osman and Cavet, 2008). The integral inner membrane CusA binds cytoplasmic Cu and feeds the CusC OMP via the periplasmic CusB MFP, which can also directly bind periplasmic Cu^{2+}. While RND complexes share a common structure in Gram-negative bacteria, they diverge enough to accommodate for different metals. For instance, in *Pseudomonas putida*, the CzcCBA system confers increased resistance against Zn^{2+}, Cd^{2+}, and Pb^{2+} (Leedjärv et al., 2008). In *Caulobacter crescentus*, the CzrCBA and NczCBA systems are involved in Cd and Zn, and Ni and Co efflux, respectively (Valencia et al., 2013). A similar system also exists in *Helicobacter pylori*, where CznABC mediates Cd, Zn, and Ni homeostasis. A tight regulation of cellular metal homeostasis is particularly important in the success of *H. pylori* infection (Stähler et al., 2006). In *Cupriavidus metallidurans*, the CzcCBA system confers higher resistance to Co, Cd, Zn, and Ni (Nies, 2003).

23.2.2.1.3 Cation Diffusion Facilitator

The third major type of bacterial efflux pumps is the cation diffusion facilitators (CDF) family. These membrane metalloproteins are classically composed of six transmembrane helices, two of which possess metal-binding sites. The third TM domain usually acts as a hydrophobic gate. A histidine-rich loop (IL-2) between the fourth and the fifth TM domain has a metal selectivity purpose (Fig. 23.4) (Kolaj-Robin et al., 2015). CDF mostly transport Zn^{2+}, Co^{2+}, Cd^{2+}, Ni^{2+},

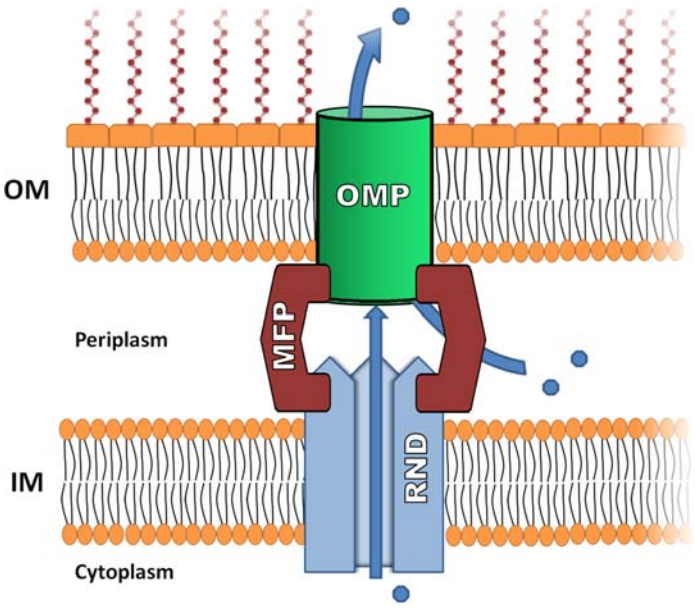

FIGURE 23.3 Classic structure of the HME-RND transporter family. The complex articulate itself around a RND protein (RND, in blue, anchored in the inner membrane), a periplasmic MFP (in red), and an OMP (in green). Metal ions (blue octagons) are delivered either from the periplasm or directly from the cytoplasm. *OM*, outer membrane; *IM*, inner membrane; *HME*, heavy metal efflux; *RND*, resistance-nodulation-division; *MFP*, membrane fusion protein; *OMP*, outer membrane channel protein.

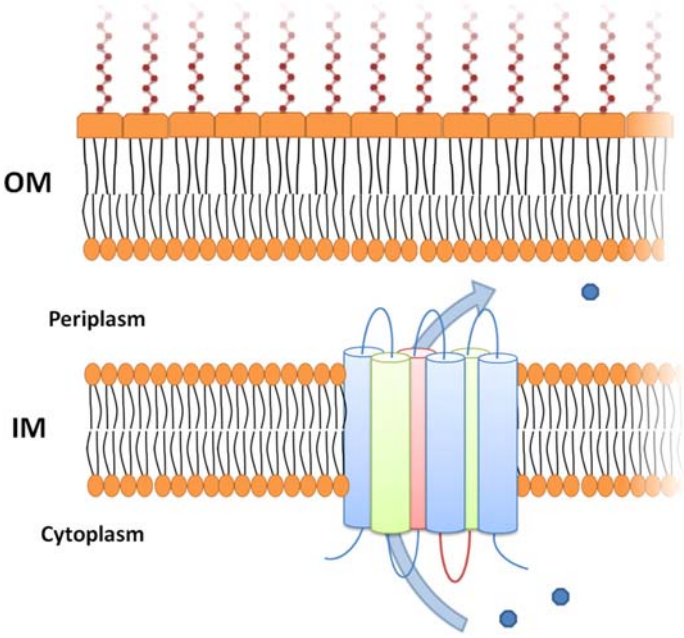

FIGURE 23.4 CDF are usually composed of six transmembrane helices (or TM domain). The second and fifth TM domain, depicted in green, comprise metal binding sites. The third helix, in pink, serves as a hydrophobic gate. The histidine-rich loop (IL-2, in dark red, linking the fourth and fifth TM domain) has a metal selectivity purpose. *OM*, outer membrane; *IM*, inner membrane; *CDF*, cation diffusion facilitators.

and Fe^{2+} ions by diffusion along gradients (Higuchi et al., 2009; Nies, 2003). In *E. coli*, ZitB and YiiP antiporters export Zn^{2+} against H^{+} (Chao and Fu, 2004; Wei and Fu, 2005). This system is conserved across a large number of bacteria, including extremophiles such as the hyperthermophilic bacterium *Thermotoga maritima* (Higuchi et al., 2009).

In *B. subtilis*, MneP and MneS CDF proteins are controlled by the Mn sensor and regulator MntR (Huang et al., 2017). *MneP* and *mneS* mutants exhibit an increased Mn sensitivity and accumulate 12 times more Mn ions than the wild-type strain (Huang et al., 2017).

23.2.2.1.4 ABC Transporters

The ABC transporters family is the most conserved transport system in living organisms (Higgins, 2001; Jones and George, 2004). ABC transporters are generally composed of (1) a TM domain anchored in the cytoplasmic membrane and acting as a permease and (2) a cytoplasmic nucleotide-binding domain featuring an ABC (Fig. 23.5). ABC transporters ensures the transport of a wide variety of substrates such as sugars, amino acids, and metals (Fath and Kolter, 1993). In *E. coli*, YbbP and YbbA have been reported as two subunits of a putative metal exporting ABC system (Moussatova et al., 2008). Even though ABC metal exporters turn out to be less prevalent in bacteria than in the other domains of life, yet they are crucial in metal extrusion in many microorganisms, including unicellular fungi and algae. In *S. cerevisiae*, Yor1 is proposed to transport Cd-bound glutathione (GSH) across the plasma membrane in order to maintain a proper cellular Cd concentration (Culotta and Scott, 2013). In addition, the Fe-specific Atm1 ABC transporter was identified in the *S. cerevisiae* mitochondrial inner membrane, where it would protect mitochondrial DNA from Fe-induced oxidative damage by regulating mitochondrial Fe homeostasis. Accordingly, *Atm1* mutants accumulate up to 30 times more mitochondrial Fe than the wild-type strain (Chloupková et al., 2003; Radisky et al., 1999; Schueck et al., 2001). In *Arabidopsis thaliana*, the ABC transporter AtPDR8 is upregulated in the presence of both Cd and Pb and provides an increased resistance to both metals (Kim et al., 2007).

23.2.2.1.5 Others Transport Systems

Several efflux systems do not belong to any of the aforementioned categories. Yet, they play an important role in metal homeostasis. For instance, the Fe integral inner membrane MbfA exporter has been identified in the Gram-negative bacteria *Bradyrhizobium japonicum* (Sankari and O'Brian, 2014). Interestingly, *mbfa* gene expression is induced by Fe only, suggesting that its function may be specific to this metal (Sankari and O'Brian, 2014).

In *E. coli*, the expression of the RcnA inner membrane Ni/Co pump, previously known as YhoM, is induced by Ni and Co. Accordingly, a *rcnA* mutant exhibits an increased sensitivity to Ni and Co by accumulating nearly twice more Ni than the wild-type strain. RncA overexpression leads to a drastic decrease of the cellular Ni concentration below the

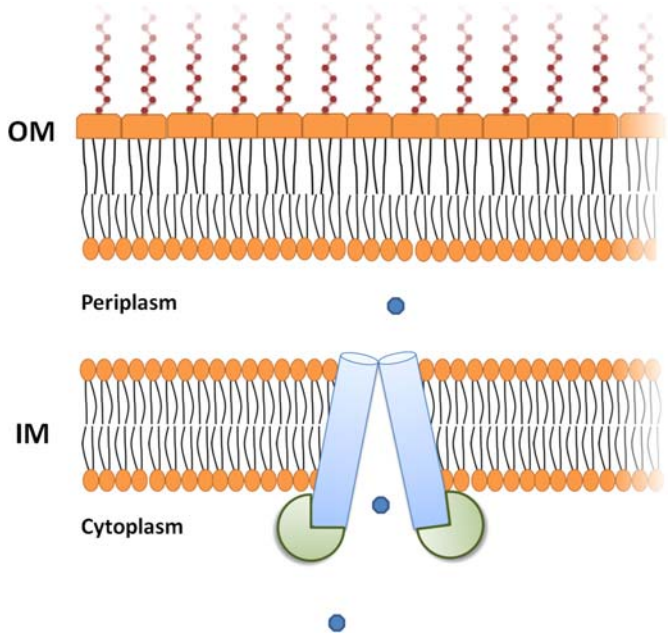

FIGURE 23.5 Schematic representation of an ABC transporter. The transmembrane domains (in light blue) are anchored in the cytoplasmic membrane, where they serve as permeases. The cytoplasmic NBD (in green) featuring an ATP-binding cassette, uses the energy of ATP hydrolysis to modify the conformation of the complex to allow the transportation of substrates. *OM*, outer membrane; *IM*, inner membrane; *NBD*, nucleotide-binding domain.

wild-type level. However, RncA does not harbor any typical genetic signature from other known efflux system, suggesting that it belongs to a novel family (Bleriot et al., 2011; Rodrigue and Effantin, 2005).

Nonspecific multidrug efflux pumps have been shown to mediate the export of a broad variety of compounds and molecules, including metals (Blanco et al., 2016). Various bioinformatics tools facilitate the prediction of potential periplasmic export proteins and outer membrane efflux proteins based on sequence homology, without, however, predicting their substrate (Johnson and Church, 1999).

23.2.2.2 Storage and Detoxification

Owing to their cytotoxicity, free metals ions must remain scarce in the intracellular bacterial space. In eukaryotic cells, free Zn^{2+} concentration is in the picomolar range (Maret, 2015). In bacteria, free Cu is estimated at less than one atom/cell, which is in agreement with the extreme sensitivity of the CueR sensor within the zeptomolar range (Changela et al., 2003). In order to maintain such a low amount of free metal ions and to limit metal-associated damages, bacteria evolved molecules such as chelators, scavenging proteins, and chaperones, displaying a strong affinity for metals.

23.2.2.2.1 Metallochaperones

Chaperones are small cytoplasmic or periplasmic proteins acting as metal carriers. Chaperones not only isolate toxic free metal ions, but they also ensure their correct delivery to their cognate protein targets (Bagai et al., 2008; Harrison et al., 1999; Waldron and Robinson, 2009). In the periplasm of *E. coli*, CusF binds Cu^{+} ions and delivers them for export to CusB within the CusABC RND efflux pump (Bagai et al., 2008). MerP binds Hg^{2+} cations and transfers them to the inner membrane MerT transporter, which feeds the cytoplasmic MerA mercuric reductase for Hg^{2+} detoxification into Hg^{0} (Das, 2017; Moore et al., 1990). Some chaperones provide protection against multiple metals. The periplasmic Zn chaperone ZinT binds not only Zn but also Co, Cd, and Hg (Colaço et al., 2016; Kershaw et al., 2007). Despite some contradictory results about ZinT function, *zinT* expression seems to rely on the Zn-specific regulator Zur. ZinT chaperone would deliver Zn to the ZnuABC inner-membrane Zn importer, therefore playing an important role under Zn starvation as well. *ZinT* expression is also upregulated upon periplasmic Cd stress (Colaço et al., 2016). In addition, ZinT binds a wide array of metals and increases the resistance against Cd, Co, and Hg. It was even hypothesized that ZinT can deliver Co^{2+} ions to the previously described Ni/Co pump RcnA/B (Colaço et al., 2016).

In *B. subtilis*, Cu^{+} ions are delivered to the CopA P_{1b}-type ATPase by the CopZ chaperone (Radford et al., 2003). CopZ binds Cu^{+} via a typical MxCxxC binding domain (Cobine et al., 2002). This conserved domain is present in the majority of bacterial Cu chaperones identified so far (Harrison et al., 1999). Most of these metallochaperones display a βαββαβ ("open-faced β sandwich") folding (Harrison et al., 1999; Pontel et al., 2015). *E. hirae* CopZ is a cytoplasmic

chaperone that delivers Cu^+ ions to the CopY repressor, triggering its release from the cop operon promoter and allowing *cop* transcription. CopZ therefore acts as an indirect activator of the *cop* operon (Cobine et al., 1999; Cobine et al., 2002) In *E. coli*, no CopZ homolog has been identified. However, a 2017 study demonstrated that the CopA mRNA is translated into a chaperone protein through a ribosomal frameshifting (Meydan et al., 2017). The *copA* gene therefore encodes both the ATPase and its chaperone, highlighting the amazing optimization potential of bacterial genomes.

23.2.2.2.2 Metallothioneins

Metallothioneins (MTs) are small cytoplasmic or periplasmic proteins binding metals via thiolate bounds within cysteine residues (Hamer, 1986). While their main biological function is still a matter of debate, they have been shown to bind Zn, Cu, Hg, Cd, As, or Ag (Chandrangsu et al., 2017; Culotta and Scott, 2013; Peer et al., 2006). Unlike metallochaperones, MT do not play a role in directed metal transport. MTs are found in eukaryotes and bacteria and often exhibit a "buffer-like" function to limit the toxicity of free metal ions. In *Synechococcus* species, the Smta MT has been shown to bind not only Zn^{2+} but also possibly other ions, as its expression is also induced by Cu^{2+} and Cd^{2+} (Borkow and Gabbay, 2005; Bruins et al., 2000; Culotta and Scott, 2013). In *Providencia vermicola*, the MT BmtA sequesters Pb in the periplasm, leading to increased Pb resistance (Sharma et al., 2017).

23.2.2.2.3 Glutathione

GSH is a thiol compound produced by many organisms, including certain bacteria. In *E. coli*, it is synthesized in a two-step reaction from three amino acid precursors: Glu, Cys, and Gly (Masip et al., 2006). This reaction is catalyzed by GshA and GshB. GSH has a broad range of biological functions, including protection against various stresses, such as pH variation, osmotic shock, or toxic products (Masip et al., 2006; Montoya, 2013; Potter et al., 2012; Wang and Ballatori, 1998). As an antioxidant, GSH plays a critical role in the defense against ROS (Potter et al., 2012). In *E. coli*, GSH protects against H_2O_2-induced oxidative stress (Masip et al., 2006).

Many Gram-positive bacteria, such as *Streptococcus mutans*, are lacking the GSH synthesis pathway (Sherrill and Fahey, 1998; Vergauwen et al., 2013). It was shown that *S. mutans* imports GSH from the environment through two ABC transporters: TcyBC and GshT, a solute-binding protein possessing a high affinity for GSH (Vergauwen et al., 2013). A homologous system is present in the Gram-positive *S. pneumoniae*, where extracellular GSH is imported by the GshT ABC transporter (Potter et al., 2012). A *S. pneumoniae* GshT mutant is unable to grow properly when challenged with toxic Cu, Zn, or Cd concentrations (Potter et al., 2012). In *Novosphingobium aromaticivorans*, an Atm1-like ABC exporter has been associated with GSH transport in the context of heavy metals detoxification (Lee et al., 2014).

GSH mercaptides are also known to binds metals, such as Cu, Cr, or Zn, via nonenzymatic reactions, providing a chelating effect and preventing the potential toxicity of free metal ions (Helbig et al., 2008; Ballatori, 1994; Wang and Ballatori, 1998).

The GSH oligomer phytochelatin is mainly present in plants where it sequesters various metal ions. It is also an important means of metal detoxification for numerous microorganisms such as unicellular algae or fungi (Helbig et al., 2008). In *Schizosaccharomyces pombe*, Cd^{2+}-bound phytochelatin is translocated into a vacuolar compartment by the *hmt1*-encoded ABC transporter, thereby isolating the toxic metal from valuable cellular material (Ortiz et al., 1992; Ortiz et al., 1995).

23.2.2.2.4 Ferritins

Dedicated resistance systems can limit metal toxicity by combining sequestration with an oxidoreduction reaction. Ferritin, bacterioferritin, and ferritin-like proteins are multimeric proteins involved in the storage and detoxification of free Fe ions (Carrondo, 2003; Das, 2017). Ferritin proteins are conserved among most living organisms, from bacteria to mammals, underlying their utmost importance in the regulation of cellular Fe distribution and availability. Ferritin is composed of 24 subunits forming a spherical shape that can hold up to 4500 Fe atoms and therefore acts as a Fe buffer and storage under both Fe starvation and excess. In addition, ferritin uses O_2 to oxidize Fe^{2+} ions at the ferroxidase catalytic site within each ferritin subunit (Andrews et al., 2003). The soluble Fe^{2+} cations are thus stored in the less toxic Fe^{3+} ferrihydrite minerals (He et al., 2016) and can remobilize Fe^{2+} ions upon Fe starvation (Andrews et al., 2003; Pulliainen et al., 2005).

Dps proteins (DNA-binding proteins for starved cells) are Fe detoxification proteins, similar to ferritins in the sense they also form roughly spherical shapes that encapsulate Fe ions (Andrews et al., 2003). They are sometimes referred to as ferritin-like proteins, although they are composed of only 12 subunits, limiting the number of bound Fe ions (about

500). Yet, Dps proteins are primarily involved in DNA protection against ROS during stationary phase (Almiron et al., 1992). Dps Fe-binding ability was demonstrated much later (Zhao et al., 2002).

23.2.2.2.5 Multicopper Oxidases

Multicopper oxidases (MCOs) use Cu ions as cofactors to oxidize a broad range of substrates (Komori and Higuchi, 2015; Solomon et al., 1996). Classically, MCOs harbor three Cu-binding sites. The mononuclear T1 Cu site accepts electrons and transfer them to a trinuclear cluster, which is composed of a mononuclear T2 Cu site and a binuclear T3 Cu center, binding and reducing O_2 (Galli et al., 2004; Solomon et al., 1996). Specific MCOs are involved in metal resistance by using the metal as a substrate (Butterfield et al., 2013; Solomon et al., 2008). In *E. coli*, the periplasmic MCO CueO oxidizes Cu^+ into the less toxic Cu^{2+} by using O_2 as a final acceptor (Grass and Rensing, 2001). Cu^+ oxidation will therefore result in a four electrons reduction of O_2 into two H_2O molecules (Djoko et al., 2010; Grass and Rensing, 2001). Near the T1 Cu site, CueO also displays a methionine-rich region binding a labile Cu ion in the context of a phenol oxidase activity (Cortes Castrillona et al., 2015; Djoko et al., 2010; Roberts et al., 2003).

Cu-oxidizing MCOs tend to be conserved, although small structural and functional variations can be observed. For instance, the *Rhodobacter capsulatus* CutO MCO provides Cu tolerance, despite the lack of an extra methionine-rich region (Wiethaus et al., 2006).

23.2.2.2.6 Other Detoxification Systems

MerA is a mercuric iron reductase dedicated to the detoxification of the deleterious Hg^{2+} ions into the volatile and near-inert Hg^0 in the cytoplasm of many bacteria (Moore et al., 1990). This system is conserved in various Gram-negative and Gram-positive bacteria such as *E. coli*, *B. subtilis*, *Bacillus thuringiensis*, and *P. aeruginosa* (Barkay et al., 2003; Das, 2017; Moore et al., 1990; Schiering et al., 1991).

Some metal reductases are coupled to efflux systems in order to provide their protective effect. For instance, the ArsC arsenate reductase turns the pentavalent As^{5+} (arsenate) into the trivalent As^{3+} (arsenite). Arsenate is an analog of phosphate that impairs phosphorylations in metabolic reactions. Arsenate also prevents ATP synthesis by inhibiting oxidative phosphorylations (Tamaki and Frankenberger, 1992). Arsenite is, however, regarded as more toxic than arsenate, owing to its ability to bind thiol groups (Kaur et al., 2009; Kaur et al., 2011; Silver and Misra, 1984; Tamaki and Frankenberger, 1992). Nevertheless, the reduction of arsenate into arsenite is necessary for As homeostasis considering the specificity of the ArsA and ArsB exporters for arsenite (Bruins et al., 2000). Interestingly, in some bacteria such as certain *Bacillus alcaligenes*, or *Pseudomonas* species, As^{3+} is oxidized into the less toxic As^{5+} (Osborne and Ehrlich, 1976; Tamaki and Frankenberger, 1992; Turner, 1949).

23.3 METAL RESISTANCE ASSOCIATED WITH PHENOTYPIC PLASTICITY

23.3.1 Biofilm

A biofilm is a complex microbial aggregate attached to inert or living surfaces and enclosed in an extracellular matrix composed of proteins, amyloid fibers, exopolysaccharides, and extracellular DNA (Flemming and Wingender, 2010; Watnick and Kolter, 2000). In natural habitats, biofilm is the prevalent microbial lifestyle and provides multiple advantages to the matrix-embedded microorganisms. For instance, the extracellular polymeric matrix not only captures and concentrates environmental nutrients but also acts as a protective barrier against environmental challenges or antimicrobial factors (Serra and Hengge, 2014; Watnick and Kolter, 2000).

When *P. aeruginosa* biofilms are subjected to Cu^{2+} stress, brown Cu precipitates accumulate in the extracellular space, suggesting that the matrix chelates and aggregates Cu ions, increasing metal resistance (Harrison et al., 2005). Increased resistance of biofilms to other metals such as Pb, Co, Ni, and Zn has also been described, likely resulting from metal ions binding to the polymeric matrix (Harrison et al., 2005; Teitzel and Parsek, 2003).

23.3.2 Persister Cells

Persistence is a typical example of phenotypic heterogeneity within a genetically homogenous population. Persister cells are metabolically less active cells, akin to a "dormancy" state. The remaining metabolic activities are mostly focused on energy production (Radzikowski et al., 2016). Persisters have been shown to catabolize carbon sources and perform cellular respiration (Amato et al., 2014; Mok et al., 2015; Orman and Brynildsen, 2013). Persister cells appear in a constant and stochastic manner or following an environmental stress, where the persisters rate can reach 1% in biofilm or

in stationary phase (Gefen and Balaban, 2009; Wu et al., 2012). The presence of persister cells in microbial populations ensures that a small subpopulation can survive to stress conditions, where a phenotypically homogeneous population would be eradicated (Fruci and Poole, 2012). Interestingly, this dormancy state protects them from toxic compounds acting preferentially on growing bacteria (Lewis, 2010).

In *P. aeruginosa*, planktonic persisters exhibit an increased resistance to Cu, Ni, and Co stresses, although the precise underlying molecular mechanisms remain to be elucidated (Harrison et al., 2005). In *E. coli*, metals-induced ROS have been shown to induce a decrease of membrane potential, leading to a reduced metabolic activity and an increased persisters level in the population (Wang et al., 2017). The decrease of membrane potential might be mediated by the SOS response, which was shown to activate the expression of *tisB* in *E. coli*, leading to the disruption of the proton motive force and the decrease of intracellular ATP level (Dörr et al., 2010). Owing to their ability to trigger ROS production, some metals could therefore induce an SOS response leading to the generation of persister cells more prone to survive under metal stress.

23.3.3 Bet-Hedging

Stochasticity is inherent to most biological processes. From transcription to protein assembly and bistability of specific systems, random variations are inevitable (Raj and van Oudenaarden, 2008; Veening et al., 2008). In addition, the distribution of cellular material upon cell division might not reach a perfect 1:1 ratio between the incipient progenies resulting in random phenotypic variations within the bacterial population, irrespective of environmental cues (Raj and van Oudenaarden, 2008; Seger and Brockmann, 1987). This phenotypic plasticity relates to a bet-hedging strategy providing rapid Darwinian adaptation to a changing environment. Because no genetic change is involved, this strategy is regarded as more flexible, and reversible at the population scale. The trade-off of this stochasticity is a partial loss of fitness in the population, sometimes leading to adverse effects or suboptimal conditions (Raj and van Oudenaarden, 2008; Veening et al., 2008). Bet-hedging has been observed in various bacterial species. In *S. meliloti*, polyhydroxybutyrates (PHB) are not equally distributed between the siblings. The old pole tends to retain more PHB in a stochastic way. This leads to variations of PHB levels among the clonal population. Bacteria with a high-level of PHB are more likely to be metabolically dormant, akin to persisters, and better resist to stress (Ratcliff and Denison, 2011).

A recent study on Zn resistance in *E. coli* demonstrated stochastic cell-to-cell fluctuations of the ZntA exporter (Takahashi et al., 2015). Because ZntA is very sensitive and because free cellular Zn must remain very scarce, the slightest variation in the amount of ZntA may be crucial for one bacterium relative to its counterparts within the clonal population. Therefore, some bacteria will be "primed" to respond to certain stress conditions, such as an increase in Zn concentration, despite being suboptimal otherwise (Takahashi et al., 2015).

23.3.4 Sporulation

In response to environmental changes, some bacteria, such as *Bacillus* spp. or *Clostridium* spp., undergo sporulation in order to generate the so-called metabolically inactive dormant spores (Leggett et al., 2012; Tan and Ramamurthi, 2014). In *B. subtilis*, sporulation results from a transcriptional reprogramming of more than 500 genes (Schultz et al., 2009). When favorable growth conditions are restored, spores germinate and resume their vegetative cell cycle.

The stress resistance capacity of a spore mostly resides in its structure, featuring inwards an exosporium, a spore coat, an outer membrane, a cortex, a germ cell wall, and an inner membrane before reaching the core, which contains the bacterial chromosome, RNA, ribosomes, and most of the bacterial enzymes. The spore coat, composed of a series of thin and concentric layers, acts as a "sieve" excluding large toxic molecules but remains permeable to small molecules, such as those triggering spore germination (McKenney and Eichenberger, 2012; Nicholson et al., 2000). The spore coat also provides a good protection against bacteriophages and oxidizing agents, UV radiation, ozone, and peroxinite (Genest et al., 2002; Laaberki and Dworkin, 2008; Riesenman and Nicholson, 2000). The cortex is mostly constituted of peptidoglycan and maintains the spore in a partially dehydrated state, allowing a high resistance to heat (Beaman and Gerhardt, 1986; Imae and Strominger, 1976).

In *Clostridium difficile*, dormant spores are less sensitive to Cu stress than the vegetative form (Wheeldon et al., 2008). Similarly, *Bacillus anthracis* endospores were proven to better resist to contact-killing with a Cu surface than the vegetative cells (Bleichert et al., 2014). Albeit still unknown, the mechanisms underlying this resistance might be related to the structure of the spore itself and to spore-specific proteins. In *Bacillus* species, the exosporium contains metal-oxidizing enzymes such as the MCO that catalyze the two-step Mn oxidation (Mn^{2+} to Mn^{4+}), resulting in Mn mineralization and encrustation in the outer layer (Butterfield et al., 2013). The structure of *B. subtilis* spore makes it

more resistant than the vegetative form to metal by-products such as ROS (Zuber, 2009). Indeed, the spore coat acts as a first-line barrier to limit the entry of peroxides. Moreover, the poor hydration of the core is unfavorable to ROS generation (Zuber, 2009).

It is currently unclear whether sporulation is induced upon metal stress, although it is well established that metals are required for this process (Kojetin et al., 2005). Surprisingly, in *Clostridium tyrobutyricum*, *Streptomyces* spp., *B. subtilis*, and *Pasteuria penetrans*, high Zn^{2+} and Cu^{2+}concentrations reduce the sporulation rate (Kojetin et al., 2005; Majzlik et al., 2011; Mato Rodriguez and Alatossava, 2010).

23.3.5 Fructification

Morphological and developmental changes also constitute a means of coping with local metal stress. The *Glomereaceae* fungi family members extend their presymbiotic hyphae and expand their extraradical mycelium when exposed to high Cd and Pb concentrations, reaching less metal concentrated areas (Pawlowska and Charvat, 2004). Similar avoidance strategies have been highlighted in other fungi and even in plants, such as *Filipendula ulmaria.* In *F. ulmaria*, growth inhibition of the roots near Cd-rich soil layers is compensated by an increase in the growth rate of deeper roots, further away from the stress (Balsberg, 2013; Tyler et al., 1989).

23.4 CASE STUDY: *CAULOBACTER CRESCENTUS* BIMODAL STRATEGY

The oligotrophic alphaproteobacterium *C. crescentus* constitutes a striking example of functional diversity. Its cell cycle culminates with an asymmetrical cell division yielding two morphologically and physiologically distinct progenies, one flagellated swarmer (SW) cell and one sessile stalked (ST) cell. This phenotypic discrepancy implies that both cell types will tackle metal stress by using distinct strategies.

23.4.1 *Caulobacter crescentus* Cell Cycle

The SW cell is limited to the G1 phase and is therefore unable to replicate its DNA. In the context of a differentiation process, the SW cell will loosely attach to a surface, shed its flagellum, retract its pili, and synthesize a stalk at the same pole. The resulting ST cell is now strongly bound to the surface via a polysaccharidic holdfast located at the tip of the stalk and immediately starts chromosome replication (S phase). After completion of DNA replication, the growing ST cell enters the G2 phase and turns into a predivisional (PD) cell that will grow a new flagellum at the pole opposite to the stalk. The PD cell will then undergo an asymmetrical cell division yielding a new SW cell and a ST cell, immediately starting a new round of DNA replication (Fig. 23.6) (Curtis and Brun, 2010).

The presence of a capsule around the ST and PD cells allows the isolation of a SW cell population by centrifugation in a silicate gradient and therefore the monitoring of the different stages of the cell cycle within a synchronized cell population (Kirkpatrick and Viollier, 2012; Schrader and Shapiro, 2015).

23.4.2 SW Cell Defense Strategy Against Cu

In the early 20th century, Walter Bradford Cannon coined the "fight or flight" response as a physiological process initiated in mammals subjected to a threat (Cannon, 1932).

In *C. crescentus*, the SW cells have been proposed to seek optimal environments before initiating DNA replication (England et al., 2010). We demonstrated that upon Cu stress, SW cells accumulate a high amount of cellular Cu and actively flee from the Cu source within minutes (Lawarée et al., 2016). Briefly, a SW cells population was isolated by centrifugation and loaded into a microfluidic chamber where they could swim freely. At opposite sides of the chamber, a control and a Cu-containing agarose plug had been cast prior the injection of the cells. The dynamics of the SW cells was then monitored for 25 minutes by time-lapse microscopy within two fields located in the vicinity of both plugs and quantified. SW cells population decreases by about 50% next to the Cu plug, whereas the number of SW cells located near the control plug remains stable, accounting for a SW cell-specific "flight-like" response. We also showed that an artificial decrease of Cu concentration within the SW cells impairs their flight, suggesting that their chemotactic response relies on high levels of cellular Cu. Preliminary results suggest that this flight response also takes place when the SW cells are exposed to Zn and Cd. This indicates that the motile form of *C. crescentus* is able to sense a local increase of metal concentration in its environment and actively responds to it (Fig. 23.6).

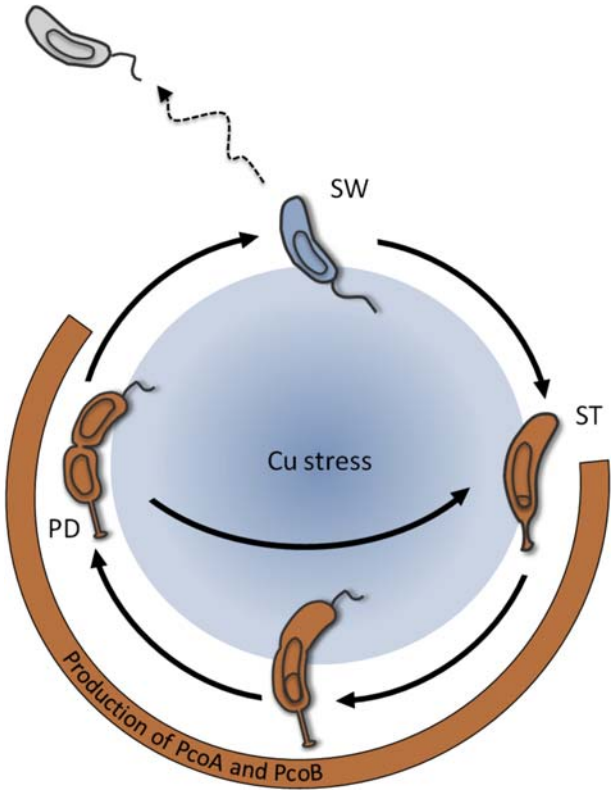

FIGURE 23.6 Bimodal defense strategy of *Caulobacter crescentus* to Cu stress. *Caulobacter crescentus* asymmetrical cell cycle culminates with the generation of a motile SW cell and a sessile ST cell. Upon Cu stress, the SW cell engages a negative chemotactic response, whereas the ST cell and the resulting PD cell rely on a ready-to-use PcoAB detoxification/efflux system to ensure their survival. *SW*, swarmer; *ST*, stalked; *PD*, predivisional.

23.4.3 Cu Detoxification by the ST Cell-Specific PcoAB System

The irreversible binding of the ST cell to a substrate implies that this cell type will have to initiate efficient protection mechanisms to maintain a proper Cu homeostasis in the presence of toxic Cu concentrations. We have shown that the *pcoAB* operon is upregulated during the SW−ST transition until cell division. *pcoAB* operon encodes an efficient Cu detoxification/efflux system composed of the PcoA and PcoB proteins. PcoA displays a classical periplasmic MCO activity, similar to the previously described CueO. It was then proposed to detoxify the periplasm by oxidizing Cu^{+} into the less toxic Cu^{2+}. PcoB is located in the outer membrane where it acts as an efflux pump (Fig. 23.6). Accordingly, upon Cu stress, a *pcoAB* mutant accumulates up to 2.5 times more cellular Cu than the wild type strain, drastically impairing its growth (Lawarée et al., 2016).

Unlike the plasmid-encoded PcoABCDRSE system initially discovered in an *E. coli* strain isolated from feces of pigs fed with Cu (Osman and Cavet, 2008; Tetaz and Luke, 1983), the PcoAB system is not inducible in *C. crescentus*. This discrepancy together with the fact that only PcoA and PcoB are conserved in *C. crescentus* suggest a divergent evolution in the composition and the regulation of these homologous systems, likely due to the distinct bacterial lifestyles.

C. crescentus intrinsic dimorphism thereby provides a bimodal strategy involving a negative chemotactic response and a ready-to-use Cu detoxification system to increase the chances to survive in a toxic environment.

23.5 CONCLUSION

Bacteria have evolved a broad diversity of mechanisms to overcome the challenges associated with metal duality. The combination of metal influx/efflux systems and the production of metal-binding molecules to maintain a proper metal homeostasis allowed bacteria to colonize various hostile environments. Horizontal gene transfers favored the propagation of these metal defense strategies similarly to antibiotics resistance. In the latter context, various bacterial species also evolved combined antibiotic and metal resistance systems by sharing specific regulators or efflux pumps to cope with toxic metals and antibiotics, attesting the amazing resilience and adaptation ability of the microbial world.

REFERENCES

Achard, M.E.S., Stafford, S.L., Bokil, N.J., Chartres, J., Bernhardt, P.V., Schembri, M.A., et al., 2012. Copper redistribution in murine macrophages in response to Salmonella infection. Biochem. J. 444, 51–57. Available from: http://doi.org/10.1042/BJ20112180.

Almiron, M., Link, A.J., Furlong, D., Kolter, R., 1992. A novel DNA-binding protein with regulatory and protective roles in starved *Escherichia coli*. Genes Dev. 6 (12 B), 2646–2654. Available from: http://doi.org/10.1101/gad.6.12b.2646.

Amato, S.M., Fazen, C.H., Henry, T.C., Mok, W.W.K., Orman, M.A., Sandvik, E.L., et al., 2014. The role of metabolism in bacterial persistence. Front. Microbiol. 5 (Mar), 1–9. Available from: http://doi.org/10.3389/fmicb.2014.00070.

Andrews, S.C., Robinson, A.K., Rodríguez-Quiñones, F., 2003. Bacterial iron homeostasis. FEMS Microbiol. Rev. 27 (2–3), 215–237. Available from: https://doi.org/10.1016/S0168-6445(03)00055-X.

Argüello, J.M., Gonzalez-Guerrero, M., Raimunda, D., 2011. Bacterial transition metal P1B-ATPases, transport mechanism and roles in virulence. Biochemistry 50 (46), 9940–9949. Available from: http://doi.org/10.1021/bi201418k.Bacterial.

Argüello, J.M., Raimunda, D., Padilla-Benavides, T., 2013. Mechanisms of copper homeostasis in bacteria. Front. Cell. Infect. Microbiol. 3 (November), 1–14. Available from: http://doi.org/10.3389/fcimb.2013.00073.

Bagai, I., Rensing, C., Blackburn, N., McEvoy, M., 2008. Direct metal transfer between periplasmic proteins identifies a bacterial copper chaperone. Biochemistry 47 (44), 11408–11414. Available from: http://doi.org/10.1021/bi801638m.Direct.

Ballatori, N., 1994. Glutathione mercaptides as transport forms of metals. Adv. Pharmacol. 27 (C), 271–298. Available from: https://doi.org/10.1016/S1054-3589(08)61036-4.

Balsberg, A., 2013. Plant biomass, primary production in disappearance a Filipendula meadow ecosystem, and the effects of cadmium. Nordic Soc. Oikos 38 (1), 72–90.

Barkay, T., Miller, S.M., Summers, A.O., 2003. Bacterial mercury resistance from atoms to ecosystems. FEMS Microbiol. Rev. 27 (2–3), 355–384. Available from: https://doi.org/10.1016/S0168-6445(03)00046-9.

Beaman, T., Gerhardt, P., 1986. Heat resistance of bacterial spores correlates with protoplast dehydration, mineralization, and thermal adaptation. Appl. Environ. Microbiol. 52 (6), 1242–1246.

Becker, K.W., Skaar, E.P., 2014. Metal limitation and toxicity at the interface between host and pathogen. FEMS Microbiol. Rev. Available from: http://doi.org/10.1111/1574-6976.12087.

Beinert, H., 2000. Iron–sulfur proteins: ancient structures, still full of surprises. J. Biol. Inorg. Chem. 5 (1), 2–15. Available from: http://doi.org/10.1007/s007750050002.

Benson, D.R., Rivera, M., 2013. Metallomics and the Cell, 12, https://doi.org/10.1007/978-94-007-5561-1.

Blanco, P., Hernando-Amado, S., Reales-Calderon, J., Corona, F., Lira, F., Alcalde-Rico, M., et al., 2016. Bacterial multidrug efflux pumps: much more than antibiotic resistance determinants. Microorganisms 4 (1), 14. Available from: http://doi.org/10.3390/microorganisms4010014.

Bleichert, P., Espírito Santo, C., Hanczaruk, M., Meyer, H., Grass, G., 2014. Inactivation of bacterial and viral biothreat agents on metallic copper surfaces. Biometals . Available from: http://doi.org/10.1007/s10534-014-9781-0.

Bleriot, C., Effantin, G., Lagarde, F., Mandrand-Berthelot, M.A., Rodrigue, A., 2011. RcnB is a periplasmic protein essential for maintaining intracellular Ni and Co concentrations in *Escherichia coli*. J. Bacteriol. 193 (15), 3785–3793. Available from: http://doi.org/10.1128/JB.05032-11.

Borkow, G., Gabbay, J., 2005. Copper as a biocidal tool. Curr. Med. Chem. 12 (18), 2163–2175. Available from: http://doi.org/10.2174/0929867054637617.

Bruins, M.R., Kapil, S., Oehme, F.W., 2000. Microbial resistance to metals in the environment. Ecotoxicol. Environ. Saf. 45 (3), 198–207. Available from: http://doi.org/10.1006/eesa.1999.1860.

Butterfield, C.N., Soldatova, A.V., Lee, S.-W., Spiro, T.G., Tebo, B.M., 2013. Mn(II, III) oxidation and MnO_2 mineralization by an expressed bacterial multicopper oxidase. Proc. Natl. Acad. Sci. U.S.A. 110 (29), 11731–11735. Available from: http://doi.org/10.1073/pnas.1303677110.

Cannon, W.B., 1932. In: W. W. N. & Company (Ed.), The Wisdom of the Body. W. W. Norton, New York, NY (W.W. Norto). W.W. Norton & Company.

Carrondo, M.A., 2003. Ferritins, iron uptake and storage from the bacterioferritin viewpoint. EMBO J. 22 (9), 1959–1968. Available from: http://doi.org/10.1093/emboj/cdg215.

Chandrangsu, P., Rensing, C., Helmann, J.D., 2017. Metal homeostasis and resistance in bacteria. Nat. Rev. Microbiol. 15 (6), 338–350. Available from: http://doi.org/10.1038/nrmicro.2017.15.

Changela, A., Chen, K., Xue, Y., Holschen, J., Outten, C.E., O'Halloran, T.V., et al., 2003. Molecular basis of metal-ion selectivity and zeptomolar sensitivity by CueR. Science (New York, N.Y.) 301 (5638), 1383–1387. Available from: http://doi.org/10.1126/science.1085950.

Chao, Y., Fu, D., 2004. Kinetic study of the antiport mechanism of an *Escherichia coli* zinc transporter, ZitB. J. Biol. Chem. 279 (13), 12043–12050. Available from: http://doi.org/10.1074/jbc.M313510200.

Chloupková, M., LeBard, L.S., Koeller, D.M., 2003. MDL1 is a high copy suppressor of ATM1: evidence for a role in resistance to oxidative stress. J. Mol. Biol. 331 (1), 155–165. Available from: https://doi.org/10.1016/S0022-2836(03)00666-1.

Cobine, P., Wickramasinghe, W.A., Harrison, M.D., Weber, T., Solioz, M., Dameron, C.T., 1999. The *Enterococcus hirae* copper chaperone CopZ delivers copper(I) to the CopY repressor. FEBS Lett. 445 (1), 27–30. Available from: https://doi.org/10.1016/S0014-5793(99)00091-5.

Cobine, P.A., George, G.N., Jones, C.E., Wickramasinghe, W.A., Solioz, M., Dameron, C.T., 2002. Copper transfer from the Cu(I) chaperone, CopZ, to the repressor, Zn(II)CopY: Metal coordination environments and protein interactions. Biochemistry 41 (18), 5822–5829. Available from: http://doi.org/10.1021/bi025515c.

Colaço, H.G., Santo, P.E., Matias, P.M., Bandeiras, T.M., Vicente, J.B., 2016. Roles of *Escherichia coli* ZinT in cobalt, mercury and cadmium resistance and structural insights into the metal binding mechanism. Metallomics 8 (3), 327−336. Available from: http://doi.org/10.1039/C5MT00291E.

Cortes Castrillona, L., Wedd, A.G., Xiao, Z., 2015. The functional roles of the three copper sites associated with the methionine-rich insert in the multicopper oxidase CueO from *E. coli*. Metallomics. Available from: http://doi.org/10.1039/C5MT00001G.

Cotton, G., Wilkinson, C.A., Murillo, M., Bochmann, F.A., 1999. In: W.-Interscience (Ed.), Advanced Inorganic Chemistry, sixth ed. John Wiley & Sons, Inc., New York, NY, USA.

Culotta, V., Scott, R.A., 2013. In: Culotta, V., Scott, R.A. (Eds.), Metals in Cells. John Wiley & Sons Ltd, The Atrium, Southern Gate, Chichester, West Sussex, UK.

Curtis, P.D., Brun, Y.V., 2010. Getting in the loop: regulation of development in *Caulobacter crescentus*. Microbiol. Mol. Biol. Rev.: MMBR 74 (1), 13−41. Available from: http://doi.org/10.1128/MMBR.00040-09.

Dann, C.E., Wakeman, C.A., Sieling, C.L., Baker, S.C., Irnov, I., Winkler, W.C., 2007. Structure and mechanism of a metal-sensing regulatory RNA. Cell 130 (5), 878−892. Available from: http://doi.org/10.1016/j.cell.2007.06.051.

Das, 2017. Handbook of Metal−Microbe Interactions and Bioremediation. CRC Press Taylor & Francis Group, Boca Raton, FL.

Djoko, K.Y., Chong, L.X., Wedd, A.G., Xiao, Z., 2010. Reaction mechanisms of the multicopper oxidase CueO from *Escherichia coli* support its functional role as a cuprous oxidase. J. Am. Chem. Soc. 132 (6), 2005−2015. Available from: http://doi.org/10.1021/ja9091903.

Dörr, T., Vulić, M., Lewis, K., 2010. Ciprofloxacin causes persister formation by inducing the TisB toxin in *Escherichia coli*. PLoS Biol. 8 (2), 29−35. Available from: http://doi.org/10.1371/journal.pbio.1000317.

Dupont, C.L., Grass, G.B., Rensing, C., 2011. Copper toxicity and the origin of bacterial resistance—new insights and applications. Metallomics 11, 1109−1118.

England, J.C., Perchuk, B.S., Laub, M.T., Gober, J.W., 2010. Global regulation of gene expression and cell differentiation in *Caulobacter crescentus* in response to nutrient availability. J. Bacteriol. 192 (3), 819−833. Available from: http://doi.org/10.1128/JB.01240-09.

Failla, M.L., 2003. Trace elements and host defense: recent advances and continuing challenges. J. Nutr. 133 (2003), 1443−1447. Available from: https://doi.org/10.1093/jn/133.5.1443S.

Fath, M.J., Kolter, R., 1993. ABC transporters: bacterial exporters. Microbiol. Rev. 57 (4), 995−1017. Available from: https://doi.org/10.1016/S0005-2736(99)00158-3.

Festa, R.A., Thiele, D.J., 2011. Copper: an essential metal in biology. Curr. Biol. 21 (21), R877−R883. Available from: http://doi.org/10.1016/j.cub.2011.09.040.

Flemming, H.C., Wingender, J., 2010. The biofilm matrix. Nat. Rev. Microbiol. 8 (9), 623−633. Available from: http://doi.org/10.1038/nrmicro2415.

Fontecave, M., Ollagnier-de-Choudens, S., 2008. Iron−sulfur cluster biosynthesis in bacteria: mechanisms of cluster assembly and transfer. Arch. Biochem. Biophys. 474 (2), 226−237. Available from: http://doi.org/10.1016/j.abb.2007.12.014.

Fruci, M., Poole, K., 2012. Bacterial stress responses as determinants of antimicrobial resistance. J. Antimicrob. Chemother. 1 (May 2012), 115−136. Available from: http://doi.org/10.1002/9781119004813.ch10.

Fullmer, C.S., Edelstein, S., Wasserman, R.H., 1985. Lead-binding properties of intestinal calcium-binding proteins. J. Biol. Chem. 260 (11), 6816−6819.

Furnholm, T.R., Tisa, L.S., 2014. The ins and outs of metal homeostasis by the root nodule actinobacterium Frankia. BMC Genomics 15, 1092.

Galli, I., Musci, G., Bonaccorsi Di Patti, M.C., 2004. Sequential reconstitution of copper sites in the multicopper oxidase CueO. J. Biol. Inorg. Chem. 9 (1), 90−95. Available from: http://doi.org/10.1007/s00775-003-0501-4.

Gefen, O., Balaban, N.Q., 2009. The importance of being persistent: heterogeneity of bacterial populations under antibiotic stress: review article. FEMS Microbiol. Rev. 33 (4), 704−717. Available from: http://doi.org/10.1111/j.1574-6976.2008.00156.x.

Genest, P.C., Setlow, B., Melly, E., Setlow, P., 2002. Killing of spores of *Bacillus subtilis* by peroxynitrite appears to be caused by membrane damage. Microbiology 148 (1), 307−314. Available from: http://doi.org/10.1099/00221287-148-1-307.

Gordge, M.P., Meyer, D.J., Hothersall, J., Neild, G.H., Payne, N.N., Noronha-Dutra, A., 1995. Copper chelation-induced reduction of the biological activity of *S*-nitrosothiols. Br. J. Pharmacol. 114 (5), 1083−1089.

Graham, S.C., Guss, J.M., 2008. Complexes of mutants of *Escherichia coli* aminopeptidase P and the tripeptide substrate ValProLeu. Arch. Biochem. Biophys. 469 (2), 200−208. Available from: http://doi.org/10.1016/j.abb.2007.10.009.

Graham, S.C., Lilley, P.E., Lee, M., Schaeffer, P.M., Kralicek, A.V., Dixon, N.E., et al., 2006. Kinetic and crystallographic analysis of mutant *Escherichia coli* aminopeptidase P: insights into substrate recognition and the mechanism of catalysis. Biochemistry 45 (3), 964−975. Available from: http://doi.org/10.1021/bi0518904.

Grass, G., Rensing, C., 2001. CueO is a multi-copper oxidase that confers copper tolerance in *Escherichia coli*. Biochem. Biophys. Res. Commun. 286, 902−908. Available from: http://doi.org/10.1006/bbrc.2001.5474.

Grass, G., Rensing, C., Solioz, M., 2011. Metallic copper as an antimicrobial surface. Appl. Environ. Microbiol. 77 (5), 1541−1547. Available from: http://doi.org/10.1128/AEM.02766-10.

Guan, G., Pinochet-Barros, A., Gaballa, A., Patel, S.J., Argüello, J.M., Helmann, J.D., 2015. PfeT, a P1B4 -type ATPase, effluxes ferrous iron and protects *Bacillus subtilis* against iron intoxication. Mol. Cell 98 (4), 787−803.

Hamer, D.H., 1986. Metallothionein. Annu. Rev. Biochem. 55, 913.

Harrison, J.J., Turner, R.J., Ceri, H., 2005. Persister cells, the biofilm matrix and tolerance to metal cations in biofilm and planktonic *Pseudomonas aeruginosa*. Environ. Microbiol. 7 (7), 981−994. Available from: http://doi.org/10.1111/j.1462-2920.2005.00777.x.

Harrison, M.D., Jones, C.E., Dameron, C.T., 1999. Copper chaperones: function, structure and copper-binding properties. J. Biol. Inorg. Chem. 4, 145−153. Available from: http://doi.org/10.1007/s007750050297.

Hawkes, S.J., 1997. What is a "heavy metal"? J. Chem. Educ. 74 (11), 1374. Available from: http://doi.org/10.1021/ed074p1374.

He, D., Hughes, S., Vanden-Hehir, S., Georgiev, A., Altenbach, K., Tarrant, E., et al., 2016. Structural characterization of encapsulated ferritin provides insight into iron storage in bacterial nanocompartments. eLife 5 (August), 1–31. Available from: http://doi.org/10.7554/eLife.18972.

Helbig, K., Bleuel, C., Krauss, G.J., Nies, D.H., 2008. Glutathione and transition-metal homeostasis in *Escherichia coli*. J. Bacteriol. 190 (15), 5431–5438. Available from: http://doi.org/10.1128/JB.00271-08.

Higgins, C.F., 2001. ABC transporters: physiology, structure and mechanism—an overview. Res. Microbiol. 152 (3–4), 205–210. Available from: http://doi.org/10.1016/S0923-2508(01)01193-7.

Higuchi, T., Hattori, M., Tanaka, Y., Ishitani, R., Nureki, O., 2009. Crystal structure of the cytosolic domain of the cation diffusion facilitator family protein. Proteins: Struct. Funct. Bioinf. 76 (3), 768–771. Available from: http://doi.org/10.1002/prot.22444.

Hiniker, A., Collet, J.F., Bardwell, J.C.A., 2005. Copper stress causes an in vivo requirement for the *Escherichia coli* disulfide isomerase DsbC. J. Biol. Chem. 280, 33785–33791. Available from: http://doi.org/10.1074/jbc.M505742200.

Horsburgh, M.J., Wharton, S.J., Karavolos, M., Foster, S.J., 2002. Manganese: elemental defence for a life with oxygen? Trends Microbiol. 10 (11), 496–501. Available from: http://doi.org/10.1016/S0966-842X(02)02462-9.

Hossain, M.A., Piyatida, P., da Silva, J.A.T., Fujita, M., 2012. Molecular mechanism of heavy metal toxicity and tolerance in plants: central role of glutathione in detoxification of reactive oxygen species and methylglyoxal and in heavy metal chelation. J. Bot. 2012 (Cd), 1–37. Available from: http://doi.org/10.1155/2012/872875.

Huang, X., Shin, J.-H., Pinochet-Barros, A., Su, T.T., Helmann, J.D., 2017. *Bacillus subtilis* MntR coordinates the transcriptional regulation of manganese uptake and efflux systems. Mol. Microbiol. 103, 253–268. Available from: http://doi.org/10.1158/1940-6207.CAPR-14-0359.Nrf2-dependent.

Imae, Y., Strominger, J.L., 1976. Relationship between cortex content and properties of *Bacillus sphaericus* spores. J. Bacteriol. 126 (2), 907–913.

Imlay, J.A., 2014. The mismetallation of enzymes during oxidative stress. J. Biol. Chem. 289 (41), 28121–28128. Available from: http://doi.org/10.1074/jbc.R114.588814.

Inesi, G., Pilankatta, R., Tadini-Buoninsegni, F., 2014. Biochemical characterization of P-type copper ATPases. Biochem. J. 463 (2), 167–176. Available from: http://doi.org/10.1042/BJ20140741.

Johnson, J.M., Church, G.M., 1999. Alignment and structure prediction of divergent protein families: periplasmic and outer membrane proteins of bacterial efflux pumps. J. Mol. Biol. 287 (3), 695–715. Available from: http://doi.org/10.1006/jmbi.1999.2630.

Jones, P.M., George, A.M., 2004. The ABC transporter structure and mechanism: perspectives on recent research. Cell. Mol. Life Sci. 61 (6), 682–699. Available from: http://doi.org/10.1007/s00018-003-3336-9.

Kaur, S., Kamli, M.R., Ali, A., 2009. Diversity of arsenate reductase genes (arsc genes) from arsenic-resistant environmental isolates of *E. coli*. Curr. Microbiol. 59 (3), 288–294. Available from: http://doi.org/10.1007/s00284-009-9432-9.

Kaur, T., Singh, A., Goel, R., 2011. Mechanisms pertaining to arsenic toxicity. Toxicol. Int. 18 (2), 87. Available from: http://doi.org/10.4103/0971-6580.84258.

Kershaw, C.J., Brown, N.L., Hobman, J.L., 2007. Zinc dependence of zinT (yodA) mutants and binding of zinc, cadmium and mercury by ZinT. Biochem. Biophys. Res. Commun. 364 (1), 66–71. Available from: http://doi.org/10.1016/j.bbrc.2007.09.094.

Kim, D.Y., Bovet, L., Maeshima, M., Martinoia, E., Lee, Y., 2007. The ABC transporter AtPDR8 is a cadmium extrusion pump conferring heavy metal resistance. Plant J. 50 (2), 207–218. Available from: http://doi.org/10.1111/j.1365-313X.2007.03044.x.

Kirkpatrick, C.L., Viollier, P.H., 2012. Decoding Caulobacter development. FEMS Microbiol. Rev. 36 (1), 193–205. Available from: http://doi.org/10.1111/j.1574-6976.2011.00309.x.

Kojetin, D.J., Thompson, R.J., Benson, L.M., Naylor, S., Waterman, J., Davies, K.G., et al., 2005. Structural analysis of divalent metals binding to the *Bacillus subtilis* response regulator Spo0F: the possibility for in vitro metalloregulation in the initiation of sporulation. Biometals 18 (5), 449–466. Available from: http://doi.org/10.1007/s10534-005-4303-8.

Kolaj-Robin, O., Russell, D., Hayes, K.A., Pembroke, J.T., Soulimane, T., 2015. Cation diffusion facilitator family: structure and function. FEBS Lett. 589 (12), 1283–1295. Available from: http://doi.org/10.1016/j.febslet.2015.04.007.

Komori, H., Higuchi, Y., 2015. Structural insights into the O_2 reduction mechanism of multicopper oxidase. J. Biochem. 158 (4), 293–298. Available from: http://doi.org/10.1093/jb/mvv079.

Laaberki, M.H., Dworkin, J., 2008. Role of spore coat proteins in the resistance of *Bacillus subtilis* spores to *Caenorhabditis elegans* predation. J. Bacteriol. 190 (18), 6197–6203. Available from: http://doi.org/10.1128/JB.00623-08.

Laity, J.H., Lee, B.M., Wright, P.E., 2001. Zinc finger proteins: new insights into structural and functional diversity. Curr. Opin. Struct. Biol. 11 (1), 39–46. Available from: https://doi.org/10.1016/S0959-440X(00)00167-6.

Lawarée, E., Gillet, S., Louis, G., Tilquin, F., Le Blastier, S., Cambier, P., et al., 2016. *Caulobacter crescentus* intrinsic dimorphism provides a prompt bimodal response to copper stress. Nat. Microbiol. 1 (9), 16098. Available from: http://doi.org/10.1038/nmicrobiol.2016.98.

Lee, J.Y., Yang, J.G., Zhitnitsky, D., Lewinson, O., Rees, D.C., 2014. Structural basis for heavy metal detoxification by an Atm1-type ABC exporter. Science 343 (6175), 1133–1136. Available from: https://doi.org/10.1126/science.1246489.

Leedjärv, A., Ivask, A., Virta, M., 2008. Interplay of different transporters in the mediation of divalent heavy metal resistance in *Pseudomonas putida* KT2440. J. Bacteriol. 190 (8), 2680–2689. Available from: http://doi.org/10.1128/JB.01494-07.

Leggett, M.J., Mcdonnell, G., Denyer, S.P., Setlow, P., Maillard, J.Y., 2012. Bacterial spore structures and their protective role in biocide resistance. J. Appl. Microbiol. 113 (3), 485–498. Available from: http://doi.org/10.1111/j.1365-2672.2012.05336.x.

Lewis, K., 2010. Persister cells. Annu. Rev. Microbiol. 64 (1), 357–372. Available from: http://doi.org/10.1146/annurev.micro.112408.134306.

Macomber, L., Imlay, J.A., 2009. The iron–sulfur clusters of dehydratases are primary intracellular targets of copper toxicity. Proc. Natl. Acad. Sci. U.S.A. 106 (20), 8344–8349. Available from: http://doi.org/10.1073/pnas.0812808106.

Macomber, L., Rensing, C., Imlay, J.A., 2007. Intracellular copper does not catalyze the formation of oxidative DNA damage in *Escherichia coli*. J. Bacteriol. 189 (5), 1616–1626. Available from: http://doi.org/10.1128/JB.01357-06.

Majzlik, P., Strasky, A., Adam, V., Nemec, M., Trnkova, L., Zehnalek, J., et al., 2011. Influence of zinc(II) and copper(II) ions on Streptomyces bacteria revealed by electrochemistry. Int. J. Electrochem. Sci. 6 (6), 2171–2191.

Maret, W., 2015. Analyzing free zinc(II) ion concentrations in cell biology with fluorescent chelating molecules. Metallomics 7 (2), 202–211. Available from: http://doi.org/10.1039/C4MT00230J.

Masip, L., Veeravalli, K., Georgiou, G., 2006. The many faces of glutathione in bacteria. Antioxid. Redox Signaling 8 (5), 152–162. Available from: http://doi.org/10.1089/ars.2007.1634.

Mato Rodriguez, L., Alatossava, T., 2010. Effects of copper on germination, growth and sporulation of *Clostridium tyrobutyricum*. Food Microbiol. 27 (3), 434–437. Available from: http://doi.org/10.1016/j.fm.2010.01.003.

McDevitt, C.A., Ogunniyi, A.D., Valkov, E., Lawrence, M.C., Kobe, B., McEwan, A.G., et al., 2011. A molecular mechanism for bacterial susceptibility to Zinc. PLoS Pathog. 7 (11). Available from: http://doi.org/10.1371/journal.ppat.1002357.

McKenney, P., Eichenberger, P., 2012. Dynamics of spore coat morphogenesis in *Bacillus subtilis*. Mol. Microbiol. 83 (2), 245–260. Available from: http://doi.org/10.1111/j.1365-2958.2011.07936.x.

Meydan, S., Klepacki, D., Karthikeyan, S., Margus, T., Thomas, P., Jones, J.E., et al., 2017. Programmed ribosomal frameshifting generates a copper transporter and a copper chaperone from the same gene. Mol. Cell 65 (2), 207–219. Available from: http://doi.org/10.1016/j.molcel.2016.12.008.

Mok, W.W.K., Orman, M.A., Brynildsen, M.P., 2015. Impacts of global transcriptional regulators on persister metabolism. Antimicrob. Agents Chemother. 59 (5), 2713–2719. Available from: http://doi.org/10.1128/AAC.04908-14.

Molteni, C., Abicht, H.K., Solioz, M., 2010. Killing of bacteria by copper surfaces involves dissolved copper. Appl. Environ. Microbiol. 76 (12), 4099–4101. Available from: http://doi.org/10.1128/AEM.00424-10.

Montoya, M., 2013. Bacterial glutathione import. Nat. Struct. Mol. Biol. 20 (7), 775. Available from: http://doi.org/10.1038/nsmb.2632.

Moore, M.J., Distefano, M.D., Zydowsky, L.D., Cummings, R.T., Walsh, C.T., 1990. Organomercurial lyase and mercuric ion reductase: nature's mercury detoxification catalysts. Acc. Chem. Res. 23 (9), 301–308. Available from: http://doi.org/10.1021/ar00177a006.

Moussatova, A., Kandt, C., O'Mara, M.L., Tieleman, D.P., 2008. ATP-binding cassette transporters in *Escherichia coli*. Biochim. Biophys. Acta, Biomembr. 1778 (9), 1757–1771. Available from: http://doi.org/10.1016/j.bbamem.2008.06.009.

Multhaup, G., Strausak, D., Bissig, K.D., Solioz, M., 2001. Interaction of the CopZ copper chaperone with the CopA copper ATPase of *Enterococcus hirae* assessed by surface plasmon resonance. Biochem. Biophys. Res. Commun. 288 (1), 172–177. Available from: http://doi.org/10.1006/bbrc.2001.5757.

Nicholson, W.L., Munakata, N., Horneck, G., Melosh, H.J., Setlow, P., 2000. Resistance of Bacillus endospores to extreme terrestrial and extraterrestrial environments. Microbiol. Mol. Biol. Rev.: MMBR 64 (3), 548–572. Available from: http://doi.org/10.1128/MMBR.64.3.548-572.2000.

Nies, D.H., 2003. Efflux-mediated heavy metal resistance in prokaryotes. FEMS Microbiol. Rev. 27 (2–3), 313–339. Available from: https://doi.org/10.1016/S0168-6445(03)00048-2.

Odermatt, A., Suter, H., Krapf, R., Solioz, M., 1993. Primary structure of two P-type ATPases involved in copper homeostasis in *Enterococcus hirae*. J. Biol. Chem. 268 (17), 12775–12779.

Orman, M.A., Brynildsen, M.P., 2013. Establishment of a method to rapidly assay bacterial persister metabolism. Antimicrob. Agents Chemother. 57 (9), 4398–4409. Available from: http://doi.org/10.1128/AAC.00372-13.

Ortiz, D.F., Kreppel, L., Speiser, D.M., Scheel, G., McDonald, G., Ow, D.W., 1992. Heavy metal tolerance in the fission yeast requires an ATP-binding cassette-type vacuolar membrane transporter. EMBO J. 11 (10), 3491–3499.

Ortiz, D.F., Ruscitti, T., McCue, K.F., Ow, D.W., 1995. Transport of metal-binding peptides by HMT1, a fission yeast ABC-type vacuolar membrane protein. J. Biol. Chem. Available from: http://doi.org/10.1074/jbc.270.9.4721.

Osborne, F.H., Ehrlich, H.L., 1976. Oxidation of arsenite by a soil isolate of *Alcaligenes*. J. Appl. Bacteriol. 41 (2), 295–305. Available from: http://doi.org/10.1111/j.1365-2672.1976.tb00633.x.

Osman, D., Cavet, J.S., 2008. Copper homeostasis in Bacteria. Adv. Appl. Microbiol. 65 (8), 217–247. Available from: https://doi.org/10.1016/S0065-2164(08)00608-4.

Patel, S.J., Padilla-Benavides, T., Collins, J.M., Argüello, J.M., 2014. Functional diversity of five homologous Cu + -ATPases present in *Sinorhizobium meliloti*. Microbiology (United Kingdom) 160, 1237–1251. Available from: http://doi.org/10.1099/mic.0.079137-0.

Pawlowska, T.E., Charvat, I., 2004. Heavy-metal stress and developmental patterns of arbuscular mycorrhizal fungi heavy-metal stress and developmental patterns of arbuscular mycorrhizal fungi. Appl. Environ. Microbiol. 70 (11), 6643–6649. Available from: http://doi.org/10.1128/AEM.70.11.6643.

Peer, W.A., Baxter, I.R., Richards, E.L., Freeman, J.L., Murphy, A.S., 2006. Molecular biology of metal homeostasis and detoxification. In: Tamas, M., Martinoia, E. (Eds.), Topics in Current Genetics, vol. 14. Springer Science + Business Media, Berlin/Heidelberg, Germany, https://doi.org/10.1007/b98249.

Peng, C.T., Liu, L., Li, C.C., He, L.H., Li, T., Shen, Y.L., et al., 2017. Structure-function relationship of aminopeptidase P from *Pseudomonas aeruginosa*. Front. Microbiol. 8 (Dec), 1–12. Available from: http://doi.org/10.3389/fmicb.2017.02385.

Pontel, L., Checa, S., Soncini, F., 2015. In: Saffarini, D. (Ed.), Bacteria–Metal Interactions. Springer (Springer). Available from: http://doi.org/10.1007/978-3-319-18570-5.

Porcheron, G., Garénaux, A., Proulx, J., Sabri, M., Dozois, C.M., 2013. Iron, copper, zinc, and manganese transport and regulation in pathogenic Enterobacteria: correlations between strains, site of infection and the relative importance of the different metal transport systems for virulence. Front. Cell. Infect. Microbiol. 3 (December), 1–24. Available from: http://doi.org/10.3389/fcimb.2013.00090.

Potter, A.J., Trappetti, C., Paton, J.C., 2012. *Streptococcus pneumoniae* uses glutathione to defend against oxidative stress and metal ion toxicity. J. Bacteriol. 194 (22), 6248–6254. Available from: http://doi.org/10.1128/JB.01393-12.

Pulliainen, A.T., Kauko, A., Haataja, S., Papageorgiou, A.C., Finne, J., 2005. Dps/Dpr ferritin-like protein: insights into the mechanism of iron incorporation and evidence for a central role in cellular iron homeostasis in *Streptococcus suis*. Mol. Microbiol. 57 (4), 1086–1100. Available from: http://doi.org/10.1111/j.1365-2958.2005.04756.x.

Radford, D.S., Kihlken, M.A., Borrelly, G.P.M., Harwood, C.R., Le Brun, N.E., Cavet, J.S., 2003. CopZ from *Bacillus subtilis* interacts in vivo with a copper exporting CPx-type ATPase CopA. FEMS Microbiol. Lett. 220 (1), 105–112. Available from: https://doi.org/10.1016/S0378-1097(03)00095-8.

Radisky, D.C., Babcock, M.C., Kaplan, J., 1999. The yeast frataxin homologue mediates mitochondrial iron efflux. J. Biol. Chem. 274 (8), 4497–4499.

Radzikowski, J.L., Vedelaar, S., Siegel, D., Ortega, Á.D., Schmidt, A., Heinemann, M., 2016. Bacterial persistence is an active σ^S stress response to metabolic flux limitation. Mol. Syst. Biol. 12 (9), 882. Available from: http://doi.org/10.15252/msb.20166998.

Raj, A., van Oudenaarden, A., 2008. Stochastic gene expression and its consequences. Cell 135 (2), 216–226. Available from: http://doi.org/10.1016/j.cell.2008.09.050.Stochastic.

Rani, A., Kumar, A., Lal, A., Pant, M., 2014. Cellular mechanisms of cadmium-induced toxicity: a review. Int. J. Environ. Health Res. 24 (4), 378–399. Available from: http://doi.org/10.1080/09603123.2013.835032.

Ratcliff, W.C., Denison, R.F., 2011. Bacterial persistence and bet hedging in *Sinorhizobium meliloti*. Commun. Integr. Biol. 4 (1), 98–100. Available from: http://doi.org/10.4161/cib.4.1.14161.

Rensing, C., Grass, G., 2003. *Escherichia coli* mechanisms of copper homeostasis in a changing environment. FEMS Microbiol. Rev. 27 (2–3), 197–213. Available from: https://doi.org/10.1016/S0168-6445(03)00049-4.

Rensing, C., Mitra, B., Rosen, B.P., 1997. The zntA gene of *Escherichia coli* encodes a Zn(II)-translocating P-type ATPase. Proc. Natl. Acad. Sci. U.S.A. 94 (26), 14326–14331. Available from: http://doi.org/10.1073/pnas.94.26.14326.

Riesenman, P.J., Nicholson, W.L., 2000. Role of the spore coat layers in *Bacillus subtilis* spore resistance to hydrogen peroxide, artificial UV-C, UV-B, and solar UV radiation. Appl. Environ. Microbiol. 66 (2), 620–626. Available from: http://doi.org/10.1128/AEM.66.2.620-626.2000.

Roberts, S.A., Wildner, G.F., Grass, G., Weichsel, A., Ambrus, A., Rensing, C., et al., 2003. A labile regulatory copper ion lies near the T1 copper site in the multicopper oxidase CueO. J. Biol. Chem. 278 (34), 31958–31963. Available from: http://doi.org/10.1074/jbc.M302963200.

Rodrigue, A., Effantin, G., Mandrand-Berthelot, M.A., 2005. Identification of rcnA (yohM), a nickel and cobalt resistance gene in *Escherichia coli*. J. Bacteriol. 187 (8), 2912–2916. Available from: http://doi.org/10.1128/JB.187.8.2912-2916.2005.

Sankari, S., O'Brian, M.R., 2014. A bacterial iron exporter for maintenance of iron homeostasis. J. Biol. Chem. 289 (23), 16498–16507. Available from: http://doi.org/10.1074/jbc.M114.571562.

Santo, C.E., Taudte, N., Nies, D.H., Grass, G., 2008. Contribution of copper ion resistance to survival of *Escherichia coli* on metallic copper surfaces. Appl. Environ. Microbiol. 74 (4), 977–986. Available from: http://doi.org/10.1128/AEM.01938-07.

Santo, C.E., Morais, P.V., Grass, G., 2010. Isolation and characterization of bacteria resistant to metallic copper surfaces. Appl. Environ. Microbiol. 76 (5), 1341–1348. Available from: http://doi.org/10.1128/AEM.01952-09.

Schiering, N., Kabsch, W., Moore, M.J., Distefano, M.D., Walsh, C.T., Pai, E.F., 1991. Structure of the detoxification catalyst mercuric ion reductase from Bacillus sp strain-Rc607. Nature . Available from: http://doi.org/10.1038/352168a0.

Schrader, J.M., Shapiro, L., 2015. Synchronization of *Caulobacter crescentus* for investigation of the bacterial cell cycle. J. Visualized Exp. 2 (98), 1–6. Available from: http://doi.org/10.3791/52633.

Schueck, N.D., Woontner, M., Koeller, D.M., 2001. The role of the mitochondrion in cellular iron homeostasis. Mitochondrion 1 (1), 51–60. Available from: https://doi.org/10.1016/S1567-7249(01)00004-6.

Schultz, D., Wolynes, P.G., Jacob, E.B., Onuchic, J.N., 2009. Deciding fate in adverse times: sporulation and competence in *Bacillus subtilis*. Proc. Natl. Acad. Sci. U.S.A. 106 (50), 21027–21034. Available from: http://doi.org/10.1073/pnas.0912185106.

Seger, J., Brockmann, J., 1987. What is bet-hedging. Oxf. Surv. Evol. Biol. 4 (November), 182–211.

Serra, D.O., Hengge, R., 2014. Stress responses go three dimensional—the spatial order of physiological differentiation in bacterial macrocolony biofilms. Environ. Microbiol. 16 (6), 1455–1471. Available from: http://doi.org/10.1111/1462-2920.12483.

Sharma, J., Shamim, K., Dubey, S.K., Meena, R.M., 2017. Metallothionein assisted periplasmic lead sequestration as lead sulfite by *Providencia vermicola* strain SJ2A. Sci. Total Environ. 579, 359–365. Available from: http://doi.org/10.1016/j.scitotenv.2016.11.089.

Sherrill, C., Fahey, R.C., 1998. Import and metabolism of glutathione by *Streptococcus mutans*. J. Bacteriol. 180 (6), 1454–1459.

Silver, S., Misra, T.K., 1984. Bacterial transformations of and resistances to heavy metalsBasic Life Sci. 28 (67), 23–46. Retrieved from. Available from: http://www.ncbi.nlm.nih.gov/pubmed/6367730.

Solioz, M., Stoyanov, J.V., 2003. Copper homeostasis in *Enterococcus hirae*. FEMS Microbiol. Rev. 27 (2–3), 183–195. Available from: https://doi.org/10.1016/S0168-6445(03)00053-6.

Solomon, E.I., Sundaram, U.M., Machonkin, T.E., 1996. Multicopper oxidases and oxygenases. Chem. Rev. 96 (7), 2563–2606. Available from: http://doi.org/10.1021/cr9500460.

Solomon, E.I., Augustine, A.J., Yoon, J., 2008. O_2 reduction to H_2O by the multicopper oxidases. Dalton Trans. 30, 3921–3932. Available from: http://doi.org/10.1039/b800799c.O.

Stähler, F.N., Odenbreit, S., Haas, R., Wilrich, J., Van Vliet, A.H.M., Kusters, J.G., et al., 2006. The novel *Helicobacter pylori* CznABC metal efflux pump is required for cadmium, zinc, and nickel resistance, urease modulation, and gastric colonization. Infect. Immun. 74 (7), 3845–3852. Available from: http://doi.org/10.1128/IAI.02025-05.

Takahashi, H., Oshima, T., Hobman, J.L., Doherty, N., Clayton, S.R., Iqbal, M., et al., 2015. The dynamic balance of import and export of zinc in *Escherichia coli* suggests a heterogeneous population response to stressJ. R. Soc. Interface. 12 (106), 20150069. Available from: http://doi.org/10.1098/rsif.2015.0069.

Tamaki, S., Frankenberger Jr, W., 1992. Environmental biochemistry of arsenicRev. Environ. Contam. Toxicol. (United States) 124 (March), 71 pages. Available from: http://doi.org/10.1007/978-1-4612-2864-6.

Tan, I., Ramamurthi, K., 2014. Spore formation in *Bacillus subtilis*. NIH Public Access 6 (3), 212–225. Available from: http://doi.org/10.1126/scisignal.2001449.Engineering.

Teitzel, G.M., Parsek, M.R., 2003. Heavy metal resistance of biofilm and planktonic *Pseudomonas aeruginosa*. Appl. Environ. Microbiol. 69 (4), 2313–2320. Available from: http://doi.org/10.1128/AEM.69.4.2313.

Tetaz, T.J., Luke, R.K.J., 1983. Plasmid-controlled resistance to copper in *Escherichia coli*. J. Bacteriol. 154 (3), 1263–1268.

Tian, H., Boyd, D., Beckwith, J., 2000. A mutant hunt for defects in membrane protein assembly yields mutations affecting the bacterial signal recognition particle and Sec machinery. Proc. Natl. Acad. Sci. U.S.A. 97 (9), 4730–4735. Available from: http://doi.org/10.1073/pnas.090087297.

Turner, A.W., 1949. Bacterial oxidation by arsenite. Nature 164, 915–916. Available from: http://doi.org/10.1038/164076a0.

Tyler, G., Balsberg Pahlsson, A.-M., Bengtsson, G., Baath, E., Tranvik, L., 1989. Heavy-metal ecology of terrestrial plants, microorganisms and invertebrates. Water Air Soil Pollut. 47, 189–215.

Valencia, E.Y., Braz, V.S., Guzzo, C., Marques, M.V., 2013. Two RND proteins involved in heavy metal efflux in *Caulobacter crescentus* belong to separate clusters within proteobacteria. BMC. Microbiol. 13, 79. Available from: http://doi.org/10.1186/1471-2180-13-79.

Veening, J.-W., Smits, W.K., Kuipers, O.P., 2008. Bistability, epigenetics, and bet-hedging in bacteria. Annu. Rev. Microbiol. 62 (1), 193–210. Available from: http://doi.org/10.1146/annurev.micro.62.081307.163002.

Vergauwen, B., Verstraete, K., Senadheera, D.B., Dansercoer, A., Cvitkovitch, D.G., Guédon, E., et al., 2013. Molecular and structural basis of glutathione import in Gram-positive bacteria via GshT and the cystine ABC importer TcyBC of *Streptococcus mutans*. Mol. Microbiol. 89 (2), 288–303. Available from: http://doi.org/10.1111/mmi.12274.

Wakeman, C.A., Goodson, J.R., Zacharia, V.M., Winkler, W.C., 2014. Assessment of the requirements for magnesium transporters in *Bacillus subtilis*. J. Bacteriol. 196 (6), 1206–1214. Available from: http://doi.org/10.1128/JB.01238-13.

Waldron, K.J., Robinson, N.J., 2009. How do bacterial cells ensure that metalloproteins get the correct metal? Nat. Rev. Microbiol. 7, 25–35. Available from: http://doi.org/10.1038/nrmicro2074.

Wang, T., El Meouche, I., Dunlop, M.J., 2017. Bacterial persistence induced by salicylate via reactive oxygen species. Sci. Rep. 7 (March), 1–7. Available from: http://doi.org/10.1038/srep43839.

Wang, W., Ballatori, N., 1998. Endogenous glutathione conjugates: occurrence and biological functions. Pharmacol. Rev. 50 (3), 335–356.

Watnick, P., Kolter, R., 2000. Biofilm, City of Microbes 182 (10), 2675–2679.

Wedepohl, K.H., 1995. The composition of the continental crust. Geochim. Cosmochim. Acta 59 (7), 1217–1232. Available from: https://doi.org/10.1016/0016-7037(95)00038-2.

Wei, Y., Fu, D., 2005. Selective metal binding to a membrane-embedded aspartate in the *Escherichia coli* metal transporter YiiP (FieF). J. Biol. Chem. 280 (40), 33716–33724. Available from: http://doi.org/10.1074/jbc.M506107200.

Wheeldon, L.J., Worthington, T., Lambert, P.A., Hilton, A.C., Lowden, C.J., Elliott, T.S.J., 2008. Antimicrobial efficacy of copper surfaces against spores and vegetative cells of *Clostridium difficile*: the germination theory. J. Antimicrob. Chemother. 62 (3), 522–525. Available from: http://doi.org/10.1093/jac/dkn219.

Wiethaus, J., Wildner, G.F., Masepohl, B., 2006. The multicopper oxidase CutO confers copper tolerance to *Rhodobacter capsulatus*. FEMS Microbiol. Lett. 256, 67–74. Available from: http://doi.org/10.1111/j.1574-6968.2005.00094.x.

Winterbourn, C.C., 1995. Toxicity of iron and hydrogen peroxide: the Fenton reaction. Toxicol. Lett. 82–83 (C), 969–974. Available from: https://doi.org/10.1016/0378-4274(95)03532-X.

Wu, Y., Vulić, M., Keren, I., Lewis, K., 2012. Role of oxidative stress in persister tolerance. Antimicrob. Agents Chemother. 56 (9), 4922–4926. Available from: http://doi.org/10.1128/AAC.00921-12.

Yocum, C.F., Pecoraro, V.L., 1999. Recent advances in the understanding of the biological chemistry of manganese. Curr. Opin. Chem. Biol. 3 (2), 182–187. Available from: https://doi.org/10.1016/S1367-5931(99)80031-3.

Yu, W., Farrell, R.A., Stillman, D.J., Winge, D.R., 1996. Identification of SLF1 as a new copper homeostasis gene involved in copper sulfide mineralization in *Saccharomyces cerevisiae*. Mol. Cell. Biol. 16 (5), 2464–2472. Available from: http://doi.org/10.1128/MCB.16.5.2464.

Zhao, G., Ceci, P., Ilari, A., Giangiacomo, L., Laue, T.M., Chiancone, E., et al., 2002. Iron and hydrogen peroxide detoxification properties of DNA-binding protein from starved cells. A ferritin-like DNA-binding protein of *Escherichia coli*. J. Biol. Chem. 277 (31), 27689–27696. Available from: http://doi.org/10.1074/jbc.M202094200.

Zuber, P., 2009. Management of oxidative stress in Bacillus. Annu. Rev. Microbiol. 63, 575–597. Available from: http://doi.org/10.1146/annurev.micro.091208.073241.

nature microbiology

LETTERS

PUBLISHED: 4 JULY 2016 | ARTICLE NUMBER: 16098 | DOI: 10.1038/NMICROBIOL.2016.98

Caulobacter crescentus intrinsic dimorphism provides a prompt bimodal response to copper stress

Emeline Lawarée[1], Sébastien Gillet[1], Gwennaëlle Louis[1], Françoise Tilquin[1], Sophie Le Blastier[1], Pierre Cambier[2] and Jean-Yves Matroule[1]*

Stress response to fluctuating environments often implies a time-consuming reprogramming of gene expression. In bacteria, the so-called bet hedging strategy, which promotes phenotypic stochasticity within a cell population, is the only fast stress response described so far[1]. Here, we show that *Caulobacter crescentus* asymmetrical cell division allows an immediate bimodal response to a toxic metals-rich environment by allocating specific defence strategies to morphologically and functionally distinct siblings. In this context, a motile swarmer cell favours negative chemotaxis to flee from a copper source, whereas a sessile stalked sibling engages a ready-to-use PcoAB copper homeostasis system, providing evidence of a prompt stress response through intrinsic bacterial dimorphism.

To maintain their fitness, all living organisms must adapt as quickly as possible to sudden changes in their environment. In animals, the bimodal fight-or-flight response triggers drastic physiological changes that prime the individual for fighting or fleeing[2]. In bacteria, bet hedging provides a prompt response to fluctuating environments by promoting a stochastic phenotypic diversity within the cell population. This strategy contrasts with time-consuming stress responses such as sporulation in *Bacillus* and heterocysts formation in *Anabaena*.

Here, we show that the *Caulobacter crescentus* intrinsic cell dimorphism, resulting from an asymmetrical cell division (Supplementary Fig. 1), prompts the morphologically and functionally distinct swarmer (SW) and stalked (ST) siblings for an immediate bimodal response to a toxic Cu-rich environment. In relation to bet hedging, this original strategy saves the significant gene reprogramming underlying classical stress responses.

In most living organisms, Cu is a cofactor for key metalloenzymes[3], yet it becomes toxic at high concentrations, as are frequently encountered by free-living, symbiotic and pathogenic bacteria. Cu duality therefore implies a tight regulation of its intracellular homeostasis[3]. To determine the cellular Cu homeostasis in isolated *C. crescentus* motile SW cells and sessile ST cells, we developed a method combining atomic absorption spectrometry (AAS) with flow cytometer cell counting to provide a more relevant approach than conventional methods based on protein normalization. Interestingly, under moderate Cu stress conditions (see Supplementary Information), there is a clear discrepancy between Cu concentrations in the SW cell (9.4 mM) and the ST cell (2.8 mM) (Fig. 1a), arguing for a cell type-specific regulation of Cu homeostasis. Remarkably, this difference is only observed under toxic Cu conditions (Supplementary Fig. 2). As previously described[4], the cellular Cu concentration exceeds the extracellular Cu concentration (even under optimal conditions). This might result from Cu complexation by cellular chaperones and chelators in order to limit Cu toxicity and to store Cu ions for further use[5]. Complexed Cu would not account for the Cu osmotic balance, thereby maintaining Cu influx in spite of a high cellular Cu concentration[6].

The prototypical *Escherichia coli* Cu homeostasis Cue, Cus and Pco systems are conserved in *C. crescentus* (Supplementary Table 1)[7]. However, the *C. crescentus* chromosome-encoded PcoA and PcoB are the sole conserved members of the *E. coli* plasmid-encoded Pco system (Supplementary Table 1). When monitoring the growth of *cueR*, *copA*, *cusR*, *cusA*, *cusB*, *cusC* and *pcoAB* mutants under moderate Cu stress, only the *pcoAB* mutant (Δ*AB*) exhibits a higher Cu sensitivity than the wild-type (WT) strain (Fig. 1b). Ectopic overexpression of *pcoAB* in the *pcoAB* mutant (Δ*AB*/p*AB*) (Supplementary Fig. 3) restores the WT phenotype (Fig. 1b), indicating that PcoA and/or PcoB take(s) part in the Cu stress response. In addition, disruption of the *cue* and *cus* regulons in the Δ*AB* strain does not potentiate its Cu sensitivity (Supplementary Fig. 4), suggesting that the PcoAB system predominates in *C. crescentus*.

Given the inducibility of the Cu homeostasis network in *E. coli*[8–10], we sought to monitor the expression of the PcoAB system under moderate Cu stress. Interestingly, Cu does not significantly affect the *pcoB* mRNA level, which is used as a hallmark of *pcoAB* operon transcription (Supplementary Fig. 5a). This observation is supported by the steady-state level of PcoA and PcoB proteins under the same conditions (Supplementary Fig. 5b), suggesting that the PcoAB system is expressed in a Cu-independent manner.

A transcriptomic analysis performed throughout the *C. crescentus* cell cycle suggests that the *pcoAB* operon is expressed during SW-to-ST cell differentiation (see Supplementary Fig. 1 for more information on *C. crescentus* differentiation)[11]. Consistent with this observation, our study shows a preferential accumulation of *pcoB* mRNA (Fig. 1c) and PcoA and PcoB proteins (Fig. 1d) in the ST cell, irrespective of Cu treatment (Supplementary Fig. 6). Proteolysis of the CtrA master regulator, which occurs during SW-to-ST cell differentiation, together with subsequent firing of *ctrA* gene transcription in the early ST cell, are used as indicators of cell cycle progression[12]. This ST cell-specific expression of PcoA and PcoB may therefore explain the discrepancy of Cu accumulation between the SW and ST cells (Fig. 1a). Accordingly, Cu-treated Δ*AB* ST cells exhibit a significant (2.5×) increase in cellular Cu concentration (Fig. 1a), which is associated with a low and constant level of cells replicating their chromosome (S phase), indicative of a blockage of DNA replication (Fig. 1e and Supplementary Fig. 7b). In addition, Cu triggers a Δ*AB* cell growth defect but no cell death (Supplementary Fig. 8), suggesting a bacteriostatic effect of Cu under our experimental conditions. In the Δ*AB*/p*AB* strain, Cu homeostasis together with DNA replication and growth are fully restored, and even potentiated (Fig. 1a,b,e and Supplementary Fig. 7a,c). Collectively, these data argue for a Cu detoxification response initiated by the Cu-exposed ST cell,

[1]Unité de Recherche en Biologie des Micro-organismes, University of Namur, 61 Rue de Bruxelles, 5000 Namur, Belgium. [2]Unité de Recherche en Biologie Végétale, University of Namur, 61 Rue de Bruxelles, 5000 Namur, Belgium. *e-mail: jean-yves.matroule@unamur.be

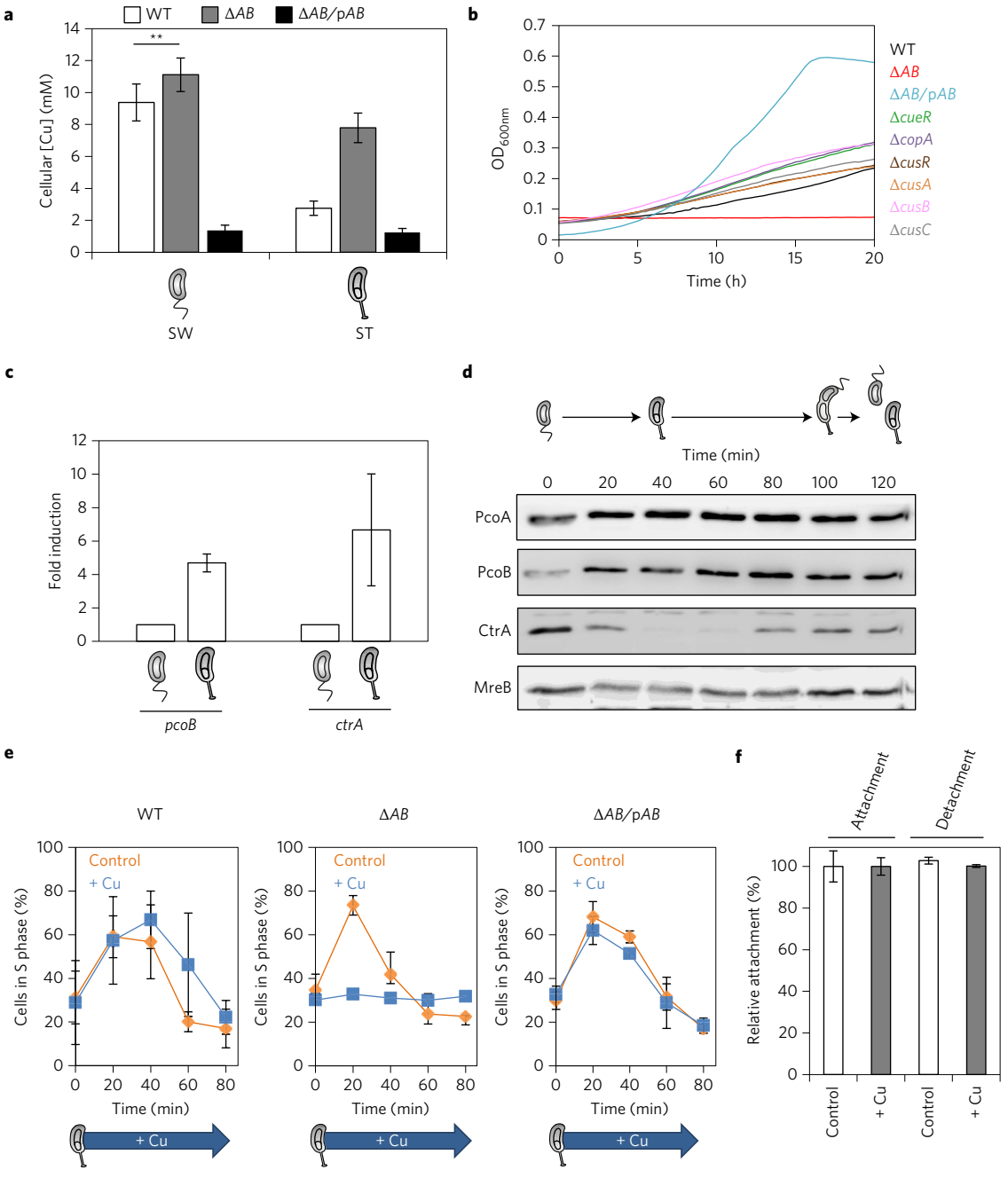

Figure 1 | Cu detoxification response in Cu-treated ST cells. a, Cellular Cu concentration in SW and ST cells subjected to a moderate (1.16 mM) Cu stress. *pcoAB* knockout strain and the corresponding completed strain are abbreviated to Δ*AB* and Δ*AB*/p*AB*, respectively (mean ± s.d., biological replicates = 3, technical replicates = 3). **b**, Growth profiles of WT, Δ*AB*, Δ*cueR*, Δ*copA*, Δ*cusR*, Δ*cusA*, Δ*cusB*, Δ*cusC* and Δ*AB*/p*AB* strains subjected to a moderate (1.16 mM) Cu stress (mean, relative standard deviation between 0.0087 and 0.1413, biological replicates = 3, technical replicates = 2). OD, optical density. **c**, *pcoB* mRNA level in SW or ST cells. The *ctrA* gene is a landmark of SW-to-ST cell differentiation (mean ± s.d., biological replicates = 3, technical replicates ≥ 9). **d**, PcoA and PcoB expression levels throughout cell cycle. CtrA is an indicator of cell cycle progression whereas MreB is the loading control (representative experiment, biological replicates = 3). **e**, Percentage of cells in the S phase measured by flow cytometry when WT, Δ*AB* and Δ*AB*/p*AB* ST cells are subjected to a moderate (1.16 mM) Cu stress (mean ± s.d., biological replicates = 3). **f**, Relative attachment of *C. crescentus* in attachment or detachment assays under control (white) or 1.16 mM Cu (grey) conditions (mean ± s.d., biological replicates = 3, technical replicates = 3). *P* values were calculated using a *t*-test (**$P < 0.01$).

which enrols a ready-to-use Cu homeostasis PcoAB system to lower the cellular Cu concentration to a level compatible with DNA replication. This implies that the ST cell adhesive properties are maintained in spite of the Cu. Here, we show that moderate Cu stress does not prevent ST cells attaching to a surface; nor does it trigger ST cell detachment (Fig. 1f).

In *E. coli*, the Pco system supports the Cue and Cus systems in Cu resistance[12] but has remained poorly characterized so far. To identify the respective functions of *C. crescentus* PcoA and PcoB, we generated single *pcoA* (Δ*A*) and *pcoB* (Δ*B*) knockouts, which display similar Cu sensitivity to the Δ*AB* mutant (Fig. 2a). The Δ*B*/p*B* strain features a WT-like Cu tolerance (Fig. 2a). In contrast, the Δ*A*/p*A* strain is not complemented (Fig. 2a), suggesting a polar effect of *pcoA* invalidation on PcoB production (Fig. 2b). Consistent with this hypothesis, the transformation of p*AB* into the Δ*A* mutant restores both PcoA and PcoB expression together with Cu tolerance

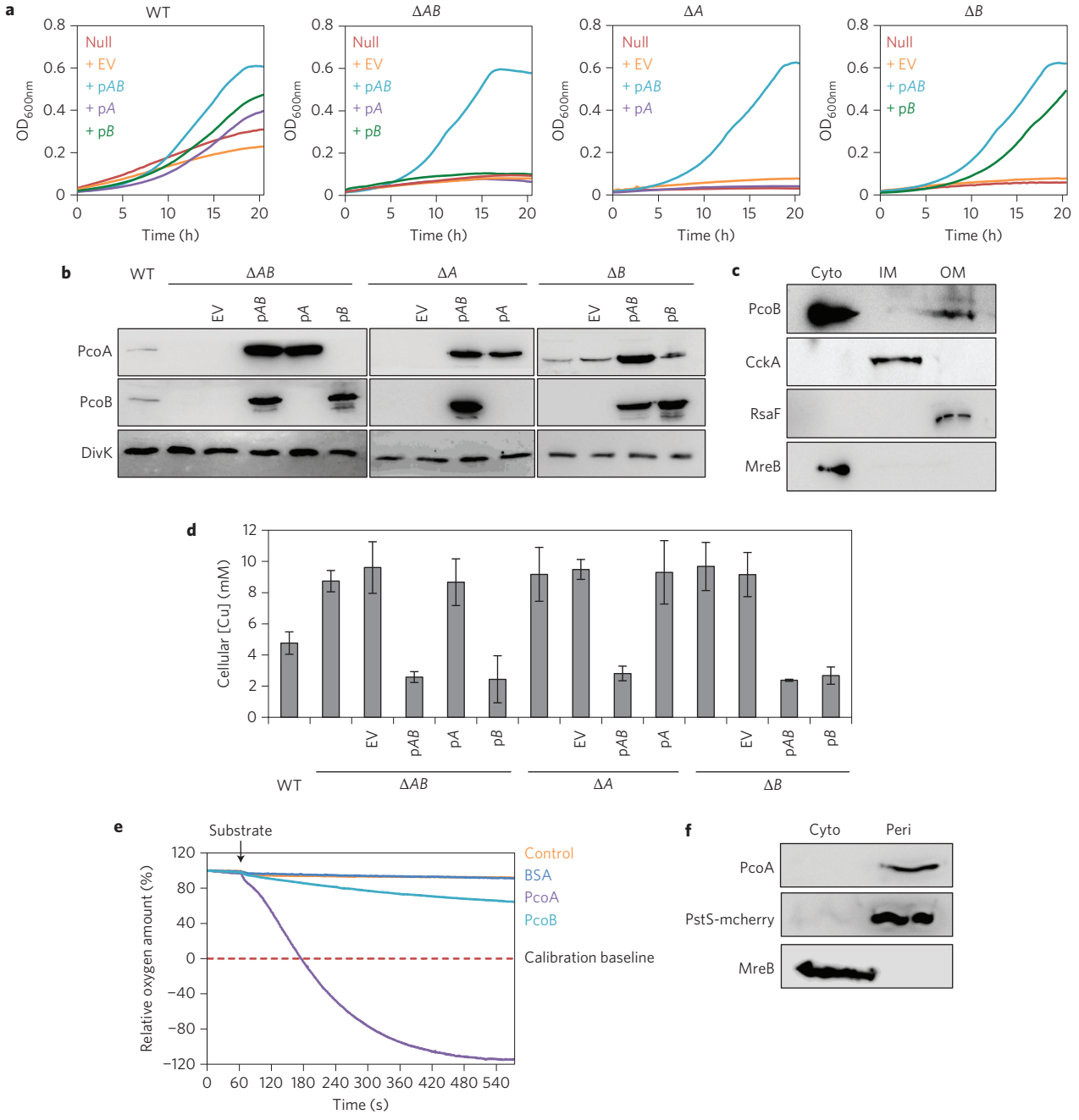

Figure 2 | Respective roles of PcoA and PcoB during the Cu detoxification response. a, Growth profiles of WT, Δ*AB*, Δ*A* and Δ*B* strains transformed with empty vector (EV), p*AB*, p*A* or p*B* under moderate (1.16 mM) Cu stress. *pcoAB*, *pcoA* and *pcoB* knockout strains are abbreviated to Δ*AB*, Δ*A* and Δ*B*, respectively (mean, relative standard deviation between 0.0031 and 0.1025, biological replicates = 3, technical replicates = 2). **b**, PcoA and PcoB expression levels in WT, Δ*AB*, Δ*A* and Δ*B* strains transformed with empty vector (EV), p*AB*, p*A* or p*B*. DivK is the loading control (representative experiment, biological replicates = 3). **c**, Expression level of PcoB in the cytoplasm (Cyto), inner membrane (IM) and outer membrane (OM). MreB, CckA and RsaF were used as Cyto, inner membrane (IM) and outer membrane (OM) controls, respectively. Cyto fraction was concentrated four times to visualize the MreB positive control, resulting in an intense PcoB band in the cytoplasm (representative experiment, biological replicates = 3). **d**, Cellular Cu concentrations in WT, Δ*AB*, Δ*A* and Δ*B* strains transformed with EV, p*AB*, p*A* or p*B* under moderate (1.16 mM) Cu stress (mean ± s.d., biological replicates = 3, technical replicates = 3). **e**, Relative oxygen amount measured with control buffer, BSA, PcoA and PcoB. The red dashed line represents the calibration baseline (representative experiment, biological replicates = 3). **f**, Expression levels of PcoA in the cytoplasm (Cyto) and in the periplasm (Peri). MreB and PstS-mcherry were used as Cyto and Peri controls, respectively (representative experiment, biological replicates = 3).

at a similar extent to the Δ*AB*/p*AB* and Δ*B*/p*AB* strains (Fig. 2a). Neither p*A* nor p*B* alone are able to sustain Cu tolerance in the Δ*AB* genetic background, suggesting that both PcoA and PcoB cooperate to maintain a proper Cu homeostasis.

PcoB contains a high proportion of histidines in its *N*-terminal region and is predicted to form a β-barrel in the outer membrane (Swiss-Model, Biozentrum). In accordance with this prediction, PcoB is found in the outer membrane (OM), but not in the inner membrane (IM) (Fig. 2c). MreB, CckA and RsaF are used as cytoplasmic, IM and OM controls, respectively[14–16]. Interestingly, the cellular Cu concentration of the Δ*B* and Δ*A*/p*A* strains is similar to the Cu level measured in the Δ*AB* mutant (Fig. 2d), indicating that

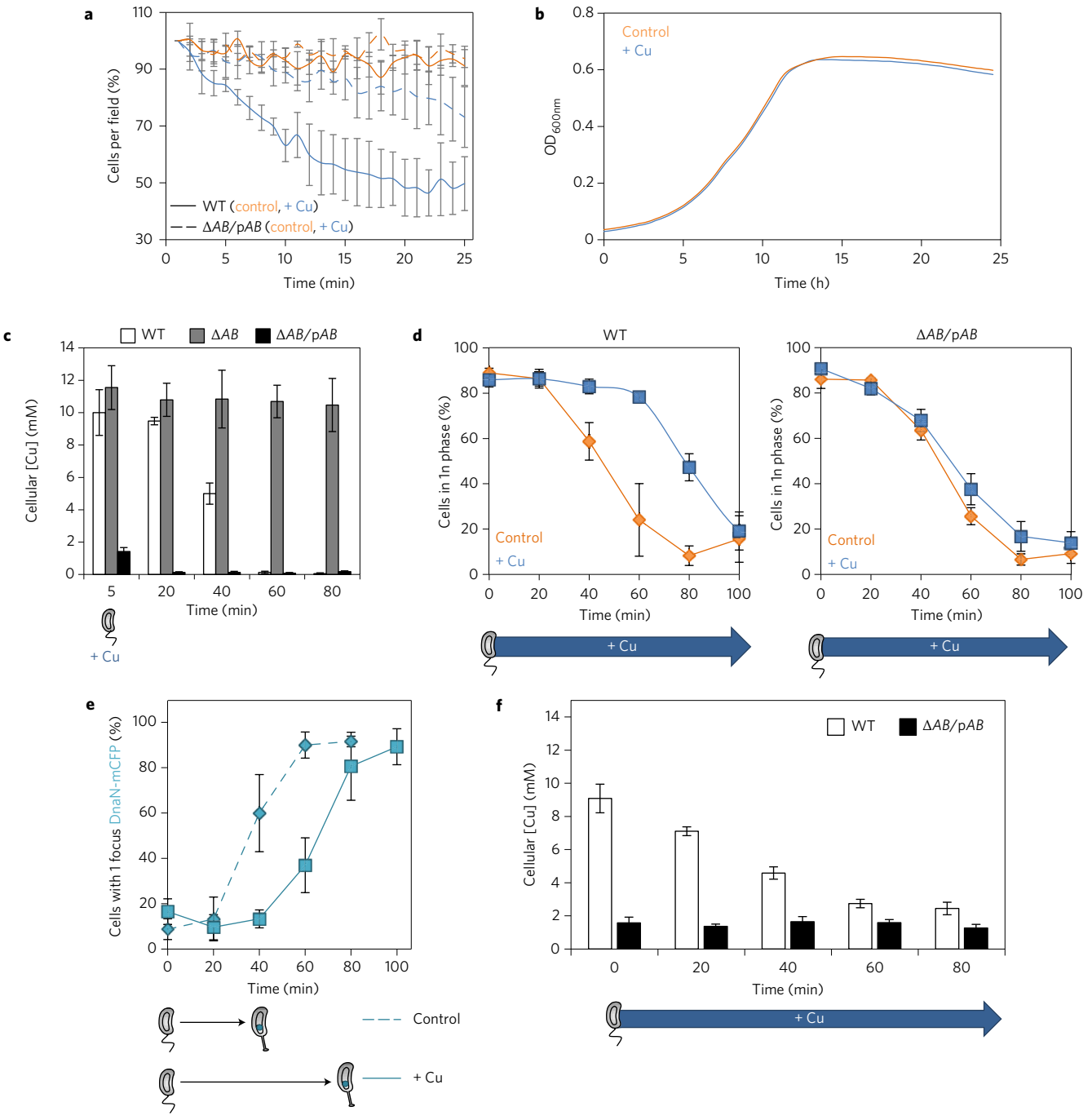

Figure 3 | Cu-treated SW cells escape. a, Percentage of WT (continuous line) or Δ*AB*/p*AB* (dashed line) SW cells in the vicinity of the control plug (orange) or the 1.16 mM Cu plug (blue) (mean ± s.d., biological replicates = 3). **b**, Growth profile of SW cells subjected to 5 min moderate (1.16 mM) Cu stress (blue) and grown for 24 h in a Cu-free culture medium. Untreated SW cells are in orange (mean, relative standard deviation between 0.0054 and 0.0972, biological replicates = 3, technical replicates = 2). **c**, Cellular Cu level in WT, Δ*AB* and Δ*AB*/p*AB* strains when SW cells are subjected to 5 min moderate (1.16 mM) Cu stress (mean ± s.d., biological replicates = 3, technical replicates = 3). **d**, Percentage of cells containing one chromosome (1n) in the WT and Δ*AB*/p*AB* strains when SW cells are grown in 1.16 mM Cu (mean ± s.d., biological replicates = 3). **e**, Localization of DnaN-CFP when SW cells are grown in a Cu-free culture medium (dashed line; *n* cells = 2,830) or in 1.16 mM Cu (continuous line; *n* cells = 3,756) (mean ± s.d., biological replicates = 3). **f**, Cellular Cu level in WT and Δ*AB*/p*AB* strains when SW cells are grown in 1.16 mM Cu (mean ± s.d., biological replicates = 3, technical replicates = 3).

the absence of PcoB results in an enhanced cellular Cu accumulation. Alternatively, PcoB overexpression in the Δ*AB*/p*B* strain, which is expected to mimic a clean single Δ*A* mutant without polar effects on *pcoB*, restores the cellular Cu concentration to the Δ*AB*/p*AB* strain level (Fig. 2d). Collectively, these data argue for a role of PcoB as a Cu efflux pump. Remarkably, the Δ*AB*/p*B* strain remains sensitive to Cu in spite of the low cellular Cu level (Fig. 2a,d), suggesting that the PcoB-mediated Cu efflux is not sufficient to compensate for the lack of PcoA in Δ*AB*/p*B* cells.

Owing to the PcoA homology to the periplasmic *E. coli* CueO multi-copper oxidase (MCO) (Supplementary Table 1)[17], we sought to investigate its ability to oxidize Cu^{+} into Cu^{2+} and to catalyse a four-electron reduction of O_2 into H_2O. Within a few seconds of adding a Cu^{+} substrate, recombinant PcoA-His triggers a strong decrease in

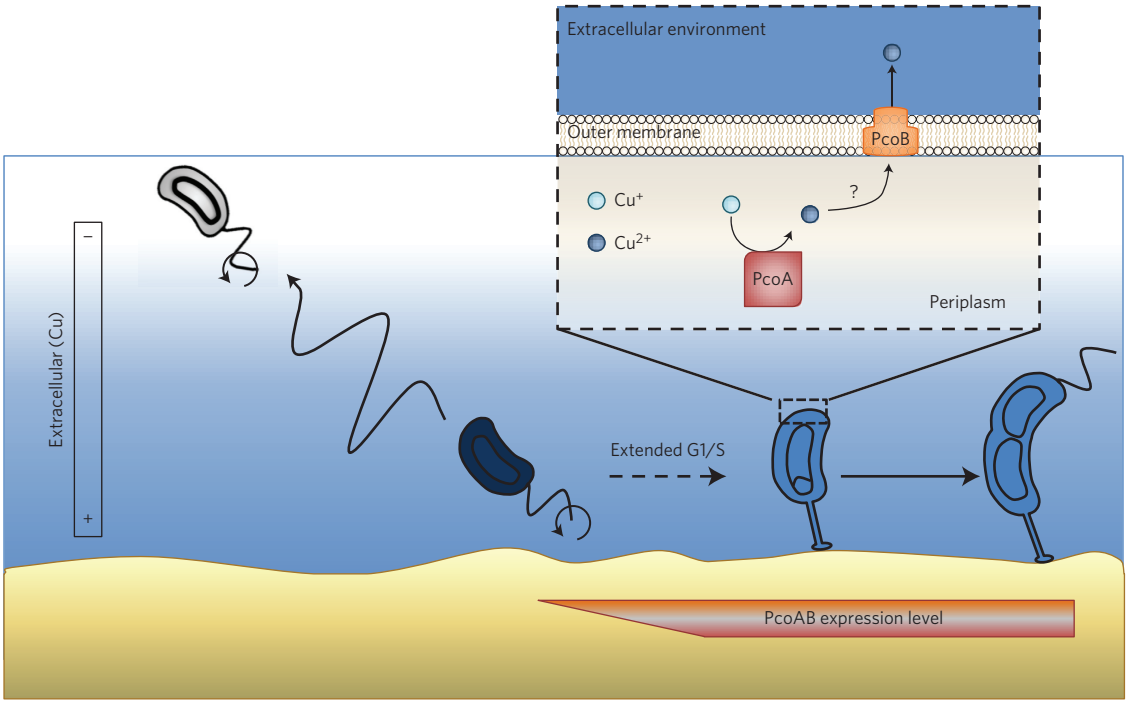

Figure 4 | Model of the *C. crescentus* bimodal response. In a Cu-rich environment, the sessile ST cell triggers a Cu detoxification response relying on the cell type-specific PcoAB defence system involved in Cu detoxification and efflux. In the same context, the SW cell accumulates a high level of Cu (dark blue), which may act as an internal cue to escape towards a Cu-free ecological niche. If restrained to the Cu-rich environment, the SW cell will eventually differentiate into a ST cell and promote a Cu detoxification response.

O_2 concentration, which stabilizes after 9 min far below the calibration baseline (Fig. 2e). Conversely, the slow and weak decrease in O_2 concentration observed with the control buffer, a BSA solution and PcoB-His probably results from a slight Cu^+ self-oxidation. In accordance with its oxidase activity and its homology to *E. coli* CueO, PcoA is mainly found in the periplasmic fraction (Fig. 2f). PstS-mcherry and MreB are used as periplasmic and cytoplasmic controls, respectively.

Together, our data suggest that in a ST cell subjected to moderate Cu stress, PcoA oxidizes toxic Cu^+ to less toxic Cu^{2+} (ref. 3), which is in turn transferred to the outer membrane PcoB efflux pump, thereby contributing to Cu detoxification in the growing ST cells.

The faint PcoAB level detected in the SW cell (Fig. 1d) leads to an important accumulation of cellular Cu in these cells (Fig. 1a). One may hypothesize that in this context, the SW cell will prioritize the escape towards a Cu-free environment. To test this hypothesis, we adapted a live chemotaxis imaging assay to visualize Cu-stressed SW cell dynamics over 25 min after 1.16 mM Cu exposure (Supplementary Fig. 9). Consistent with our hypothesis, the SW cell population decreases by about 50% next to the Cu plug, while the number of SW cells located near the control plug remains stable (Fig. 3a), suggesting a SW cell-specific escape response. Once they have reached a more appropriate ecological niche, Cu-loaded SW cells presumably resume their normal developmental programme. This hypothesis is supported by the typical growth profile (Fig. 3b) and cell cycle progression (Supplementary Fig. 10) of SW cells exposed to Cu for 5 min and then inoculated in fresh culture medium. This latter observation probably results from the decrease in cellular Cu concentration by PcoAB during SW-to-ST cell differentiation (Fig. 3c).

One may question the biological significance of maintaining such a high and potentially toxic Cu concentration in the SW cell before initiating the PcoAB-dependent Cu homeostasis. We propose that a high cellular Cu level acts as an internal cue to trigger a negative chemotactic response. In agreement with this hypothesis, we show that the artificial decrease in the Cu level mediated by overexpression of PcoAB in the SW cells (Fig. 3c) strongly impacts bacterial escape, because 80% of the Δ*AB*/p*AB* SW cells remain in the vicinity of the Cu plug when challenged in the live chemotaxis imaging assay (Fig. 3a).

When the SW cell is confined to a Cu-rich environment (for example, in a culture tube), polar localization of the SW-to-ST cell differentiation markers PleC-meGFP and SpmX-mcherry is delayed (40 min) (Supplementary Fig. 11). The lag in SW cell differentiation is accompanied by a 40 min extension of the G1/S transition (Fig. 3d and Supplementary Fig. 12a). Using the β-sliding clamp DnaN-mCFP fluorescent fusion as a landmark of DNA pol III positioning[18,19], we notice a similar delay in the timing of localization of DnaN-mCFP at the stalked pole where DNA replication initiates (Fig. 3e). This observation suggests that Cu stress affects entry into the S phase by impeding DNA polymerase III recruitment to the replication origin.

Interestingly, the G1/S transition takes place when the cellular Cu concentration matches the Cu level measured in the Cu-treated ST cells (Figs 1a and 3f), suggesting that the extension of the cell cycle results from a delayed Cu homeostasis and the onset of Cu detoxification. Consistent with this hypothesis, PcoAB expression is initiated 20 min later under Cu stress (Supplementary Fig. 6a). In addition, constitutive overexpression of PcoAB in the Δ*AB*/p*AB* SW cells and its associated enhanced Cu homeostasis restores a typical cell cycle progression in a Cu-rich environment (Fig. 3d,f and Supplementary Fig. 12). One may hypothesize that Cu impacts cell cycle progression through (1) Cu^{2+}-mediated thiol group oxidation or metal displacement from metal binding sites in the periplasm[3,20] and/or (2) Cu^+-mediated Fe displacement from Fe–S clusters in the cytoplasm[21]. These alterations may therefore impede the function of key proteins involved in cellular processes such as transcription, translation and DNA replication[22].

Finally, preliminary experiments show that toxic concentrations of Zn and Cd trigger a negative chemotaxis response in SW cells (Supplementary Fig. 13a) without affecting the adhesive properties of ST cells (Supplementary Fig. 13b). This suggests that the

C. crescentus bimodal response may be extrapolated to other toxic trace elements, even though the underlying molecular mechanisms are probably different.

Cell dimorphism resulting from an asymmetrical cell division is widespread among the very diverse alpha-proteobacteria class, which encompasses intracellular mammalian pathogens (for example, *Brucella* spp.), plant pathogens (for example, *Agrobacterium* spp.), plant symbionts (for example, *Rhizobium* spp.) and free-living bacteria (for example, *C. crescentus*)[23]. However, the keystone of this peculiar conserved feature has remained quite puzzling so far. A recent study demonstrated that the *Brucella abortus* infectious form is restrained to the progenies (1n cells), suggesting a key role of specific cell cycle stages in pathogenicity[24]. However, the contribution of cell dimorphism in the *Brucella* infection process remains unknown. Our study provides new insights into the bacterial stress response by demonstrating how intrinsic dimorphism primes bacteria for an immediate bimodal response to a heavy metal stress (Fig. 4).

Methods

Strains, plasmids and growth conditions. *C. crescentus* was grown at 30 °C in Hutner base imidazole-buffered glucose glutamate (HIGG) minimal medium[25] with 5 μg ml^{-1} kanamycin, 25 μg ml^{-1} spectinomycin, 5 μg ml^{-1} streptomycin and/or $CuSO_4.5H_2O$ when required. Exponentially growing cultures were used for all experiments. Plasmids were mobilized from *E. coli* strain S17-1 into *C. crescentus* by conjugation[26]. Strains and plasmids are listed in Supplementary Table 2, and the strategies for their construction are available upon request. When appropriate, synchronized populations were obtained as described in ref. 27.

Growth curve measurements. Bacterial cultures (triplicates for each condition) in the exponential growth phase were diluted in HIGG medium to a final optical density at 660 nm (OD_{660nm}) of 0.05 and inoculated in 96-well plates. Bacteria were then grown for 24 h at 30 °C under continuous shaking in a BioTek ELx808 absorbance reader, where OD_{600nm} was measured every 15 min. Different $CuSO_4.5H_2O$ concentrations were added when appropriate.

Atomic absorption spectrometry. Cells were fixed for 20 min at 4 °C in 2% paraformaldehyde and then washed three times with an ice-cold wash buffer (10 mM Tris-HCl, pH 6.8, 100 μM EDTA). The pelleted cells were lysed under 2.4 kbar in 1 M HNO_3 using a cell disrupter (Cell Disruption System, one shot model, Constant). Intracellular Cu was measured using a Shimadzu Atomic Absorption Spectrophotometer AA-7000F. Cellular Cu concentration was calculated as the (total Cu)/(number of cells × cell volume) ratio. SW, ST and predivisional cell volumes were 0.408, 0.46 and 0.634 μm^3, respectively. The average cell volume in the mixed population was 0.5 μm^3. A total of 2×10^9 to 10×10^9 bacteria were counted for each condition.

Reverse transcription quantitative polymerase chain reaction. Bacteria (50 ml) cultivated in HIGG at 30 °C ($OD_{660} = 0.4$) were collected by centrifugation. The recovered pellet was washed twice in sterile PBS and finally resuspended in 100 μl of 10% SDS and 20 μl proteinase K (proteinase K, recombinant, PCR Grade, Roche). The resuspended pellet was incubated for 1 h at 37 °C under mild shaking. A guanidinium thiocyanate-phenol-chloroform extraction was then conducted with TriPure Isolation Reagent (Roche), as described in the protocol available on the manufacturer's website (https://lifescience.roche.com/wcsstore/RASCatalogAssetStore/Articles/NAPI_Manual_page_156-163.pdf).

RNA (2 μg) was treated for 30 min with DNAse I (Thermo Scientific) at 37 °C followed by DNAse I inactivation with 50 mM EDTA for 10 min at 65 °C. The RNA was then reverse transcribed with Superscript II reverse transcriptase (Invitrogen) with hexamer random primers as described by the manufacturer. A condition without reverse transcriptase was also conducted in parallel as a negative control.

cDNA (0.3 μg) was then mixed with SybrGreen mix (FastStart Universal SYBR Green Master (Rox); Roche) and the appropriate primers sets (concentrations available upon request) and subjected to qPCR in a LightCycler96 (Roche). A total of 45 three-step cycles were performed as follows: 95 °C for 10 s, 60 °C for 10 s and 72 °C for 10 s. Melting curves were then performed to assess primer specificity. Target mRNA fold change was calculated as $2^{-\Delta\Delta Ct}$, where 16S ARN was used as the reference gene. Each biological replicate was analysed in at least six technical replicates.

Flow cytometry

Cell counting. Bacteria were fixed for 20 min at 4 °C with 2% paraformaldehyde. Fixed cells were diluted 1:100 in a phosphate buffered saline solution and counted with a BD FACSVerse flow cytometer. Data were analysed with the BD FACSuite V1.0.5 software.

DNA quantification. Exponentially growing cells were fixed with cold 70% (vol/vol) ethanol as described previously[28]. Fixed cells were incubated for 30 min in fluorescence-activated cell sorting (FACS) staining buffer pH 7.2 (10 mM Tris-HCl, pH 6.8, 1 mM EDTA, 50 mM Na citrate and 0.01% TritonX-100) supplemented with 20 mg ml^{-1} RnaseA. DNA was then labelled by washing the cells in FACS staining buffer pH 7.2 supplemented with 0.2 μM Sytox Green (Life Technologies). Labelled cells were analysed on a BD FACSCalibur flow cytometer. The data were analysed with the CellQuest Pro software. A total of 5×10^4 bacteria were analysed for each condition.

Bacterial cell counting. Exponentially growing bacteria were treated for 8 h with different $CuSO_4$ concentrations at 30 °C under continuous shaking. Bacteria were then collected and serially diluted in HIGG medium. A volume of 20 μl of each dilution was plated on HIGG agar. After 48 h incubation at 30 °C, the total bacterial charge was estimated by counting colony forming units. To ensure the statistical validity of the results, the experiment was repeated three times (biological triplicate). Each biological replicate was inoculated on three different HIGG agar plates (technical replicate).

Bacterial live/dead assay. Exponentially growing cells were incubated for 8 h with the appropriate amount of $CuSO_4$. Bacteria were then diluted in 0.85% NaCl and stained with the LIVE/DEAD BacLight bacterial viability kit (Molecular Probes) according to the manufacturer's protocol. The percentage of live or dead bacteria was determined by fluorescence microscopy.

Antibodies production and western blotting. Exponentially growing cells were pelleted and resuspended in SDS–polyacrylamide gel electrophoresis (PAGE) loading buffer. Boiled protein samples were then resolved on 12% SDS–polyacrylamide gels and electrotransferred to polyvinylidene difluoride (PVDF) membrane. PVDF membranes were probed with polyclonal rabbit anti-PcoA (1:5,000), anti-PcoB (1:1,000), anti-CtrA (1:5,000) and anti-MreB (1:10,000) antibodies. Polyclonal goat anti-rabbit immunoglobulins/horseradish peroxidase secondary antibody was used at 1:10,000 (DAKO).

Attachment/detachment assay. For the attachment assay, exponentially growing CB15 cells were incubated for 15 min with appropriate Cu concentrations. Cells were then inoculated for 2 h in a 96-well plate at 30 °C under continuous shaking. Cell attachment to the polystyrene surface was quantified as described in ref. 29. For the detachment assay, exponentially growing CB15 cells were grown overnight in a 96-well plate at 30 °C under continuous shaking. Appropriate Cu concentrations were then added on cells for 15 min. Cell detachment from the polystyrene surface was quantified as described in ref. 29.

Cellular fractionation

Inner and outer membrane fractions. The inner and outer membrane fractions of *C. crescentus* were collected by ultracentrifugation after sodium lauryl sarconisate and sodium carbonate treatment, as described in ref. 30.

Cell cultures (300 ml) were grown in HIGG at 30 °C to an OD_{660} of 0.5. Bacteria were centrifuged for 10 min at 4,000*g* at 4 °C, and washed three times in 50 ml of 50 mM (pH 8) ammonium bicarbonate. Cells were finally resuspended in 5 ml ammonium bicarbonate and sonicated on ice (20 rounds of 5 s sonication at maximum intensity). The lysate was centrifuged for 20 min at 12,000*g* at 4 °C, and the pellet containing the unbroken cells and debris was discarded. The supernatant was then ultracentrifuged for 40 min at 100,000*g* to dissociate the cytoplasmic fraction (supernatant) from the total membrane fraction (pellet). The cytoplasmic fraction was stored at −20 °C. The pellet was then resuspended in 1 ml of 1% sodium lauryl sarconisate and centrifuged for another 40 min at 100,000*g* and 4 °C. The subsequent supernatant containing the solubilized inner membrane was concentrated with a speedvac and stored at −20 °C. The pellet containing the outer membrane fraction was washed in 1 ml of 2.5 M NaBr and incubated for 30 min on ice. This was then ultracentrifuged for 40 min at 100,000*g* at 4 °C. The supernatant was discarded and the pellet was incubated for 1 h in 1 ml of 100 mM Na_2CO_3 for further enrichment of the outer membrane fraction, before being spun again for 40 min at 100,000*g* at 4 °C. The resulting pellet was resuspended in SDS–PAGE loading buffer and stored at −20 °C.

Periplasmic fraction. Bacterial cultures (10 ml; $OD_{660} = 0.4$) were centrifuged for 5 min at 3,500*g*. The resulting pellet was washed twice in 1 ml filtrated PBS, resuspended in 1 ml resuspension buffer (RS) buffer (0.2 M Tris-HCl, pH 7.6) and then incubated with another 1 ml RS buffer containing 1 M sucrose and 0.25% of Zwittergent 3. The resulting mix was incubated for 10 min at room temperature and centrifuged for 15 min at 7,000*g*. The supernatant, containing the periplasmic components, was separated from the cytoplasmic pellet. A portion (280 μl) of the periplasmic fraction was mixed with 80 μl Laemmli buffer 5× and 40 μl of 1 M dithiothreitol (DTT). The cytoplasmic pellet was resuspended in 70 μl H_2O, 20 μl 5× Laemmli buffer and 10 μl 1 M DTT.

Oxidase assay. The oxidase activity of PcoA and PcoB was assessed *in vitro* by measuring their oxygen consumption rate with an oxygraph (Hansatech Instruments) when mixed with a Cu^+ substrate as described for CueO in ref. 31. Briefly, 50 μg recombinant PcoA-His or PcoB-His were resuspended in 700 μl of 0.1 M sodium acetate buffer (pH 5.5), loaded in the Oxygraph sensor cell and supplemented with 1 mM $CuSO_4$ in order to fill the labile copper ligation site. Three minute later, 500 μM solubilized Tetrakis(acetonitrile)copper(I) hexafluorophosphate ($[Cu(CH_3CN)_4]PF_6$, Sigma Aldrich) substrate were added as a caged source of Cu^+, thereby limiting Cu^+

self-oxidation. Oxygen consumption was recorded with the Oxygraph for 30 min and the data were then plotted. BSA (50 μg) was used as a negative control.

Live chemotaxis imaging. Live chemotaxis imaging was adapted from the 'plug assay' designed in Emonet's laboratory (Yale University). Briefly, chemotaxis devices were made by casting solubilized 10:1 polydimethylsiloxane (PDMS Slygard 184, Dow Corning) in a small glass pot ($d = 50$ mm, $h = 30$ mm; glassware from Lenz Laborglass Instrument) where coverslips had previously been placed in order to mould the future bacterial chambers. After a degassing phase, the mixed PDMS was heated for 1 h at 70 °C. Unmoulded PDMS devices were then mounted on a microscopy glass slide. The slide and the PDMS cube were washed successively with acetone (only the slide), isopropanol and methanol and rinsed with milli-Q water. Both components were blown dry between each wash. Three inlets and one outlet channels were drilled in the PDMS, which was then firmly pressed against the slide to seal the device. Melted 1.5% agarose H_2O (10 μl) with or without 1.16 mM Cu was loaded into the chamber through both external inlet channels to generate the plugs. Isolated SW cells (150 μl, $OD_{660\ nm} = 0.01$) were in turn injected into the bacterial chamber through the central inlet channel (Supplementary Fig. 9a).

Images were collected every minute for 25 min in one focal plan (near the liquid surface) in the vicinity of the Cu or the control plug with a Zen Observer Z.1 inverted microscope equipped with a Zeiss ×20/0.4 Ph2 objective equipped with a Zeiss Axiocam 506 mono digital camera. All image capture and processing was performed with the Zen Pro lite software (blue version).

Quantitative analysis of time-lapse images was performed with MATLAB software (MathWorks) (Supplementary Fig. 9b).

Fluorescence microscopy. Cells in the exponential growth phase were immobilized on 1% agarose HIGG pads. Fluorescence microscopy was performed using a Zeiss Axio Imager.Z1 microscope equipped with a Zeiss ×100/1.3 oil Ph3 objective and appropriate filter sets. Images were collected with a Hamamatsu C11440 digital camera. All image capture and processing was performed with Zen Pro 2012 software (blue version).

Received 12 November 2015; accepted 23 May 2016; published 4 July 2016

References

1. Veening, J. W., Smits, W. K. & Kuipers, O. P. Bistability, epigenetics, and bet-hedging in bacteria. *Annu. Rev. Microbiol.* **62,** 193–210 (2008).
2. Cannon, W. B. *Bodily Changes in Pain Hunger Fear and Rage* (D. Appleton & Co., 1920).
3. Osman, D. & Cavet, J. S. Copper homeostasis in bacteria. *Adv. Appl. Microbiol.* **65,** 217–247 (2008).
4. Bagwell, C. E., Milliken, C. E., Ghoshroy, S. & Blom, D. A. Intracellular copper accumulation enhances the growth of *Kineococcus radiotolerans* during chronic irradiation. *Appl. Environ. Microbiol.* **74,** 1376–1384 (2008).
5. Palumaa, P. Copper chaperones. The concept of conformational control in the metabolism of copper. *FEBS Lett.* **587,** 1902–1910 (2013).
6. Ma, Z., Jacobsen, F. E. & Giedroc, D. P. Metal transporters and metal sensors: how coordination chemistry controls bacterial metal homeostasis. *Chem. Rev.* **109,** 4644–4681 (2009).
7. Rensing, C. & Grass, G. *Escherichia coli* mechanisms of copper homeostasis in a changing environment. *FEMS Microbiol. Rev.* **27,** 197–213 (2003).
8. Outten, F. W., Outten, C. E., Hale, J. & O'Halloran, T. V. Transcriptional activation of an *Escherichia coli* copper efflux regulon by the chromosomal MerR homologue, cueR. *J. Biol. Chem.* **275,** 31024–31029 (2000).
9. Outten, F. W., Huffman, D. L., Hale, J. A. & O'Halloran, T. V. The independent Cue and Cus systems confer copper tolerance during aerobic and anaerobic growth in *Escherichia coli*. *J. Biol. Chem.* **276,** 30670–30677 (2001).
10. Stoyanov, J. V., Hobman, J. L. & Brown, N. L. CueR (YbbI) of *Escherichia coli* is a MerR family regulator controlling expression of the copper exporter CopA. *Mol. Microbiol.* **39,** 502–511 (2001).
11. Fang, G. *et al.* Transcriptomic and phylogenetic analysis of a bacterial cell cycle reveals strong associations between gene co-expression and evolution. *BMC Genomics* **14,** 450 (2013).
12. Skerker, J. M. & Laub, M. T. Cell-cycle progression and the generation of asymmetry in *Caulobacter crescentus*. *Nature Rev. Microbiol.* **2,** 325–337 (2004).
13. Lee, S. M. *et al.* The Pco proteins are involved in periplasmic copper handling in *Escherichia coli*. *Biochem. Biophys. Res. Commun.* **295,** 616–620 (2002).
14. Jacobs, C., Hung, D. & Shapiro, L. Dynamic localization of a cytoplasmic signal transduction response regulator controls morphogenesis during the *Caulobacter* cell cycle. *Proc. Natl Acad. Sci. USA* **98,** 4095–4100 (2001).
15. Jacobs, C., Ausmees, N., Cordwell, S. J., Shapiro, L. & Laub, M. T. Functions of the CckA histidine kinase in *Caulobacter* cell cycle control. *Mol. Microbiol.* **47,** 1279–1290 (2003).
16. Reichelt, M., von Specht, B. U. & Hahn, H. P. The *Caulobacter crescentus* outer membrane protein Omp58 (RsaF) is not required for paracrystalline S-layer secretion. *FEMS Microbiol. Lett.* **201,** 277–283 (2001).
17. Huffman, D. L. *et al.* Spectroscopy of Cu(II)-PcoC and the multicopper oxidase function of PcoA, two essential components of *Escherichia coli* Pco copper resistance operon. *Biochemistry (Moscow)* **41,** 10046–10055 (2002).
18. Fernandez-Fernandez, C., Grosse, K., Sourjik, V. & Collier, J. The β-sliding clamp directs the localization of HdaA to the replisome in *Caulobacter crescentus*. *Microbiol. Read. Engl.* **159,** 2237–2248 (2013).
19. Oakley, A. J. *et al.* Flexibility revealed by the 1.85 A crystal structure of the beta sliding-clamp subunit of *Escherichia coli* DNA polymerase III. *Acta Crystallogr. D* **59,** 1192–1199 (2003).
20. Hiniker, A., Collet, J.-F. & Bardwell, J. C. A. Copper stress causes an *in vivo* requirement for the *Escherichia coli* disulfide isomerase DsbC. *J. Biol. Chem.* **280,** 33785–33791 (2005).
21. Macomber, L. & Imlay, J. A. The iron–sulfur clusters of dehydratases are primary intracellular targets of copper toxicity. *Proc. Natl Acad. Sci. USA* **106,** 8344–8349 (2009).
22. Py, B., Moreau, P. L. & Barras, F. Fe–S clusters, fragile sentinels of the cell. *Curr. Opin. Microbiol.* **14,** 218–223 (2011).
23. Hallez, R., Bellefontaine, A.-F., Letesson, J.-J. & De Bolle, X. Morphological and functional asymmetry in α-proteobacteria. *Trends Microbiol.* **12,** 361–365 (2004).
24. Deghelt, M. *et al.* G1-arrested newborn cells are the predominant infectious form of the pathogen *Brucella abortus*. *Nature Commun.* **5,** 4366 (2014).
25. Poindexter, J. S. Selection for nonbuoyant morphological mutants of *Caulobacter crescentus*. *J. Bacteriol.* **135,** 1141–1145 (1978).
26. Ely, B. in *Methods in Enzymology* Vol. 204 (ed. Miller, J. H.) 372–384 (Academic, 1991).
27. Evinger, M. & Agabian, N. Envelope-associated nucleoid from *Caulobacter crescentus* stalked and swarmer cells. *J. Bacteriol.* **132,** 294–301 (1977).
28. Winzeler, E. & Shapiro, L. Use of flow cytometry to identify a *Caulobacter* 4.5 S RNA temperature-sensitive mutant defective in the cell cycle. *J. Mol. Biol.* **251,** 346–365 (1995).
29. Levi, A. & Jenal, U. Holdfast formation in motile swarmer cells optimizes surface attachment during *Caulobacter crescentus* development. *J. Bacteriol.* **188,** 5315–5318 (2006).
30. Le Blastier, S. *et al.* Phosphate starvation triggers production and secretion of an extracellular lipoprotein in *Caulobacter crescentus*. *PLoS ONE* **5,** e14198 (2010).
31. Achard, M. E. S. *et al.* The multi-copper-ion oxidase CueO of *Salmonella enterica* serovar Typhimurium is required for systemic virulence. *Infect. Immun.* **78,** 2312–2319 (2010).

Acknowledgements

The authors thank C. Jacobs-Wagner, J. Collier, L. Shapiro, P. Viollier and J. Smit for providing strains and antibodies. The authors acknowledge the microscopy platform of the De Duve Institute (UCL) for allowing access to the Zen Observer Z.1 inverted microscope, and thank C. Staudt (URPhym, UNamur) for technical support regarding the oxygraph and R. Stephan from the GIGA Flow Cytometry Facility (ULg) for technical support with FACS cell counting. Finally, the authors thank C. Jacobs-Wagner, J.-F. Collet, G. Cornelis and X. De Bolle for critical reading of the manuscript and the URBM members for discussions. This work was supported by the University of Namur. E.L. and S.G. were supported by the Belgian Fund for Industrial and Agricultural Research Associate (FRIA).

Author contributions

E.L., S.G., G.L., F.T., S.L.B. and P.C. performed the experiments. E.L., S.G. and G.L. analysed the data. E.L. and J.-Y.M. initiated and designed the research. E.L., S.G. and J.-Y.M. wrote the manuscript.

Additional information

Supplementary information is available online. Reprints and permissions information is available online at www.nature.com/reprints. Correspondence and requests for materials should be addressed to J.Y.M.

Competing interests

The authors declare no competing financial interests.